Aqueous phase catalysis using mono– and bimetallic transition metal complexes

Leah Charlie Matsinha

University of Cape Town

August 2015

Supervisor:

Student: Signed by candidate

Aqueous phase catalysis using mono– and bimetallic transition metal complexes

A thesis submitted to the

University of Cape Town

in fulfilment of the requirements for the degree of

Doctor of Philosophy

by

Leah Charlie Matsinha

Supervisor: Assoc. Professor Gregory S. Smith

Co-supervisor: Professor Selwyn F. Mapolie

Co-supervisor: Dr Gerhard A. Venter

Department of Chemistry,

University of Cape Town,

South Africa

Declaration

I know the meaning of Plagiarism and declare that all of the work in the document, **"Aqueous phase catalysis using mono– and bimetallic transition metal complexes"**, is my own work and to the best of my knowledge has never been submitted for examination for any degree at any university. All sources of information are cited and fully referenced.

Leah Charlie Matsinha ……..

Date 28 August 2015 ……..

Acknowledgements

I would like to thank God, for the gift of life and all the blessings bestowed upon me to pursue a doctoral degree in chemistry. He has allowed a vast array of people to be part of my life during my doctoral studies and I would like to take this opportunity to publicly thank these people.

Firstly, I would also like to thank my supervisors, Associate Professor Gregory Smith, Professor Selwyn Mapolie and Dr Gerhard Venter for their ideas, suggestions and lots of patience throughout the project. It has been a great privilege working with them and their passion for teaching and research assisted me during this work and will definitely continue to help me in my career as a researcher. Thank you all for asking all the insightful questions, helpful suggestions and invaluable training throughout my doctoral studies. On the administrative side, I would like to thank Mrs Deirdre Brooks who was always smiling and ready to assist at all times.

The analytical chemistry staff at the University of Cape Town Mr Pete Roberts, and Mr Gianpierro Benincasa did a great job and I would like to thank them for all the assistance and work they did. Many thanks also go to Hong Su for the work she did on single-crystal X-ray diffraction studies.

My humble gratitude also goes to the Centre for Catalysis Research (c*change), Canon Collins Trust, Department of Science and Technology and the University of Cape Town for funding.

My heartfelt thanks also go to the organometallic research group for the support, help and constructive criticism. I learnt a lot from the research group and at the same time got a good dose of laughter. I would also like to thank Dr Banothile Makhubela, Dr Preshendren Govender, Dr Tameryn Stringer, James Biwi and Shepherd Siangwata for proof reading my thesis.

I would like to dedicate this thesis to Patrick Charlie and Christine Charlie (*parents*), Benjamin, Patrick and Kevin (*brothers*), my fiancé Drek Kandengwa and friends. Thank you all for the support and unconditional love.

Abstract

The synthesis and characterization of monomeric and dimeric salicylaldimine water-soluble ligands is discussed. The salicylaldimine ligands (**2.3**-**2.10**) were synthesised *via* Schiff base condensation reactions of various amines with water-soluble sulfonated salicylaldehydes (**2.1** and **2.2**). The ligands were characterized using various analytical and spectroscopic techniques. Complexation reactions of these water-soluble ligands (**2.3**-**2.10**) with $[Rh(COD)Cl]_2$ gave the corresponding water-soluble mononuclear (**2.11**-**2.14**) and binuclear (**2.15**-**2.18**) Rh(I) complexes. All the complexes were characterized using nuclear magnetic resonance spectroscopy, infrared spectroscopy, single crystal X-ray diffraction (for complex **2.14**), mass spectrometry, elemental analysis and melting point determinations.

The water-soluble Rh(I) complexes (**2.11**-**2.18**) were evaluated as aqueous biphasic hydroformylation catalyst precursors. The reaction conditions were optimised at 90 °C, 50 bar syngas pressure for 8 hours, with 2.87 x 10^{-3} mmol Rh loading. The mononuclear catalysts (**2.11**-**2.14**) displayed excellent chemoselectivity for aldehydes (>99%), whilst the binuclear Rh(I) analogues (**2.15**-**2.18**) showed slightly lower aldehyde chemoselectivity (>89%). The incorporation of the tertiary butyl moiety in catalysts **2.14, 2.16** and **2.18** presents greater steric bulk around the metal which resulted in better regioselectivity for nonanal. Through recycling experiments, the mononuclear catalysts (**2.11**-**2.14**) could be recycled up to five times while the binuclear analogues (**2.15**-**2.18**) could be recycled three times. A significant amount of Rh particles was formed using the binuclear catalysts, with a concomitant formation of internal olefins. Inductively coupled plasma optical spectrometry experiments confirm that no leaching of the mononuclear and binuclear catalysts (**2.11**-**2.18**) into the organic layer occurs. Analyses of the aqueous layers after the recycling experiments show that <1% metal is present in solution. The mercury drop experiments show suppressed catalyst activity and therefore the activity is due to a combination of homogeneous catalysis and catalysis mediated by Rh nanoparticles suspended in the aqueous layer.

The synthesis and characterization of water-soluble thiosemicarbazone ligands (**4.1** and **4.3**) *via* Schiff base condensation reactions of a sulfonated salicylaldehyde **2.1** with either a thiosemicarbazide or a dithiosemicarbazide is also described. Both ligands displayed excellent water-solubility at room temperature and were characterized using various analytical and spectroscopic techniques. Complexation reactions of these ligands with either $[PdCl_2(PPh_3)_2]$ or

$[PdCl_2(PTA)_2]$ resulted in the corresponding water-soluble mononuclear and binuclear thiosemicarbazone Pd(II) complexes (**4.4**-**4.7**). The Pd(II) complexes (**4.4**-**4.7**) were characterized using ^{1}H NMR, $^{13}C\{H\}$ NMR, $^{31}P\{H\}$ NMR and infrared spectroscopy, electrospray ionisation mass spectrometry (negative ion-mode), elemental analysis, and melting point determinations. The stability of the complexes was investigated using complex **4.4** as a representative example of the series. The complex displayed excellent stability at 70 ˚C over a period of 24 hours in water, using ^{1}H NMR and $^{31}P\{H\}$ NMR spectroscopy. Hydrolysis of the imine functionality was not observed and the $^{31}P\{H\}$ NMR spectroscopy also confirmed the presence of an unaltered phosphorus species at the end of the experiment.

The Pd(II) thiosemicarbazone complexes (**4.4**-**4.7**) were evaluated as catalyst precursors in the Suzuki-Miyaura cross-coupling reaction in aqueous medium. The reaction was optimised using Na_2CO_3 as base at 70 ˚C for 24 hours. The binuclear catalysts (**4.6**-**4.7**) displayed comparable activity to the mononuclear analogues (**4.4**-**4.5**). The mononuclear catalysts (**4.4**-**4.5**) were versatile and coupled substrates containing various substituents, with iodobenzene giving better results than bromobenzene as expected. Catalyst **4.4** could only be recycled efficiently twice with a significant drop in conversion of the aryl halide to products occurring in the third recycle. Mercury poisoning tests ruled out the formation of any catalytic active nanoparticles, suggesting that the catalytic reaction follows a homogeneous pathway.

A computational investigation of the oxidative addition of iodobenzene to catalyst **4.4** (with PPh_3 replaced by PH_3 to reduce the computational effort) is described. The water-soluble thiosemicarbazone complex **4.4** was found to be very stable in water at elevated temperatures. Moreover, in the Suzuki-Miyaura cross-coupling reactions nanoparticle formation was not observed. The mercury poisoning experiment also supported the fact that the Suzuki-Miyaura cross-coupling reactions were entirely homogeneous with absence of Pd(0) species/particles. As a result of these findings, the possibility of reduction of Pd(II) to Pd(0) for oxidative addition of the aryl halide to occur was ruled out. The feasibility of a Pd(II)/Pd(IV) mechanism during the oxidative addition of iodobenzene to thiosemicarbazone complex was therefore investigated. The DFT calculations showed that the Pd(II) to Pd(IV) redox is feasible with the highly stable Pd(II) complexes, which was found not to form any Pd(0) during experimental studies. The overall oxidative addition reaction is endergonic with a $\Delta G^{o} = +138.8$ kJ/mol.

Publications, conference contributions and awards

Journal Articles

1. Recoverable and recyclable water-soluble sulfonated salicylaldimine Rh(I) complexes for 1-octene hydroformylation in aqueous biphasic media.
   L. C. Matsinha, S. F. Mapolie and G. S. Smith, *Dalton Transactions*, 2015, **44**, 1240-1248.

2. Water-Soluble Palladium(II) Sulfonated Thiosemicarbazone Complexes: Facile Synthesis and Preliminary Catalytic Studies in the Suzuki-Miyaura cross-coupling reaction in Water.
   L. C. Matsinha, J. Mao, S. F. Mapolie, and G. S. Smith, *European Journal of Inorganic Chemistry*, 2015, 4088-4094.

Conference Contributions

1. **Suzuki-Miyaura cross-coupling reactions in neat water using water-soluble Pd(II) catalyst precursors** (Oral Presentation). CATSA Conference, St George's Hotel, Pretoria (9-12 November 2014).
   L. C. Matsinha, J. Mao, S. F. Mapolie and G. S. Smith.

2. **Aqueous biphasic hydroformylation of 1-octene using water-soluble Rh(I) complexes as catalyst precursors** (Oral Presentation). 41st International Conference on Coordination Chemistry, Suntec City, Singapore (21 -25 July 2014).
   L. C. Matsinha, S. F. Mapolie and G. S. Smith.

3. **The use of syngas for the production of aldehydes using recyclable Rh(I) catalysts** (Poster presentation). SYNGAS Convention, Cape Town (29 March-1 April 2015).
   L. C. Matsinha, Selwyn F. Mapolie and Gregory S. Smith.

4. **Water-soluble Ru(II) and Rh(I) complexes for aqueous biphasic hydroformylation of 1-octene** (Poster presentation). Green Chemistry Symposium G2C2, Cape Town (24-26 August 2014).
   L. C. Matsinha, S. F. Mapolie and G. S. Smith.

Awards

1. **Canon Collins Scholars Conference Award**, (Impact Award), Cape Town, South Africa, 2015.
2. **Department of Science and Technology**, Women in Science Award, Johannesburg, South Africa, 2013.

List of Abbreviations

Å	Angstrom
acac	Acetylacetone
Ar	Aromatic or aryl
br s	Broad singlet (NMR)
°C	Degrees Celsius
CD_3OD	Methanol-d_4
CHCN	Acetonitrile
cm^{-1}	Wavenumbers (reciprocal centimetres)
COD	Cyclooctadiene
COSY	Correlation spectroscopy
C_p	Cloud point
$^{13}C\{H\}$ NMR	Proton-decoupled carbon nuclear magnetic resonance
def-2-SVP	basis set of the def2-type
EtOH	Ethanol
Et_2O	Diethyl ether
DFT	Density functional theory
DMF	Dimethylformamide
DMSO-d_6	Dimethyl sulfoxide-d_6
D_2O	Deuterium oxide
ESI-MS	Electrospray ionisation mass spectrometry
Et_2O	Diethyl ether
FT-IR	Fourier Transform Infrared
GC	Gas chromatography
^1H NMR	Proton nuclear magnetic resonance
HOMO	Highest occupied molecular orbital
Hz	Hertz
ICP-OES	Inductively coupled plasma optical emission spectroscopy
IFP	Institut Francais du Petrole
IRC	Intrinsic reaction coordinate
J	Coupling constant
m	Multiplet (NMR)
Max	Maximum

MeOH	Methanol
Min	Minimum
NBO	Natural bond orbitals analysis
NHC	N-Heterocyclic carbene
OAc	Acetate
OPGPP	Octylpolyglycol phenylene phosphite
ORTEP	Oak ridge thermal ellipsoid plot
PEO-DPPSA	N,N-dipolyoxyethylene-substituted-4-(diphenylphosphino) benzenesulfonamide
PEO-TPP	Poly(ethylene oxide) triphenylphosphine
Ph	Phenyl
ppb	Parts per billion
ppm	Parts per million
PTA	1,3,5-Triaza-7-phosphaadamantane
QST2	Quadratic synchronous transit method
RCH/RP	Ruhrchemie/Rhône-Poulenc
s	Singlet (NMR)
SHOP	Shell higher olefin process
SMD	a universal continuum solvent model (D stands for density)
t	Triplet
TBAB	Tetrabutylammonium bromide
^{t}Bu	Tertiary butyl
TEM	Transmission electron microscope
TOF	Turn over frequency
TPPDS	Triphenylphosphine disulfonate
TPPMS	Triphenylphosphine monosulfonate
TPPTS	Triphenylphosphine trisulfonate
TPTC	Thermoregulated phase transfer catalysis
TS	Transition state
SulphoXantPhos	2,7-bis(SO_3Na)-4,5-bis(diphenylphosphino)-9,9-dimethylxanthene
Syngas	Synthesis gas
UOP	Universal Oil Products

Table of Contents

Chapter 1: Background on catalysis and the literature review on catalysis in unusual solvents 1

1.1 Introduction 1

1.2 Multiphase (biphasic, liquid/liquid) homogeneous catalysis 2

1.3 The hydroformylation reaction 5

1.3.1 Sulfonated ligands for aqueous biphasic hydroformylation 8

1.3.2 Cyclodextrins in aqueous biphasic hydroformylation 12

1.3.3 Thermoregulated phase transfer ligands in aqueous biphasic hydroformylation 14

1.3.4 Fluorous/organic biphasic catalysis in hydroformylation of olefins 18

1.4 The Suzuki-Miyaura cross-coupling reaction 21

1.4.1 Sulfonated Pd complexes for Suzuki-Miyaura cross-coupling reactions in water 23

1.5 Homobimetallic complexes in catalysis 26

1.5.1 Homobimetallic catalysts for the hydroformylation reaction 27

1.5.2 Homobimetallic catalysts for the Suzuki-Miyaura cross-coupling reaction 27

1.6 Closing Remarks 30

1.7 Aims and objectives of the thesis 31

1.7.1 Specific aims and objectives 31

1.8 References 33

Chapter 2: Synthesis and characterization of water-soluble mono- and binuclear salicylaldimine Rh(I) complexes 41

2.1 Introduction 41

2.2 Synthesis and characterization of water-soluble *N,O*-chelating Schiff base ligands 42

2.2.1 Synthesis and characterization of sulfonated monosodium 5- sulfanato salicylaldehydes 42

2.2.2 Synthesis and characterization of monomeric *N,O*-chelating Schiff base ligands 44

2.2.3 Synthesis and characterization of dimeric *N,O*-chelating Schiff base ligands 45

2.3 Synthesis and characterization of water-soluble mononuclear *N,O*-Rh(I) complexes 47

2.4 Synthesis and characterization of water-soluble binuclear *N,O*-Rh(I) complexes 51

2.5 Overall Summary 54

2.6 Experimental 55

General Details....55
2.7 Synthesis and characterization of sulfonated aldehydes and the corresponding imine ligands....55
2.7.1 Synthesis of water-soluble salicylaldimine ligand **2.4**....55
2.7.2 Synthesis of water-soluble salicylaldimine ligand **2.5**....56
2.7.3 Synthesis of water-soluble salicylaldimine ligand **2.7**....56
2.7.4 Synthesis of water-soluble salicylaldimine ligand **2.8**....57
2.7.5 Synthesis of water-soluble salicylaldimine ligand **2.9**....57
2.7.6 Synthesis of water-soluble salicylaldimine ligand **2.10**....58
2.8 Synthesis and characterization of sulfonated water-soluble Rh(I) complexes....59
2.8.1 Synthesis of mononuclear complex **2.11**....59
2.8.2 Synthesis of mononuclear complex **2.12**....59
2.8.3 Synthesis of mononuclear complex **2.13**....60
2.8.4 Synthesis of mononuclear complex **2.14**....61
2.8.5 Synthesis of mononuclear complex **2.15**....62
2.8.6 Synthesis of mononuclear complex **2.16**....62
2.8.7 Synthesis of mononuclear complex **2.17**....63
2.8.8 Synthesis of mononuclear complex **2.18**....64
2.8.9 X-ray Crystallography....64
2.9 References....65
Chapter 3: Aqueous biphasic hydroformylation of 1-octene using water-soluble Rh(I) complexes as catalyst precursors....67
3.1 Introduction....67
3.2 Aqueous biphasic hydroformylation of 1-octene....68
3.2.1 Optimisation of the reaction conditions....69
3.2.2 Chemoselectivity and regioselectivity of the mononuclear catalyst precursors **2.11**-**2.14**....70
3.2.3 Recyclability of the mononuclear catalysts **2.11**-**2.14**....71
*Chemoselectivity of catalysts **2.11**-**2.14***....71
Electronic effects....72
*Regioselectivity of catalysts **2.11**-**2.14***....74
Steric effects....74
3.2.4 Chemoselectivity and regioselectivity of the binuclear catalysts precursors **2.15**-**2.18**....76

Electronic effects 77
Steric effects 79
3.2.5 Recyclability of the binuclear catalysts **2.15-2.18.** 80
3.2.6 Mononuclear catalysts versus binuclear catalysts 81
3.3 Inductively coupled plasma optical spectrometry experiments 82
3.4 Mercury poisoning experiments 83
3.5 Overall Summary 84
3.6 Experimental 85
3.7 References 86
Chapter 4: Synthesis and characterization of water-soluble mono- and binuclear thiosemicarbazone Pd(II) complexes 89
4.1 Introduction 89
4.2 Synthesis and characterization of water-soluble sulfonated salicylaldimine thiosemicarbazone ligands 90
4.2.1 Synthesis and characterization of sulfonated monothiosemicarbazone salicylaldimine ligand **4.1** 90
4.2.2 Synthesis and characterization of sulfonated dithiosemicarbazone salicylaldimine ligand **4.3**. 92
4.3 Synthesis and characterization of water-soluble Pd(II) sulfonated salicylaldimine thiosemicarbazone complexes 94
4.3.1 Synthesis and characterization of water-soluble mononuclear Pd(II) sulfonated salicylaldimine thiosemicarbazone complexes **4.4** and **4.5**. 94
4.3.2 Synthesis and characterization of water-soluble binuclear Pd(II) sulfonated salicylaldimine thiosemicarbazone complexes **4.6** and **4.7**. 97
4.4 Stability experiments for the water-soluble Pd(II) complex 4.4 in water at 70 ˚C. 99
4.5 Overall Summary 101
4.6 Experimental 101
4.7 Synthesis and characterization of water-soluble sulfonated thiosemicarbazone ligands 102
4.7.1 Synthesis and characterization of sulfonated monothiosemicarbazone salicylaldimine ligand **4.1** 102
4.7.2 Synthesis and characterization of sulfonated dithiosemicarbazone salicylaldimine ligand **4.3** 102
4.8 Synthesis and characterization of water-soluble sulfonated thiosemicarbazone Pd(II) complexes 103

4.8.1 Synthesis and characterization of sulfonated mononuclear Pd(II) thiosemicarbazone complex **4.4**. 103
4.8.2 Synthesis and characterization of sulfonated mononuclear Pd(II) thiosemicarbazone complex **4.5**. 104
4.8.3 Synthesis and characterization of sulfonated mononuclear Pd(II) thiosemicarbazone complex **4.6**. 104
4.8.4 Synthesis and characterization of sulfonated mononuclear Pd(II) thiosemicarbazone complex **4.7**. 105
4.9 References 106
Chapter 5: Aqueous phase Suzuki-Miyaura cross-coupling reactions using water-soluble Pd(II) complexes as catalyst precursors 108
5.1 Introduction 108
5.2 Aqueous phase Suzuki-Miyaura cross-coupling reactions using water-soluble thiosemicarbazone complexes **4.4**-**4.7**. 109
5.3 Effects of the base 111
5.4 Effects of temperature 113
5.3.3 Effects of nuclearity 114
5.4 Suzuki-Miyaura cross-coupling reactions between various substrates using **4.4** and **4.5**. 116
5.5 Catalyst recycling in the aqueous phase Suzuki-Miyaura cross-coupling reactions using catalyst **4.4** 117
5.6 Overall Summary 119
5.7 Experimental 119
5.8 Characterization of the Suzuki-Miyaura cross-coupling reaction products 120
5.8.1 Characterization of 1,1-biphenyl 120
5.8.2 Characterization of 4-methyl-1,1-bipheyl 120
5.8.3 Characterization of 4-methoxyl-1,1-bipheyl 121
5.8.4 Characterization of 4-methyl-2-nitro-1,1-biphenyl 121
5.8.5 Characterization of 4-(tert-butyl)-1,1-biphenyl 121
5.8.6 Characterization of [1,1-biphenyl]-4-carboxylic acid 121
5.8.7 Characterization of 4-methyl-1,1-biphenyl 122
5.8.8 Characterization of [1,1'-biphenyl]-4-carbaldehyde 122
5.8.9 Characterization of 4-(tert-butyl)-1,1-biphenyl 122
5.8.10 Characterization of 4-methyl-1,1-biphenyl 122
5.8.11 Characterization of [1,1-biphenyl]-4-carboxylic acid 123

5.8.12 Characterization of 4-methyl-2-nitro-1,1-biphenyl....123
5.8.13 Characterization of [1,1-biphenyl]-4-carboxylic acid....123
5.8.14 Characterization of 4-methoxyl-1,1-biphenyl....123
5.8.15 Characterization of 4-methyl-1,1-biphenyl....124
5.8.16 Characterization of 4-(tert-butyl)-1,1-biphenyl....124
5.8.17 Characterization of [1,1-biphenyl]-4-carboxylic acid....124
5.8.18 Characterization of 1,1-biphenyl....124
5.8.19 Characterization of [1,1-biphenyl]-4-carboxylic acid....125
5.8.20 Characterization of [1,1-biphenyl]-4-carboxylic acid....125
5.8.21 Characterization of 4-methyl-1,1-biphenyl....125
5.8.22 Characterization of 4-methyl-1,1-biphenyl....125
5.8.23 Characterization of 4-(tert-butyl)-1,1-biphenyl....126
5.9 References....126
Chapter 6:Theoretical study on the oxidative addition of iodobenzene to Pd(II) thiosemicarbazone complex....128
6.1 Introduction....128
6.2 Mechanism of Oxidative addition of iodobenzene to Pd(II) thiosemicarbazone complex **4.4**....130
6.3 Overall Summary....135
6.4 Computational details....136
6.5 References....136
Chapter 7: Overall summary, conclusions and future outlook....139
7.1 Synthesis and characterization of water-soluble Rh(I) complexes and application as catalysts precursors in the aqueous biphasic hydroformylation of 1-octene....139
7.2 Synthesis and characterization of water-soluble Pd(II) thiosemicarbazone complexes and their application in aqueous phase Suzuki-Miyaura cross-coupling reactions....140
7.3 Theoretical investigation of the oxidative addition of iodobenzene to water-soluble thiosemicarbazone complex in aqueous medium....141
7.4 Future outlook....141
7.4.1 Aqueous biphasic hydroformylation reactions....141
7.4.2 Aqueous phase Suzuki-Miyaura cross-coupling reactions....142
7.4.3 Theoretical studies on the oxidative addition of iodobenzene to thiosemicarbazone Pd(II) complex....142
7.5 References....142

Chapter 1

Background on catalysis and literature review on catalysis in unusual solvents

1.1 Introduction

Catalysis is one of the most important enabling technologies that supports the world's economy today.[1] Industries such as the petroleum, agrochemicals, electronics and polymer industries rely heavily on catalysis and catalyst demand is estimated to reach $19.5 billion in 2016.[2,3] The application of catalysis makes industrial processes economically viable because reaction times are shortened and energy costs are reduced. Moreover, catalytic transformations reduce waste generation.[4] The significance of catalysis can also be appreciated by a survey of the Nobel Prizes for chemistry in the past 60 years. Examples include, the work by Ziegler and Natta on catalysis as applied in polymer synthesis (1963),[5] Wilkinson and Fischer on organometallic compounds (1973),[6] the work on asymmetric hydrogenation and oxidation reactions by Knowles, Noyori and Sharpless on chirally catalysed reactions (2001),[7] the work by Chauvin, Grubbs and Schrock on metathesis reactions (2005)[8] and lastly Negishi, Heck and Suzuki-Miyaura in their work on palladium catalysed reactions in organic synthesis (2010).[9]

Catalysis is also one of the important principles of Green Chemistry (Table 1.1) mainly because it substitutes classical stoichiometric methodologies with cleaner catalytic alternatives.[10] Implementation of the principles of Green Chemistry is vital for sustainable development of chemical processes which determines most of the concepts in the chemical industry.[4,11-12] The key strategy is the development of technologies that are more selective while occurring under mild conditions which are not time consuming (to save energy) and produce less by-products and waste.[13]

Catalytic reactions can be divided into homogeneous catalysis and heterogeneous catalysis. Most industrial processes use heterogeneous catalysts because they can be easily separated from the products, but selectivity and reaction rates are limited by the multiphase nature of the system. However, homogeneous catalysts have been found to be more efficient in terms

of selectivity and reaction rates. Unfortunately, the use of organic solvents to dissolve the catalysts raises problems of environmental pollution since these solvents are often toxic.

Table 1.1 Principles of Green Chemistry.[13]

Principles of Green Chemistry	
1. Prevent waste	7. Use of renewable feed stocks
2. Atom efficiency	8. Reduce derivatives
3. Less hazardous chemical synthesis	9. Catalysis
4. Designing safer chemicals	10. Design for degradation
5. Safer solvents and auxiliaries	11. Real-time analysis for pollution prevention
6. Design for energy efficiency	12. Inherently safer chemicals for accident prevention

Moreover, reactants, products and catalyst are in the same phase which results in difficulties in catalyst separation from products and high energy consumption to separate the mixtures.[14] Table 1.2 shows some of the advantages and disadvantages of homogeneous and heterogeneous catalysis.

Table 1.2 Advantages and disadvantages of homogeneous and heterogeneous catalysis.[15]

	Stirred tank homogeneous operation	**Fixed bed heterogeneous operation**
Conversion	High conversions	Low conversions
Separation	- Filtration after chemical decomposition -Distillation -Extraction	No separation problems
Additional equipment required	Yes	No
Catalyst recycling	Difficult	Easy
Cost of catalyst losses	High	Minimal
Catalyst concentration in product	Low	-

Bridging the gap between homogeneous and heterogeneous catalysis is essential in order for a catalyst to be efficient. Improving the recovery of highly selective homogeneous catalysts by developing multiphase solvent systems is a potential solution.

1.2 Multiphase (biphasic, liquid/liquid) homogeneous catalysis

All multiphasic systems aim to overcome the major problem of homogeneous catalysis which is catalyst recovery and product separation.[16] The concept of biphasic catalysis involves two

immiscible layers with one containing the catalyst and the second layer containing the substrate/s (Figure 1.1). The active catalyst remains in one layer so that the reactants and products which are entirely soluble in the second layer can easily be phase separated from the catalyst.

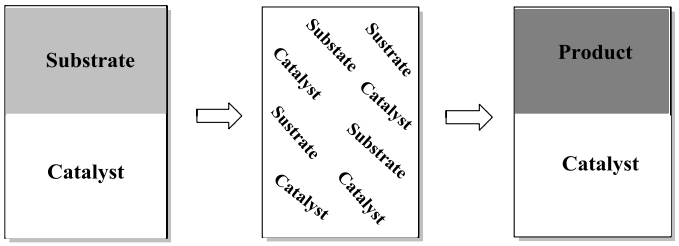

Figure 1.1 Aqueous biphasic catalysis.[17]

Many biphasic approaches for catalysis have been developed and include aqueous/organic biphasic systems,[11,18–25] thermoregulated phase transfer biphasic systems,[26–32] fluorous/organic biphasic systems,[33–44] and ionic liquid biphasic systems.[45-46] Several of these solvent combinations have been applied on an industrial scale in various organic transformation reactions. Some examples are shown Table 1.3.

Table 1.3 Biphasic catalysis in industry.[11]

Process	Company	Active metal	Solvent
Oligomerization of ethylene (SHOP)	Shell	Ni	Butane-1,4-diol
Hydroformylation of propylene and butylene	Ruhrchemie/Rhône-Poluenc (RCH/RP)	Rh	Water
Hydrogenation of unsaturated aldehydes	Rhône-Poluenc	Ru	Water
Telomerization of butadiene	Kuraray	Pd	Water/Sulfolane
Dimerization of propylene	Institut Francais du Petrole (IFP)	Ni	Ionic liquids
Oligomerization of ethylene	Universal Oil Products (UOP)	Ni	Sulfolane

Aqueous biphasic systems are the most popular because they make use of water. This is because of ecological reasons and water offers many advantages as a reaction medium.[12,13,47] Water is polar and easy to separate from non-polar solvents, non-flammable, incombustible, widely available in suitable quality, odourless and has high solubility in many gases.[11] Since many organometallic complexes have poor solubility in water, it is important to design catalysts that are readily soluble in water to ensure catalyst immobilization in the aqueous

phase. Polar groups have been found to be advantageous in terms of enhancing activity, selectivity and water-solubility and preventing catalyst transfer to the organic phase during catalyst recovery.[19] The application of aqueous biphasic catalysis has been commercialised and examples of ligands used in some petrochemical processes are shown in Table 1.4.

Table 1.4 Petrochemical processes involving aqueous biphasic catalysis.

Reaction	**Active metal**	**Ligand**
Hydroformylation [48,49]	Rh	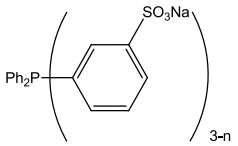 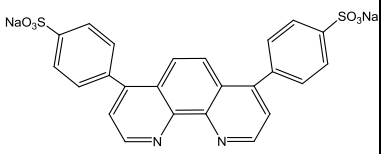 **1.1** n=0 (TPPTS); **1.2** n=2 (TPPMS); **1.3** n=3 (TPPDS) **1.4**
Hydrogenation[50,51]	Rh, Ru, Ir	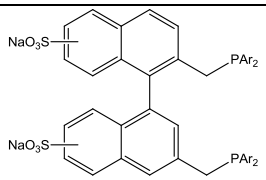 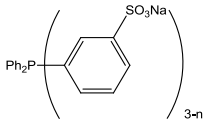 **1.5** **1.1 - 1.3**
Carbonylation[52,53]	Pd	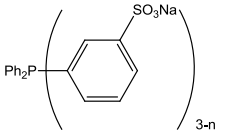 **1.1 - 1.3**
Wacker oxidation[54]	Pd	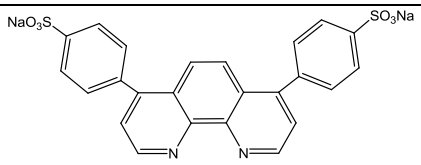 **1.1**
Dimerization of butadiene[55]	Pd	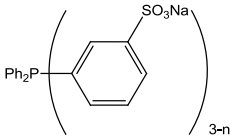 **1.1 - 1.3**
Metathesis[56]	Ru	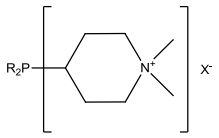 R = Cy, ^{t}Bu; X = Cl, I (**1.6** – **1.9**)

There is however a general restriction regarding the use of water as a reaction medium in homogeneous catalysis. Water-solubility of organic substrates decreases with increase in the carbon chain length. For example, in the hydroformylation reaction, the reactivity of the alkenes C_3 - C_9 has been explained by the difference in solubility of the olefins. Therefore co-solvents, co-ligands, surfactants, counter-ions, micelle-forming agents or surface-active ligands are usually added to improve water-solubility of substrates.[19,57]

Aqueous biphasic catalysis has been applied extensively in the hydroformylation reaction and this will be discussed in more detail in the next section. A wide range of organic transformations have also been successfully performed in neat water using water-soluble transition metal complexes as catalysts. This is in an effort to make catalyst recovery and recyclability possible and also make use of a cheaper and environmentally friendly solvent. One such reaction is the Suzuki-Miyaura cross-coupling reaction and this will also be discussed herein in more detail.

1.3 The hydroformylation reaction

The hydroformylation reaction is one of the largest homogeneously catalysed reactions in industry. This process is a transition metal-catalysed conversion of olefins in the presence of syngas (a mixture of carbon monoxide and hydrogen gas) to form linear and branched aldehydes (Scheme 1.1).[58]

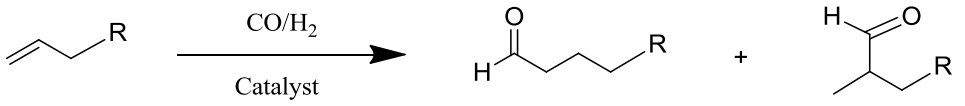

R = alkyl or aromatic group

Scheme 1.1. The hydroformylation reaction.

Since the discovery of hydroformylation by Otto Roelen,[55] the use of aldehydes has been estimated to be over 9.6 million tons per year.[59] This process has catalysts based on various metals but Co and Rh for example, $Co_2(CO)_8$ and $HRh(CO)(PPh_3)_3$, have been mostly explored.[60] The mechanism for the reaction was first described for Co-based catalysts, however Rh has since proved to be a better metal for catalysing this reaction in terms of activity and selectivity, the mechanism for Rh-catalysed hydroformylation has also been described (Scheme 1.2).[61]

The catalytic cycle starts with a 16-electron Rh-H fragment **1.11** which coordinates with an olefin at the empty coordination site on Rh to form a 5-coordinate intermediate **1.12**. Migratory insertion of olefin into Rh-H results in a 4-coordinate Rh-alkyl compound **1.13**, to which CO coordinates for form **1.14**. Migratory insertion of CO into the metal-alkyl bond results in the formation of an acyl complex of rhodium **1.15**. The hydrogenolysis of compound by hydrogen **1.15** results in **1.16** followed by reductive elimination of either linear or branched aldehydes, with the regeneration of the active Rh-H complex **1.11** occurring simultaneously.

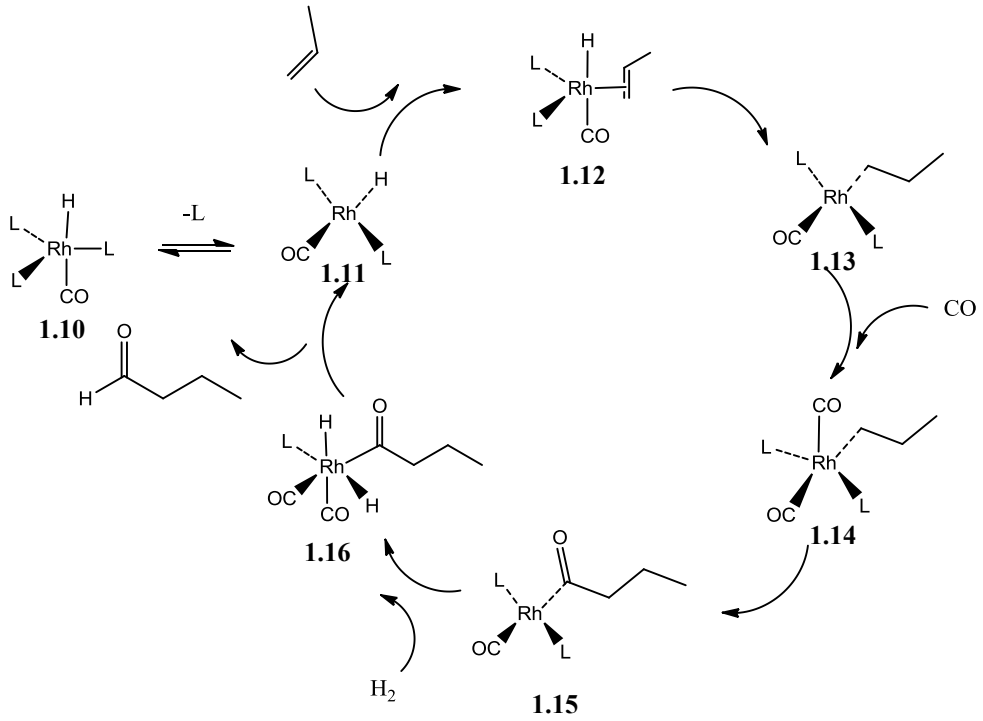

Scheme 1.2 Mechanism of Rh-catalysed hydroformylation.[62]

The regioselectivity of the catalyst is an important factor in olefin hydroformylation because either linear or branched aldehydes can be formed.[63] This can be controlled by various factors such as effects of the catalysts or potential directing effects of functional groups appended to the substrate. Moreover, olefin hydroformylation can have side and subsequent reactions. These include isomerisation of the olefin substrate to form internal olefins, hydrogenation of the olefin forming an alkane or hydrogenation of aldehydes to form alcohols. The aldehydes produced can be used as feedstocks in the production of pharmaceuticals, fragrances and agrochemicals.[64] Apart from this, aldehydes give access to a wide range of compounds such as amines, acetals, diols and carboxylic acids.

In 1984, the aqueous biphasic hydroformylation of propene and butene was developed and commercialised as the Ruhrchemie/Rhône-Poulenc (RCH/RP) process.[65] The RCH/RP process uses the highly water-soluble ligand triphenylphosphine trisulfonate (TPPTS), with a water-solubility of 1100 mg/mL at room temperature.[66] The rhodium complex $[HRh(CO)(TPPTS)_3]$ (Figure 1.2) is supported in the aqueous phase while the product and substrate form the organic phase. This is a very good demonstration of catalysis in water on a large scale, and it gives good results when employing low molecular weight terminal olefins as substrates. The Ruhrchemie/Rhône-Poulenc process and the use of TPPTS-modified Rh-hydrido carbonyl complex as catalyst has been extensively described in the literature. [48,65,67]

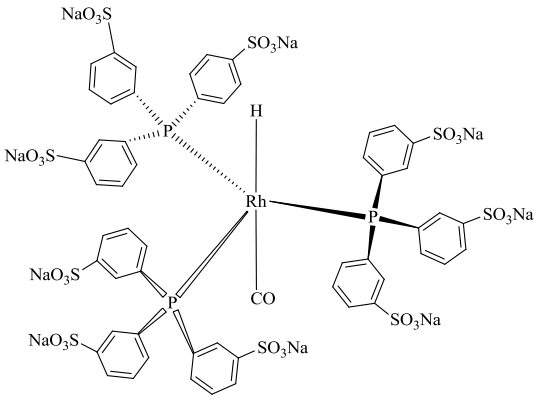

1.17

Figure 1.2 Active catalyst $[HRh(CO)(TPPTS)_3]$ for the Ruhrchemie/Rhône Poulenc process.

Most organometallic complexes are insoluble in water, therefore the design of ligands with suitable hydrophilic functionalities which constrain the catalytically active metal species in the aqueous phase is the main task.[19] Ligands can partition into the aqueous phase when these suitable hydrophilic groups are incorporated. Polar groups display advantageous properties in terms of selectivity and activity and they sharply induce water-solubility. When they are introduced into the structure of the metal complexes, these polar groups prevent the catalyst from moving into the organic-phase after the reaction.[68] The most commonly used polar groups are phosphonates, sulfonates, quaternary ammonium and hydroxyl groups. These have been extensively used with various transition metals in hydroformylation catalysis.[19,49]

1.3.1 Sulfonated ligands for aqueous biphasic hydroformylation

The first and most easily used water-solubilising substituent is the sulfonate. It is the most attractive water-solubilising moiety because it can easily be introduced and it is stable under a variety of reaction conditions.[19] Metal sulfonates are usually introduced onto the aryl substituents of phosphines by electrophilic sulfonation using a mixture of SO_3 and H_2SO_4 or in some cases just H_2SO_4. Sulfonation of the aryl rings connected to the phosphorus atom occurs exclusively in the meta-position. This is due to the directing effects of the protonated phosphorus centre. Harsh conditions are usually used (20-40% oleum at elevated temperatures) during sulfonation due to the protonated phosphorus centre that has a tendency to deactivate the aryl ring to sulfonation. Triphenylphosphine sulfonation was first reported by Chatt.[69] In this work, 25% SO_3 in H_2SO_4 was used to give the monosulfonated triphenylphosphine derivative (*m*-TPPTS). The trisulfonated derivative was then first prepared by Kuntz using 20% oleum.[20, 21] During the time when hydroformylation was developed at Rhône-Poulenc, Co-based catalysts dominated propene hydroformylation, however Rh-phosphine catalysts were known to be more active. Due to the high cost of Rh compared to Co, recovery of the expensive metal became critical and hence the development of the water-soluble Rh(I) complex $[HRh(CO)(TPPTS)_3]$ (Figure 1.2).

The catalyst is not sensitive to sulfur and other 'oxo' poisons.[67] This together with the simple but effective decanting operation allows organic impurities and other by-products to be removed at the separation stage, accumulation of activity-decreasing poisons in the catalyst solution is prevented. Therefore, no further pre-treatment or purification steps are required for the catalyst containing-aqueous phase.[67] This technology is currently in operation at five plants world-wide, producing about 800 000 tons of aldehydes annually. The operation (RCH/RP) has been seen to be robust, simple and has displayed excellent economics due to minimal leaching of the Rh metal into the organic phase that lies in the ppb range.[70]

A continuous aqueous biphasic process was also developed using $[Rh(COD)Cl]_2$ (where COD is cyclooctadiene) and an excess of *m*-TPPTS for the hydroformylation of propene to afford butanal and *iso*butanal with 24:1 linear/branches ratio.[66,71] Upon completion of the reaction, the two-phase mixture was separated easily and the aqueous layer contained the Rh-TPPTS complex, excess TPPTS and a small amount of aldehydes, while the organic phase contained the products and a small amount of water. The slight excess of TPPTS was required to stabilise the catalyst system and improve the activity.[72]

Another example that has been reported in the literature involved the synthesis and application of hydrophilic sulfonate salicylaldimine dendrimers in aqueous biphasic hydroformylation of 1-octene.[17] These were synthesized following similar sulfonating methods. The sulfonated ligands (Figure 1.3) were used to generate water-soluble Rh(I) metallodendrimers and their mononuclear analogues were used for the production of aldehydes.

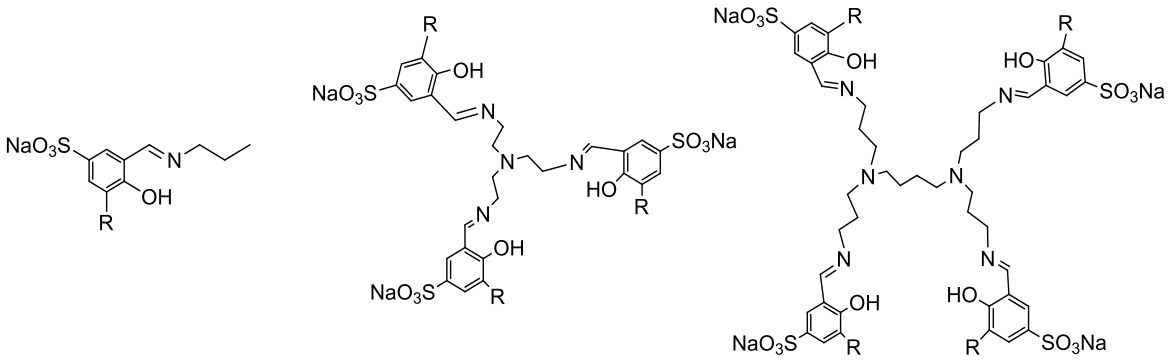

R = H (**1.18-1.20**), R = ^{t}Bu (**1.21-1.22**)

Figure 1.3 Monomeric and multimeric water-soluble sulfonated salicylaldimine ligands. [17]

The water-soluble complexes were prepared by reaction of these water-soluble ligands with $[Rh(COD)Cl]_2$ to form mono- and multimetallic organometallic catalysts. The catalysts proved to be active in the hydroformylation of 1-octene with excellent aldehyde chemoselectivity. Most importantly, the catalysts exhibited good recyclability, over five cycles, with consistent chemo- and regioselectivities.[17] Catalyst recovery was performed by simply decanting the organic products from the catalyst-containing aqueous phase. Unfortunately, Rh leaching into the organic phase was observed upon analysis of the aqueous layer using inductively coupled plasma mass spectrometry.

Monflier and co-workers have also described the synthesis of two water-soluble ligands **1.23** and **1.24** containing sulfonate groups to impart hydrophilicity (Figure 1.4). The Rh complex $Rh(acac)(CO_2)$ (where acac is acetylacetone) was used as the catalyst precursor in the hydroformylation of methyl-4-pentenoate and acetoxystyrene.[21]

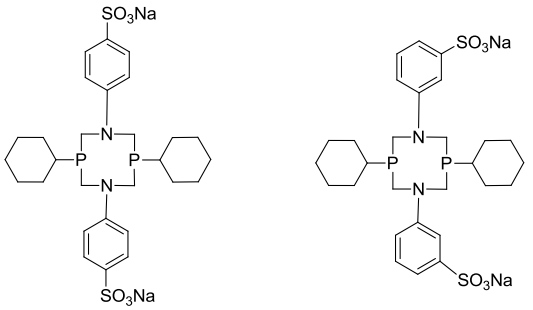

1.23 **1.24**

Figure 1.4 Water-soluble diphosphadiazacyclooctanes ligands. [21]

This system displayed an excellent aldehyde chemoselectivity with almost no isomerisation observed in some of the reactions. The conversion of the substrates was found to be dependent on ligand: Rh ratio but the recyclability of the catalysts was not reported.

Another application of sulfonated ligands used in the hydroformylation reaction was described by Peng.[25] The substrates used include 1-hexene, 1-octene and 1-dodecene with $Rh(CO_2)(acac)$ as the catalyst precursor.[25] Sulfonation of the phosphines resulted in water-soluble ligands (**1.25 – 1.27**).

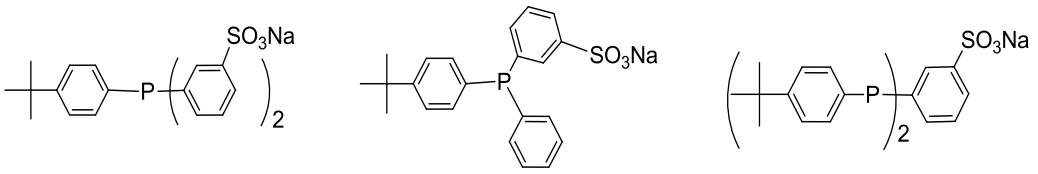

1.25 **1.26** **1.27**

Figure 1.5 Structures of the water-soluble phosphine ligands.

The hydroformylation catalyst precursor $Rh(acac)(CO_2)$ produced aldehydes in good yield under relatively mild conditions. The sulfonated phosphine ligands and their corresponding Rh complexes were found to form aggregates in water which helped to improve water-solubility of the organic substrates. No significant loss in activity was observed with the catalyst generated from the phosphine **1.25**. This could be attributed to the fact that the phosphine forms micelles spontaneously and the catalytically active aggregates allow for easy product and catalyst separation. The authors were of the opinion that ligand **1.25** fulfils the requirements for aqueous biphasic hydroformylation of higher olefins.[25]

Deng and co-workers reported the synthesis of a water-soluble ligand (Scheme 1.3) and this together with Rh(acac)(CO_2) were used in the asymmetric hydroformylation of vinyl acetate and styrene.[73]

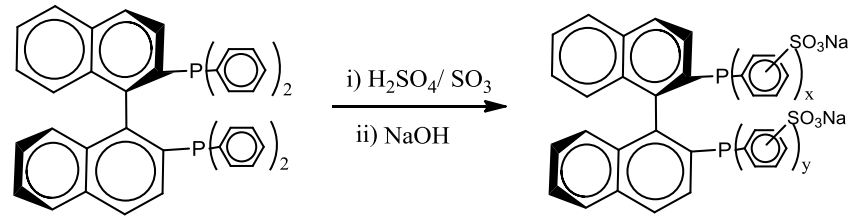

(R)-BINAPS (**1.28**) R=BINAP-nSO_3Na ; n=x+y = 3-4 (**1.29**)

Scheme 1.3 Synthesis of sulphonate ligand **1.29**.

The conversion of vinyl acetate was only 28% but with 99.8% selectivity. Secondly and most importantly, the catalysts generated from this water-soluble ligand could be recycled up to 6 times without significant losses in the activity, enantio- and regioselectivity. The same ligand (**1.29**) was also utilised in the hydrogenation of dimethyl itaconate using Ru as the metal.

Hamerla and co-workers reported the synthesis of a hydrophilic metal-ligand complex for the hydroformylation of 1-dodecene.[74] The complex (Figure 1.6) was synthesized by coordinating a water-soluble ligand 2,7-bis(SO_3Na)-4,5-bis(diphenylphosphino)-9,9-dimethylxanthene) (SulphoXantPhos) to Rh(CO_2)(acac). This system was used in the presence of an anionic surfactant to improve olefin solubility in water.

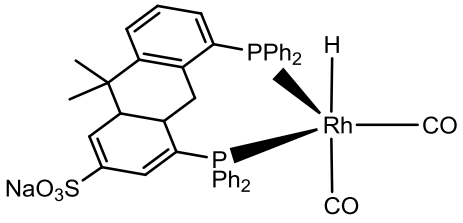

1.30

Figure 1.6 Metal-ligand complex used in the multiphasic hydroformylation of 1-dodecene.

Normal and reverse micelles were formed in the system and these acted as phase transfer agents for either the substrate or the catalysts and hence enhancing the performance of the system. Very high linear/branched ratios were obtained as high as 98:2. Leaching of catalyst was also minimal with less than 1 ppm metal found in the organic layer after separation.

Apart from sulfonated ligands, cyclodextrins have also been employed to enhance hydroformylation using the aqueous biphasic medium approach.

1.3.2 Cyclodextrins in aqueous biphasic hydroformylation

Cyclodextrins are cyclic oligosaccharides of six α-cyclodextrin, seven β-cyclodextrin, eight γ-cyclodextrin or more glucopyranose units linked by α-(1,4) bonds.[75] The most notable property of cyclodextrins is their ability to form inclusion complexes (host-guest complexes) with a wide range of compounds by molecular complexation.[75] In the complexes, the guest molecule is held within the cavity of the cyclodextrin host molecule. The lipophilic cavity of the cyclodextrin provides an environment into which non-polar moieties can enter to form inclusion complexes (Figure 1.7).[76] The physicochemical properties of the guest molecules are affected when they have been included into the cyclodextrin. These include solubility and stability of labile guests. As a result, these cyclodextrin based systems find use in a wide range of applications and this includes aqueous biphasic hydroformylation.

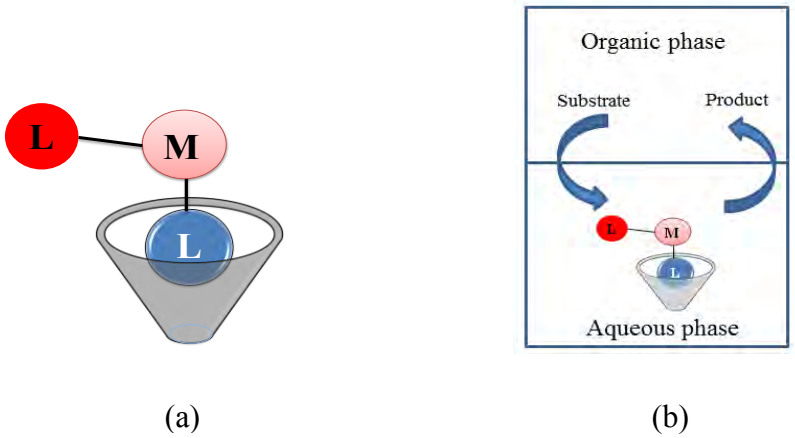

(a) (b)

Figure 1.7 An inclusion complex (a) and aqueous biphasic catalysis using water-soluble inclusion complex (b).

Monflier and co-workers reported the application of a cyclodextrin based organometallic complexes as catalysts for the hydroformylation of styrene in water (Figure 1.8).[77] Complex **1.31** showed good catalytic activity and gave a 95% conversion of styrene after 6 hours at 80 °C. Complex **1.32** gave a conversion of 91% under similar hydroformylation conditions. The nature of the nitrogen alkyl substituents resulted in the slight differences in activity of the two complexes.

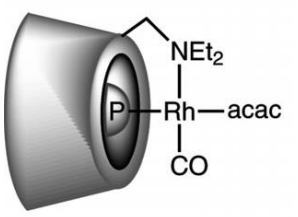

(**1.31**)

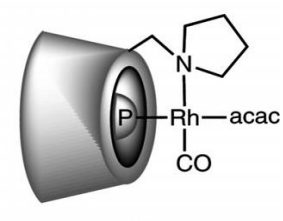

(**1.32**)

Figure 1.8 Cyclodextrin based Rh complexes used in aqueous biphasic hydroformylation.

Another Rh-based cyclodextrin complex $[Rh(L)(COD)BF_4]^+$ has been described in hydroformylation of various olefinic substrates.[78] A high selectivity and activity was reported using this complex with ligands **1.33** and **1.34** (Figure 1.9). The reaction was performed at 80 ^oC and 20 bar syngas (1:1 CO/H_2) pressure. An aldehyde chemoselectivity of 99% was observed with 1-octene as the substrate using ligand **1.33**. However, catalyst reusability was disappointing with only 50% conversion being recorded in the second run. The same ligand was also used in the hydroformylation of *E*-3-hexene and 4-vinylcyclohexene.

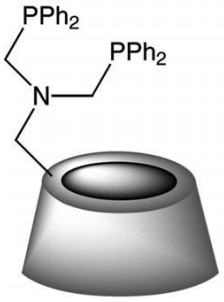

(**1.33**)

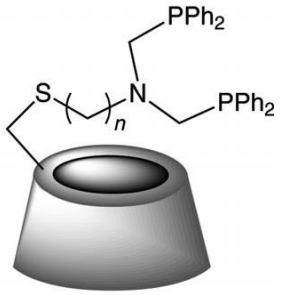

(**1.34**)

Figure 1.9 Ligands used to generate organometallic complex $[Rh(L)(COD)BF_4]^+$ in the hydroformylation of various olefinic substrates, where L = **1.33** and **1.34**.

Various cyclodextrins have been used as mass transfer agents in hydroformylation,[19] for example, the conversion of 1-decene into corresponding aldehydes was performed in the presence of cyclodextrins as mass transfer agents.[79] When water-soluble ligands such as phosphanes are also used, they are able to act as water-solubilising groups for organometallic complexes in water.[19] When combined with cyclodextrins, phosphines such as **1.35 - 1.37** can give interesting properties because the whole supramolecular species can now act as both a mass transfer agent and as a coordinating species.[80]

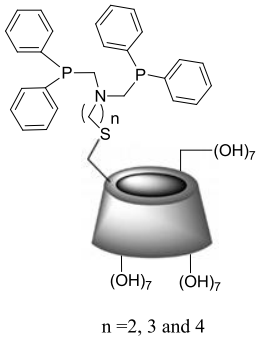

(**1.35-1.36**)

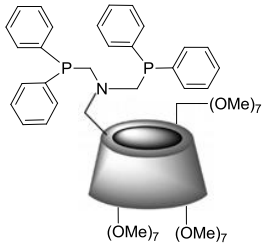

(**1.37**)

Figure 1.10 Cyclodextrin-functionalised phosphines.

When the functionalised cyclodextrins were employed in the hydroformylation of various olefins (1-octene, *E*-3-hexene and allylbenzene), an unexpectedly high catalytic activity was observed. The systems were found to be over 150 times more active at 80 ^{o}C than the Rh/TPPTS at 120 ^{o}C. Catalyst recovery was simple; unfortunately Rh was detected in the organic layer using atomic absorption spectrophotometry thus showing loss of the metal during the reaction. Reuse of the aqueous phase yielded a residual catalytic activity of only 50%.

As a follow-up to this work a phosphane-based α-cyclodextrin was synthesized. [81] The ligand easily formed complexes with a number of metals such as Pt, Pd, Au, Ag and Rh. The Rh complex formed was used in hydroformylation of 1-octene (water/methanol; 60/40). Both conversion and aldehyde chemoselectivity were seen to be over 99%, but unfortunately catalyst leaching was also seen. The results proved that the ligands are valuable for this chemical transformation under aqueous biphasic conditions.[81] Many reports have been given on the use of cyclodextrins for aqueous biphasic hydroformylation of olefins.[82–85] Apart from cyclodextrins, thermoregulated phase transfer ligands have also been used in aqueous biphasic hydroformylation.

1.3.3 Thermoregulated phase transfer ligands in aqueous biphasic hydroformylation

Attaching polyethylene glycol chains onto an active metal catalyst has been used as a strategy to prepare catalysts that can be used in aqueous biphasic catalysis. For example, a water-soluble rhodium polyethylene glycolate was prepared by reacting rhodium trichloride with polyethylene glycol and this catalyst was used as a catalyst in the hydroformylation of

various olefins such as 1-dodecene, 2, 4, 4-trimethylpentene and styrene in biphasic systems. [86] The catalyst was reported to be very active with turn over frequencies (TOFs) in the range of interest for industrial applications. From this example, we see that polyethylene glycols can be used as water-solubilising substituents, but they have an interesting inverse-temperature dependent solubility when the correct hydrophobic/hydrophilic ratios are maintained. As a result they have found application in thermoregulated phase transfer catalysis. This approach is very important especially in biphasic hydroformylation of higher olefins due to their poor water-solubility as illustrated in Figure 1.11.

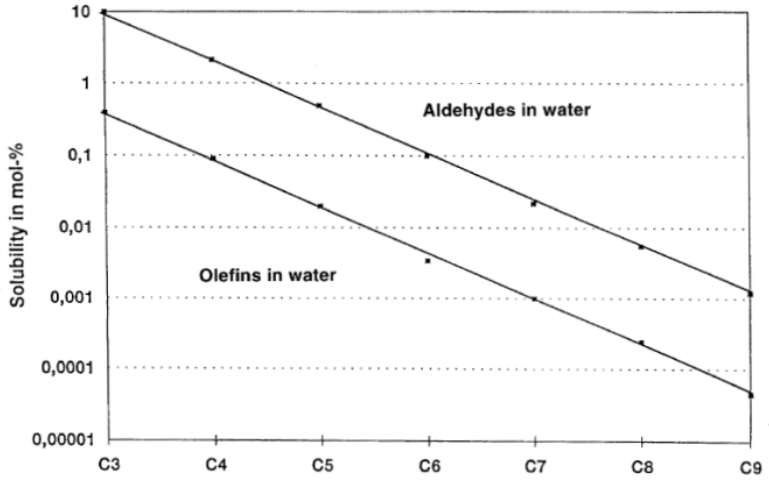

Figure 1.11 Dependence of the solubility in water on the number of carbon atoms in the olefins used and in resulting aldehydes.[67]

The decrease in the water-solubility with an increase with the number of C atoms in olefinic substrates and resulting aldehydes results in decrease in the reactivity of catalyst in aqueous medium. This is why extensive work has been done in the aqueous biphasic hydroformylation of shorter chain olefins. Other biphasic systems have therefore been explored to solve the problem of poor water-solubility of higher olefins and thermoregulated phase transfer catalysis has become an interesting alternative for biphasic hydroformylation of higher olefins.

Thermoregulated ligands exhibit an inverse temperature-dependant solubility in water and possess a distinct cloud point pertaining to typical non-ionic surfactants.[87] The cloud point is the temperature above which an aqueous solution of a water-soluble surfactant becomes turbid. This allows transition metal complexes to transfer to the organic phase to catalyse the reaction at a temperature higher than the cloud point (C_p). This two-phase process in which the catalyst is able to transfer between the aqueous and the organic phase is termed

thermoregulated phase transfer catalysis (TPTC). Since this technique ensures that the substrate and the catalyst stay in the same phase during the reaction (Figure 1.12), even extremely water immiscible substrates can get into contact with the water-soluble catalyst.[87]

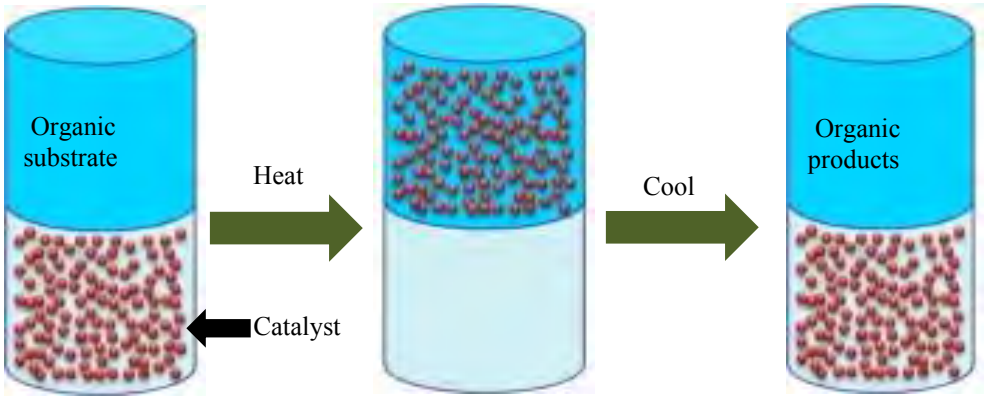

Figure 1.12 Thermoregulated phase transfer catalysis.[87]

The use of thermoregulated ligands in aqueous biphasic hydroformylation has been studied extensively over the past few years.[88] An investigation of catalyst recovery and separation in TPTC was done by Behr.[89] This is a very important step for an economically viable process which makes use of an expensive metal such as Rh. In this study, 1-dodecene was used as the substrate, with a Rh catalyst. After optimising the reaction conditions, the catalyst could be reused up to 30 times. In this study, the metal leaching was reduced by separating products from the catalyst at very low temperatures (-10 ^{o}C). High catalyst ratios also resulted in increased leaching of Rh into the product phase. This is the first systematic investigation into whether catalyst leaching can be controlled and which of these influencing factors are significant.[89] In TPTC, proper design of the ligands is vital to achieve the proper inverse temperature dependant water-solubility property. The synthesis (Scheme 1.4) of one such ligand poly(ethylene oxide)-substituted triphenylphosphines (PEO-TPP) has been described and its application in hydroformylation evaluated.[87]

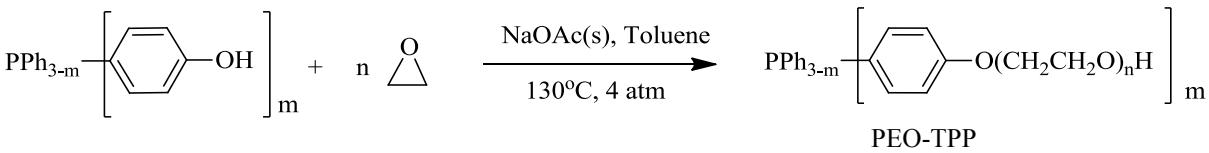

PEO-TPP

(n = 8–29) and m = 1 (**1.38**), m = 2 (**1.39**) and m = 3 (**1.40**)

Scheme 1.4 Synthesis of poly(ethylene oxide)-substituted triphenylphosphines (PEO-TPPs). [87]

The two-phase hydroformylation using the Rh/TPPTS catalyst previously employed in the Ruhrchemie/Rhône-Poulenc process was performed. This catalyst gave conversion of only 20 % in the aqueous biphasic hydroformylation of higher olefins.[90] When the reaction was performed *via* the TPTC system using Rh/PEO-TPP complexes, a satisfactory catalytic reactivity was observed.[87] At temperatures lower than C_p, PEO-TPP modified Rh catalyst remained in the aqueous phase because the partitioning of the catalyst between water and the solvent favours that the catalyst remains in water. On heating to temperatures higher than C_p, the catalyst transferred into the organic layer which is the reaction site. At the end of the reaction, after cooling to temperatures lower than C_p, the catalyst returned to the aqueous phase. In this work, the hydroformylation rates of 1-hexene and 1-decene were similar, indicating that the size of the terminal olefin did not affect the reactivity the system.[87]

The use of Rh nanoparticles stabilised by a thermoregulated ligand in the hydroformylation of 1-decene and 1-dodecene in water/1-butanol has also been reported.[91] The catalytic system converted all the substrates at temperatures above 60 ^{o}C. Recycling of the catalyst was done by simple phase separation. Another ligand, octylpolyglycol phenylene phosphite (OPGPP) **1.41** (Figure 1.13), was used in TPTC of styrene using $Rh(CO_2)(acac)$ as catalyst precursor.[29]

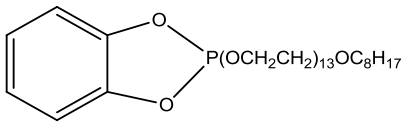

(1.41)

Figure 1.13 Thermoregulated octylpolyglycol phenylene phosphite (OPGPP) ligand.[29]

The ligand OPGPP has a cloud point of 56.5 ^{o}C. The active catalyst was generated *in situ* from OPGPP and $Rh(CO_2)(acac)$. This catalyst gave a styrene conversion of over 99%. It was observed that the conversion of styrene to products increased with increasing in P:Rh ratio. In this work the authors reported that the ratio of water: substrate has no effect on reactivity because of the inverse temperature-dependant solubility in water of the ligand.[29]

The synthesis and application of thermoregulated ligands **1.43**-**1.45** in biphasic hydroformylation of 1-decene has also been described.[92] Similar to other thermoregulated catalysed systems, the metal complexes are soluble in the aqueous phase at low temperature ($<C_p$) and can precipitate from water into the organic phase on heating to temperatures above the cloud point ($>C_p$). Synthesis of the ligands is described in Scheme 1.5.

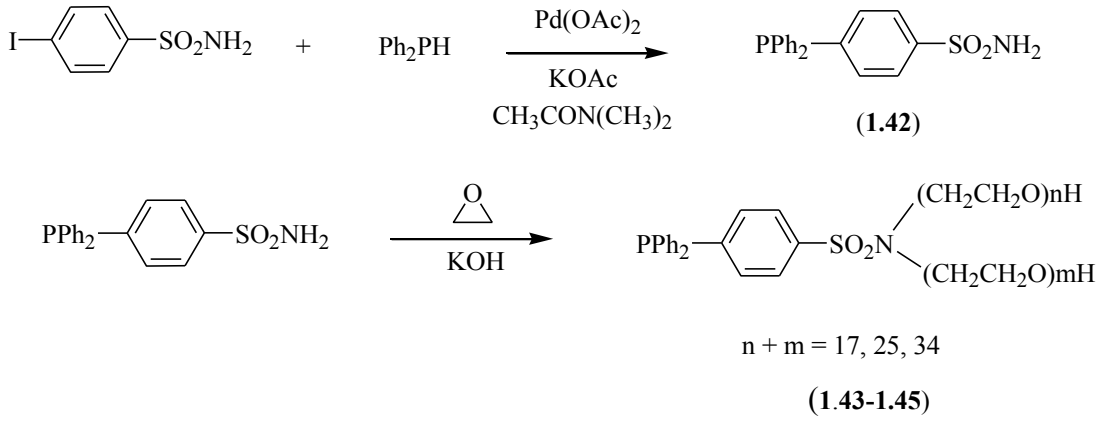

Scheme 1.5 Synthesis of thermoregulated ligands **1.43** – **1.45**.

The precursor **1.42** was prepared by Pd-catalysed P-C coupling between 4-I-$C_6H_4SO_2NH_2$ and Ph_2PH. The product of this coupling reaction was then ethoxylated with ethylene oxide to produce thermoregulated ligands (PEO-DPPSA) **1.43-1.45**. The ligands **1.43-1.45** have cloud points of 51 ^oC, 59 ^oC and 68 ^oC respectively. The aqueous-organic biphasic hydroformylation of 1-decene was carried out using Rh/PEO-DPPSA, which was prepared *in situ* from $RhCl_3.3H_2O$ and PEO-DPPSA (m + n = 25). Under the experimental conditions tested, it was observed that total aldehyde production increased with an increase in temperature, however the linear: branched aldehyde ratio decreases. The authors suggested that this is due to increased rate of isomerisation at elevated temperatures.[92]

Thermoregulated phase transfer biphasic catalysis has been shown to be effective for hydroformylation of olefins. Another biphasic catalytic system that has also been explored over the years is fluorous/organic catalysis. Most importantly, it has been successfully applied in hydroformylation of various olefins.

1.3.4 Fluorous/organic biphasic catalysis in hydroformylation of olefins

Horvâth and Râbai were the first to introduce the temperature-dependant miscibility of highly fluorinated solvents and organic solvents in fluorous biphasic catalysis.[93] The thermomorphic nature of ligands used in this application allows for fluorous solvents to be immiscible in organic solvents at low temperatures and miscible with them at higher temperatures.[41] Fluorous molecules are designed in order to mimic the reactivity of conventional organic molecules, yet to be soluble in fluorous solvents due to their high fluorine content. These fluorous molecules have two regions, a highly fluorinated group that controls the fluorous solubility of the molecule and an organic region that resemble a conventional organic

molecule. For example, phosphines have been used widely in organic and organometallic co-ordination.[41] An example of a fluorinated phosphine oxide and how it can be easily separated from reaction mixture is shown in Scheme 1.6.

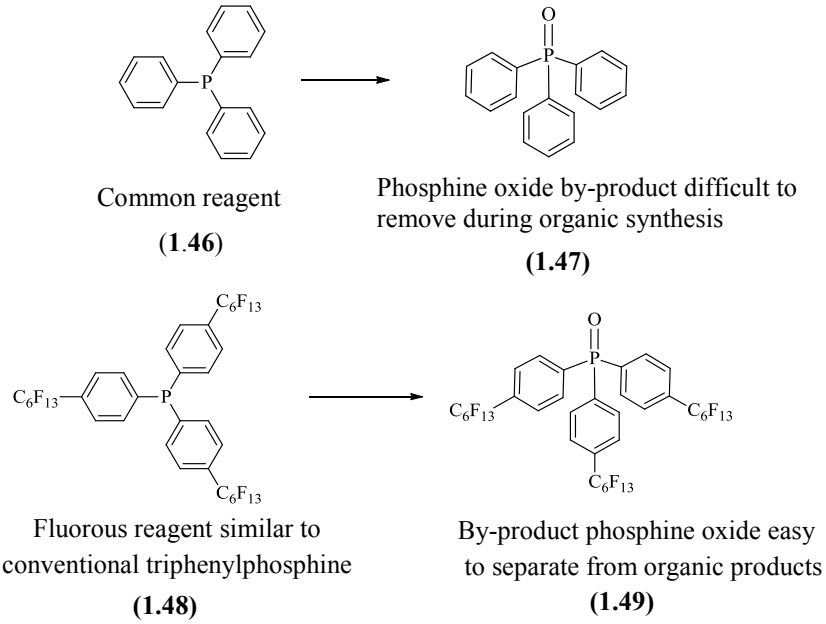

Scheme 1.6 Fluorous ligands synthesized for easy recovery for conventional organic solvents.

The fluorous triphenylphosphine was designed in such a way that it reacts in the same way as the organic triphenylphosphine. The highly electronegative fluorine atoms are far enough from the reaction centre (phosphorous atom), so that the aromatic rings act as effective 'spacer groups.' Phosphine oxides such as **1.49** are easily removed especially if they are unwanted reaction by-products. This example illustrates the advantage of using fluorous ligands especially because of ease of separation.[41]

In catalytic applications, a fluorous phase containing the fluorous catalyst is mixed with an organic phase containing the organic substrates. When this is heated up, a homogeneous system is formed, which allows the catalyst to come into contact with the organic phase (Figure 1.14). At the end of the reaction, the system is cooled down rendering two separate phases, the organic phase and the fluorous phase. The fluorous catalyst can then be recovered and be reused for a new catalytic cycle.[94] If the catalyst is designed to be selectively soluble in the fluorous phase; any product formed during the catalytic cycle that is organic can easily be separated by simple decantation. The major advantage of this system over aqueous biphasic catalysis is that one homogeneous mixture is formed under hydroformylation conditions.[95]

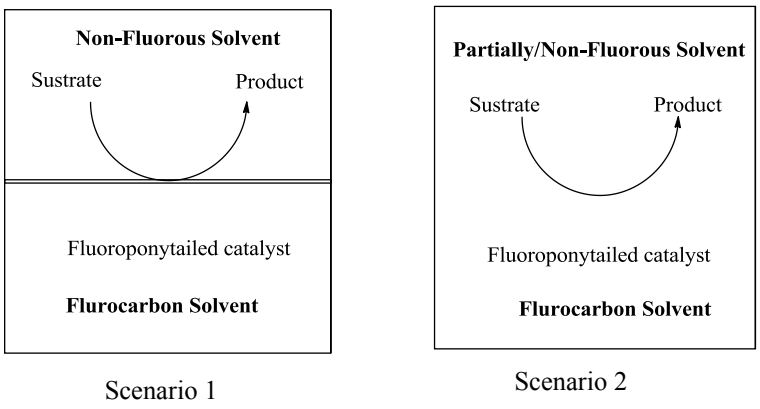

Figure 1.14 Two scenarios in fluorous biphasic catalysis.[96]

Fluorous systems can be applied in catalysis either at room temperature in the biphasic mode (Figure 1.14, scenario 1) or at elevated temperature (Figure 1.14, scenario 2) in a single phase.[93,96] The synthetic strategy for fluoroponytailed ligands and their subsequent fluorocarbon-soluble metal-ion complexes is that the CF_2 group α to the heteroatom that can potentially bind to the metal ion be two or three methylene spacer groups away.[96] Another strategy is to attach the ponytail to an aromatic ring so that this electron-withdrawing effect is not experienced.[97, 98]

One of the first organic transformations to be performed under fluorous biphasic conditions was hydroformylation.[95, 93] In the system explored by Horvâth, Rh complexes of fluorous trialkylphosphine $P(CH_2CH_2C_6F_{13})_3$ were used. This system demonstrated very good hydroformylation activity of 1-decene, with very good retentions in the fluorous phase. The catalyst could be recycled up to 9 times with only a 4.2% loss of Rh catalyst. The only problem encountered was the poor aldehyde chemoselectivity of the catalyst, as isomerisation competed effectively.[93] The same system was used in the hydroformylation of 1-nonene and 2-nonene and the catalyst displayed good selectivity and high reaction rates at low Rh catalyst loading. Leaching was limited to only 0.05%.[93, 94]

Cole-Hamilton and co-workers also described the hydroformylation of 1-octene for the production of nonanal under a fluorous system.[44] In this study, the fluorous solvent used was perfluoromethylcyclohexane and they found that the hydroformylation of 1-octene was more complicated than if one phase existed under the conditions tested. The phase behaviour of 1-octene was seen to be affected by temperature and ratio of 1-octene used.

The hydroformylation of various olefins such as 1-octene, 1-decene, 1-dodecene, 2-octene, 4-octene and cyclohexene using a fluorous solvent was also reported in the literature.[99] In this work they observed that reactivity of internal olefins was lower than that of terminal olefins. Isomerisation was found to be competitive and cyclic olefins were reported to be inactive substrates. The catalyst was easily recovered and reused and it maintained activity during the first 3 cycles. However, conversion dropped drastically in the fourth cycle due to Rh leaching into the organic phase. The fluorous ligands used for these tests are shown below (Figure 1.15).

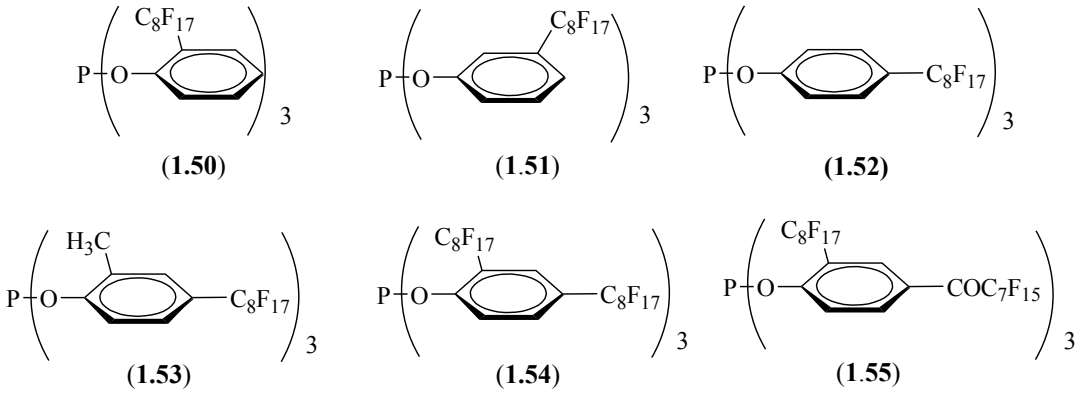

Figure 1.15 Phosphite ligands used in the fluorous biphasic hydroformylation of various olefins.

The catalytic systems formed by the different fluorous phosphite ligands **1.50-1.55** with $Rh(acac)(CO)_2$ were found to be very active with TOFs greater than 3000 hr^{-1}. However, the different systems exhibited different activities depending on the position and number of substituents on the aromatic ring. For example, the *para*-substituted phosphite **1.52** gave activity that was three times lower than what was observed when the bulky *ortho*-substituted phosphite **1.50** was used. The *meta*-substituted ligand **1.51** gave intermediate activity between **1.50** and **1.52**. Isomerisation was also observed in all systems. Catalysts formed using ligands **1.50**, **1.51** and **1.55** were tested for reusability and it was found that the catalysts could be recycled up to four times. Apart from the hydroformylation reaction, several transition metal catalysed organic transformations have been carried out either in aqueous biphasic systems or in neat water. More pertinent to our studies is the Suzuki-Miyaura cross-coupling reaction which is discussed in more detail in the following section.

1.4 The Suzuki-Miyaura cross-coupling reaction

The Suzuki-Miyaura cross-coupling reaction, also known as the Suzuki-Miyaura cross-coupling reaction involves the coupling of arylboronic acids to aryl halides in the presence of

a transition metal catalyst to form biphenyl products and was first published in 1979 by Akira Suzuki-Miyaura (Scheme 1.7).[100,101]

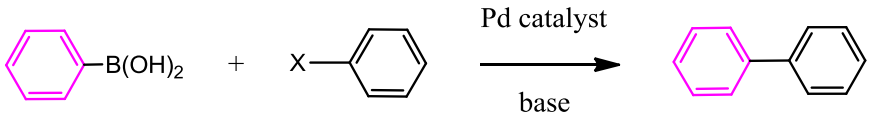

Scheme 1.7 The Suzuki-Miyaura cross-coupling reaction.

The reaction gives access to biphenyl products that are relevant to the pharmaceutical industry. The organoboron substrates are highly stable in cross-coupling reactions, have high selectivity, non-toxicity and have high tolerance towards various functional groups. This gives the Suzuki-Miyaura cross-coupling reaction a practical advantage over other cross-coupling reactions such as Kharash coupling, Negishi coupling, Stille coupling, Himaya coupling and Kumada coupling reactions.[102] Moreover, the Suzuki-Miyaura cross-coupling reaction employs milder reaction conditions and more readily available diverse boronic acids.[103] The reaction has been extensively studied and explored as a result. [100,102] The mechanism of the Suzuki-Miyaura cross-coupling reaction is shown in Scheme 1.8.

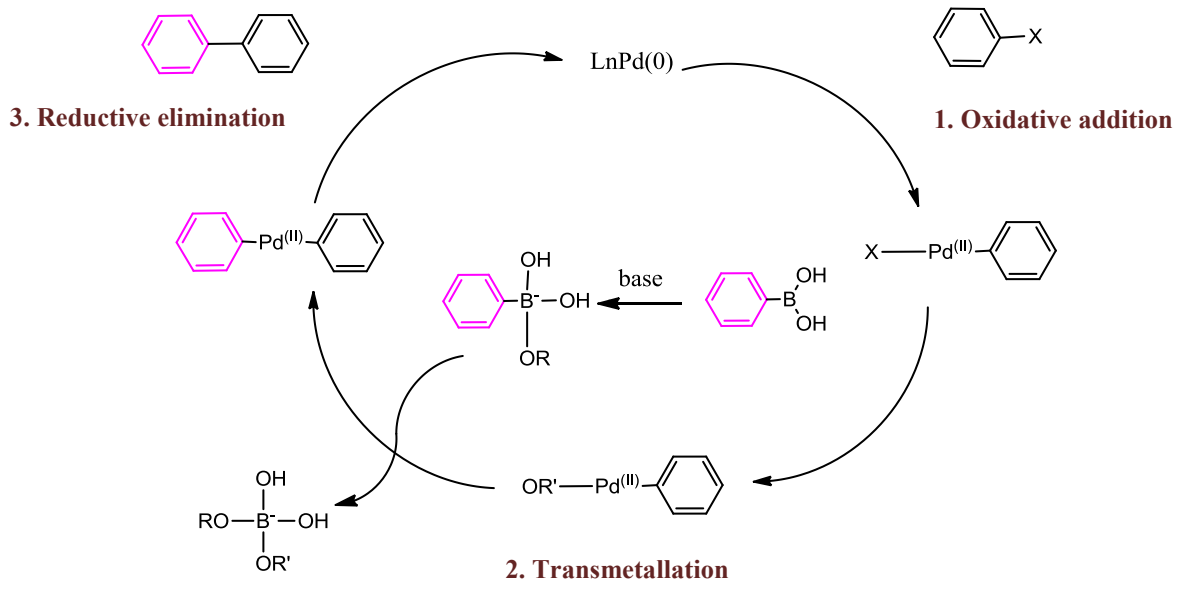

Scheme 1.8 Suzuki-Miyaura cross-coupling reaction mechanism.[104]

The reaction proceeds *via* a three-step mechanism which entails oxidative addition of a carbon electrophile to an unsaturated Pd(0) species to afford a Pd(II) species, followed by transmetallation in which the carbon electrophile is transferred from the boron to the Pd

centre and then finally reductive elimination.[105,106] The oxidative addition and the reductive elimination steps are very common steps in many transition metal-catalysed reactions.[107] However the transmetallation step and the role of the base in the Suzuki-Miyaura cross-coupling reaction have not been established.[108] Initially, Suzuki and co-workers suggested that the base substitutes the halide in the Pd complex before the transmetallation step.[100,101,109,110] Mechanistic experiments using electrospray mass spectrometry do not show the presence of an intermediate formed due to the replacement of the halide by the base.[111] In another study, Smith and co-workers proposed that the base binds the boronic acid to form a reactive species.[112] Later Matos proposed that the base either replaces the halide in the Pd complex or binds to the organoboron species depending on the affinity of the latter.[113]

As a result of the broad tolerance to different functional groups, the application of the Suzuki-Miyaura cross-coupling reaction has become very common in the pharmaceutical industry. The design of drug candidates using the Suzuki-Miyaura cross-coupling reaction has become very popular since the reaction has been found to be versatile, effective, functional group tolerant under mild reaction conditions.[114] Similar to the hydroformylation reaction, extensive research has also been carried out in the aqueous medium in an effort to make the reaction greener and since water is a useful alternative reaction medium. It also enables easy catalyst recovery from the organic products and hence makes catalyst recycling possible.

1.4.1 Sulfonated Pd complexes for Suzuki-Miyaura cross-coupling reactions in water

The first report on the Suzuki-Miyaura cross-coupling reaction in water was reported in 1990 by Casalnuovo.[115] In this work, a Pd(0) catalyst $Pd[(PPh_2(m\text{-}C_6H_5SO_3M)]_3$ (where M is Na) was utilised in the C-C bond formation reaction and was viable in aqueous medium. Since this pioneering work, extensive research has been done in this area. Zhou and co-workers have reported the application of water-soluble Pd complexes (Figure 1.16) and their use as catalysts for the Suzuki-Miyaura cross-coupling reaction.[116] In this work, a catalyst loading of 0.01 mol% was employed in either neat water or a water and ethanol solvent mixture. Most importantly was the easy catalyst recovery and recycling. The catalysts (**1.56**-**1.57**) could be used efficiently twice however very little product was obtained in the third cycle. Tetrabutylammonium bromide (TBAB) was used to accelerate the rate of coupling.

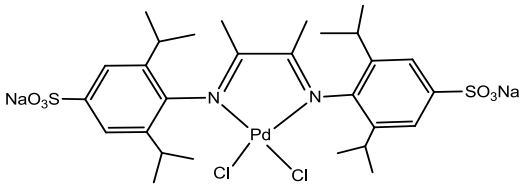

(**1.56**)

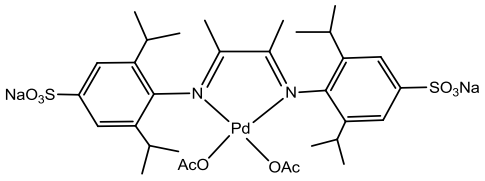

(**1.57**)

Figure 1.16 Diimine Pd catalysts for the Suzuki-Miyaura cross-coupling reaction.[116]

The use of phase transfer agents for catalytic processes has been reported to enhance product yields, improve purity, generation of small volumes of waste and ultimately improve the energy efficiency of these processes.[117] This is in line with some of the principles of Green Chemistry. In particular TBAB has been shown to be essential in a number of C-C bond forming reactions in water.[118–121] The addition of tetraalkylammonium salts also enhances the rate of transition-metal-catalysed reactions mainly palladium cross-coupling reactions. Water-soluble palladium complexes containing *N*-heterocyclic carbenes (Figure 1.17) were also utilised as catalysts for the Suzuki-Miyaura cross-coupling reaction in water under aerobic conditions.[122]

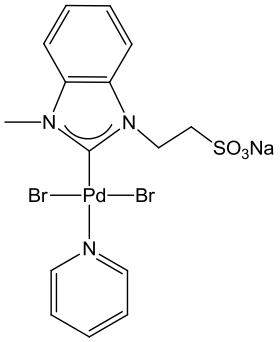

(1.58)

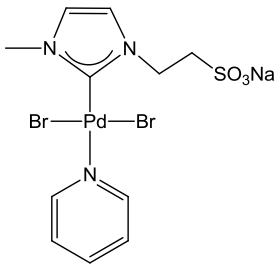

(1.59)

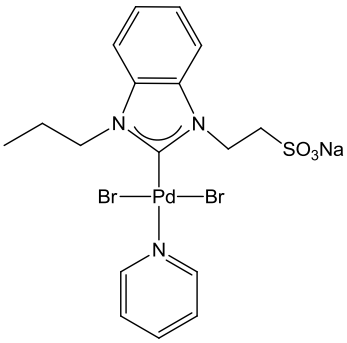

(1.60)

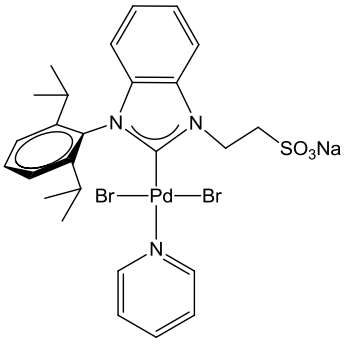

(**1.61**)

Figure 1.17 Sulfonate functionalized Pd-NHC complexes.[122]

These complexes were used at room temperature and complex **1.61** proved to be the most efficient. The catalyst could promote the coupling reactions of a wide range of substrates and could be recycled effectively 4 times. However, the active catalyst formed nanoparticles which are believed to be the active species. This was confirmed by experiments such as TEM experiments, kinetic studies and the mercury drop test.

The application of sulfonate functionalized Pd-NHC complexes in the Suzuki-Miyaura cross-coupling reaction in water has also been reported.[123] In this work the authors describe the synthesis of four complexes that adopt a monodentate, bis-chelating and pincer coordination form. These complexes display excellent water-solubility and display poor solubility in most organic solvents. The catalysts showed good activity in the Suzuki-Miyaura cross-coupling reactions of either bromobenzene or chlorobenzene with phenylboronic acid. The best catalyst gave good results in a water/isopropanol mixture. The recyclability of these catalysts was not tested in this work.

Hanhan also described the synthesis and characterization of binuclear Pd(II) complexes and their application as Suzuki-Miyaura cross-coupling reaction catalysts (Figure 1.18).[124] The mononuclear analogues with general structure similar to that of **1.62** were also synthesized and the authors observed that the binuclear nature of complex **1.63** improved the activity of the catalyst. Further to that, steric and electronic modification of the ligands had great influence of the performance of the catalysts.

The authors believed that the two metal sites behave as two isolated mononuclear catalysts and work independently of each other for **1.63**. This work proves that two metals are better than one with improved results being observed when the binuclear catalysts were employed. Upon completion of the reaction, the products were extracted and the catalyst-containing aqueous layer could be reused effectively up to 14 times. Moreover, the catalysts were shown to be homogeneous after performing the mercury drop test.

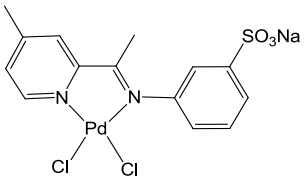

(1.62)

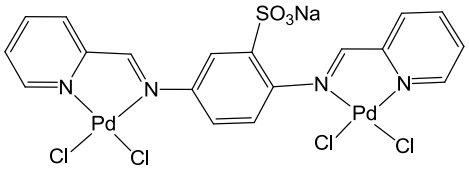

(1.63)

Figure 1.18 Water-soluble iminopyridyl Pd(II) complexes.

A water-soluble Pd(II) cationic 2,2-bipyridyl catalysts for the Suzuki-Miyaura cross-coupling reaction in water has been reported in the literature.[121] The catalyst proved to be stable in air and displayed good activity for activated and deactivated aryl bromides. The catalyst shows good recyclability with a slight decrease in activity each time the catalyst is recycled. The system gave satisfactory results with aryl chlorides, however elevated temperatures were required. Palladacycles are another interesting class of compounds that have been applied as catalysts in the Suzuki-Miyaura cross-coupling reaction.[125–127]

1.5 Homobimetallic complexes in catalysis

Bimetallic metal complexes have been found to be advantageous over their mononuclear analogues. The two metal centres in binuclear complexes can have varying oxidation states which can further stabilise these complexes.[128] The interaction between metal centres has also been observed to increase rates of transformations and improve the yields.[129] From a structural point of view, bimetallic catalysts may be classified into several types such as the single-framed bimetallic systems, separate bimetallic systems, bridged bimetallic systems and tethered bimetallic systems (Figure 1.19).[130] When catalytic sites are combined, co-operative reaction pathways may be induced, resulting in improved activity and/or selectivity. The metal separation in the bimetallic systems plays a crucial role and the optimal metal separation distance must be 3.5 - 6 Å.[131] Therefore, catalysts containing two metals within an approximate distance and arrangement can potentially lead to better reactivity.

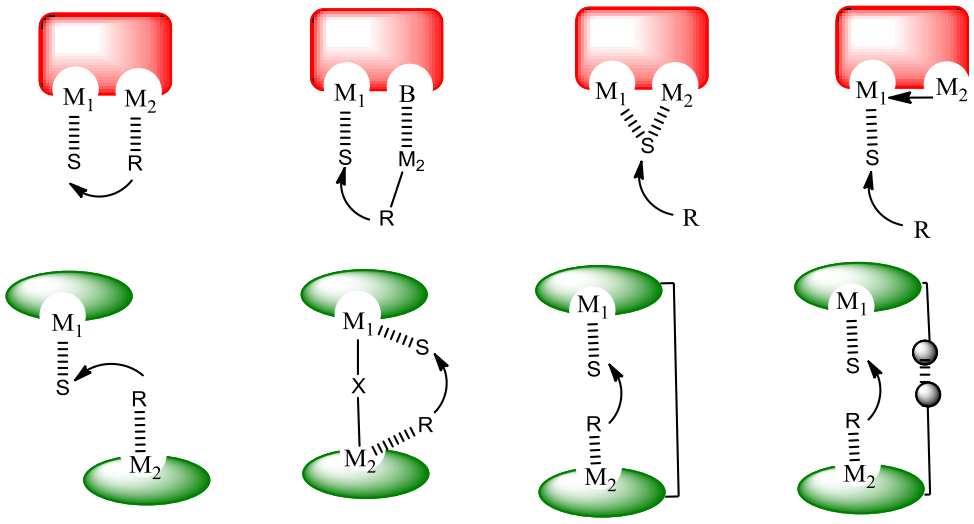

M_1 and M_2 are the metal centres

Figure 1.19 Schematic representation of bimetallic catalysts.[130]

The first type of bimetallic catalysts has the two metals in a single ligand and this is normally achieved through ionic coordination of multiple metals or ligands. [130] These catalysts contain two metal sites through direct complexation. Each metal is responsible for activating the electrophile or nucleophile during a catalytic cycle. In the other type of bimetallic systems, both metal centres simultaneously activate the one reactant whilst the other system has one metal centre activating the reactant and the other metal centre stabilising the reacting metal centre, through metal-metal redox cooperativity.[130] Various ligand types may be used as donor centres that can influence the particular type of bimetallic catalyst. The application of homobimetallic catalysts have been applied into many organic transformations[132–134] including the hydroformylation reaction and the Suzuki-Miyaura cross-coupling reactions and evidence of enhanced performance was seen for both reactions in the presence of a second metal.

1.5.1 Homobimetallic catalysts for the hydroformylation reaction

The synthesis and characterization of a water-soluble binuclear Rh complex and its application in hydroformylation has been reported.[135] The sulfonated complex was found to be active in the aqueous biphasic hydroformylation of a range of substrates, namely, cyclohexene, styrene, 1-hexene, 2,3-dimethyl-1-butene and allylbenzene. The complex displayed excellent stability and was reported to be resistant to sulphur poisoning.

The Rh-catalysed hydroformylation of natural olefins (terpene and allylbenzene) using binuclear Rh complexes has also been reported. In all reactions, moderate to high reactivity and aldehyde chemoselectivity was observed.[136] Due to the biphasic nature of the reaction, the catalyst could easily be recovered and could be recycled up to five times without any loss in activity or selectivity. Pardey also reported the application of a binuclear dithiolato-bridged Rh(I) complex for the hydroformylation of 1-hexene, cyclohexene, 2,3-dimethyl-1-butene and 2-methylpent-2-ene.[137] *In-situ* hydroformylation of the olefins present using this catalyst presented promising results for future industrial applications applicable to gasoline.

1.5.2 Homobimetallic catalysts for the Suzuki-Miyaura cross-coupling reaction

In 2013, Hanhan and co-workers described the synthesis and characterization of binuclear complexes for the Suzuki-Miyaura cross-coupling reaction in water.[124] The reaction rates for the binuclear complexes were better than those experienced with the mononuclear complexes.

The catalysts were highly water-soluble and could be easily recovered and recycled up to 10 times without loss in catalytic activity. In this work, the authors demonstrate that two metals are better than one for the Suzuki-Miyaura cross-coupling reaction.

Bera and co-workers also reported the synthesis, characterization and catalytic activity of dipalladium(I) complexes in the Suzuki-Miyaura cross-coupling reaction.[138] The best catalyst was found to be active with aryl boronic acids and aryl chlorides, and provided very high yields of biphenyl products in short reaction times. Cooperativity between the two metal centres was observed with the oxidative addition and reductive elimination occurring simultaneously on the dipalladium species.

Palladacycles have high thermal stability and contain 5-membered Pd containing rings.[139–141] Palladacycle intermediates are believed to be powerful tools for various biphenyl products *via* cross-coupling reactions. In 2000, Cheprakov reported that palladacycles are structurally robust catalysts,[142] but get disassembled during the activation stage (during a catalytic transformation) and usually release a phosphine (if present), making them very popular catalyst precursors. The use of this class of complexes has also been extended to catalysis in water for the Suzuki-Miyaura cross-coupling reaction. Shaughnessy reported the preparation and catalytic evaluation of a family of water-soluble palladacycles (Figure 1.20). [143]

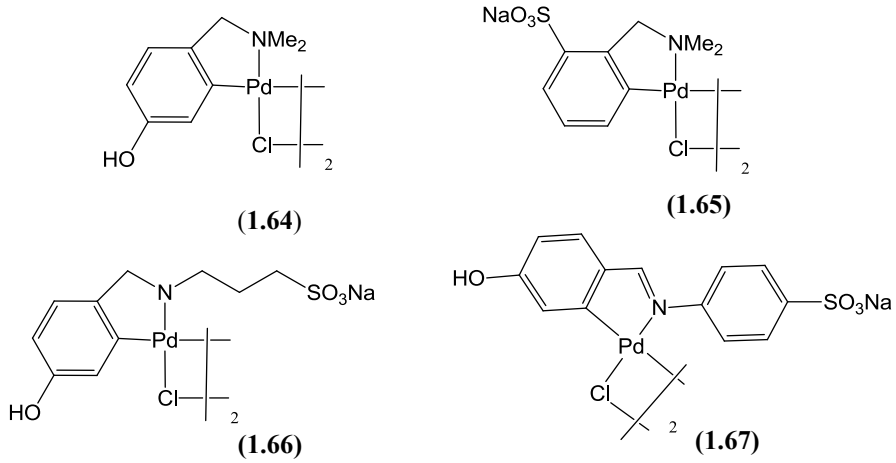

Figure 1.20 Water-soluble palladacycles.[143]

Catalysts **1.64** and **1.67** gave the best activity in the Suzuki-Miyaura cross-coupling reactions in neat water. The scope of the catalysts was explored using a range of electron deficient, neutral and electron rich aryl bromide substrates. Catalysts **1.64** and **1.67** gave moderate yields with 4-chlorobenzonitrile. Complex **1.64** gave high yields in the coupling reactions

involving deactivated aryl bromides with catalyst loadings as low as 0.02 mol%. The same catalyst **1.64** could be recycled up to 12 times and yields greater than 85% were obtained throughout the recycling experiments.[143]

The coupling of various aryl bromides with phenylboronic acid using water/DMF mixture has also been reported.[144] The catalyst loading was as low as 0.001 mol% and excellent yields of the biphenyl products were formed. The oxime-derived catalyst (Figure 1.21) was found to be thermally stable and not sensitive to air and water.

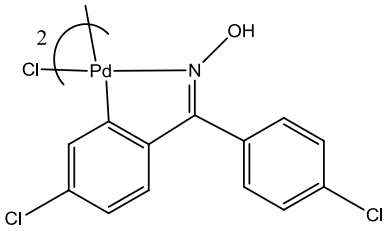

(1.68)

Figure 1.21 Thermally stable palladacycle for coupling of aryl chlorides.

In related work, synthesis of an air stable oxime-based palladacycle **1.69** (Scheme 1.9) which was tested in the Suzuki-Miyaura cross-coupling reaction of inactivated chlorides in neat water was reported in the literature.[118]

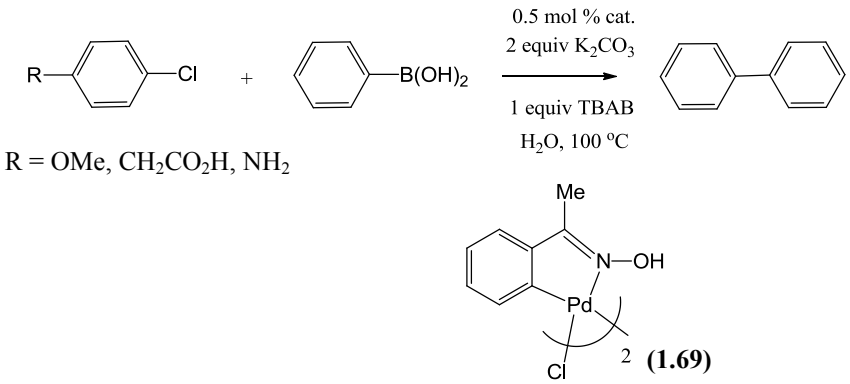

Scheme 1.9 Suzuki-Miyaura cross-coupling reaction catalysed by palladacycle **1.69**.[118]

It was observed that the catalysts produce biaryls products using a wide range of substrates in aqueous solution in varying yields. The catalyst could be recycled effectively 3 times and a significant drop in activity was observed in the fourth recycle. In 2005, Chen and co-workers also reported the synthesis and application of benzylic palladacycles (Scheme 1.10) for the Suzuki-Miyaura cross-coupling reaction in water, under aerobic conditions.[145] The catalyst

1.70 displayed high activity in the coupling of aryl bromides with phenylboronic acid with turnover numbers as high as 10^6. The catalysts was also active in the coupling of aryl chlorides with phenyl boronic acids, but however, TBAB was required for these reactions and the reaction times were extended. Catalyst recycling for this complex was not reported.

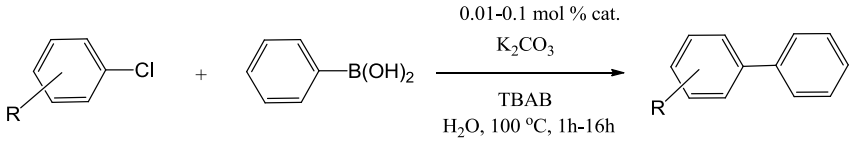

R = 4-MeCO, 4-NO_2, 2,4-$(NO_2)_2$, 4-OMe, H

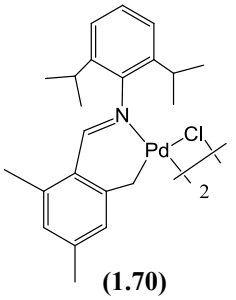

(1.70)

Scheme 1.10 Suzuki-Miyaura cross-coupling reaction catalysed by palladacycle **1.70**.[145]

The synthesis and application of a sulfonated palladacyclic complex in the Suzuki-Miyaura cross-coupling reaction has also been reported.[146] The system was very efficient in the coupling for the coupling of aryl bromides with moderate to good yields obtained. The substrate scope was extended to *ortho*-substituted aryl bromides to afford various biphenyls.

Mono- and binuclear cyclopalladated complexes have also been synthesized by Fairlamb and co-workers and these were tested as catalysts for the Suzuki-Miyaura cross-coupling reaction.[147] The activity of these catalysts was reported to be dependent on the type of ligand utilised. The presence of a phosphine ligand resulted in an improvement in the catalytic activity of the catalysts. Furthermore, the authors demonstrated the recyclability of these catalysts using polyethylene oxide and methanol solvent mixture. The polar phase could be recycled several times giving cross-coupled products in good yields (>95%).

1.6 Closing Remarks

The application of water as an alternative solvent in the area of catalysis has been on the increase over recent years in an effort to develop systems that are greener for the chemical industry. It has also been observed that most catalysts used for various organic transformations are based on metals that belong to the Platinum Group Metals, which are

relatively expensive and fast depleting. Therefore, it is of utmost importance to develop catalysts that are very active, with excellent selectivity for the desired products, used at low catalyst loading together with readily available and cheap solvents such as water. Moreover, incorporating two metals into a catalyst could result in cooperativity which could result in improved catalyst performance at low catalyst loading. This together with easy catalyst recovery and recyclability of these catalysts is motivation for some of the work reported in this thesis.

1.7 Aims and objectives of the thesis

The overall aims of this project were to synthesise and characterize water-soluble mononuclear and binuclear Rh(I) and Pd(II) complexes and to evaluate their activity as catalysts in the aqueous biphasic hydroformylation of 1-octene and the Suzuki-Miyaura cross-coupling reaction in aqueous medium respectively.

1.7.1 Specific aims and objectives

The specific objectives of this thesis were:

- To synthesise and characterize water-soluble monomeric and dimeric *N,O*-chelating salicylaldimine Schiff base ligands (Figure 1.22).

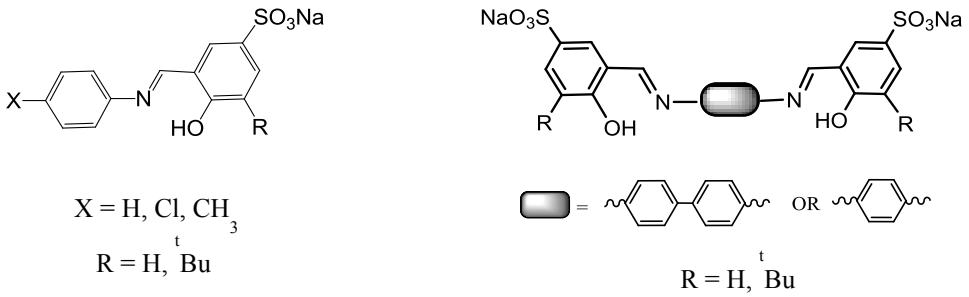

Figure 1.22 General structure of monomeric and dimeric *N,O*-chelating Schiff base ligands.

- Synthesis and characterization of a series of new water-soluble Rh(I) mono- and binuclear complexes (Figure 1.23).

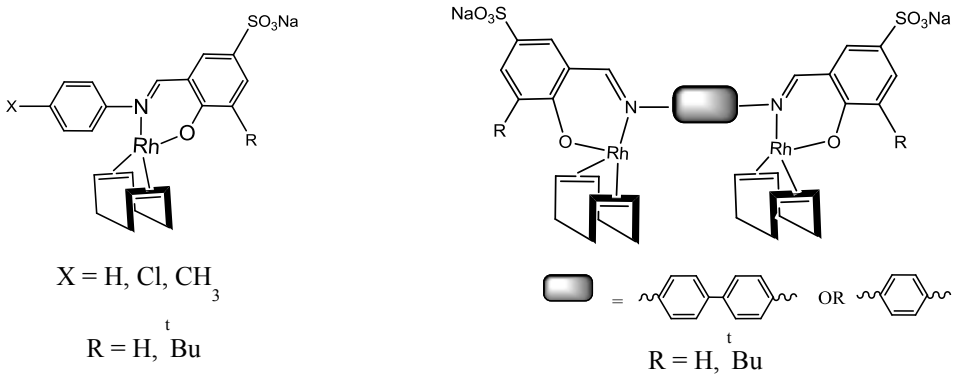

Figure 1.23 General structure of mononuclear and binuclear Rh(I)complexes.

- Application of the water-soluble mono- and binuclear Rh(I) complexes in the aqueous biphasic hydroformylation of 1-octene.
- Synthesis and characterization water-soluble monomeric and dimeric thiosemicarbazone ligands (Figure 1.24).

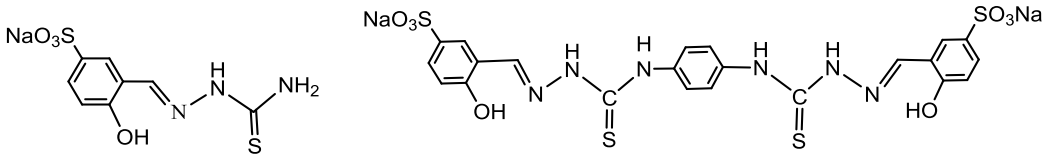

Figure 1.24 General structure of mono- and dithiosemicarbazone ligands.

- Synthesis and characterization water-soluble mononuclear and binuclear thiosemicarbazone Pd(II) complexes (Figure 1.25).

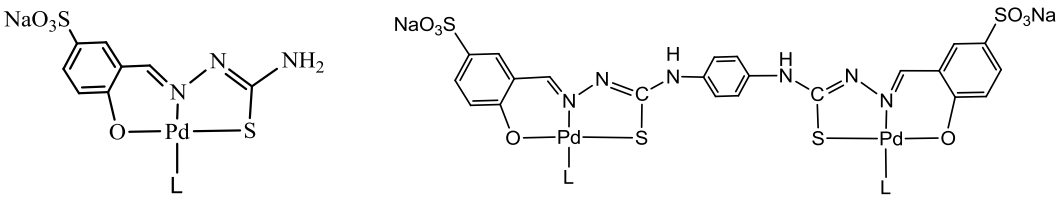

Figure 1.25 General structure of water-soluble mono- and dithiosemicarbazone complexes.

- Application of the water-soluble mono and binuclear Pd(II) thiosemicarbazone complexes in the aqueous phase Suzuki-Miyaura cross-coupling reaction.

- Perform density functional theory experiments (DFT) on the oxidative addition of iodobenzene to a thiosemicarbazone complex and whether it is feasible for a Pd(II)/Pd(IV) redox to be followed during oxidative addition.

1.8 References

1 C. A. Busacca, D. R. Fandrick, J. J. Song and C. H. Senanayake, *Adv. Synth. Catal.*, 2011, **353**, 1825–1864.

2 The Freedonia group, in *World catalysts, Industry study with forecasts for 2016 and 2021*, 2010, pp. 4 –36.

3 J. N. Armor, *Catal. Today*, 2011, **163**, 3–9.

4 R. A. Sheldon, *J. Chem. Tech. Biotechnol.*, 1997, **50**, 381–388.

5 A. Shamiri, M. Chakrabarti, S. Jahan, M. Hussain, W. Kaminsky, P. Aravind and W. Yehye, *Materials*, 2014, **7**, 5069–5108.

6 The Royal Swedish Academy of Sciences - press release, *Nobel Prize. Chem.*, 1973, 1–2.

7 The Royal Swedish Academy of Sciences - Press release, *Nobel Prize Chem.*, 2001, 1–6.

8 The Royal Swedish Academy of Sciences - Press release, *Nobel Prize Chem.*, 2005, 1–12.

9 J. E. Harvey and B. Halton, *Chem. New Zeal.*, 2011, 49-51.

10 R. Sheldon, I. Arends and U. Hanefeld, in *Green Chemistry and Catalysis*, Wiley-VCH Verlag GmbH & Co. KGaA, Weinheim, 2007, pp. 1–40.

11 E. A. Karakhanov and A. L. Maksimov, *Russ. J. Gen. Chem.*, 2009, **79**, 1370–1383.

12 R. A. Sheldon, *Green Chem.*, 2005, **7**, 267–278.

13 P. T. Anastas and J. C. Warner, in *Green Chemistry: Theory and Practice*, 1998 University Press: New York, 1998, pp. 30.

14 J. A. Widegren and R. G. Finke, *J. Mol. Catal. A Chem.*, 2003, **198**, 317–341.

15 W. Keim, *Green Chem.*, 2003, **5**, 105–111.

16 D. J. Adams, P. J. Dyson and S. Tavener, in *Chemistry In Alternative Reaction Media*, John Wiley and Sons Ltd, West Sussex, 2004, pp. 1–36.

17 E. B. Hager, B. C. E. Makhubela and G. S. Smith, *Dalton Trans.*, 2012, **41**, 13927–13935.

18 L. Obrecht, P. C. J. Kamer and W. Laan, *Catal. Sci. Technol.*, 2013, **3**, 541–551.

19 K. H. Shaughnessy, *Chem. Rev.*, 2009, **109**, 643–710.

20 T. Borrmann, H. W. Roesky and U. Ritter, *J. Mol. Catal. A Chem.*, 2000, **153**, 31–48.

21 J. Boulanger, H. Bricout, S. Tilloy, A. Fihri, C. Len, F. Hapiot and E. Monflier, *Catal. Commun.*, 2012, **29**, 77–81.

22 C. J. Cobley and P. G. Pringle, *Catal. Sci. Technol.*, 2011, **1**, 239–242.

23 A. A. Dabbawala, H. C. Bajaj, H. Bricout and E. Monflier, *Appl. Catal. A Gen.*, 2012, **413-414**, 273–279.

24 A. A. Dabbawala, H. C. Bajaj, H. Bricout and E. Monflier, *Catal. Sci. Technol.*, 2012, **2**, 2273–2278.

25 Q. Peng, Y. Yang, C. Wang, X. Liao and Y. Y. Ã, *Catal. Letters*, 2003, **88**, 219–225.

26 Y. Brunsch and A. Behr, *Angew. Chem. Int. Ed. Engl.*, 2013, **52**, 1586–1589.

27 L. Bai, L. Zhang, J. Pan, J. Zhu, Z. Cheng and X. Zhu, *Macromolecules*, 2013, **46**, 2060–2066.

28 A. Behr, Y. Brunsch and A. Lux, *Tetrahedron Lett.*, 2012, **53**, 2680–2683.

29 R. Chen, X. Liu and Z. Jin, *J. Organomet. Chem.*, 1998, **571**, 201–204.

30 N. Liu, C. Liu, B. Yan and Z. Jin, *Appl. Organomet. Chem.*, 2011, **25**, 168–172.

31 S. Liu, C. Xie, S. Yu, F. Liu and Z. Song, *Ind. Eng. Chem. Res.*, 2011, **50**, 2478–2481.

32 D. Wu, Y. Wang, G. Li, J. Jiang and Z. Jin, *Catal. Commun.*, 2014, **44**, 54–56.

33 L. P. Barthel-Rosa, J. A. Gladysz, O. Chemie, F. Alexander and D. Erlangen, *Coord. Chem. Rev.*, 1999, **190-192**, 587–605.

34 M. S. Yu, D. P. Curran and T. Nagashima, *Org. Lett.*, 2005, **7**, 3677–3680.

35 D. J. Adams, D. J. Cole-Hamilton, E. G. Hope, P. J. Pogorzelec and A. M. Stuart, *J. Organomet. Chem.*, 2004, **689**, 1413–1417.

36 T. Mathivet, E. Monflier, Y. Castanet, A. Mortreux and J.-L. Couturier, *Tetrahedron*, 2002, **58**, 3877–3888.

37 R. A. Cook, J. E. Bond and P. A. Stevens, *J. Am. Chem. Soc.*, 1998, **120**, 3133–3143.

38 T. Mathivet, É. Monflier, Y. Castanet, A. Mortreux and J. Couturier, *Comptes Rendus Chim.*, 2002, **5**, 417–424.

39 W. Chen, L. Xu and J. Xiao, *Chem. Commun.*, 2000, 839–840.

40 D. P. Curran, S. Hadida, S. Kim and Z. Luo, *J. Am. Chem. Soc.*, 1999, **121**, 6607–6615.

41 A. P. Dobbs and M. R. Kimberley, *J. Fluor. Chem.*, 2002, **118**, 3–17.

42 R. H. Fish, *Chem. Eur. J.*, 1999, **94720**, 1677–1680.

43 D. F. Foster, D. J. Adams, D. Gudmunsen, A. M. Stuart, E. G. Hope and D. J. Cole-Hamilton, *Chem. Commun.*, 2002, 722–723.

44 Y. Huang, E. Perperi, G. Manos and D. J. Cole-Hamilton, *J. Mol. Catal. A Chem.*, 2004, **210**, 17–21.

45 R. J. Cornmell, C. L. Winder, S. Schuler, R. Goodacre and G. Stephens, *Green Chem.*, 2008, **10**, 685–691.

46 C. M. Gordon, *Catal. React. Kinet. Inorg. React. Mech.*, 2001, **222**, 101–117.

47 P. G. Jessop, *Green Chem.*, 2011, **13**, 1391–1398.

48 W. A. Herrmann, C. W. Kohlpaintner, H. Bahrmann and W. Konkol, *J. Mol. Catal.*, 1992, **73**, 191–201.

49 W. A. Herrmann and W. R. Thiel, *Chem. Ber.*, 1990, **123**, 1953–1961.

50 R. T. Smith, R. K. Ungar, L. J. Sanderson and M. C. Baird, *Organometallics*, 1983, **2**, 1138–1144.

51 F. Joó, P. Csiba and A. Bényei, *J. Chem. Soc. Chem. Commun.*, 1993, 1602–1604.

52 F. B. S. Tilloy, E. Monflier, *New J. Chem*, 1997, 529–531.

53 F. W. B. Einstein and E. Kiehlmann, *Can. J. Chem.*, 1985, **63**, 2176–2180.

54 G. Brink, I. W. C. E. Arends, G. Papadogianakis and R. A. Sheldon, *Chem. Commun.*, 1998, vol. 195, pp. 2359–2360.

55 O. Roelen, *US Pat.*, 1982, 4.356.333.1982.

56 B. Mohr, D. M. Lynn and R. H. Grubbs, *Organometallics*, 1996, **15**, 4317–4325.

57 H. Nowothnick, A. Rost, T. Hamerla, R. Schomäcker, C. Müller and D. Vogt, *Catal. Sci. Technol.*, 2013, **3**, 600–605.

58 S. K. Sharma and R. V. Jasra, *Catal. Today*, 2015, **247**, 70-81.

59 A. K. S. N. Bizzari, M. Blagoev, *CEH Mark. Rep.*, 2006, 682.7000.

60 R. L. Pruett and J. A. Smith, *J. Org. Chem.*, 1969, **34**, 327–330.

61 J. D. Unruh and J. R. Christenson, *J. Mol. Cat.*, 1982, **14**, 19–34.

62 S. Bhaduri and D. Mukeshi, in *Homogeneous Catalysis: Mechanisms and Industrial applications*, John Wiley and Sons Ltd, New York, 2000, vol. 8, pp. 55–105.

63 L. C. Matsinha, P. Malatji, A. T. Hutton, G. A. Venter, S. F. Mapolie and G. S. Smith, *Eur. J. Inorg. Chem.*, 2013, 4318–4328.

64 G. T. Whiteker and C. J. Cobley, *Top Organomet. Chem.*, 2012, 35–46.

65 B. Cornils, *Org. Process Res. Dev.*, 1998, **1**, 121–127.

66 E. G. Kuntz, *Chemtech*, 1987, **17**, 570–575.

67 B. Cornils, in *Modern Solvent Systems in Industrial Homogeneous Catalysis*, Hoechst AG, Frankfurt, 1999, vol. 206, pp. 133–149.

68 E. A. Karakhanov and A. L. Maksimov, *Russ. J. Gen. Chem.*, 2009, **79**, 1370–1383.

69 A. Andriollo, A. Bolívar, F. A. López and D. E. Páez, *Inorg. Chim. Acta*, 1995, **238**, 187–192.

70 L. Obrecht, P. C. J. Kamer and W. Laan, *Catal. Sci. Technol.*, 2013, **3**, 541–551.

71 E. G. Kuntz, *FR Pat. 2.349.562.1976*, 1976.

72 J. F. Jenck, *French Pat. 2.478.078*, 1980.

73 C. Deng, G. Ou, J. She and Y. Yuan, *J. Mol. Catal. A Chem.*, 2007, **270**, 76–82.

74 T. Hamerla, A. Rost, Y. Kasaka and R. Schomäcker, *ChemCatChem.*, 2013, **5**, 1854–1862.

75 E. M. M. Del Valle, *Process Biochem.*, 2004, **39**, 1033–1046.

76 T. Loftsson and M. E. Brewster, *J. Pharm. Sci.*, 1996, **85**, 1017–1025.

77 F. Hapiot, H. Bricout, S. Tilloy and E. Monflier, *Eur. J. Inorg. Chem.*, 2012, 1571–1578.

78 M. T. Reetz, *Top. Catal.*, 1997, **4**, 187–200.

79 B. Sueur, L. Leclercq, M. Sauthier, Y. Castanet, A. Mortreux, H. Bricout, S. Tilloy and E. Monflier, *Chem. A Eur. J.*, 2005, **11**, 6228–6236.

80 S. Tilloy, C. Binkowski-Machut, S. Menuel, H. Bricout and E. Monflier, *Molecules*, 2012, **17**, 13062–13072.

81 D. N. Tran, F. Legrand, S. Menuel, H. Bricout, S. Tilloy and E. Monflier, *Chem. Commun.*, 2012, **48**, 753–755.

82 F. Hapiot, A. Ponchel, S. Tilloy and E. Monflier, *Comptes Rendus Chim.*, 2011, **14**, 149–166.

83 G. Fremy, R. Grzybek, E. Monflier, A. Mortreux, A. M. Trzeciak and J. Ziolkowski, *J. Organomet. Chem.*, 1995, **505**, 11–16.

84 T. Mathivet, C. Méliet, Y. Castanet, A. Mortreux, L. Caron, S. Tilloy and E. Monflier, *J. Mol. Catal. A Chem.*, 2001, **176**, 105–116.

85 E. Monflier, H. Bricout, F. Hapiot, S. Tilloy, A. Aghmiz and A. M. Masdeu-Bultó, *Adv. Synth. Catal.*, 2004, **346**, 425–431.

86 T. Borrmann, H. W. Roesky and U. Ritter, *J. Mol. Catal. A Chem.*, 2000, **153**, 31–48.

87 X. Zheng, J. Jiang, X. Liu and Z. Jin, *Catal. Today*, 1998, **44**, 175–182.

88 N. Liu, C. Liu, B. Yan and Z. Jin, *Appl. Organomet. Chem.*, 2011, **25**, 168–172.

89 Y. Brunsch and A. Behr, *Angew. Chemie Int. Ed.*, 2013, **52**, 1586–1589.

90 B. Cornils, A. G. Ruhrchemie and H. Bahrmann, *Pat. 3420491*, 1985.

91 K. Li, Y. Wang, J. Jiang and Z. Jin, *Chinese J. Catal.*, 2010, **31**, 1191–1194.

92 C. Liu, J. Jiang, Y. Wang, F. Cheng and Z. Jin, *J. Mol. Catal. A Chem.*, 2003, **198**, 23–27.

93 I. T. Horvâth and J. Râbai, *Science,* 1994, **266**, 1994, 72–75.

94 W. Zhang, *Tetrahedron*, 2003, **59**, 4475–4489.

95 I. T. Horváth, G. Kiss, R. A. Cook, J. E. Bond, P. A. Stevens, J. Rábai and E. J. Mozeleski, *J. Am. Chem. Soc.*, 1998, **120**, 3133–3143.

96 R. H. Fish, *Chem. Eur. J.*, 1999, **5**, 1677–1680.

97 G. Pozzi, F. Montanari and S. Quici, *Chem. Commun.*, 1997, 69–70.

98 G. Pozzi, F. Cinato, F. Montanari and S. Quici, *Chem. Commun.*, 1998, 877–878.

99 T. Mathivet, É. Monflier, Y. Castanet, A. Mortreux and J.-L. Couturier, *Comptes Rendus Chim.*, 2002, **5**, 417–424.

100 A. Suzuki, *J. Organomet. Chem.*, 1999, **576**, 147–168.

101 N. Miyaura and A. Suzuki, *Chem. Rev.*, 1995, **95**, 2457–2483.

102 A. J. J. Lennox and G. C. Lloyd-Jones, *Chem. Soc. Rev.*, 2014, **43**, 412–443.

103 S. Kotha, K. Lahiri and D. Kashinath, *Tetrahedron*, 2002, **58**, 9633–9695.

104 J. So, K. Olech, Ś. Agnieszka, D. Zaj and J. Cabaj, *J. Chem. Educ.*, 2013, **3**, 19–32.

105 M. Sumimoto, N. Iwane, T. Takahama and S. Sakaki, *J. Am. Chem. Soc.*, 2004, **126**, 10457–10471.

106 L. J. Goossen, D. Koley, H. L. Hermann and W. Thiel, *Organometallics*, 2006, **25**, 54–67.

107 A. A. C. Braga, N. H. Morgon, G. Ujaque and F. Maseras, *J. Am. Chem. Soc.*, 2005, **127**, 9298–9307.

108 H. Kurosawa and Guinot V., in *Fundamentals in molecular catalysis*, Elsevier, Amsterdam, 2003, pp. 1–522.

109 A. Suzuki, *J. Organomet. Chem.*, 2002, **653**, 83–90.

110 N. Miyaura, *J. Organomet. Chem.*, 2002, **653**, 54–57.

111 A. O. Aliprantis and J. W. Canary, *J. Am. Chem. Soc.*, 1994, **116**, 6985–6986.

112 G. B. Smith, G. C. Dezeny, D. L. Hughes, A. O. King and T. R. Verhoeven, *J. Org. Chem.*, 1994, **59**, 8151–8156.

113 K. Matos and J. A. Soderquist, *J. Org. Chem.*, 1998, **63**, 461–470.

114 N. Yasuda, *J. Organomet. Chem.*, 2002, **253**, 279–287.

115 A. L. Casalnuovo and J. C. Calabrese, *J. Am. Chem. Soc.*, 1990, **112**, 4324–4330.

116 J. Zhou, X. Guo, C. Tu, X. Li and H. Sun, *J. Organomet. Chem.*, 2009, **694**, 697–702.

117 M. Makosza, *Pure Appl. Chem.*, 2000, **72**, 1399–1403.

118 L. Botella and C. Nájera, *Angew. Chem. Int. Ed.,* 2002, **41**, 179–181.

119 C. Baleizao, A. Corma, H. Garcia and A. Leyva, *ChemInform*, 2003, **34**, 606–607.

120 L. Bai, J. Wang and Y. Zhang, *Green Chem.*, 2003, **5**, 615–617.

121 W. Wu, S. Chen and F. Tsai, *Tetrahedron Lett.*, 2006, **47**, 9267–9270.

122 R. Zhong, A. Pöthig, Y. Feng, K. Riener, W. A. Herrmann and F. E. Kühn, *Green Chem.*, 2014, **16**, 4955–4962.

123 F. Godoy, C. Segarra, M. Poyatos and E. Peris, *Organometallics*, 2011, **30**, 684–688.

124 M. E. Hanhan, C. Cetinkaya and M. P. Shaver, *Appl. Organomet. Chem.*, 2013, **27**, 570–577.

125 D. Zim, A. S. Gruber, G. Ebeling, J. Dupont and A. L. Monteiro, *Org. Lett.*, 2000, **2**, 2881–2884.

126 D. Zim, S. M. Nobre and A. L. Monteiro, *J. Mol. Catal. A Chem.*, 2008, **287**, 16–23.

127 V. Farina, *Adv. Synth. Catal.*, 2004, **346**, 1553–1582.

128 B. Xia, H. Zhang, C. Che, K. Leung, D. L. Phillips, N. Zhu and Z Zhou, *J. Am. Chem. Soc.*, 2003, **125**, 10362–10374.

129 N. Guo, L. Li and T. J. Marks, *J. Am. Chem. Soc.*, 2004, **126**, 6542–6543.

130 J. Park and S. Hong, *Chem. Soc. Rev.*, 2012, **41**, 6931–6943.

131 B. L. Feringa, M. I. Chemistry, N. Occurring, D. Active, S. D. Catalysts, D. P. Catalysts, D. R. Catalysts, H. Systems and T. C. Systems, *Tetrahedron*, 1998, **54**, 12985–13011.

132 H. Pellissier, *Tetrahedron*, 2013, **69**, 7171–7210.

133 M. G. Timerbulatova, M. R. D. Gatus, K. Q. Vuong, M. Bhadbhade, G. Algarra, S. A. Macgregor and B. A. Messerle, *Organometallics*, 2013, **32**, 5071-5081.

134 F. Heshmatpour, R. Abazari and S. Balalaie, *Tetrahedron*, 2012, **68**, 3001–3011.

135 S. W. S. Choy, M. J. Page, M. Bhadbhade and B. A. Messerle, *Organometallics*, 2013, **32**, 4726–4729.

136 P. J. Baricelli, L. G. Melean, M. Rosales, R. Mariandry, M. dos Santos and E. Escalante, *J. Chem. Chem. Eng*, 2013, **7**, 299–305.

137 A. J. Pardey, J. D. Suarez, M. C. Ortega, C. Longo, J. J. Perez-Torrente and L. A. Oro, *Open Catal. J.*, 2010, **3**, 44–49.

138 R. K. Das, B. Saha, S. M. W. Rahaman and J. K. Bera, *Chem. A Eur. J.*, 2010, **16**, 14459–14468.

139 I. P. Beletskaya and A. V. Cheprakov, *J. Organomet. Chem.*, 2004, **689**, 4055–4082.

140 T. Mahamo, F. Zheng, A. Sivaramakrishna, J. R. Moss and G. Smith, *J. Organomet. Chem.*, 2008, **693**, 103–108.

141 V. Farina, *Adv. Synth. Catal.*, 2004, **346**, 1553–1582.

142 I. P. Beletskaya and A. V. Cheprakov, *Chem. Rev.*, 2000, **100**, 3009–3066.

143 R. Huang and K. H. Shaughnessy, *Organometallics*, 2006, **25**, 4105–4112.

144 D. A. Alonso, C. Nájera and M. C. Pacheco, *Org. Lett.*, 2002, **67**, 5588–5594.

145 C. Chen, Y. Liu, S. Peng and S. Liu, *Tetrahedron Lett.*, 2005, **46**, 521–523.

146 L. Hong and W. Yangjie, *Appl. Organomet. Chem.*, 2008, **22**, 233–236.

147 I. J. S. Fairlamb, A. R. Kapdi, A. F. Lee, G. Sánchez, G. López, J. L. Serrano', L. Garcia, J. Pérez and E. Pérez, *Dalton Trans.*, 2004, 3970-3981.

Chapter 2

Synthesis and characterization of water-soluble mono- and binuclear salicylaldimine Rh(I) complexes

The following chapter forms part of the following publication:

Recyclable and recoverable water-soluble sulfonated Rh(I) complexes for 1-octene hydroformylation in aqueous biphasic media.
Leah C. Matsinha, Selwyn F. Mapolie and Gregory S. Smith, *Dalton Transactions,* 2015, **44**, 1240-1248.

2.1 Introduction

Most organometallic complexes used for catalytic applications display poor water-solubility. However extensive research has been done towards the synthesis of water-soluble complexes for various transition-metal catalysed organic transformations in aqueous media.[1–16] The design of ligands with suitable hydrophilic functionalities which constrain the catalytically active metal species in the aqueous phase has been used as a strategy to achieve highly water-soluble complexes.[17] The most common approach is to attach a hydrophilic substituent onto a known hydrophobic ligand. One of the most common ionic substituents is the sulfonate moiety.[17–19]

Schiff base ligands are a well-known class of ligands which are synthesized *via* simple condensation reactions between an amine and an aldehyde or ketone. Schiff base ligands are easy to prepare, have wide structural variety and subtle steric and electronic control.[20] As a result, many metal complexes based on Schiff bases have been synthesized and used for a wide range of applications including catalysis and biological evaluation.[17–19,21–26]

Incorporating a sulfonate group on existing Schiff base ligands can give access to highly water-soluble ligands that can consequently be used in the synthesis of water-soluble transition metal complexes.[7,18,27] The synthetic approach of such complexes usually begins with the sulfonation of either the aldehyde/ketone or the amine, then followed by a Schiff base condensation reaction which results in the formation of a water-soluble imine ligand.[18]

Previously, we reported the synthesis of a water-soluble mononuclear salicylaldimine Ru-arene complex and its application in aqueous biphasic hydroformylation of 1-octene.[22] This catalyst displayed poor selectivity for aldehydes (21%), however 77% of these aldehydes was nonanal which indicates that the catalyst has good regioselectivity for the linear aldehyde. The recyclability of the catalyst was not very efficient as it could only be used 3 times. As an extension of this work, instead of using Ru, Hager and co-workers synthesized a series of water-soluble mononuclear salicylaldimine Rh(I) complexes and their dendritic analogues.[18] The catalytic activity of the mononuclear complexes was superior to that of the Ru(II) complex reported in the previous work. The chemoselectivity and regioselectivity of the mononuclear catalysts was also better than the results obtained for the Ru(II) complex. The metallodendimers were prepared *in situ* and their hydroformylation activity was lower than that of the mononuclear complexes.

As a result of the good chemoselectivity and activity of the sulfonated Rh(I) salicylaldimine complexes, the synthesis and characterization of a series of mononuclear and binuclear water-soluble salicylaldimine Rh(I) complexes is discussed in this chapter. Various electron-withdrawing and electron-donating groups were incorporated to further expand the investigation on the catalytic performance, recovery and recyclability of these water-soluble Rh(I) salicylaldimine complexes in aqueous biphasic hydroformylation of 1-octene.

2.2 Synthesis and characterization of water-soluble *N,O*-chelating Schiff base ligands

2.2.1 Synthesis and characterization of sulfonated monosodium 5- sulfanato salicylaldehydes

The preparation of all the ligands was done using sulfonated monosodium salicylaldehydes **2.1** and **2.2.**[18,28] The synthesis of these aldehydes involved a 3-step synthesis (Scheme 2.1). Step 1 involved the protection of either salicylaldehyde or 3-*tert*-butyl-2-hydroxybenzaldehyde using aniline. The products were obtained as either a yellow crystalline solid or an orange oil. The ^{1}H NMR spectra of both imine containing compounds obtained from the reactions show a signal at 8.61 ppm and 8.58 ppm, respectively, which is evidence for the formation of the imine functionality. The infrared spectra also confirm the presence of the imine bond due to the appearance of an intense absorption band at either 1612 cm^{-1} (R = H) or 1619 cm^{-1} (R = ^{t}Bu).

The second step involved heating the imine product in concentrated sulfuric acid to afford a beige solid. Acid catalysed imine hydrolysis of this solid was the last step to afford the desired sulfonated aldehyde **2.1** and **2.2**. In the case of **2.2**, the sulfonated salicylaldimine was difficult to crystallise from concentrated sulfuric acid at room temperature, so the black oil was cooled to 0 ^{o}C to aid precipitation.

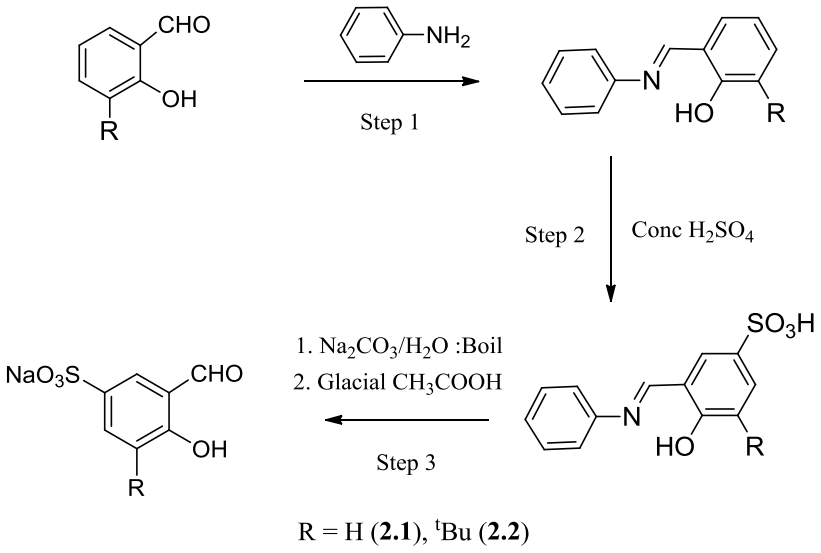

Scheme 2.1. Synthesis of monosodium 5-sulfanatosalicyldehydes.

Both products **2.1** and **2.2** display excellent water-solubility at room temperature. The two aldehydes were characterized using ^{1}H NMR, ^{13}C{^{1}H} NMR and infrared spectroscopy, mass spectrometry and elemental analysis.

In the ^{1}H NMR spectrum of **2.1**, the aldehyde proton is observed at 9.87 ppm. The proton *ortho* to the aldehyde functionality is the most deshielded aromatic proton and is observed as a singlet at 8.03 ppm. Two doublets with coupling constants of 9.26 Hz and 7.42 Hz respectively are observed for the other two aromatic protons. The spectrum for **2.2** is very similar to that of **2.1** except that at 1.35 ppm a singlet for the tertiary butyl substituent, integrating for 9 protons is observed. This is similar to what has been previously reported for these compounds.[18]

The infrared spectra for both compounds show the OH absorption band in the range 3200 – 3600 cm^{-1}. The mass spectra of both aldehydes were recorded in the negative ion-mode and the molecular ion peak for each compound was observed at either m/z = 201.2104 or m/z = 257.5691 for **2.1** and **2.2** respectively. After confirming the identity of the sulfonated

aldehydes, these were used as reactants for Schiff base condensation reactions with various amines to yield a series of water-soluble *N,O*-chelating ligands.

2.2.2 Synthesis and characterization of monomeric *N,O*-chelating Schiff base ligands

The monomeric sulfonated imine ligands were prepared by stirring the appropriate sulfonated aldehyde with an equimolar amount of the amine at room temperature for 16 hours (Scheme 2.2). Ligand **2.3** precipitated from the solution. Ligands **2.4-2.5** were isolated after the solvent was removed from the reaction mixture. Ligand **2.6** was obtained as a sticky oil that was difficult to isolate. As a result, the synthesis of the corresponding complex from **2.6** was performed in a one-pot synthetic step and is discussed later in the chapter. All the ligands display good water-solubility in the range 0.35 – 8.00 mg/mL at room temperature.

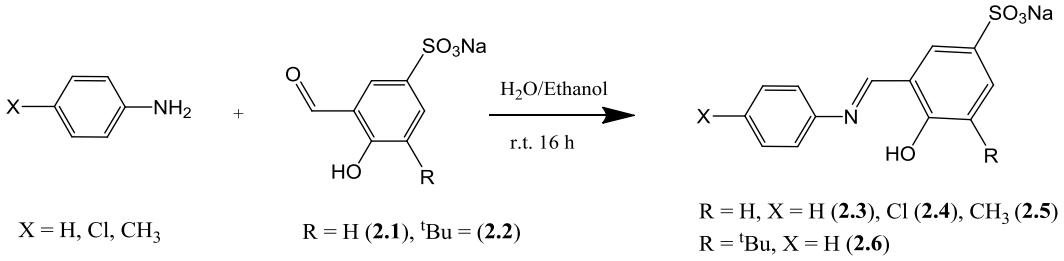

Scheme 2.2 Synthesis of water-soluble monomeric sulfonated Schiff base ligands **2.3**-**2.6**.

In the ^{1}H NMR spectra of the ligands (**2.3**-**2.6**), the imine proton appears as a singlet in the range 8.55 ppm - 8.95 ppm. The aromatic protons for ligand **2.4** are observed in the region between 6.50 ppm and 8.00 ppm. The proton *ortho* to the imine appears as the most deshielded aromatic proton due to the electron withdrawing effects of the sulfonate group. The proton adjacent to the OH and the proton *para* to the imine appear as doublets with coupling constants of 7.35 Hz and 8.30 Hz respectively. A multiplet integrating for four protons is observed between 7.49 ppm and 7.39 ppm for the protons on the *4-chloro* substituted aromatic ring. The ^{1}H NMR spectra for the other monomeric ligands (**2.3**-**2.6**) display similar trends and confirm the suggested structures. The ^{13}C{^{1}H} NMR spectrum of the ligands showed the expected number of carbon signals.

The absorption band for the imine functionality is also observed in the infrared spectra of the ligands and appears as an intense band between 1615 cm^{-1} and 1621 cm^{-1}. The ESI-MS spectra show peaks for [M]$^{-}$ in the negative ion-mode at m/z = 366.0580 and 290.3182 for

2.4 and **2.5** respectively, where M is the molecular anion. The results from the elemental analyses of the ligands (**2.3**-**2.5)** agree with the proposed structures.

2.2.3 Synthesis and characterization of dimeric *N,O*-chelating Schiff base ligands

The dimeric ligands were prepared by dissolving either *p*-phenylenediamine or benzidine in ethanol followed by the addition of two equivalents of the appropriate sulfonated aldehyde (Scheme 2.3). This was either refluxed or stirred at room temperature to afford the products as solids. Ligand **2.7** was collected as an orange brown solid after washing with dichloromethane and has a water-solubility of 0.2 mg /mL at room temperature. Ligand **2.8** was collected as a yellow-brown solid and displays good solubility in methanol and water (0.07 mg/mL). Compound **2.9** was isolated as a bright yellow powder. The ligand is insoluble in dichloromethane, ethanol, acetonitrile and toluene. The compound displays partial solubility in methanol and a water-solubility of 0.1 mg/mL. Ligand **2.10** was also isolated as a bright yellow solid that is soluble in water (1.7 mg/mL) and methanol.

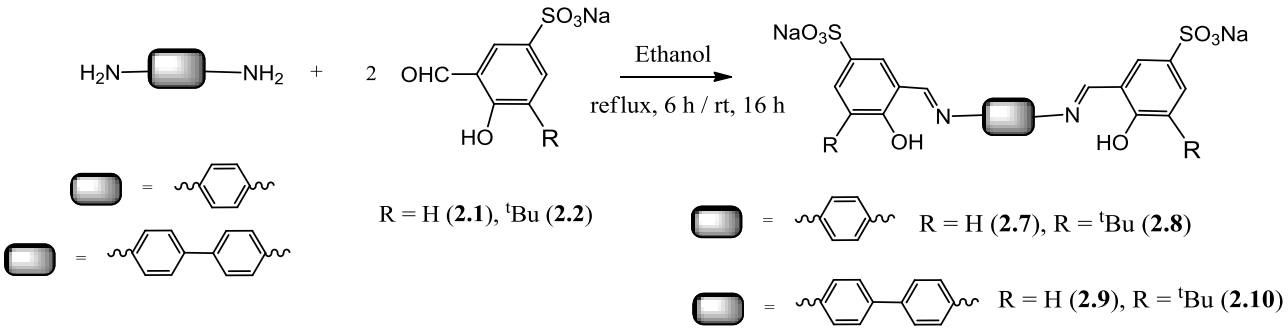

Scheme 2.3 Synthesis of water-soluble dimeric sulfonated Schiff base ligands **2.7 - 2.10**.

The ^{1}H NMR spectra of the ligands confirmed the successful synthesis of the compounds. The spectra are very similar, all displaying peaks for the imine protons and each integrating for two protons. The ^{1}H NMR spectrum of ligand **2.7** is shown in Figure 2.1. The phenolic proton is observed as a singlet downfield in the region between 13 ppm and 13.5 ppm.

The signal for the imine protons H-5 is observed at 9.06 ppm and integrates for 2 protons confirming the dimeric nature of the ligand. A singlet H-6 is also observed at 7.54 ppm for the 4 protons of the bridging phenylene spacer, further confirming the symmetric structure. This has been observed for similar symmetrical compounds that have been reported in the literature.[21] Two doublets are observed for protons at positions H-2 and H-3 as shown in

Figure 2.3, with coupling constants of 8.4 Hz and 8.5 Hz respectively. For **2.10** the ^{1}H NMR spectrum shows a singlet at 9.11 ppm for the two imine protons. Two multiplets are seen at 7.83 ppm and 7.61 ppm for the 8 aromatic protons and the spectrum also confirms the symmetric nature of this ligand.

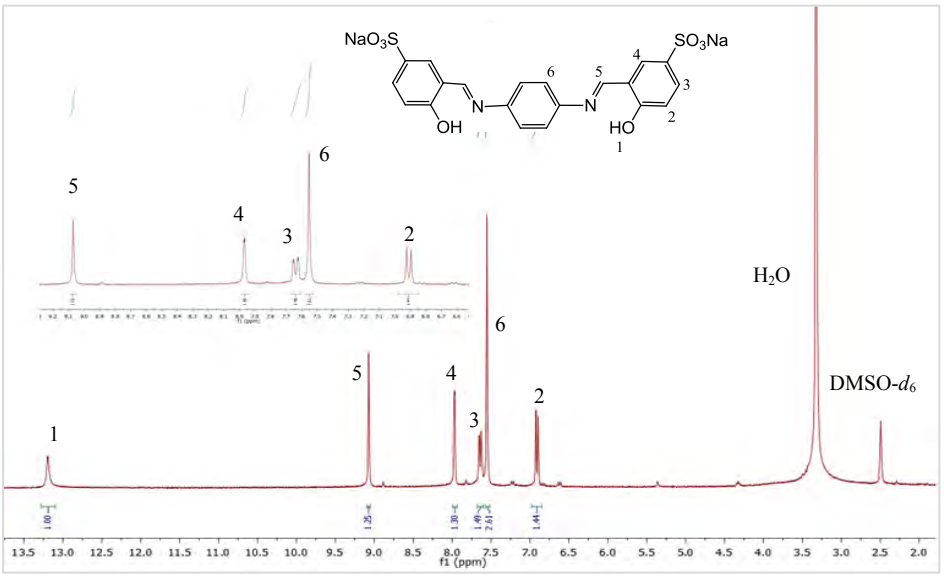

Figure 2.1 ^{1}H NMR spectrum for sulfonated dimeric ligand **2.7** in DMSO-d_6 at 30 ˚C.

The infrared spectra of the dimeric ligands show intense absorption bands at 1615 cm^{-1} (**2.7**), 1621 (**2.9**) and 1617 cm^{-1} (**2.10**) for the imine functionalities in the ligands. The electrospray ionisation mass spectra were recorded in the negative ion-mode for all ligands and Figure 2.2 shows the spectrum of ligand **2.10**.

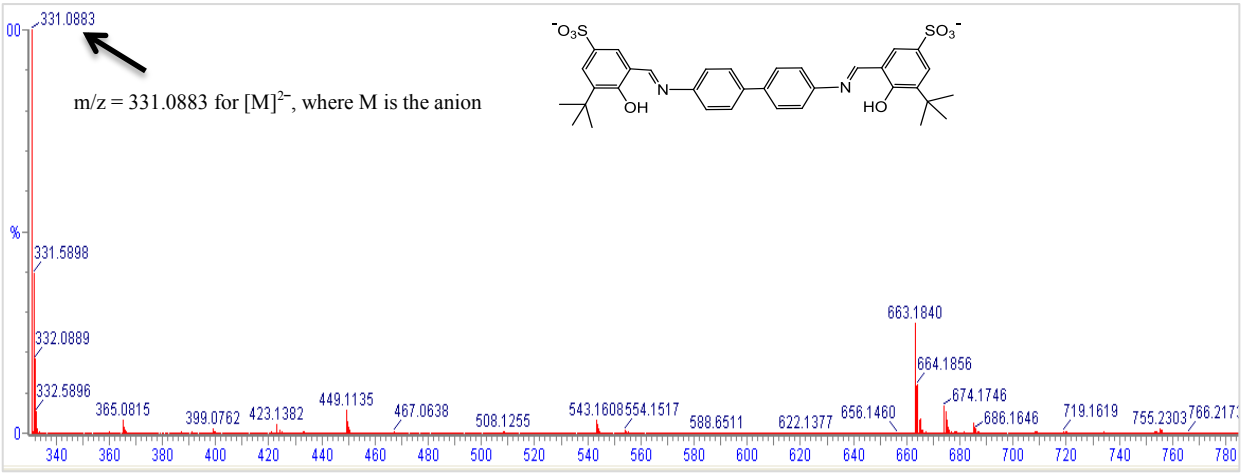

Figure 2.2 Electrospray ionisation mass spectrum for ligand **2.10** recorded in the negative ion-mode.

The molecular ion peak for ligand **2.10** was observed at m/z = 331.0883 for $[M]^{2-}$ (Figure 2.2). The molecular ion peaks for **2.7** and **2.9** were observed at either m/z = 237.2240 or 275.2751 for ligands **2.7** and **2.9** respectively. In all cases M is the molecular anion.

2.3 Synthesis and characterization of water-soluble mononuclear *N,O*-Rh(I) complexes

Sulfonated salicylaldimine ligands (**2.3-2.5**) were dissolved or suspended in a minimum amount of water and/or ethanol. Deprotonation of the phenolic proton was performed using an equimolar amount of 1M KOH. The metal precursor $[Rh(COD)Cl]_2$[29] was suspended in ethanol or methanol and this was added to the ligand and stirred at room temperature (Scheme 2.4). Synthesis of complex **2.14** (R = ^{t}Bu and X =H) was performed in a one-pot synthetic process because the ligand was difficult to isolate. All the complexes (**2.11-2.14)** were recovered as bright yellow solids that are stable at room temperature and display good water-solubility at room temperature (4 mg/mL – 5 mg/mL) and are insoluble in hexane and diethyl ether.

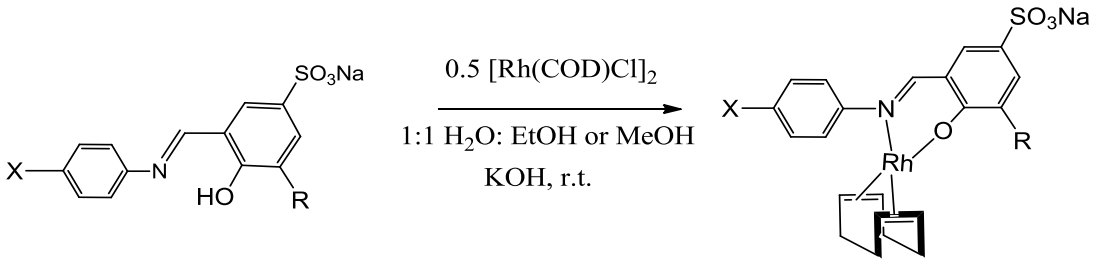

R = H, X = H (**2.3**), Cl (**2.4**), CH_3 (**2.5**)
R = ^{t}Bu, X = H (**2.6**)

R = H and X = H (**2.11**), Cl (**2.12**), CH_3 (**2.13**),
R = ^{t}Bu, X = H (**2.14**)

Scheme 2.4 Synthesis of water-soluble mononuclear Rh(I) complexes **2.11**–**2.14**.

The ^{1}H NMR spectra of the mononuclear complexes (**2.11-2.14**) show a signal for the imine proton between 7.36 ppm and 8.45 ppm. The imine signal of complex **2.14** is observed at 8.13 ppm as a singlet. The ^{1}H NMR spectrum for complex **2.12** is shown in Figure 2.3 as a representative example. The protons on the cyclooctadiene moiety are observed at 4.75 ppm, 2.36 ppm and 1.83 ppm and each signal integrates for 4 protons which is in agreement with the proposed structure. Protons H-8 and H-9 are observed as two separate multiplets due to the diastereotopic nature of these methylene protons. This is similar for previously reported results for analogous compounds in the literature.[18,30,31] The aromatic protons are observed in

the region between 7.80 ppm and 6.78 ppm. Two sets of doublets are observed at 7.35 ppm and 7.04 ppm for protons H-5 and H-6 and both have a coupling constant of 8.7 Hz as a result of these protons coupling to each other.

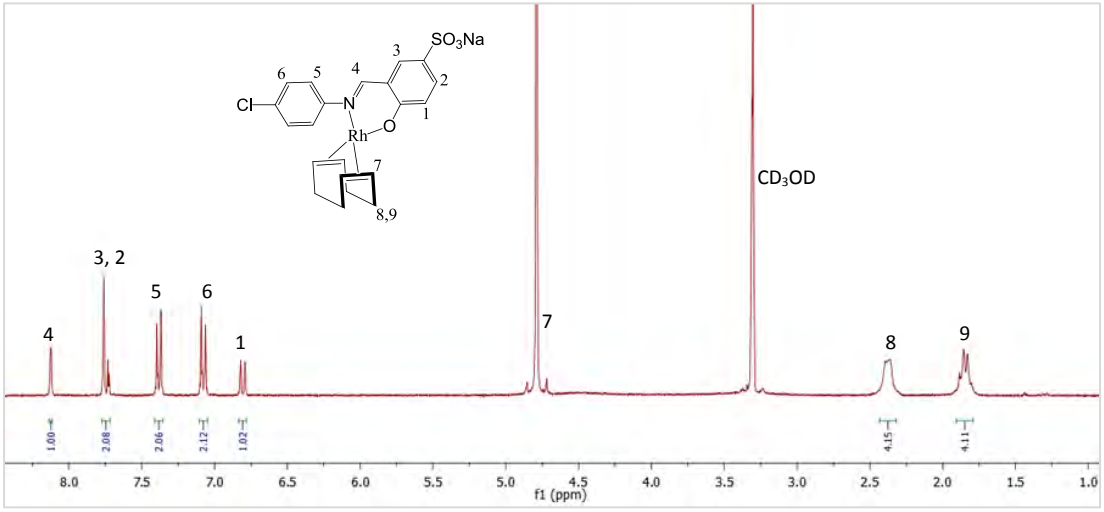

Figure 2.3. ^{1}H NMR spectrum of complex **2.12** in CD_3OD at 30˚C.

In the $^{13}C\{^{1}H\}$ NMR spectra of the complexes (**2.11-2.14**), a downfield shift of the imine carbon signal is observed upon complexation, which is further evidence for coordination of the imine nitrogen to the Rh metal centre. The number of signals observed in the spectra agrees with the number of carbon atoms in the compounds.

The infrared spectra of the complexes (**2.11-2.14**) show an imine absorption band at lower wavenumbers (1604 cm^{-1} - 1602 cm^{-1}) compared to that observed in the free ligands (1617 cm^{-1} - 1621 cm^{-1}) (Table 2.1). This phenomenon is shown in the stacked infrared spectra for ligand **2.3** and complex **2.11** shown in Figure 2.4. This shift to lower wavenumbers is due to the synergic effect. This could be as a result of the lone pair of electrons of the imine nitrogen being donated to the empty orbitals of the metal. This, together with back-donation from the metal *d*-orbitals into the empty π-anti bonding orbitals of the ligand, results in weakening of the imine bonds and consequently this lowers the imine stretching frequency.

Table 2.1 Imine infrared absorptions bands (cm^{-1}) and imine ^{1}H NMR chemical shifts (ppm) for (ligands) and complexes.

Compound	^{1}H NMR Imine (ppm)	IR Imine (cm^{-1})
2.11	(8.40) 7.36	(1621) 1603
2.12	(8.94) 8.21	(1617) 1604
2.13	(8.99) 8.31	(1619) 1604
2.14	(-) 8.13	(-) 1602

(-) Ligand was not isolated and all results for the ligands are shown in brackets.

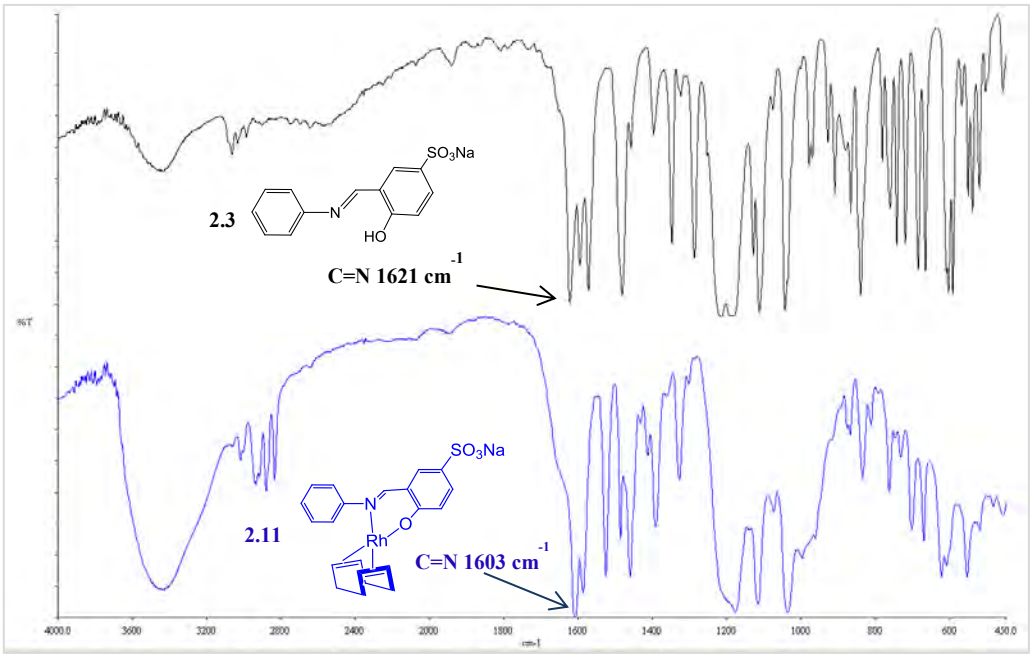

Figure 2.4. Stacked infrared spectra for ligand **2.3** and complex **2.11** showing the shift of the imine vibration.

Complex **2.14** was also characterized using single-crystal X-ray diffraction. The crystals were obtained by slow diffusion of diethyl ether into a concentrated solution of **2.14** dissolved in acetonitrile. The ball and stick representation of complex **2.14** is shown in Figure 2.5.

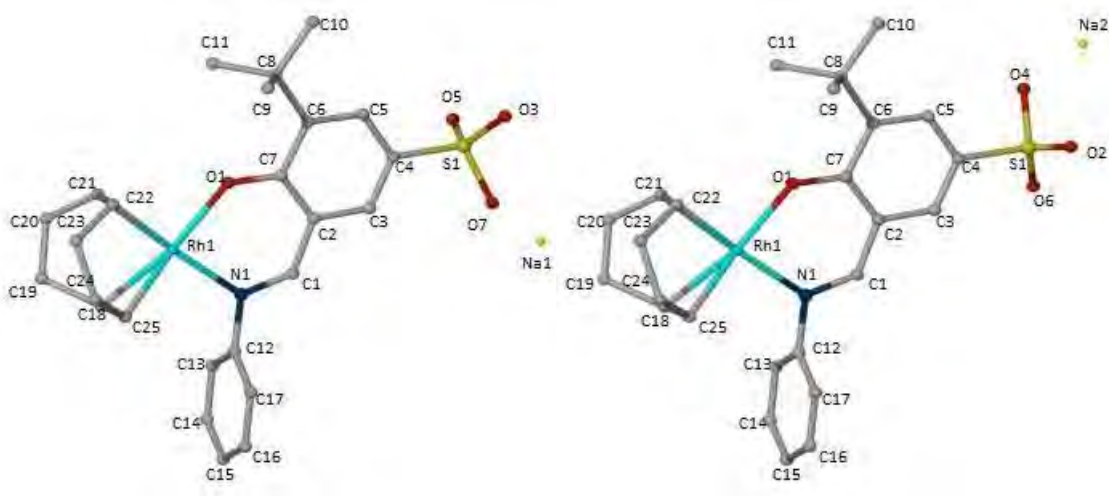

Figure 2.5 Ball and stick representation of **2.14** determined by single crystal X-ray diffraction. The hydrogen atoms have been omitted in the structures for clarity; (i) and (ii) show the different orientations of the sulfonate moiety.

Diethyl ether and acetonitrile solvent molecules co-crystallized with the complex during crystal formation and these have been omitted in Figure 2.7 for clarity. The molecular structure of complex **2.14** shows a square planar geometry around the Rh metal, with the *N,O*-chelating ligand and the cycloodiene moiety coordinated to the Rh metal centre. The bond angles around the Rh metal centre are between 81° and 96°. This is similar to what has been reported for similar compounds in the literature.[32] The oxygen atoms on the sulfonate group (O2 - O7) and the sodium atoms (Na1 and Na2) are disordered over two positions (i) and (ii) and these were refined with 50% site occupancy factors. A slightly distorted tetrahedral geometry is observed around the sulfur atom with bond angles between 105˚ and 120˚. From the data obtained, O7-S1 and O4-S1 are the longest bonds around the sulfur atom and hence represents the S-O single bonds of the sulfonate moiety. Selected crystallographic data, bond angles and bond distances are summarised in Tables 2.2 and 2.3.

The electrospray ionisation mass spectra of the water-soluble anionic complexes were recorded in the negative ion-mode and show peaks at m/z = 520.8143, 500.9313 and 542.4602 for $[M]^-$ for **2.12**, **2.13** and **2.14** respectively were M is the anion.

Table 2.2. Crystallographic data selected for the molecular structure of **2.14**.

	2.14· ½ CHCN· ½ Et_2O
Chemical formula	$C_{28}\,H_{35.50}\,N_{1.50}\,NaO_{4.50}\,RhS$
Formula weight	623.04
Crystal system	Monoclinic
Space group	*C2/c*
Crystal colour and shape	Red block
Crystal size (mm)	0.18 x 0.12 x 0.08
a/Å	31.483(3)
b/Å	20.1500(17)
c/Å	0.3174(8)
α (◦)	90.00
β (◦)	90.00
γ (◦)	90.00
V/Å ^{3}	6286.4(9)
Z	8
T/K	173(2)
D_c/g cm^{-3}	1.317
μ/mm^{-1}	0.656
Unique reflections	6915
Reflections used [$I > 2s$(I)]	3913
R_{int}	0.072
Final *R* indice [$I > 2s(I)$][a]	*0.0555*, wR_2 0.1657
R indices (all data)	0.1186
Goodness-of-fit	0.988
Max, Min Δρ/e A^{-3}	0.66, -0.51

Table 2.3. Selected bond angles and bond distances for molecular structure of **2.14.**

Bond Lengths (Å)			
Rh1-N1	2.062(4)	O3-S1	1.516(8)
Rh1-O1	2.037 (3)	O5-S1	1.315(8)
Rh1-C18	2.137(5)	O7-S1	1.568(8)
Rh1-C21	2.129(6)	O2-S1	1.329(12)
Rh1-C22	2.147(6)	O6-S1	1.400(8)
Rh1-C25	2.110(5)	O4-S1	1.598(8)
Na1-O7	1.484(9)	Na2-O4	1.711(10)
Bond Angles (°)			
N1-Rh1-O1	89.85(15)	O5-S1-O3	115.6(5)
N1-Rh1-C25	95.89(18)	O3-S1-O7	105.4(6)
O1-Rh1-C21	87.34(19)	O7-S1-O5	113.8(5)
O1-Rh1-C22	86.85(18)	O4-S1-O2	109.9(6)
C25-Rh1-C22	82.5(2)	O2-S1-O6	119.7(7)
C18-Rh1-C22	90.8(2)	O6-S1-O4	108.6(6)

2.4 Synthesis and characterization of water-soluble binuclear *N,O*-Rh(I) complexes

The binuclear complexes were synthesized by suspending or dissolving the dimeric ligands (**2.7-2.10**) in a minimum amount of ethanol or methanol, followed by deprotonation of the phenolic protons using an equimolar amount of NaH (Scheme 2.5). This was followed by

addition of the metal precursor $[Rh(COD)Cl]_2$ and stirring at room temperature. Complexes **2.15 - 2.18** were recovered as bright yellow solids.

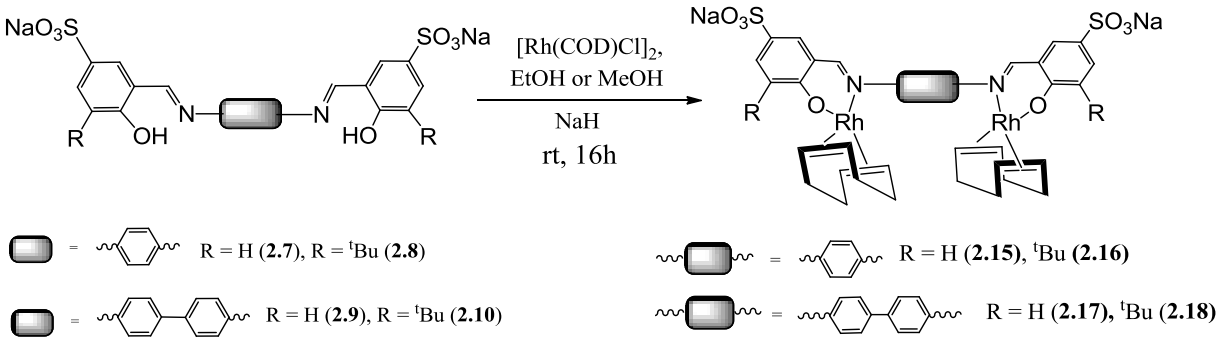

Scheme 2.5 Synthesis of water-soluble mononuclear Rh(I) complexes **2.15** – **2.18**.

All the complexes were recovered in moderate yields (60% - 86%) and display good water-solubility at room temperature 0.05 mg/mL (**2.15**), 0.01 mg/mL (**2.17**) and 0.03 mg/mL (**2.18**). Complexes **2.15** and **2.17** are partially soluble in methanol, chloroform, acetone and acetonitrile. The complexes were characterized using various spectroscopic techniques such as nuclear magnetic resonance, mass spectrometry and infrared spectroscopy. The ^{1}H NMR spectrum for the binuclear complex **2.15** is shown in Figure 2.6.

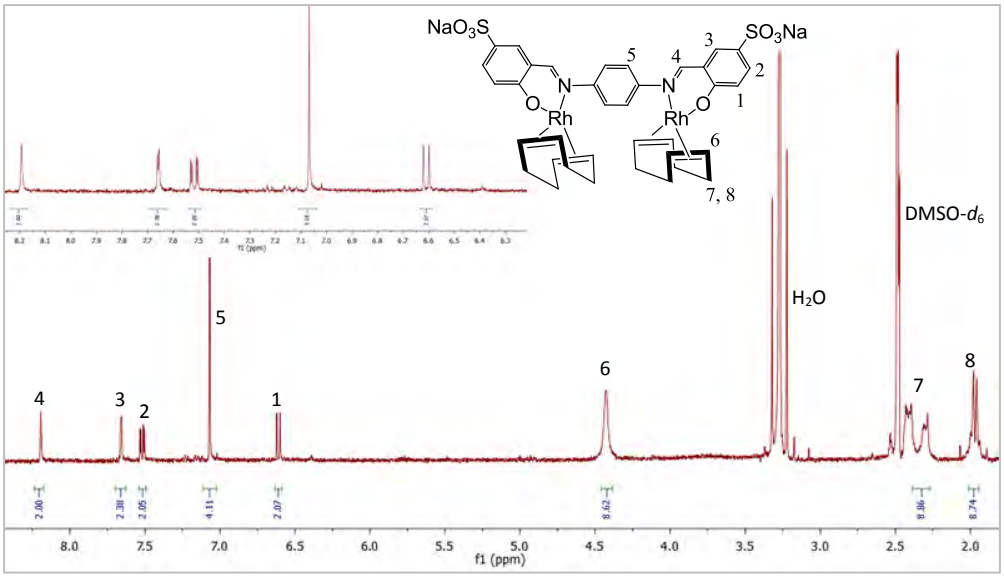

Figure 2.6. ^{1}H NMR spectrum for complex **2.15** in DMSO-d_6 at 30˚C.

In the ^{1}H NMR spectrum for complex **2.15,** the imine proton H-4 is observed at 8.19 ppm. At 7.66 ppm a singlet is observed for the proton H-3 adjacent to the sulfonate moiety. The

proton *para* to the imine H-2 is observed at 7.53 ppm. A doublet is seen further upfield at 6.62 ppm for the proton H-1 adjacent to the phenolic oxygen with a coupling constant of 6.00 Hz observed. Of interest, is a singlet observed at 7.07 ppm integrating for 4 protons of the phenylene spacer. This confirms the symmetrical nature of the complex and that all four protons exist in the same chemical environment. Similar to the mononuclear complexes, the cyclooctadiene moiety protons are observed between 4.50 ppm and 1.50 ppm.

The ^{1}H NMR spectrum for complex **2.17** shows trends very similar to those observed in the spectrum of **2.16.** The main difference is that the peaks in the spectrum of **2.17** are broadened. However the integration agrees with the suggested structure. The signals for the cyclooctadiene moieties are observed as multiplets at 3.98 ppm, 2.31 ppm and 1.74 ppm each peak integrating for 8 protons.

For complex **2.18,** a singlet is observed downfield at 8.20 ppm and similar to the other complexes described, an upfield shift from 9.11 ppm (in the free ligand) is also observed. The aromatic protons are observed between 7.15 ppm and 7.75 ppm and the symmetrical nature of the compound is reflected by the integration in the spectrum. Further upfield, at 4.28 ppm and 4.07 ppm, two signals integrating for 4 protons each are observed. These are assigned to the olefinic protons of the cyclooctadiene moiety. Two kinds of olefin proton resonances arise from the two sets of two equivalent protons *trans* to the N and *trans* to the O, respectively. This phenomenon has been extensively studied by Enamullah and co-workers for similar compounds.[32,30,33] At 2.35 ppm and 1.84 ppm, two multiplets are observed for the methylene protons of the cyclooctadiene due to their diastereotopic nature because they are on the same carbon but in different chemical environments. Finally, at 1.32 ppm a multiplet integrating for 18 protons of the tertiary butyl moiety is observed.

In the ^{13}C{^{1}H} NMR spectra of the binuclear complexes (**2.15-2.18**), three peaks were observed for the cycloodiene moiety in the region between 30 ppm and 90 ppm. The signals for the aromatic carbons are observed in the region 110 ppm and 160 ppm and the number of signals corresponds to the number of carbon atoms present in each complex. The signal for the imine carbon is the most deshielded due to the electron withdrawing effects of the nitrogen together with the anisotropic effect of the C=N bond, and is observed in the region 163 ppm and 166 ppm for all of the complexes.

The complexes (**2.15-2.18**) were also characterized using infrared spectroscopy. Similar to their mononuclear analogues, a shift in the imine absorption band to lower wavenumbers is

observed. The absorption bands for the imine functionality in the free ligands are between 1615 cm^{-1} and 1621 cm^{-1}, whilst the same vibrations are observed at lower wavenumbers between 1600 cm^{-1} and 1604 cm^{-1} in the metal complexes. This is evidence for coordination of the imine nitrogen to the Rh center. The results from infrared spectroscopy are summarized in the Table 2.4.

Table 2.4 Imine Infrared absorptions (cm^{-1}) and imine ^{1}H NMR chemical shifts (ppm) for (ligands) and complexes

Compound	^{1}H NMR Imine (ppm)	IR Imine (cm^{-1})
2.15	(9.06) 8.19	(1615) 1606
2.16	(9.11) 8.19	(1621) 1600
2.17	(9.08) 8.22	(1621) 1602
2.18	(9.11) 8.20	(1617) 1600

Data for the ligands are shown in brackets.

The complexes (**2.15**-**2.18**) were also characterized using high resolution electrospray ionisation mass spectrometry and were recorded in the negative ion-mode. A molecular ion peak was observed at m/z = 447.3087 and m/z = 485.7807 for complexes **2.15** and **2.17** respectively.

2.5 Overall Summary

A series of new water-soluble sulfonated monomeric and dimeric ligands (**2.3**-**2.10**) was synthesized and characterized. All the ligands display excellent water-solubility at room temperature. These were reacted with $[Rh(COD)Cl]_2$ dimer to afford a series of mono- and binuclear complexes (**2.11**-**2.18**) with varying substituents and organic bridging spacers. All complexes have been characterized using ^{1}H NMR, $^{13}C\{H\}$ NMR and infrared spectroscopy, high resolution mass spectrometry, elemental analysis and melting point. The complexes also display excellent water-solubility at room temperature. Furthermore, single crystal X-ray diffraction experiments for **2.14** further confirm that the mode of coordination of the salicylaldimine ligand occurs *via* the *N,O* donor atoms in a bidentate fashion. All the complexes (**2.11**-**2.18**) were evaluated as catalysts precursors in the aqueous biphasic hydroformylation of 1-octene and the results for this investigation will be discussed in Chapter 3.

2.6 Experimental

General Details

All reagents and solvents were purchased from a commercial source (Sigma-Aldrich) and were used as received. Hydrated rhodium trichloride salt was received as a kind donation from Anglo-Platinum Corporation / Johnson Matthey Limited. The sulfonated aldehydes **2.1**, **2.2** and ligand **2.3**[18] and rhodium dimeric precursor[29] were prepared according to previously reported literature methods. Nuclear magnetic resonance (NMR) spectra were recorded on either a Varian XR300 MHz (^{1}H at 300.08 MHz, ^{13}C{H} at 75.46 MHz) or a Bruker Biospin GmbH (^{1}H at 400.22 MHz, ^{13}C{H} at 100.65 MHz) spectrometer at ambient temperature. Elemental analysis for C, H, N and S were carried out using a Thermo Flash 1112 Series CHNS-O Analyser. For some compounds, the analyses are outside acceptable limits and are ascribed to the inclusion of water-molecules. Infrared absorptions were measured using a Perkin-Elmer Spectrum 100 FT-IR spectrometer as KBr pellets. Mass spectrometry was carried out on a Waters API Quattro Micro Triple Quadrupole electrospray ionisation mass spectrometer. Data were recorded in the negative ion-mode.

2.7 Synthesis and characterization of sulfonated aldehydes and the corresponding imine ligands

2.7.1 Synthesis of water-soluble salicylaldimine ligand 2.4

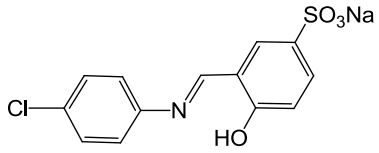

The sulfonated aldehyde **2.1** (0.221 g, 0.989 mmol) was dissolved in a minimum amount of water, followed by addition of 4-chloroaniline (0.132 g, 0.989 mmol) dissolved in ethanol. Magnesium sulphate was added and this was stirred at room temperature for 16 hours. The mixture was filtered. The filtrate was collected and the solvent was removed from the yellow solution. The product was obtained as a bright yellow solid. **Yield** (0.131 g, 61%). **Mp**: 394 ^{o}C - 395 ^{o}C. **FT-IR** (ν_{max}/cm^{-1}, KBr): 1617 (C=N). **^{1}H NMR**: DMSO-d_6, δ (ppm): 8.94 (s, 1 H, $\mathbf{H}_{imine}$), 7.96 (s, 1 H, $\mathbf{H}_{Ar}$), 7.65 (dd, ^{3}J = 8.3 Hz, ^{4}J = 2.3 Hz, 1 H, $\mathbf{H}_{Ar}$), 7.49 – 7.39 (m, 4 H, $\mathbf{H}_{Ar}$), 7.00 – 6.88 (d, ^{3}J = 8.7 Hz, 1 H, $\mathbf{H}_{Ar}$). **^{13}C{^{1}H} NMR**: DMSO-d_6, δ (ppm): 164.1,

160.7, 147.5, 140.4, 131.7, 131.5, 130.1, 129.8, 123.7, 118.5, 116.3. **Elemental Analysis**: Calculated for $C_{13}ClH_9NO_4NaS.2.5H_2O$: C, 46.92; H, 4.78; N, 3.91; S, 8.95, Found C, 47.41; H, 4.76; N, 3.44; S, 8.42. **HR-ESI-MS** (negative): m/z 366.0580 $[M]^-$, where M is the anion. $\mathbf{S_{20°C}}$ = 0.350 mg/mL in water.

2.7.2 Synthesis of water-soluble salicylaldimine ligand 2.5

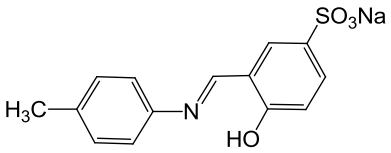

The sulfonated salicylaldehyde **2.1** (0.153 g, 0.682 mmol) was dissolved in a minimum amount of water. This was followed by drop-wise addition of a solution of *p*-toluidine (0.0710 g, 0.682 mmol) dissolved in ethanol (40 mL). Magnesium sulphate was added and the mixture was stirred at room temperature for 16 hours after which the mixture was filtered by gravity and solvent was removed from the filtrate. The residue was dried under vacuum to afford the desired product. **Yield** (0.189 g, 99%). **Mp**: Decomposes without melting, onset occurs at 336°C. **FT-IR** (ν_{max}/cm^{-1}, KBr): 1619 (C=N). **^{1}H NMR**: DMSO-d_6, δ (ppm): 13.34 (s, 1 H, O**H**), 8.99 (s, 1 H, $\mathbf{H}_{imine}$), 7.92 (dd, ^3J = 8.0 Hz, ^4J = 2.1 Hz, 1 H, $\mathbf{H}_{Ar}$), 6.30 – 7.59 (m, 1 H, $\mathbf{H}_{Ar}$), 7.37 – 7.22 (m, 4 H, H_{Ar}), 6.98 (d, ^3J = 8.7 Hz, 1 H, $\mathbf{H}_{Ar}$), 2.32 (s, 3 H, C$\mathbf{H}_3$. **^{13}C{^{1}H} NMR**: DMSO-d_6, δ (ppm): 162.8, 160.9, 145.8, 140.3, 137.0, 131.0, 130.4, 121.8, 118.5, 116.2, 114.5 , 21.1. **Elemental Analysis**: Calculated for $C_{14}H_{12}NNaO_4S.2.5H_2O$: C, 46.92; H, 4.78; N, 3.91; S, 8.95. Found C, 47.41; H, 4.76; N, 3.44; S, 3.44. **HR-ESI-MS** (negative): m/z = 290.3182 $[M]^-$, where M is the anion. $\mathbf{S_{20°C}}$ = 8.00 mg/mL in water.

2.7.3 Synthesis of water-soluble salicylaldimine ligand 2.7

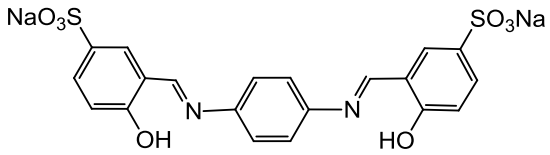

The diamine, *p*-phenylenediamine (0.0411 g, 0.371 mmol) was dissolved in ethanol (40 mL). The sulfonated aldehyde **2.1** (0.167 g, 0.743 mmol) was dissolved in a minimum amount of water and this was added drop-wise to the stirring amine. The solution was refluxed at 80 °C overnight. The yellow-brown suspension was filtered using a Büchner funnel and the solid washed with dichloromethane and then dried under vacuum to afford the product. **Yield**

(0.193 g, 99%). **Mp**.: Decomposes without melting, onset occurs at 395°C. **FT-IR** (ν_{max}/cm^{-1}, KBr): 1615 (C=N). **^{1}H NMR**: DMSO-d_6, δ (ppm): 13.21 (s, 2 H, O**H**), 9.06 (s, 2 H, **H**$_{imine}$), 7.97 (d, ^3J = 8.5 Hz, 2 H, H$_{Ar}$), 7.63 (dd, ^3J = 8.5 Hz, ^4J = 2.5 Hz, 2 H, **H**$_{Ar}$), 7.54 (s, 4 H, H$_{Ar}$), 6.90 (d, ^3J = 8.6 Hz, 2 H, H$_{Ar}$). **^{13}C{^{1}H} NMR**: DMSO-d_6, δ (ppm): 163.3, 160.9, 147.1, 140.2, 131.3, 130.1, 127.6, 123.1, 118.6, 116.3. **Elemental Analysis**: Calculated for $C_{20}H_{14}N_2Na_2O_8S_2.3H_2O$: C, 41.81; H, 3.51; N, 4.88; S, 11.16, Found: C, 41.65; H, 3.10; N, 3.71; S, 11.21. **HR-ESI-MS** (negative): m/z 237.2240 $[M]^{2-}$, where M is the anion. **S$_{20°C}$** = 0.200 mg / mL in water.

2.7.4 Synthesis of water-soluble salicylaldimine ligand 2.8

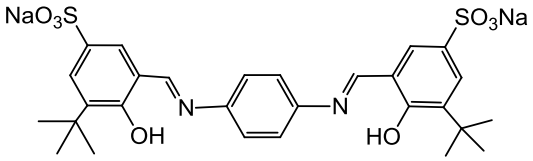

The sulfonated aldehyde **2.1** (0.0701 g, 0.250 mmol) was added to a stirring solution of, *p*-phenylenediamine (0.0141 g, 0.125 mmol) in 50 mL dry methanol. This was refluxed for 6 hours, the solvent was removed from the orange solution to afford a dark orange solid. This solid was dried under vacuum to afford the product. **Yield** (0.0601 g, 76%). **Mp**: Decomposed without melting onset at 139 °C. **FT-IR** (ν_{max}/cm^{-1}, KBr): 1621 (C=N). **^{1}H NMR**: DMSO-d_6, δ (ppm): 14.86 (s, 2 H, O**H**), 9.11 (s, 2 H, **H**$_{imine}$), 7.82 (d, ^3J = 2.1 Hz, 2 H, **H**$_{Ar}$), 7.7.-7.66 (m, 2 H, **H**$_{Ar}$), 7.61 (s, 4 H, **H**$_{Ar}$), 1.71 (s, 18 H, C**H**$_3$). **^{13}C{^{1}H} NMR**: DMSO-d_6, δ (ppm):166.2, 135.71, 129.0, 127.9, 126.9, 132.1, 122.9, 118.4, 114.7, 34.9, 29.6. **Elemental Analysis**: Calculated for $C_{28}H_{30}N_2Na_2O_8S_2$: C, 53.16; H, 4.78; N, 4.43; S, 10.14, Found: C, 53.56; H, 4.96; N, 4.01; S, 11.01. **HR-ESI-MS** (negative): m/z 293.3301 $[M]^{2-}$, where M is the anion. **S$_{20°C}$** = 0.070 mg/mL in water.

2.7.5 Synthesis of water-soluble salicylaldimine ligand 2.9

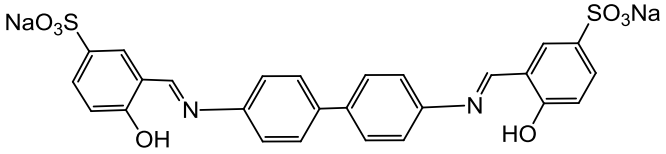

Benzidine (0.115 g, 0.632 mmol) was dissolved in ethanol (20 mL). This was followed by addition of the sulfonated aldehyde (0.279 g, 1.25 mmol) dissolved in a 1:1 water/ethanol mixture. This stirred at room temperature overnight. The bright yellow precipitate was

filtered using a Hirsch funnel, washed with ethanol and dried under vacuum to afford the product as a bright yellow solid. **Yield** (0.205 g, 55%). **Mp**: Decomposed without melting onset at 349 ^{o}C. **FT-IR** (ν_{max}/cm^{-1}, KBr): 1621 (C=N). **^{1}H NMR**: DMSO-d_6, δ (ppm): 13.23 (s, 2 H, O**H**), 9.08 (s, 2 H, $\mathbf{H}_{imine}$), 8.01 (s, 2 H, $\mathbf{H}_{Ar}$), 7.97 (dd, ^{3}J = 8.2 Hz , ^{4}J = 2.2 Hz, 2 H, $\mathbf{H}_{Ar}$), 7.82 (d, ^{3}J = 8.5 Hz, 4 H, $\mathbf{H}_{Ar}$), 7.64 – 7.61 (m, 4 H, H_{Ar}), 6.89 (m, 2 H, $\mathbf{H}_{Ar}$).**^{13}C{^{1}H} NMR**: DMSO-d_6, δ (ppm):163.5, 160.9, 147.7, 140.4, 138.4, 131.3, 128.0, 122.6, 118.6, 116.3, 115.2. **Elemental Analysis**: Calculated for $C_{26}H_{18}N_2Na_2O_8S_2$: C, 52.35; H, 3.04; N, 4.70; S, 10.75, Found: C, 52.69; H, 3.34; N, 4.46; S, 6.22. **HR-ESI-MS** (negative): m/z 275.2751 $[M]^{2-}$, where M is the anion. $\mathbf{S_{20°C}}$ = 0.110 mg/mL in water.

2.7.6 Synthesis of water-soluble salicylaldimine ligand 2.10

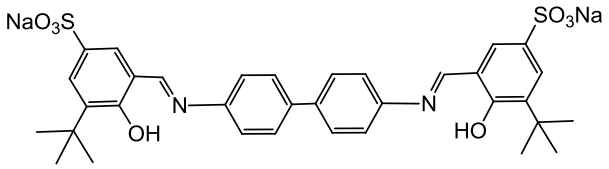

Benzidine (0.0200 g, 0.100 mmol) was dissolved in ethanol (50 mL) and to it was added the sulfonated aldehyde (0.0500 g, 0.200 mmol) in ethanol. This was stirred at room temperature for 16 hours. The bright yellow precipitate was filtered using a Büchner funnel, washed with ethanol and dried under vacuum to afford a yellow powder as the product. **Yield** (0.0600 g, 82%). **Mp**: Decomposes without melting, onset at 331 ^{o}C. **FT-IR** (ν_{max}/cm^{-1}, KBr): 1617 (C=N). **^{1}H NMR:** DMSO-d_6, δ (ppm): 14.41 (s, 2 H, OH), 9.11(s, 2 H, $\mathbf{H}_{imine}$), 7.83 (m, 8 H, $\mathbf{H}_{Ar}$), 7.61 (m, 4 H, $\mathbf{H}_{Ar}$), 1.42 (s, 18 H, C$\mathbf{H}_3$). **^{13}C{^{1}H} NMR:** DMSO-d_6, δ (ppm): 164.5, 160.9, 147.7, 140.4, 138.4, 131.3, 130.4, 127.0, 123.6, 118.8, 117.3, 31.3, 18.4. **Elemental Analysis**: Calculated for $C_{34}H_{34}N_2Na_2O_8S_2.13H_2O$: C, 43.31; H, 6.41; N, 2.97; S, 6.80, Found: C, 43.50; H, 6.19; N, 2.20; S, 9.59. **HR-ESI-MS** (negative): m/z 331.0883 $[M]^{2-}$, where M is the anion. $\mathbf{S_{20°C}}$ = 1.71 mg/mL in water.

2.8 Synthesis and characterization of sulfonated water-soluble Rh(I) complexes

2.8.1 Synthesis of mononuclear complex 2.11

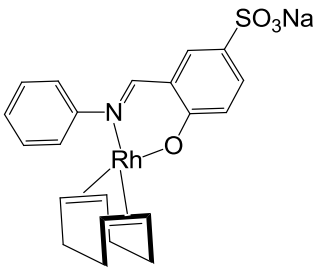

The sulfonated salicylaldimine ligand **2.3** (0.0621 g, 0.207 mmol) was deprotonated with 1M KOH for 30 minutes in 20 mL (1:1) H_2O/ethanol. The dimer $[Rh(COD)Cl]_2$ (0.0511 g, 0.104 mmol) was suspended in 10 mL ethanol and this was added drop-wise to the deprotonated ligand. The mixture was stirred at room temperature for an hour. The solvent was removed under vacuum and the residue was dissolved in a minimum amount of methanol. This was followed by addition of an excess amount of diethyl ether, a precipitate formed and was filtered using a Hirsch funnel, washed with diethyl ether and dried under vacuum to afford the product. **Yield** (0.105 g, 76%). **Mp**: 360 ^{o}C - 362 ^{o}C. **FT-IR** (ν_{max}/cm^{-1}, KBr):1603 (C=N). **^{1}H NMR:** DMSO-d_6, δ (ppm): 7.36 (s, 1 H, $\mathbf{H}_{imine}$), 6.83 (s, 1 H, $\mathbf{H}_{Ar}$), 8.83 (d, ^{3}J = 8.8 Hz, 1 H, **H**Ar), 6.60 (t, ^{3}J = 7.6 Hz, 2 H, $\mathbf{H}_{Ar}$), 6.49 – 6.38 (m, 2 H, $\mathbf{H}_{Ar}$), 6.30 (d, ^{3}J = 7.6 Hz, 2 H, $\mathbf{H}_{Ar}$), 5.83 (d, ^{3}J = 8.80 Hz, 1 H, $\mathbf{H}_{Ar}$), 4.39 (m, 4 H, C$\mathbf{H}_{COD}$), 1.70 (m, 4 H, C$\mathbf{H}_{2COD}$), 1.50 (m, 4 H, C$\mathbf{H}_{2COD}$). **^{13}C{^{1}H} NMR:** DMSO-d_6, δ (ppm): 161.8, 135.0, 134.9, 134.0, 130.1, 123.8, 122.5, 120.4, 118.5, 118.1, 116.3, 84.7, 33.7, 28.0. **Elemental Analysis**: Calculated for $C_{21}H_{21}NO_4SNaRh$: C, 49.48; H, 4.12; N, 2.74; S, 6.28, Found C, 49.15; H, 4.37; N, 2.28; S, 4.47. **HR-ESI-MS** (negative): m/z 486.3612 $[M]^{-}$, where M is the anion. **$S_{20^{o}C}$** = 5.00 mg/mL in water.

2.8.2 Synthesis of mononuclear complex 2.12

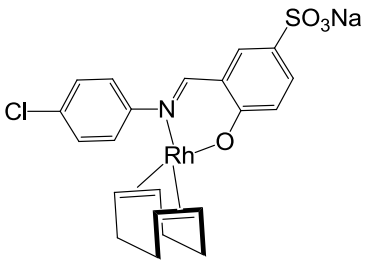

The sulfonated imine ligand **2.4** (0.0631 g, 0.188 mmol) was suspended in 20 mL of

methanol followed by addition of 0.25 mL of 1M KOH solution. The yellow solution that formed was stirred at room temperature for 30 minutes. The metal precursor $[Rh(COD)Cl]_2$ (0.0510 g, 0.0940 mmol) was suspended in 5 mL methanol and this was added drop-wise to the stirring solution. The mixture was left to stir at room temperature for 16 hours. The precipitate was filtered using a Hirsch funnel and was re-precipitated from methanol. The solid was dried under vacuum to afford the product as a bright yellow solid. **Yield** (0.0510 g, 86%). **Mp**: Decomposed without melting, onset at 373 ^{o}C. **FT-IR** (ν_{max}/cm^{-1}, KBr): 1604 (C=N). **^{1}H NMR:** CD_3OD, δ (ppm): 8.21 (s, 1 H, $\mathbf{H}_{imine}$), 7.76 – 7.80 (m, 2 H, $\mathbf{H}_{Ar}$), 7.35 (d, ^{3}J = 8.7 Hz, 2 H, $\mathbf{H}_{Ar}$), 7.04 (d, ^{3}J = 8.7 Hz, 2 H, $\mathbf{H}_{Ar}$), 6.81 - 6.78 (m, 1 H, $\mathbf{H_{Ar}}$), 4.75 (br s, 4 H, $C\mathbf{H}_{COD}$), 2.36 – 2.30 (m, 4 H, $C\mathbf{H}_{2COD}$) 1.83 (m, 4 H, $C\mathbf{H}_{2COD}$). **^{13}C{^{1}H} NMR:** CD_3OD, δ (ppm): 164.2, 131.5, 130.1, 129.8, 128.9, 125.7, 123.8, 120.4, 118.5, 116.3, 115.7, 87.7, 30.7, 27.5. **Elemental Analysis**: Calculated for $C_{21}H_{20}NO_4ClSNaRh$: C, 46.37; H, 3.68; N, 2.58; S, 5.89, Found C, 46.07; H, 3.87; N, 3.77; S, 5.12. **HR-ESI-MS** (negative): m/z 520.8142 [M]$^{-}$, where M is the anion. $\mathbf{S_{20°C}}$ = 4.70 mg/mL in water.

2.8.3 Synthesis of mononuclear complex 2.13

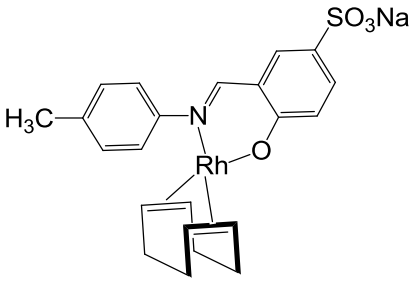

The sulfonated imine ligand **2.5** (0.0620 g, 0.197 mmol) was dissolved in a 1:1 mixture of water and ethanol (20 mL). This was followed by addition of 1M KOH (0.25 mL) and this was stirred at room temperature for 30 min. The rhodium precursor $[Rh(COD)Cl]_2$ (0.0490 g, 0.0990 mmol) was added and the mixture was left to stir at room temperature for 1h. The clear solution was filtered by gravity and the solvent was removed from the filtrate under reduced pressure. The solid was dried under vacuum to afford a yellow-brown powder as the product. **Yield** (0.0390 g, 76%). **Mp**: Decomposed without melting, onset at 262 ^{o}C. **FT-IR** (ν_{max}/cm^{-1}, KBr): 1604 (C=N). **^{1}H NMR:** DMSO-d_6, δ (ppm): 8.31 (s, 1 H, $\mathbf{H}_{imine}$), 7.62 (d, ^{3}J = 2.4 Hz, 1 H, $\mathbf{H}_{Ar}$), 7.55 (m, 1 H, $\mathbf{H}_{Ar}$), 7.19 (d, ^{3}J = 7.9 Hz, 2 H, $\mathbf{H_{Ar}}$), 6.98 (m, 2 H, $\mathbf{H}_{Ar}$), 6.64 (d, ^{3}J = 8.8 Hz, 1 H, $\mathbf{H}_{Ar}$), 4.32 (m, 4 H, $C\mathbf{H}_{COD}$), 2.32 (m, 4 H, $C\mathbf{H}_{2COD}$) 1.87 (m, 4 H,$C\mathbf{H}_{2COD}$), 1.76 (s, 3 H, $C\mathbf{H}_3$). **^{13}C{^{1}H} NMR:** DMSO-d_6, δ (ppm): 166.3, 149.7, 137.7, 135.5, 133.5, 129.4, 123.4, 122.6, 121.7, 120.6, 117.1, 74.3, 30.6, 29.5, 20.9. **Elemental Analysis**: Calculated for $C_{22}H_{23}NNaO_4RhS$: C, 50.49; H, 4.43; N, 2.68; S, 6.13, Found C,

50.72; H, 4.87; N, 2.77; S, 5.90. **HR-ESI-MS** (negative): m/z 500.9313 $[M]^-$, where M is the anion. $\mathbf{S_{20°C}}$ = 5.00 mg/mL in water.

2.8.4 Synthesis of mononuclear complex 2.14

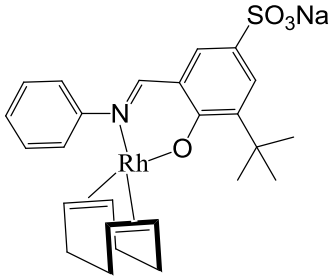

The sulfonated salicylaldehyde **2.2** (0.199 g, 0.713 mmol) was dissolved in a minimum amount of water. To this, aniline (0.0661 g, 0.713 mmol) in 20 mL ethanol was added and this was left to stir at room temperature for 16 hours. The solvent was removed under reduced pressure to afford an orange oil. This oil was dissolved in a 10 mL (1:1) ethanol/dichloromethane mixture and an equimolar amount of 1M KOH was added and the solution was stirred for 30 minutes. The metal precursor $[Rh(COD)Cl]_2$ (0.176 g, 0.357 mmol) was dissolved in dichloromethane (10mL) and this was added drop-wise to the stirring ligand solution and this was left to stir at room temperature for 1 hour. The solvent was then removed and the residue dried under vacuum to afford a yellow powder as the product. Crystals for single crystal X-ray diffraction were obtained by slow diffusion of diethyl ether into a solution of the complex (**2.14**) in acetonitrile. **Yield** (0.315 g, 78%). **Mp**: 292 - 294 ^oC. **FT-IR** (ν_{max}/cm^{-1}, KBr): 1602 (C=N). **^{1}H NMR:** DMSO-d_6, δ (ppm): 8.13 (s, 1 H, $\mathbf{H}_{imine}$), 7.54 (m, 2 H, $\mathbf{H}_{Ar}$), 7.37 (t, ^3J = 1.8 Hz, 1 H, $\mathbf{H}_{Ar}$), 7.22 (m, 1 H, $\mathbf{H}_{Ar}$), 7.09 (d, ^3J = 7.7 Hz 2H, $\mathbf{H}_{Ar}$), 6.98 (m, 1 H, $\mathbf{H}_{Ar}$), 4.27 (m, 4 H, $C\mathbf{H}_{COD}$), 2.36 (m, 4 H, $C\mathbf{H}_{2COD}$), 1.81 (m, 4 H, $C\mathbf{H}_{2COD}$). **^{13}C{^{1}H} NMR:** DMSO-d_6, δ (ppm): 165.1, 152.2, 138.7, 134.5, 132.1, 129.9, 129.1, 126.4, 123.7, 117.2, 114.7, 73.9, 39.4, 30.0, 26.4, 27.5. **Elemental Analysis**: Calculated for $C_{25}H_{29}NNaO_4RhS$: C, 53.10; H, 5.17; N, 2.48; S, 5.67. Found C, 53.07; H, 5.87; N, 2.77; S, 5.21. **HR-ESI-MS** (negative): m/z 542.4602 $[M]^-$, where M is the anion. $\mathbf{S_{20°C}}$ = 4.00 mg/mL in water.

2.8.5 Synthesis of mononuclear complex 2.15

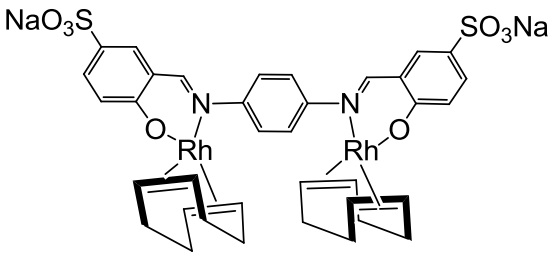

The sulfonated imine ligand **2.7** (0.0350 g, 0.0680 mmol) was dissolved in 20 mL ethanol/water (1:1) mixture and to it was added an equimolar amount of NaH. This was left to stir at room temperature for 30 minutes. Rhodium dimer $[Rh(COD)Cl]_2$ (0.0330 g, 0.0680 mmol) was suspended in ethanol (10 mL) and this was added drop-wise to the deprotonated ligand. The mixture was stirred at room temperature for 16 hours. The precipitate formed was filtered using a Hirsh funnel and dried under vacuum to afford the product as a yellow-brown solid. **Yield** (0.0510 g, 75%). **Mp**: Decomposed without melting onset at 345 ^{o}C. **FT-IR** (ν_{max}/cm^{-1}, KBr): 1606 (C=N). **^{1}H NMR:** DMSO-d_6, δ (ppm): 8.19 (s, 2 H, $\mathbf{H}_{imine}$), 7.66 (s, 2 H, $\mathbf{H}_{Ar}$), 7.53 – 7.49 (m, 4 H, $\mathbf{H}_{Ar}$), 7.07 (s, 4 H, $\mathbf{H}_{Ar}$), 6.62 (m, 2 H, $\mathbf{H}_{Ar}$), 4.43 (br s, 8 H, C$\mathbf{H}_{COD}$), 2.45 – 2.41 (m, 8 H, C$\mathbf{H}_{COD}$), 1.98 – 1.95 (m, 8 H, C$\mathbf{H}_{COD}$). **^{13}C{^{1}H} NMR:** DMSO-d_6, δ (ppm): 166.4, 159.1, 155.3, 151.6, 133.6, 133.4, 133.0, 123.5, 87.7, 30.5, 27.6. **Elemental Analysis**: Calculated for $C_{40}H_{48}N_2Na_2O_8Rh_2S_2$: C, 48.01; H, 4.83; N, 2.80; S, 6.41. Found C, 47.92; H, 4.30; N, 2.41; S, 7.31. **HR-ESI-MS** (negative): m/z 447.3087 $[M]^{2-}$, where M is the anion. $\mathbf{S_{20°C}}$ = 0.051 mg / mL in water.

2.8.6 Synthesis of mononuclear complex 2.16

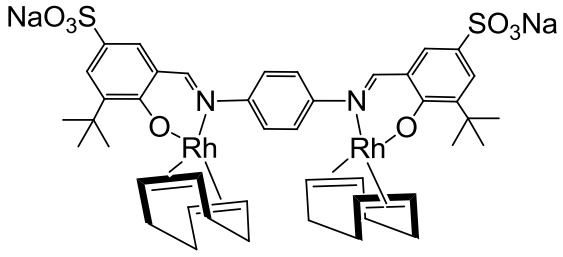

Sulfonate dimeric ligand **2.8** (0.0210 g, 0.0330 mmol) was suspended in 30 mL methanol. An equimolar amount of NaH was added and this was stirred at room temperature for 2 hours. Rhodium dimer $[Rh(COD)Cl]_2$ (0.0160 g, 0.0330 mmol) was added to the ligand and this was stirred at room temperature for 76 hours. The solvent was removed from the brown

solution and the brown solid was dried under vacuum to afford the product. **Yield** (0.0350 g, 73%). **Mp**: Decomposed without melting onset at 195 ^{o}C. **FT-IR** (ν_{max}/cm^{-1}, KBr): 1600 (C=N). **^{1}H NMR:** DMSO-d_6, δ (ppm): 8.19 (s, 2 H, $\mathbf{H}_{imine}$), 7.66 (s, 2 H, $\mathbf{H}_{Ar}$), 7.60 (d, ^{3}J = 5.6 Hz, 4 H, $\mathbf{H}_{Ar}$), 7.12 (s, 4 H, $\mathbf{H}_{Ar}$), 4.52 (m, 8 H, C$\mathbf{H}_{COD}$), 2.37-2.33 (m, 8 H, C$\mathbf{H}_{COD}$), 1.75-1.73 (m, 8 H, C$\mathbf{H}_{COD}$), 1.04 (s, 18 H, C$\mathbf{H}_{3}$). **^{13}C{^{1}H} NMR:** DMSO-d_6, δ (ppm): 165.1, 149.9, 143.0, 138.7, 134.5, 132.2, 129.2, 123.7, 117.3, 81.3, 46.9, 35.2, 30.0, 25.8. **Elemental Analysis**: Calculated for $C_{46}H_{64}N_2Na_2O_8Rh_2S_2.4H_2O$: C, 47.59; H, 6.25; N, 2.41; S, 5.52. Found C, 47.02; H, 5.98; N, 2.65; S, 6.01. **HR-ESI-MS** (negative): m/z 503.4051 $[M]^{2-}$, where M is the anion. $\mathbf{S_{20^{o}C}}$ = 0.002 mg / mL in water.

2.8.7.1 Synthesis of mononuclear complex 2.17

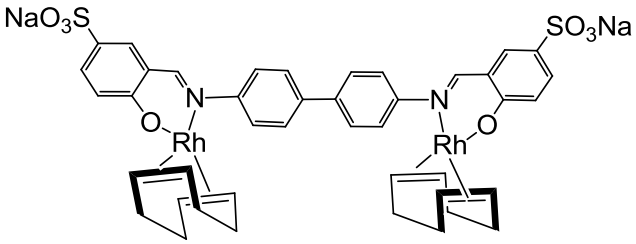

The dimeric imine ligand **2.9** (0.0550 g, 0.0930 mmol) was suspended in 20 mL methanol. To this was added an equimolar amount of NaH and the mixture stirred at room temperature for 30 minutes. Rhodium dimer $[Rh(COD)Cl]_2$ (0.0460 g, 0.0930 mmol) was also suspended in methanol (10 mL) and this was added drop-wise to the stirring ligand. The mixture was stirred at room temperature for 16 hours. The precipitate was filtered using a Büchner funnel, washed with methanol and dried under vacuum to afford a yellow- brown powder as the product. **Yield** (0.0640 g, 67%). **Mp**: Decomposed without melting onset at 325 ^{o}C. **FT-IR** (ν_{max}/cm^{-1}, KBr): 1602 (C=N). **^{1}H NMR:** DMSO-d_6, δ (ppm): 8.22 (s, 2 H, $\mathbf{H}_{imine}$), 7.70 – 7.51 (m, 8 H, $\mathbf{H}_{Ar}$), 7.12 – 7.15 (m, 4 H, $\mathbf{H}_{Ar}$), 6.62 (m, 2 H, $\mathbf{H}_{Ar}$), 3.98 (m, 4 H, C$\mathbf{H}_{COD}$), 2.31 (m, 4 H, C$\mathbf{H}_{COD}$), 1.74 (m, 4 H, C$\mathbf{H}_{COD}$). **^{13}C{^{1}H} NMR:** DMSO-d_6, δ (ppm): 163.2, 131.5, 130.1, 129.8, 128.9, 127.3, 124.7, 121.9, 122.5, 118.1, 114.3, 87.7, 30.7, 27.5. **Elemental Analysis**: Calculated for $C_{46}H_{52}N_2Na_2O_8Rh_2S_2.18H_2O$: C, 39.43; H, 6.33; N, 2.00; S, 4.58. Found C, 39.75; H, 6.18; N, 2.54; S, 4.76. **HR-ESI-MS** (negative): m/z 485.7807 $[M]^{2-}$, where M is the anion. $\mathbf{S_{20^{o}C}}$ = 0.011 mg / mL in water.

2.8.8 Synthesis of mononuclear complex 2.18

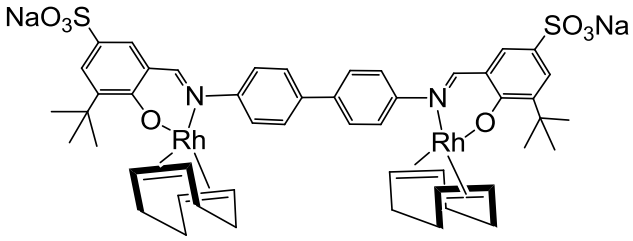

The dimeric imine ligand **2.10** (0.0150 g, 0.0200 mmol) was dissolved in 20 mL methanol and to it was added the Rh precursor $[Rh(COD)Cl]_2$ (0.0110 g, 0.0200 mmol). This was allowed to stir at room temperature for 16 hours. The solvent was removed from the yellow solution, and the residue was dried under vacuum to afford a bright yellow solid as the product. **Yield**: (0.0210 g, 86%). **Mp**: Decomposed without melting onset at 283 ^{o}C. **FT-IR** (ν_{max}/cm^{-1}, KBr): 1600 (C=N). **^{1}H NMR:** DMSO-d_6, δ (ppm): 8.20 (s, 2 H, $\mathbf{H}_{imine}$), 7.71 (d, ^{3}J = 7.7 Hz, 2 H, $\mathbf{H}_{Ar}$), 7.59 (s, 1 H, $\mathbf{H}_{Ar}$), 7.53 (s, 1 H, $\mathbf{H}_{Ar}$), 7.18 (d, ^{3}J = 8.2 Hz, 2 H, $\mathbf{H}_{Ar}$), 4.28 (m, 4 H, C$\mathbf{H}_{COD}$), 4.07 (br s, 4 H, C$\mathbf{H}_{COD}$), 2.35 (br s, 4 H, C$\mathbf{H}_{COD}$), 1.84 (m, 4 H, C$\mathbf{H}_{COD}$), 1.32 (s, 18 H, C$\mathbf{H}_{3}$). **^{13}C{^{1}H} NMR:** DMSO-d_6, δ (ppm): 164.5, 160.9, 147.7, 140.4, 138.4, 131.3, 127.0, 123.6, 118.8, 117.3, 87.7, 33.7, 31.5, 31.3, 18.4. **Elemental Analysis**: Calculated for $C_{54}H_{68}N_2Na_2O_8Rh_2S_2.6H_2O$: C, 50.00; H, 6.22; N, 2.16; S, 4.94. Found C, 49.91; H, 6.01; N, 2.36; S, 5.01. **HR-ESI-MS** (negative): m/z 541.4558 $[M]^{2-}$, where M is the anion. $\mathbf{S_{20°C}}$ = 0.030 mg/mL in water.

2.8.9 X-ray Crystallography

Single-crystal X-ray diffraction data were collected with a Bruker Kappa APEX II DUO diffractometer with graphite-monochromated Mo-*K*α radiation (λ = 0.71073 Å). Data collection was performed at 173(2) K. The temperature was controlled by an Oxford Cryostream cooling system (Oxford Cryostat). Cell refinement and data reduction were performed by using the program SAINT.[34] The data were scaled, and absorption correction was performed by using SADABS.[35] The structure was solved by direct methods by using SHELXS-97[35] and refined by full-matrix least-squares methods based on *F*2 by using SHELXL-97[35] and the graphics interface program X-Seed.[36, 37] The programs X-Seed and POV-Ray were both used to prepare molecular graphic images. The supplementary crystallographic data for **2.11** can be accessed online using CCDC code 1008938.

2.9 References

1 A. A. Dabbawala, H. C. Bajaj, H. Bricout and E. Monflier, *Appl. Catal. A Gen.*, 2012, **413-414**, 273–279.

2 A. A. Dabbawala, H. C. Bajaj, H. Bricout and E. Monflier, *Catal. Sci. Technol.*, 2012, **2**, 2273–2278.

3 Y. Fonseca, B. Fontal, M. Reyes, T. Suárez, F. Bellandi, J. C. Diaz and P. Cancines, *React. Kinet. Mech. Catal.*, 2011, **105**, 307–315.

4 G. Fremy, R. Grzybek, E. Monflier, A. Mortreux, A. M. Trzeciak and J. Ziolkowski, *J. Organomet. Chem.*, 1995, **505**, 11–16.

5 J. Boulanger, H. Bricout, S. Tilloy, A. Fihri, C. Len, F. Hapiot and E. Monflier, *Catal. Commun.*, 2012, **29**, 77–81.

6 S. N. Chen, W. Y. Wu and F. Y. Tsai, *Tetrahedron*, 2008, **64**, 8164–8168.

7 M. E. Hanhan, C. Cetinkaya and M. P. Shaver, *Appl. Organomet. Chem.*, 2013, **27**, 570–577.

8 R. Huang and K. H. Shaughnessy, *Organometallics*, 2006, **25**, 4105–4112.

9 G. K. Rao, A. Kumar, M. Bhunia, M. P. Singh and A. K. Singh, *J. Hazard. Mater.*, 2014, **269**, 18–23.

10 R. Zhong, A. Pöthig, Y. Feng, K. Riener, W. A. Herrmann and F. E. Kühn, *Green Chem.*, 2014, **16**, 4955–4962.

11 J. Zhou, X. Guo, C. Tu, X. Li and H. Sun, *J. Organomet. Chem.*, 2009, **694**, 697–702.

12 J. Zhou, X. Li and H. Sun, *J. Organomet. Chem.*, 2010, **695**, 297–303.

13 A. Andriollo, A. Bolívar, F. A. López and D. E. Páez, *Inorg. Chim. Acta*, 1995, **238**, 187–192.

14 D. Wu, J. Zhang, Y. Wang, J. Jiang and Z. Jin, *Appl. Organomet. Chem.*, 2012, **26**, 718–721.

15 S. K. Sharma and R. V. Jasra, *Catal. Today*, 2015, **247**, 70-81.

16 F. Hapiot, A. Ponchel, S. Tilloy and E. Monflier, *Comptes Rendus Chim.*, 2011, **14**, 149–166.

17 K. H. Shaughnessy, *Chem. Rev.*, 2009, **109**, 643–710.

18 E. B. Hager, B. C. E. Makhubela and G. S. Smith, *Dalton Trans.*, 2012, **41**, 13927–13935.

19 K. H. Shaughnessy, in *Metal catalysed reactions in water*, Weiheim, Wiley-VCH Verlag GmbH & Co. KGaA, 2013, pp 1-60.

20 B. K. Rai and R. Kumari, *Orient. J. Chem.*, 2013, **29**, 1164–1167.

21 L. C. Matsinha, S. F. Mapolie and G. S. Smith, *Polyhedron*, 2013, **53**, 56–61.

22 L. C. Matsinha, P. Malatji, A. T. Hutton, G. A. Venter, S. F. Mapolie and G. S. Smith, *Eur. J. Inorg. Chem.*, 2013, 4318–4328.

23 B. C. E. Makhubela, A. M. Jardine, G. Westman and G. S. Smith, *Dalton Trans.*, 2012, **41**, 10715–10723.

24 B. C. E. Makhubela, A. Jardine and G. S. Smith, *Green Chem.*, 2012, **14**, 338–347.

25 P. Govender, A. K. Renfrew, C. M. Clavel, P. J. Dyson, B. Therrien and G. S. Smith, *Dalton Trans.*, 2011, **40**, 1158–1167.

26 D. M. Boghaei and M. Gharagozlou, *J. Coord. Chem.*, 2007, **60**, 339–346.

27 J. Zhou, X. Guo, C. Tu, X. Li and H. Sun, *J. Organomet. Chem.*, 2009, **694**, 697–702.

28 A. Salanti, M. Orlandi, E. L. Tolppa and L. Zoia, *Int. J. Mol. Sci.*, 2010, **11**, 912–926.

29 J. Chatt and L. M. Venanzi, *J. Chem. Soc.*, 1957, 4735–4741.

30 M. Enamullah, A. Sharmin, M. Hasegawa, T. Hoshi, A. C. Chamayou and C. Janiak, *Eur. J. Inorg. Chem.*, 2006, 2146–2154.

31 C. Janiak, A. Chamayou, A. K. M. Royhan Uddin, M. Uddin, K. S. Hagen and M. Enamullah, *Dalt. Trans.*, 2009, **9226**, 3698–709.

32 M. Enamullah, A. K. M. R. Uddin and A. Chamayou, *Inorg. Chim. Acta*, 2007, **387**, 807–817.

33 C. Janiak, A. C. Chamayou, A. K. M. Royhan Uddin, M. Uddin, K. S. Hagen and M. Enamullah, *Dalton Trans.*, 2009, **9226**, 3698–3709.

34 SAINT, v.760a, Bruker AXC Inc., Madison, WI, 2006.

35 G. M. Sheldrick, SHELXS-97, SHELXL97, SADABS, v. 205, University of Gottingen, Germany, 1997.

36 L. J. Barbour, *J. Supramol. Chem.*, 2001, **1**, 189–191.

37 J. L. Atwood and L. J. Barbour, *Cryst. Growth Des.*, 2003, **3**, 3–8.

Chapter 3

Aqueous biphasic hydroformylation of 1-octene using water-soluble Rh(I) complexes as catalyst precursors

This chapter forms part of the following publication:

Recyclable and recoverable water-soluble sulfonated Rh(I) complexes for 1-octene hydroformylation in aqueous biphasic media.
Leah C. Matsinha, Selwyn F. Mapolie and Gregory S. Smith, *Dalton Transactions,* 2015, **44**, 1240-1248.

3.1 Introduction

The hydroformylation reaction is an important reaction for the synthesis of aldehydes, which are consequently used in the manufacture of various commodity chemicals such as agrochemicals, fragrances and pharmaceuticals.[1] The process involves the transition-metal catalysed reaction of an olefin with hydrogen and carbon monoxide as depicted in Scheme 3.1.

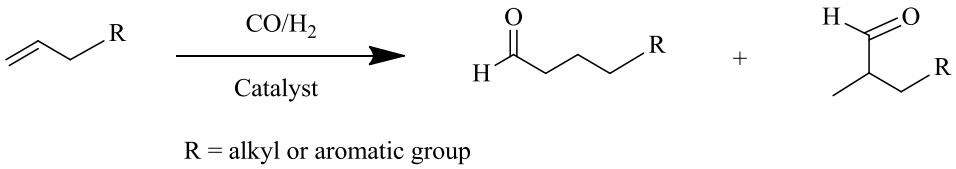

R = alkyl or aromatic group

Scheme 3.1. The hydroformylation reaction.

The reduction of the overall cost of the hydroformylation reaction is very important for the process to be economically viable. Aqueous biphasic catalysis is one way of implementing catalyst recovery and recycling strategies. This technique has been widely explored for the easy recovery of catalysts by phase separation and this technique is in operation in five plants around the world.[2] This strategy has been implemented due to the strong drive to achieve environmentally friendly, active, selective and highly economic catalysts.[3–6]

Various ligands can be used in order to fine-tune the selectivity and activity of the catalysts and ligand basicity has been seen to have an influence in the hydroformylation rates.[7] The presence of σ-donors in the ligand, increases its basic nature and this has a tendency of favouring higher hydroformylation rates.[8,9] Increasing the metal nuclearity of the catalysts is generally expected to improve catalyst activity and selectivity.[10] Binuclear complexes have been seen to exhibit unique chemistry, reactivity and selectivity compared to similar mononuclear derivatives.[6,11,12] Feringa and co-workers have reported that an increase in the number of metal centres in catalysts results in the metal centres operating cooperatively which can effectively improve activity during catalysis.[13]

The structure of the catalyst precursors is very important and hence the ligands must exhibit the appropriate electronic and structural requirements. This allows the metal centres to be within the correct distance and orientation from each other for cooperativity to take place which subsequently results in enhanced catalytic activity. The ligands must also be able to influence the hydroformylation reaction *via* the fine-tuning of its electronic and steric properties. Reducing flexibility in the bridging structures linking the two metals is one way of controlling this since it allows the accommodation of the metal centres in close proximity to each other but also prevents catalyst disintergration.[10,13] Various bridging scaffolds can be used to separate the metal centres and reports show that close proximity of the metal centres can allow the substrates to interact with both metal centres simultaneously.[6] Moreover, in binuclear complexes the two metals centres may have different oxidation states which may improve the stability of these compounds during catalysis.[14]

Herein we report the application of a series of water-soluble mono- and binuclear Rh(I) complexes as catalyst precursors for the aqueous biphasic hydroformylation of 1-octene. The mononuclear complexes have varying σ-donating and π-accepting characteristics, whilst the binuclear complexes have different bridging structures linking the two metals. The influence of the various substituents was investigated for the mononuclear series. Similarly, the binuclear complexes were tested and the effect of increasing nuclearity investigated. Moreover, the influence of the nature of the organic bridging spacers was evaluated.

3.2 Aqueous biphasic hydroformylation of 1-octene

The complexes **2.11**-**2.18** were tested as catalyst precursors in the aqueous biphasic hydroformylation of 1-octene. Scheme 3.2 shows the reaction of 1-octene with syngas (1:1,

CO/H_2) in the presence of a water-soluble Rh(I) catalyst to form aldehydes as the major products and internal olefins as the minor products.

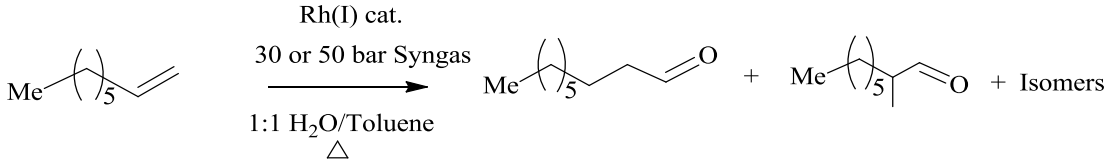

Scheme 3.2. Aqueous biphasic hydroformylation of 1-octene**.**

The biphasic system comprised of the catalyst precursor dissolved in 5 mL water and the substrate (1-octene) and internal standard (*n*-decane) dissolved in 5 mL toluene. This was pressurised and heated to the desired temperature. At the end of the experiment, the reaction was cooled followed by separation of the organic products from the catalysts by decantation. The organic layer was analysed using gas chromatography. Toluene was used because the catalyst precursors are insoluble in toluene and this solvent also been used previously for similar systems.[3,7]

3.2.1 Optimisation of the reaction conditions

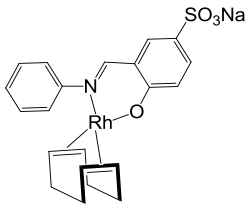

2.11

The experiments were carried out under high syngas pressure (30 bar-50 bar) and the temperature was varied between 75 ˚C and 95 ˚C. All the reactions were performed for 8 hrs. These reaction conditions were selected because similar catalyst precursors have been evaluated for the aqueous biphasic hydroformylation of 1-octene under these conditions and gave good results.[3] Catalyst precursor **2.11** was used in the optimisation experiments because it has the simplest and most representative structure for all the catalysts. All results reported are an average of two catalytic runs and calculated standard deviations are reported in the footnotes.

At 30 bar, the activity of the catalyst was 277 hr^{-1} (Entries 1 and 2, Table 3.1). The conversion of 1-octene was greater than 99% and excellent aldehyde selectivity was observed. No isomerisation activity was observed. However, very low *n:iso* ratios are recorded indicating that at 30 bar the catalyst forms slightly more branched aldehydes than nonanal.

Table 3.1 The effect of temperature and pressure on catalyst precursor **2.11**

Entry	Pressure (bar)	Temperature (°C)	Conversion %	Aldehydes %	Internal olefins %	*n:iso*	TOF/hr
1	30	75	>99	>99	-	0.96	277
2	30	95	>99	>99	-	0.75	277
3	50	75	>99	99	0.6	0.75	276
4	50	95	98	99	-	1.08	271

The reactor was charged with 1:1 toluene/H_2O (10 mL), 1-octene (0.721 g, 6.37 mmol), internal standard *n*-decane (0.180 mg, 1.26 mmol) and Rh loading **2.11** (1.50×10^{-3} g, 2.87×10^{-3} mmol). The reactor was flushed with nitrogen three times, followed by flushing twice with syngas. Standard deviations ±0.67, ± 0.78, ±0.89, ±0.56, ±0.59. TOF = (mmol of aldehydes/mmol of Rh)/time.

When the syngas pressure was increased to 50 bar, at 75 ˚C, slight isomerisation of 1-octene was observed. The *n:iso* did not change whilst the activity was similar to the catalyst's activity at 30 bar. When the temperature was increased to 95 ˚C, a considerable amount of linear aldehydes is formed as indicated by the high *n:iso* ratio (Entry 4). At 8 hours the conversion is effectivity 100% and experiments performed for shorter reaction times showed incomplete conversion of the olefin. In this work, the regioselectivity of the catalysts for nonanal (*n*-aldehyde) is of interest since previously reported catalysts did not show good regioselectivity for nonanal in aqueous biphasic medium.[3,7] Therefore, further experiments were performed under 50 bar syngas pressure and 95 ˚C for 8 hours.

3.2.2 Chemoselectivity and regioselectivity of the mononuclear catalyst precursors 2.11-2.14.

The reactions with the mononuclear catalysts **2.11**-**2.14** were performed under the determined optimum conditions. The water-soluble mononuclear catalyst precursors **2.11**-**2.14** (Figure 3.1) have turnover frequencies in the range 271-277 hr^{-1} (Table 3.2). The presence of the electron-donating and electron-withdrawing substituents does not seem to influence the activity of these catalysts since **2.12** and **2.13** show comparable activity. The catalysts display excellent aldehyde chemoselectivity, with over 99% of the products formed being aldehydes. These results are comparable with what has been reported for similar catalyst precursors by Hager and co-workers.[3]

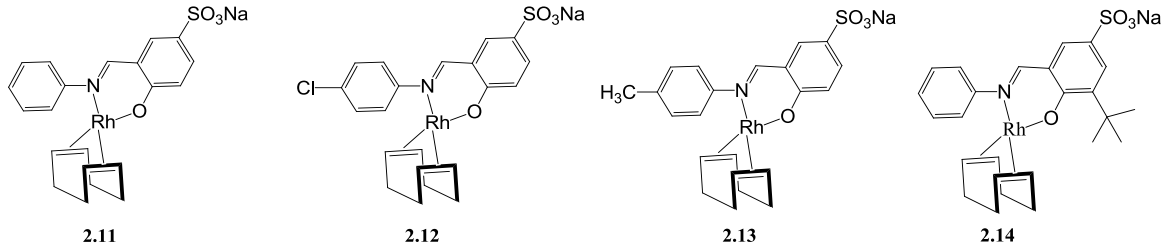

2.11 **2.12** **2.13** **2.14**

Figure 3.1 Water-soluble mononuclear complexes **2.11-2.14**.

Table 3.2 Aqueous biphasic hydroformylation of 1-octene using catalysts **2.11-2.14**.

Catalyst precursor	Pressure (bar)	Temperature (°C)	Conversion %	Aldehydes %	Internal olefins %	n:iso	TOF/hr
2.11	50	95	98	99	-	1.08	271
2.12	50	95	>99	>99	-	0.61	276
2.13	50	95	>99	>99	-	0.16	277
2.14	50	75	>99	>99	-	2.37	276

The reactions were performed in a 90 mL stainless steel pipe reactor. The reactor was charged with 1:1 toluene/H_2O (10 mL), 1-octene (6.37 mmol), internal standard *n*-decane (1.26 mmol) and Rh loading (2.87 x 10^{-3} mmol). The reactor was flushed with nitrogen three times, followed by flushing twice with syngas (1:1, CO: H_2). Standard deviations: ±0.59, ±1.78, ±1.02, ±0.89. TOF = (mmol of aldehydes/mmol of Rh)/time.

Catalyst precursors **2.12** and **2.13**, have good regioselectivity for branched aldehydes (>55%). However, with catalyst **2.14**, over 60% nonanal is formed. The presence of a bulky tertiary butyl moiety in **2.14** could be the reason for the better regioselectivity for nonanal and this is discussed in more detail in Section 3.2.3. These *N,O*-based chelating systems show inferior regioselectivity for the linear products when compared to previously reported *N,N*- and *N,P*-based catalysts for the hydroformylation of 1-octene.[15,16] Upon completion of the reaction, phase separation of the catalyst from the products was performed and the catalyst was used in a subsequent catalytic cycle and this was repeated several times for each catalyst.

3.2.3 Recyclability of the mononuclear catalysts 2.11-2.14.

Chemoselectivity of catalysts 2.11-2.14

All the catalysts (**2.11-2.14**) display excellent recyclability and could be used up to 5 times without significant drop in catalyst activity and 1-octene conversions. The catalysts maintain the aldehyde chemoselectivity above 90% throughout the 5 cycles (Figure 3.2). There is a slight decrease in aldehyde production in the fourth and fifth cycle when catalyst **2.13** (R=H, X=CH_3) was employed.

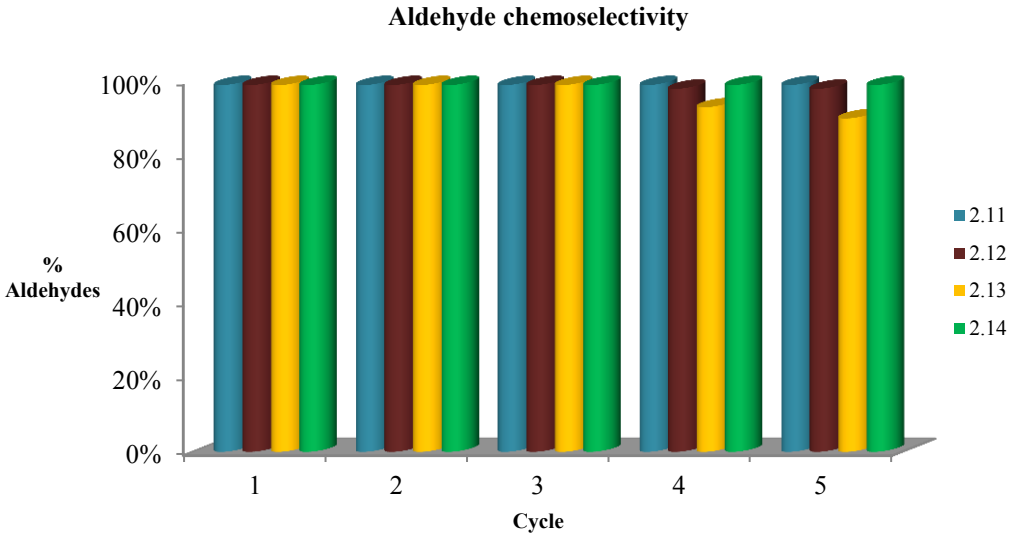

The reactions were performed in a 90 mL stainless steel pipe reactor. Solvent 1:1 toluene/water (10 mL), 1-octene (6.37 mmol), internal standard *n*-decane (1.26 mmol), Rh loading (2.87 x 10^{-3} mmol), Syngas (1:1 CO: H_2), 8 h, 95 °C, 50 bar syngas pressure.

Figure 3.2 Recyclability and aldehyde chemoselectivity for catalysts **2.11**-**2.14**.

Electronic effects

The difference in the reaction rates during hydroformylation of terminal olefins is strongly related to the σ-donor effects rather than the steric effects of the ligand. The basicity of the ligand is known to have an influence on hydroformylation reaction rates.[9] Electron-donating groups result in strong ligand basicity resulting in electron density being more readily donated to the metal centre.[17] These σ-donors result in lower hydroformylation rates due to increased back donation to the CO, which strengthens the Rh-CO bond resulting in a slower rate of CO dissociation which is required to form the active species formation of the Rh(H)(CO)L (where L is the ligand). This species is formed before olefin coordination and is a crucial step in the hydroformylation reaction. For example, trialkylphosphines are known to result in poor hydroformylation activity due to the electron-donating effects of the alkyl groups.[18] On the other hand, arylphosphines are known to give excellent hydroformylation activity due to the electron-withdrawing effects of the aromatic groups.[19] This is because electron-withdrawing substituents facilitate CO dissociation and favour easy coordination of the alkene during hydroformylation.[20] *N,O*-chelating ligands are generally strong σ-donor ligands as previously reported in the literature.[15] Figure 3.3 shows the chemoselectivity of catalysts **2.12** and **2.13** with opposite electronic effects.

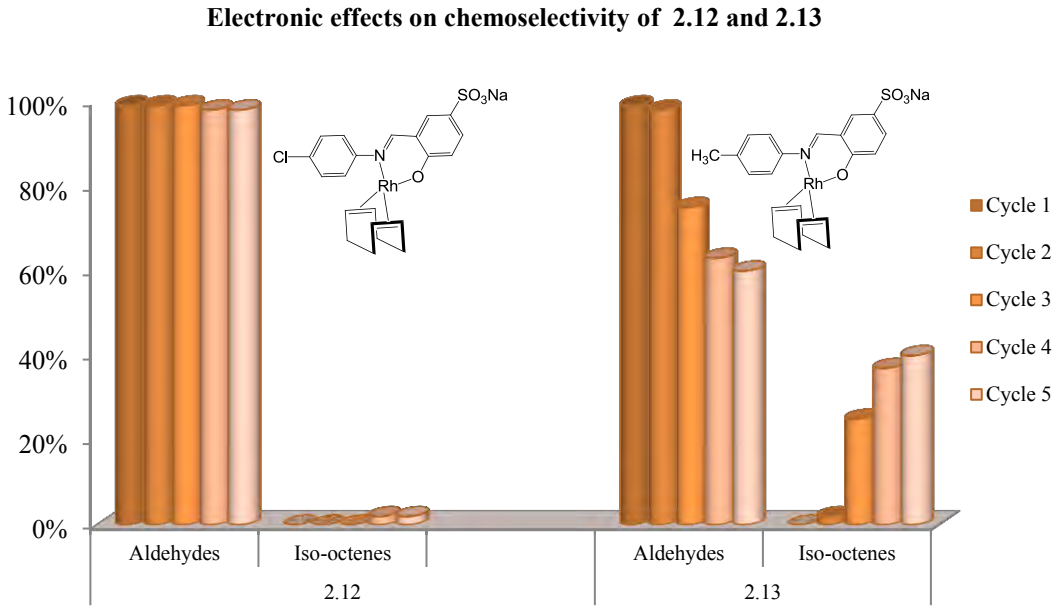

The reactions were performed in a 90 mL stainless steel pipe reactor. Solvent 1:1 toluene/water (10 mL), 1-octene (6.37 mmol), internal standard *n*-decane (1.26 mmol), Rh loading (2.87 x 10^{-3} mmol), Syngas (1:1 CO: H_2), 8 h, 95 °C, 50 bar syngas pressure.

Figure 3.3. Aldehyde chemoselectivity for catalysts **2.12-2.13** in 5 cycles.

The results show that both catalysts display excellent aldehyde chemoselectivity and the most likely key intermediate for good aldehyde chemoselectivity is the Rh-H species. However, upon recycling catalyst **2.13** for the third to the fifth time, aldehyde chemoselectivity begins to drop gradually. Isomerisation becomes more dominant; with almost 30% internal olefins being formed in the final recycle. As recycling is continued with catalyst **2.13**, a significant amount of Rh particles is observed. The isomerisation of 1-octene into 2-octene and 3-octene could be catalysed by the Rh nanoparticles present in the aqueous layer. Nanoparticles have been previously reported to favour isomerisation of olefins during the hydroformylation reaction. [7,21]

The influence of the *chloro* and the *methyl* substitutes on the chemoselectivity of the catalysts **2.12** and **2.13** was not clear in these systems since they show comparable activity in the first run. The varying chemoselectivity in the recycling experiments of **2.13** could only be due to the formation of a different active species from **2.13** which favours the formation of internal octenes. Catalyst **2.12** mantains excellent chemoselectivity for aldehydes which could be as a result of the same active species in the aqueous solution throughout the recycling experiments unlike **2.13** which forms a considerable amount of Rh particles.

Regioselectivity of catalysts ***2.11-2.14***

The regioselectivity of each catalyst varies slightly each time the catalyst is recycled, as shown in Figure 3.3. This could be a result of changes in the structure of the active catalyst with each subsequent reuse. Catalyst **2.14** displays good regioselectivity for the linear aldehyde (nonanal), whilst catalysts **2.11-2.13** favour the production of a mixture of branched aldehydes (2-methyloctanal, 2-ethylheptanal and 2-propylhexanal).

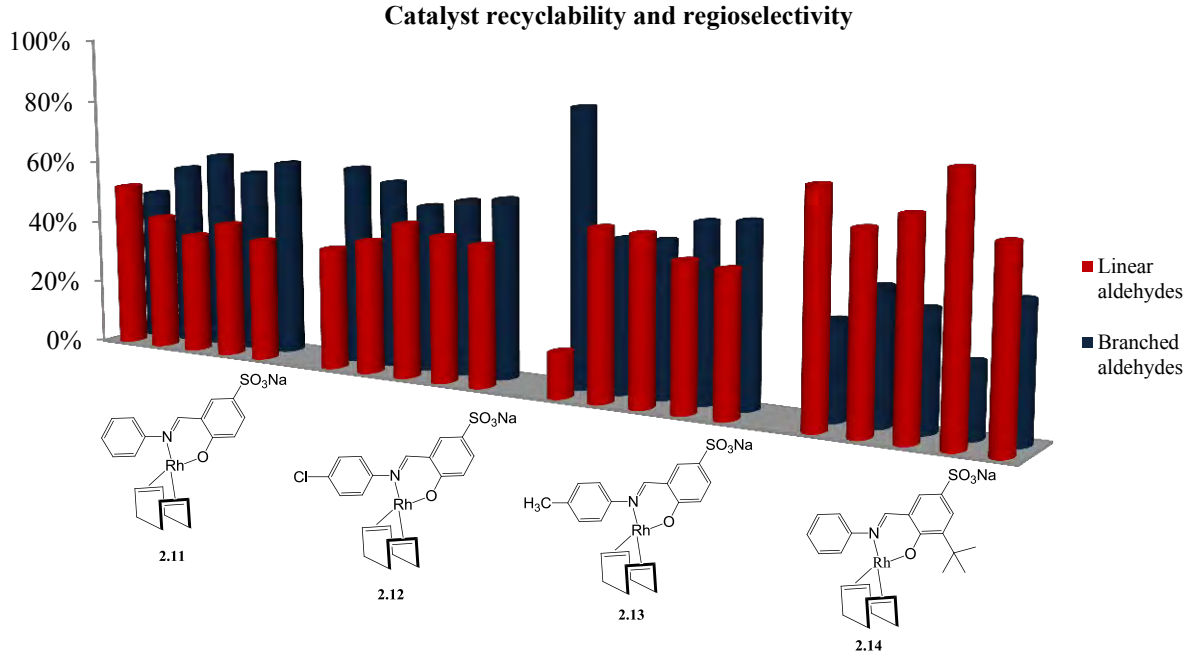

The reactions were performed in a 90 mL stainless steel pipe reactor. Solvent 1:1 toluene/water (10 mL), 1-octene (6.37 mmol), internal standard *n*-decane (1.26 mmol), Rh loading (2.87 x 10^{-3} mmol), Syngas (1:1 CO: H_2), 8 h, 95 °C, 50 bar syngas pressure.

Figure 3.3. Regioselectivity of the catalysts in five recycles.

Catalyst **2.13** shows an unusual trend; with almost 80% branched aldehydes being formed in the first run. There is a significant drop in production of these branched aldehydes in the second cycle and after this almost, 1:1 ratio of linear to branched aldehydes are formed. This is evidence of a different species being present during the reaction using **2.13**. The catalyst regioselectivity remains consistent during the later cycles.

Steric effects

Steric properties of ligands generally play a large role in the regioselectivity of a catalyst during hydroformylation. However, in some cases it is difficult to separate the influence of steric properties and electronic properties on the performance of a catalyst. The choice of

substrate can also influence the type of products that are formed. For example, electron-deficient olefins tend to give branched aldehydes because of stabilisation of the partial negative charge at the carbon bound to the metal.[22] On the other hand, 1,1-disubstituted and trisubstituted olefins favour linear aldehydes to circumvent the formation of a quaternary centre.[23] Regioselectivity can also be controlled through the design and modification of the catalyst.

Casey and co-workers reported that the migratory insertion of an olefin into Rh-H to form the Rh-alkyl species is greatly influenced by the orientation and bulkiness of the ligand.[24] This consequently determines whether linear or branched products will be formed. To investigate this phenomenon, catalyst precursors **2.11** and **2.14** were selected. The results are shown in Figure 3.4. The results indicate that **2.14** containing the tertiary butyl moiety forms more nonanal as compared to the unsubstituted analogue **2.11**.

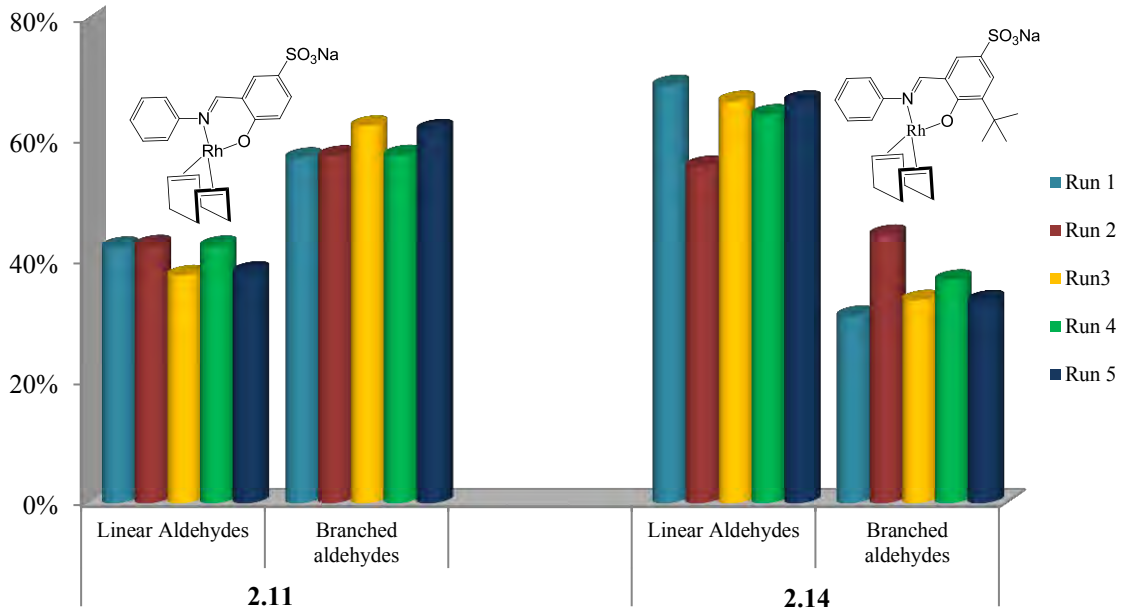

The reactions were performed in a 90 mL stainless steel pipe reactor. Solvent 1:1 toluene/water (10 mL), 1-octene (6.37 mmol), internal standard *n*-decane (1.26 mmol), Rh loading (2.87 x 10^{-3} mmol), Syngas (1:1 CO: H_2), 8 h.

Figure 3.4 Regioselectivity of catalysts **2.11** and **2.14**.

This is in agreement with literature, which has widely explored bulky ligands for application in the synthesis of hydroformylation catalysts, with the aim of forming linear aldehydes.[25–27]

3.2.4 Chemoselectivity and regioselectivity of the binuclear catalysts precursors 2.15-2.18

Similar to the mononuclear derivatives (**2.11**-**2.14**), the binuclear catalysts precursors (**2.15**-**2.18**) were tested at 50 bar syngas pressure and 95 ˚C. The Rh loading for the binuclear catalysts precursors was similar to that of the mononuclear analogues (2.87 x 10^{-3} mmol) so that comparisons can be made between the binuclear catalysts and the mononuclear catalysts. The structures of the binuclear catalyst precursors are shown in Figure 3.5. The aqueous biphasic hydroformylation reactions also proceeded for 8 hours and the results are summarised in Table 3.3. Catalysts **2.15**-**2.18** have activity greater than 210 hr^{-1}, with **2.18** displaying the lowest activity of 214 hr^{-1}. The conversion of 1-octene is excellent (84%-92%); however the 1-octene conversions are slightly lower than what is observed with the mononuclear catalysts **2.11**-**2.14**. The results for the reactions using the binuclear catalysts are summarised in Table 3.3.

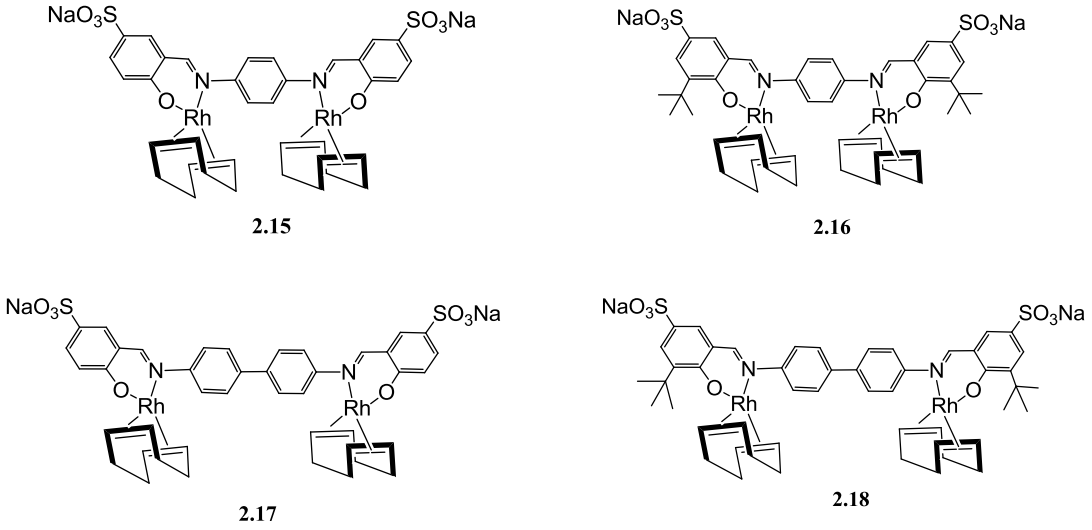

Figure 3.5. Water-soluble binuclear Rh(I) complexes **2.15**-**2.18**.

The chemoselectivity of the catalysts is excellent with over 85% aldehyde chemoselectivity observed for each catalyst. However, very small amounts of internal olefins (2-octene and 3-octene) are formed with the most being formed with **2.18**. Isomerisation is more pronounced with catalysts **2.17** and **2.18** with a biphenyl spacer. Catalysts **2.15** and **2.17** display good regioselectivity for branched aldehydes (2-methyloctanal, 2-ethylheptanal and 2-propylhexanal) whilst **2.16** and **2.18** have good regioselectivity for nonanal with *n*:*iso* ratios of 1.94 and 1.86 respectively.

Table 3.3. Aqueous biphasic hydroformylation of 1-octene using **2.15**-**2.18**.

Catalyst precursor	Conversion %	Aldehydes %	Internal olefins %	Liner Aldehydes	Branched Aldehydes	n:iso	TOF/hr
2.15	87	95	5	33	67	0.49	202
2.16	92	96	4	66	34	1.94	246
2.17	89	87	13	41	59	0.69	224
2.18	90	96	15	65	35	1.86	214

The reactions were performed in a 90 mL stainless steel pipe reactor. The reactor was charged with 1:1 toluene/H_2O (10 mL), 1-octene (0.721 g, 6.37 mmol), internal standard *n*-decane (0.180 mg, 1.26 mmol) and Rh loading **2.15-2.18** (2.87 x 10^{-3} mmol). The reactor was flushed with nitrogen three times, followed by flushing twice with syngas (1:1 CO: H_2). Standard deviations: ±1.58, ± 0.51, ±0.76, ±1.03. respectively. TOF = (mmol of aldehydes/mmol of Rh)/time.

The presence of the tertiary-butyl substituent in catalyst precursors **2.16** and **2.18** results in better regioselectivity for nonanal. This is similar to what was observed with the mononuclear derivative **2.14**. The electronic and steric effects were also investigated for catalysts **2.15**-**2.18**.

Electronic effects

It is expected that if there is cooperation between the two metal centres during catalysis employing binuclear catalysts and usually results in more active and selective.[10,28,29] However, the results obtained for the catalysts **2.15**-**2.18** are comparable to the results obtained with the mononuclear analogues (**2.11**-**2.14**). The aldehyde chemoselectivity for the binuclear catalysts **2.17**-**2.18** is slightly lower (85%-87%), whilst the activity of all the binuclear catalysts is comparable to the activity of the mononuclear catalysts.

It has also been previously reported that ligands usually impart the appropriate electronic properties during the hydroformylation reaction and most importantly must be flexible enough to allow close proximity of the metal centres without disintergrating.[10] The binuclear catalysts **2.15**-**2.18** contain structurally rigid linking aromatic rings connected to the metal centres *via* the imine nitrogen and the phenolic oxygen. The influence of the ligands on the

performance of catalysts **2.17** and **2.15** was investigated. The results are shown in Figure 3.6.

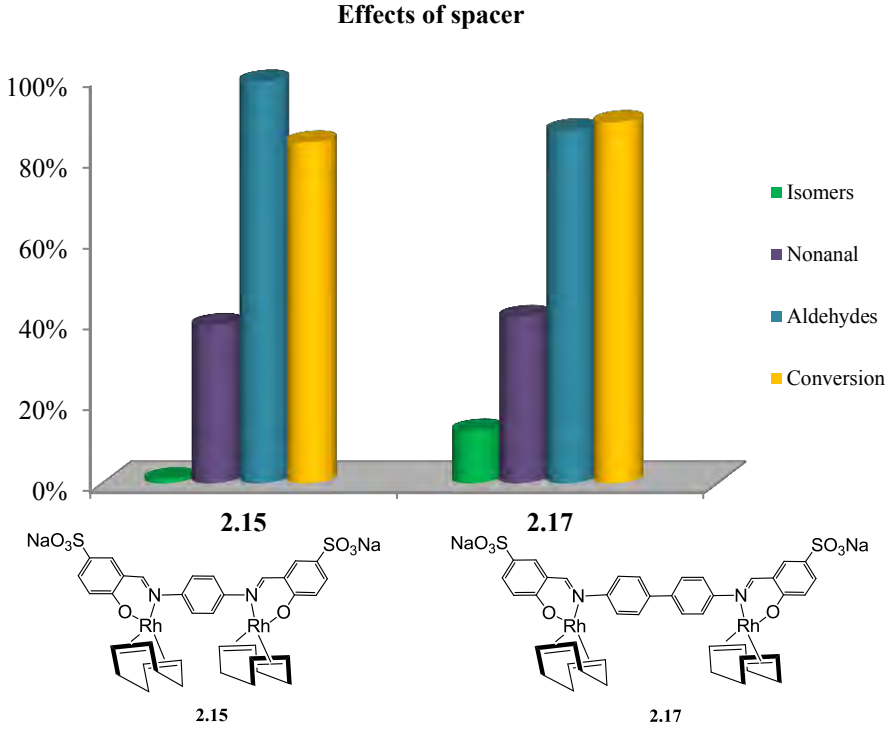

Figure 3.6. Effects of bridging spacer on catalysts **2.15** and **2.17**.

Catalysts **2.15** and **2.17** were selected as a representative example and similar trends were observed with catalysts **2.16** and **2.18**. The performance of **2.15** and **2.17** is comparable with that of **2.16** and **2.18** giving 1-octene conversions of 84% and 89% respectively. Excellent aldehyde chemoselectivity was observed for **2.15** and **2.17** (99% and 87% respectively) however 13 % of the products formed with **2.17** are a mixture of 2-octene and 3-octene. Catalyst **2.17** forms a significant amount of Rh particles in the aqueous layer (not quantified) and these could be responsible for the isomerisation activity of this catalyst. It has been previously reported in the literature that binuclear catalysts usually disintegrate into mononuclear species and/or metal nanoparticles during the hydroformylation reaction. This is because of large amounts of substrates present, i.e. H_2, CO and the olefin.[30] These nanoparticles have been reported to result in the isomerisation reaction to compete with the hydroformylation reaction.[3,7] Rh nanoparticles also produce unwanted internal olefins. Mercury poisoning experiments were conducted to investigate the influence of these Rh particles on the hydroformylation activity in these systems. This will be discussed later in this chapter.

The biphenyl spacer possibly allows easy formation of Rh nanoparticles since a significant amount of Rh particles is seen suspended in the aqueous layer after the reaction with **2.18** and

2.18. Disintegration of the catalyst precursors into nanoparticles could be occurring for these catalysts under catalytic conditions. This has been observed for other binuclear catalysts in the literature and could affect the chemoselectivity of the catalysts. [31–33] The presence of two metals in the binuclear catalysts (**2.15-2.18**) does not result in improved catalytic activity and selectivity as expected, however this has been previously observed by Stanley for binuclear catalysts.[34,35]

Steric effects

The effect of having the tertiary butyl moiety in the complexes was investigated. Catalyst precursors **2.16** and **2.18** containing the tertiary butyl moiety have good regioselectivity for nonanal and both have *n:iso* ratios of 1.94 and 1.86 respectively. Catalyst precursors **2.15** and **2.17** without the tertiary butyl substituent have *n:iso* ratios of 0.64 and 0.69 respectively. This shows that the presence of the tertiary butyl moiety influences the regioselectivity of the catalysts. Figure 3.7 shows the difference in regioselectivity for **2.17** and **2.18** and these catalysts were selected as a representative example to show the influence of the presence of the tertiary butyl moiety.

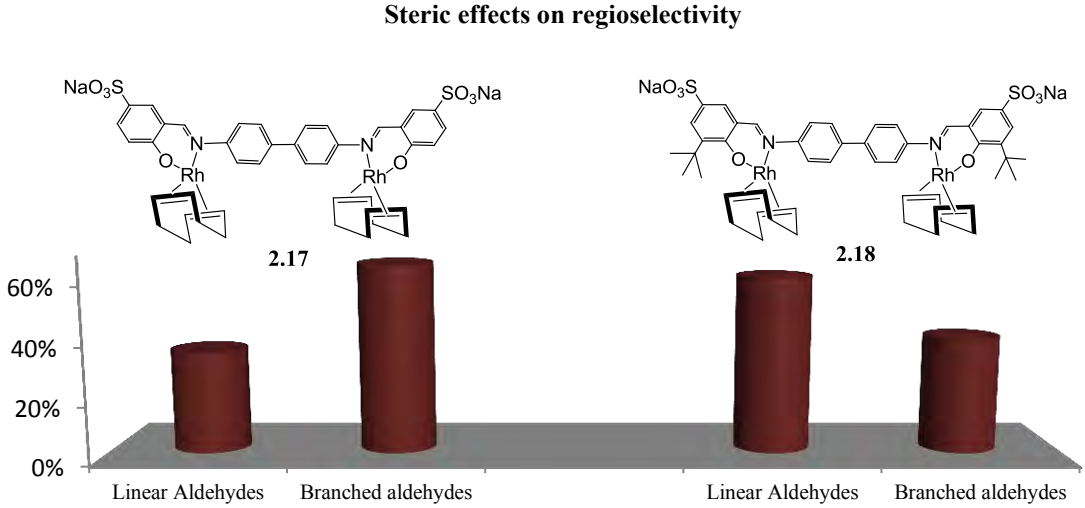

The reactions were performed in a 90 mL stainless steel pipe reactor. Solvent 1:1 toluene/water (10 mL), 1-octene (6.37 mmol), internal standard *n*-decane (1.26 mmol), Rh loading (2.87 x 10^{-3} mmol), Syngas (1:1 CO: H_2), 8 h.

Figure 3.7 Steric effects on the regioselectivity of **2.17** and **2.18**.

Catalyst **2.18** forms 65% nonanal and a 45% mixture of 2-methyloctanal, 2-ethylheptanal and 2-propylhexanal. Catalyst **2.16** forms 66% nonanal which shows comparable regioselectivity to **2.18**. In industrial aqueous biphasic hydroformylation of propene, it has been reported that

the presence of more bulky triphenylphosphine ligands favour the formation of normal butyraldehyde.[36] It shows that steric hindrances around or close to the metal result in the formation of linear products and this is displayed with catalysts **2.16** and **2.18** systems.

3.2.5 Recyclability of the binuclear catalysts 2.15-2.18.

Similar to the reactions with the mononuclear catalysts, the aqueous phase could be easily recovered by simple decantation for reuse. The catalysts **2.15-2.18** could be recycled three times with a significant change in chemoselectivity and activity after each recycle. After the first reaction, Rh particles were observed in the aqueous layer as a suspension in the aqueous layer. The aldehyde chemoselectivity of catalysts **2.15-2.18** in the recycling experiments is shown in Figure 3.8.

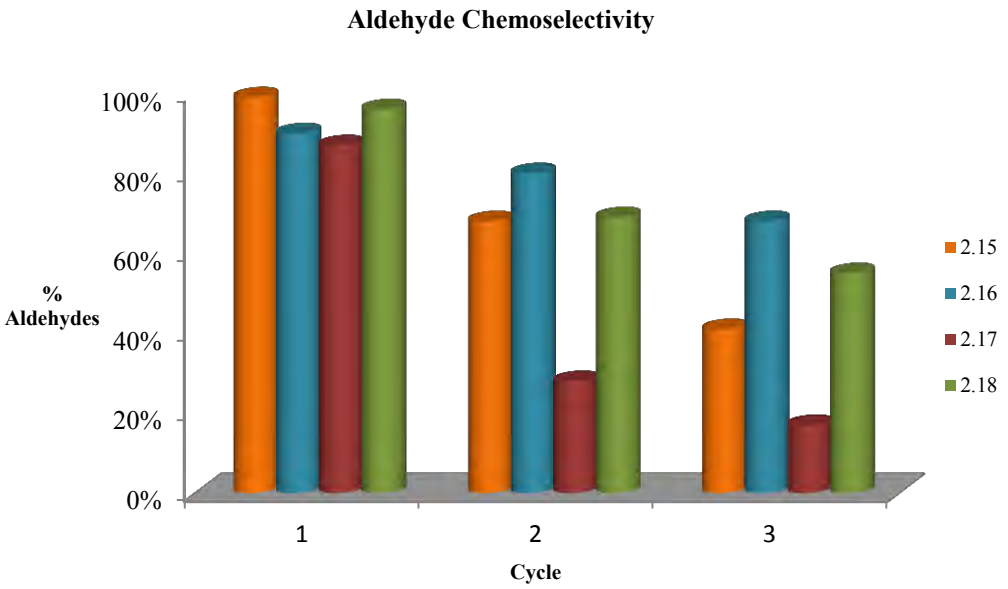

The reactions were performed in a 90 mL stainless steel pipe reactor. Solvent 1:1 toluene/water (10 mL), 1-octene (6.37 mmol), internal standard *n*-decane (1.26 mmol), Rh loading (2.87 x 10^{-3} mmol), Syngas (1:1 CO: H_2), 8 h.

Figure 3.8 Recyclability and aldehyde chemoselectivity for catalysts **2.15-2.18**.

The binuclear catalysts **2.15-2.18** display excellent aldehyde chemoselectivity in the first run, with all catalysts producing over 85% aldehydes. The amount of aldehydes formed with catalysts **2.15**, **2.16** and **2.18** are in the range 68% - 80% in the second cycle. In the third cycle, the amount of aldehydes produced was 41%, 17% and 55% with catalysts **2.15**, **2.16** and **2.18** respectively. Internal olefins (2-octene and 3-octene) are the only side products formed during the reaction and no hydrogenation is observed. The change in the chemoselectivity during the recycling experiments using the catalysts could be attributed to

the formation of a different active species each time the catalysts are reused. Catalyst **2.18** (with tertiary butyl substituent) shows better recyclability than **2.17** possibly because of the absence of the tertiary butyl moiety which probably causes **2.17** to be less stable hence its poor recyclability.

The results show that the mononuclear catalysts (**2.11-2.14**) have superior hydroformylation activity, display better recyclability in addition to maintaining excellent aldehyde chemoselectivity in 5 cycles (Figure 3.2). Catalyst precursor disintegration and/or formation of nanoparticles were more pronounced with the binuclear catalysts **2.15-2.18**. This could have resulted in lower activity and lower aldehyde chemoselectivity with the binuclear series.

3.2.6 Mononuclear catalysts versus binuclear catalysts

Since the Rh loading is the same for all the experiments (2.87 x 10^{-3} mmol), a comparison was made between the activity of the mononuclear catalysts (**2.11-2.14**) and the binuclear catalysts (**2.15-2.18**) in the first catalytic run (Figure 3.9). The activity of the catalysts was calculated based on the amount of aldehydes formed. It was observed that the mononuclear catalysts **2.11-2.14** displayed activity between 250 hr^{-1} and 270 hr^{-1} whilst the binuclear catalysts showed activity between 150 hr^{-1} and 250 hr^{-1}. The activity of the catalysts is comparable; however the activity of the binuclear catalysts was slightly lower. This is probably because each metal centre in the binuclear catalysts **2.15-2.18** acts as a single mononuclear catalyst and hence the comparable activity to the mononuclear analogues.

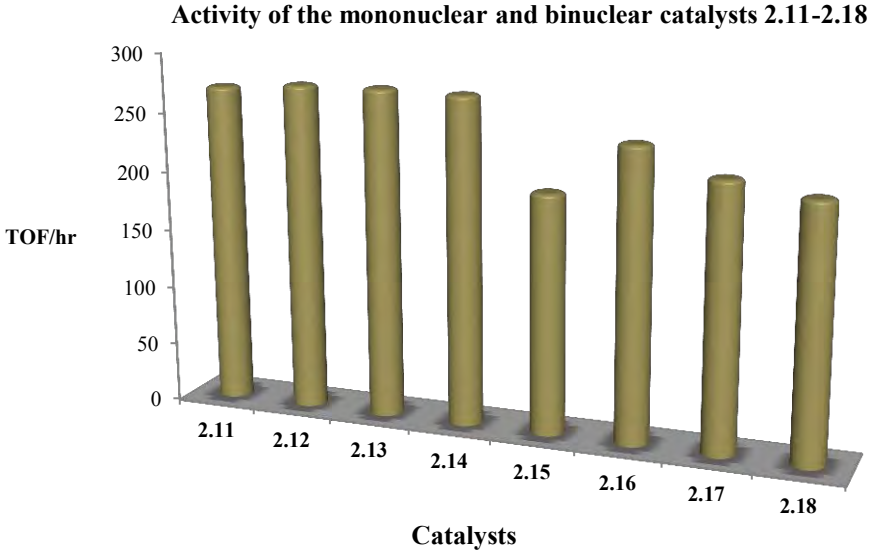

The reactions were performed in a 90 mL stainless steel pipe reactor. Solvent 1:1 toluene/water (10 mL), 1-octene (6.37 mmol), internal standard *n*-decane (1.26 mmol), Rh loading (2.87 x 10^{-3} mmol), Syngas (1:1 CO: H_2), 8 h. TOF = (mmol of aldehydes/mmol of Rh)/time.

Figure 3.9. Activity of the catalysts **2.11**-**2.18** in the first catalytic run.

Catalysis using binuclear catalysts has been widely explored and some researchers have reported absence of cooperativity between the catalytic active metal centres. For example, in a study of binuclear catalysed hydroformylation, Reek and co-workers suggested the actual active species are usually mononuclear species formed from the binuclear catalyst precursors.[30] Diéguez and co-workers have also proved using various spectroscopic techniques that disintegration of binuclear complexes is possible under hydroformylation conditions to form mononuclear catalysts which subsequently become the active catalysts.[37] Davis et al. also confirmed evidence for mononuclear catalysed hydroformylation using kinetic studies for a reaction were a binuclear catalyst was used as the precursor.[38] All these reports point to the fact that it is possible that the binuclear catalyst precursors **2.15**-**2.18** could be behaving as mononuclear catalysts and hence the comparable activity to their mononuclear analogues **2.11**-**2.14**. The structures of the catalysts previously reported in the literature are different from the structures of the binuclear catalysts reported in this chapter and therefore it is possible that the active species with the comparable activity with the mononuclear catalysts could be as a result of other factors other than catalyst disintergration.

3.3 Inductively coupled plasma optical spectrometry experiments

Analysis of the catalyst-containing aqueous layer was performed using inductively coupled plasma optical spectrometry experiments for each catalyst. Rhodium leaching into the toluene layer is a possible way the catalyst could be lost from the aqueous solution and hence the gradual decrease in activity with increase in the number of recycles. Rh and Ru leaching has been observed previously in the aqueous biphasic hydroformylation of 1-octene.[3,7] The analyses were performed to determine the amount of Rh present in solution after the final cycle for each catalyst. Sample preparation involved filtering the aqueous layer which contained suspended Rh particles, since all the catalyst precursors were completely soluble in water at the beginning of each experiment.

Less than 1% Rh was detected in solution for catalysts **2.11**-**2.14**. Only 0.5% metal was detected in the aqueous layer containing catalysts **2.13** and **2.11** whilst less than 0.1% Rh was present in the aqueous layer of **2.10** and **2.12**. At the end of the recycling experiments of the binuclear catalysts **2.15**-**2.18**, each aqueous layer contained less than 0.01% metal in solution. Analyses of the organic layer from all of the reactions using the mononuclear and binuclear catalysts **2.11**-**2.18** show that there are no traces of metal present in the organic phase.

These results indicate that there was relatively little leaching of metal catalysts from the aqueous layer into the organic layer, but the formation of nanoparticles from the homogeneous catalysts. The hydroformylation activity observed in the recycling experiments is therefore due to a combination of the homogeneous catalysts and the Rh nanoparticles. To further confirm the possibility of nanoparticle mediated hydroformylation in these systems, the mercury poisoning experiment was performed.

3.4 Mercury poisoning experiments

The mercury poisoning experiment is useful in differentiating between homogeneous and heterogeneous transition-metal catalysed reactions. Mercury(0) can form amalgams in the presence of metal particles which can be responsible for heterogeneous catalysis.[39] Poisoning of any heterogeneous catalyst present will inhibit the activity of heterogeneous catalysts and therefore this experiment can be used as an indicator of whether or not heterogeneous catalysis is taking place.

A drop of mercury was added to the reaction vessel at the start of the experiment. Even though the binuclear catalysts showed a significant amount of Rh particles in the aqueous layer, the mononuclear catalyst **2.13** was selected for this experiment. Firstly, because the catalyst could be recycled five times and hence analysis of a broader range of results could be done. Out of the mononuclear catalysts, **2.13** formed the most Rh particles. Catalyst **2.13** also formed internal olefins during the recycling experiments, which could be as a result of the presence of Rh particles in the aqueous layer. Table 3.4 shows the results obtained using **2.13** in the absence of mercury. The recyclability of the catalyst is excellent with regioselectivity and chemoselectivity remaining consistent throughout the recycles. However, there is a gradual drop in the activity of the catalyst with each recycle probably due to catalyst deactivation with increase in the number of recycles. The same reaction was repeated using **2.13** in the presence of mercury (Table 3.5).

Table 3.4. Aqueous biphasic hydroformylation of 1-octene using **2.13** in the absence of mercury.

Cycle	Pressure (bar)	Temperature (°C)	Conversion %	Aldehydes %	Iso-octenes %	n:iso	TOF/hr
1	50	95	95	92	8	0.71	241
2	50	95	89	88	12	0.74	224
3	50	95	87	74	25	0.52	214
4	50	95	86	73	27	0.55	201
5	50	95	86	71	29	0.51	186

The reactions were performed in a 90 mL stainless steel pipe reactor. The reactor was charged with 1:1 toluene/H_2O (10 mL), 1-octene (6.37 mmol), internal standard *n*-decane (1.26 mmol) and Rh loading (2.87 x 10^{-3} mmol). The reactor was flushed with nitrogen three times, followed by flushing twice with syngas (1:1, CO: H_2). Standard deviations: ±1.78, ±0.56, ±0.93, ±0.59, ±1.02. TOF = (mmol of aldehydes/mmol of Rh)/time.

It is observed from the results that the formation of Rh particles begins in the first cycle because there is a significant drop in activity from 241 hr^{-1} to 121 hr^{-1} in the presence of mercury. Upon recycling, the activity drops to 62 hr^{-1} and 52 hr^{-1} in the second and third cycles respectively. No activity is observed in the fourth cycle and fifth cycle. For Entry 3 in Table 3.5, only branched aldehydes are formed in the presence of mercury.

Table 3.5. Aqueous biphasic hydroformylation of 1-octene using catalyst precursor **2.13** in the presence of mercury.

Cycle	Pressure (bar)	Temperature (°C)	Conversion %	Aldehydes %	Iso-octenes %	n:iso	TOF/hr
1	50	95	91	48	52	2.55	121
2	50	95	64	47	53	1.45	62
3	50	95	60	35	65	-	52
4	50	95	-	-	-	-	-
5	50	95	-	-	-	-	-

The reactions were performed in a 90 mL stainless steel pipe reactor. The reactor was charged with 1:1 toluene/H_2O (10 mL), 1-octene (6.37 mmol), internal standard *n*-decane (1.26 mmol) and Rh loading (2.87 x 10^{-3} mmol). The reactor was flushed with nitrogen three times, followed by flushing twice with syngas (1:1, CO: H_2). Standard deviations: ±1.08, ±1.16, ±0.02, ±0.89, ±1.12. TOF = (mmol of aldehydes/mmol of Rh)/time.

These results indicate that a combination of homogeneous catalysis and catalysis mediated by nanoparticles is taking place in these systems. In the fourth and fifth runs in Table 3.4, activity of the catalyst is entirely due to Rh nanoparticles since no activity is observed in the presence of mercury for the same runs.

3.5 Overall Summary

The water-soluble mononuclear and binuclear complexes **2.11**-**2.18** were evaluated as catalyst precursors in the aqueous biphasic hydroformylation of 1-octene. The catalysts display very good activity, chemoselectivity and recyclability at 50 bar syngas pressure and 95 °C in the aqueous biphasic hydroformylation of 1-octene. The conversion of 1-octene is above 85% for all catalysts the first time the catalysts are used. Isomerisation of 1-octene is the only side reaction observed as evidenced by the formation of mixtures of 2-octene and 3-octene. The tertiary butyl substituent results in good regioselectivity for nonanal for catalysts **2.14**, **2.16** and **2.18**. The influence of the electron-withdrawing *chloro*- group and electron

donating methyl group was not clear as catalysts **2.12** and **2.13** showed comparable chemoselectivity and activity. The mononuclear catalysts (**2.11-2.14)** have activity that is comparable to that of the binuclear catalysts (**2.15-2.18)** with activities in the range 150 hr^{-1} – 270 hr^{-1}. This comparable activity could be as a result of the metal centres in the binuclear catalysts (**2.15-2.18**) acting as two separate mononuclear catalysts without any cooperativity.

In the recycling experiments, the catalysts could be easily recovered and be recycled up to either 5 times (mononuclear catalysts) or 3 times (binuclear catalysts). A significant amount of Rh particles was formed with the binuclear catalysts (**2.15-2.18**) which could have resulted in formation of internal olefins. Inductively coupled plasma optical spectrometry experiments confirm that no leaching of the catalysts to the organic layer occurs because no traces of metal were detected in the toluene layer. Analyses of the aqueous layers after the recycling experiments show that less than 1% metal is present in solution. Therefore the hydroformylation activity observed in these systems is due to a combination of homogeneous catalysis and catalysis mediated by Rh nanoparticles. This was confirmed by the mercury poisoning experiment, which shows suppressed activity of the catalysts in the presence of mercury.

3.6 Experimental

General Details

Hydroformylation samples were analysed on a Perkin Elmer Clarus 580 GC. Inductively coupled plasma optical emission spectroscopy experiments were carried out on ICP-OES Varian 730-ES.

General method for the hydroformylation reactions

The reactions were performed in a 90 mL stainless steel pipe reactor. The reactor was charged with 1:1 toluene/H_2O (10 mL), 1-octene (6.37 mmol), internal standard *n*-decane (1.26 mmol) and the Rh loading (2.87 x 10^{-3} mmol). The reactor was flushed with nitrogen three times, followed by flushing twice with syngas (1:1, CO: H_2). This was then pressurised and heated to the desired pressure and temperature. All reactions were done for 8 hours and samples were collected at the beginning and at the end of each reaction. Samples were analysed by gas chromatography and products were confirmed in relation to authentic internal octenes and isomers of nonanal. All reactions were performed in duplicate and results

recorded are an average of two identical experiments. Catalyst recycling was performed by decanting the organic layer followed by addition of a fresh substrate and the hydroformylation procedure was repeated.

3.7 References

1 G. T. Whiteker and C. J. Cobley, *Top Organomet. Chem.*, 2012, **42**, 35–46.

2 L. Obrecht, P. C. J. Kamer and W. Laan, *Catal. Sci. Technol.*, 2013, **3**, 541-551.

3 E. B. Hager, B. C. E. Makhubela and G. S. Smith, *Dalton Trans.*, 2012, **41**, 13927–13935.

4 K. H. Shaughnessy, *Chem. Rev.*, 2009, **109**, 643–710.

5 N. T. S. Phan, C. S. Gill, J. V Nguyen, Z. J. Zhang and C. W. Jones, *Angew. Chem. Int. Ed. Engl.*, 2006, **45**, 2209–2212.

6 M. E. Hanhan, C. Cetinkaya and M. P. Shaver, *Appl. Organomet. Chem.*, 2013, **27**, 570–577.

7 L. C. Matsinha, P. Malatji, A. T. Hutton, G. A. Venter, S. F. Mapolie and G. S. Smith, *Eur. J. Inorg. Chem.*, 2013, 4318–4328.

8 J. D. Unruh and J. R. Christenson, *J. Mol. Cat.*, 1982, **14**, 19–34.

9 E. R. Tucci, *Ind. Eng. Chem. Prod. Res. Dev.*, 1970, **9**, 516–521.

10 M. A. F. Hernandez-Gruel, G. Gracia-Arruego, A. B. Rivas, I. T. Dobrinovitch, F. J. Lahoz, A. J. Pardey, L. A. Oro and J. J. Pérez-Torrente, *Eur. J. Inorg. Chem.*, 2007, 5677–5683.

11 M. G. Timerbulatova, M. R. D. Gatus, K. Q. Vuong, M. Bhadbhade, G. Algarra, S. A. Macgregor and B. A. Messerle, *Organometallics*, 2013, **32**, 5071-5081.

12 N. Guo, L. Li and T. J. Marks, *J. Am. Chem. Soc.*, 2004, **126**, 6542–6543.

13 E. van den Beuken and B. L. Feringa, *Tetrahedron*, 1998, **54**, 12985–13011.

14 B. Xia, H. Zhang, C. Che, K. Leung, D. L. Phillips, N. Zhu and Z. Zhou, *J. Am. Chem. Soc.*, 2003, **125**, 10362–10374.

15 B. C. E. Makhubela, A. Jardine and G. S. Smith, *Green Chem.*, 2012, **14**, 338–347.

16 B. C. E. Makhubela, A. M. Jardine, G. Westman and G. S. Smith, *Dalton Trans.*, 2012, **41**, 10715–23.

17 Y. Ohgomori, S. Yoshida and Y. Watanabe, *J. Mol. Cat.*, 1987, **43**, 249–258.

18 J. K. MacDougall, M. C. Simpson, M. J. Green and D. J. Cole-Hamilton, *J. Chem. Soc. Dalton Trans.*, 1996, 1161–1172.

19 F. H. Jardine, J. A. Osborn, G. Wilkinson and G. F. Young, *Chem. Ind.*, 1965, 560–561.

20 C. S. Vasam, S. Modem, S. Kankala, G. Budige and R. Vadde, *Appl. Organomet. Chem.*, 2009, **23**, 460–466.

21 M. Kontkanen, M. Tuikka, N. Kinnunen, S. Suvanto and M. Haukka, *Catalysts*, 2013, **3**, 324–337.

22 I. Ojima, *Chem. Rev.*, 1988, **88**, 1011–1030.

23 B. Breit and W. Seiche, *Synthesis*, 2001, **1**, 1–36.

24 C. P. Casey, E. Lin Paulsen, E. W. Beuttenmueller, B. R. Proft, L. M. Petrovich, B. A. Matter and D. R. Powell, *J. Am. Chem. Soc.*, 1997, **119**, 11817–11825.

25 T. P. Clark, C. R. Landis, S. L. Freed, J. Klosin and K. A. Abboud, *J. Am. Chem. Soc.*, 2005, **127**, 5040–5042.

26 S. Yu, X. Zhang, Y. Yan, C. Cai, L. Dai and X. Zhang, *Chem. A Eur. J.*, 2010, **16**, 4938–4943.

27 Y. Yan and X. Zhang, *J. Am. Chem. Soc.*, 2006, **128** , 16058–16061.

28 S. W. S. Choy, M. J. Page, M. Bhadbhade and B. A. Messerle, *Organometallics*, 2013, **32**, 4726–4729.

29 I. Bratko and M. Gómez, *Dalton Trans.*, 2013, **42**, 10664–81.

30 D. G. H. Hetterscheid, S. H. Chikkali, B. de Bruin and J. N. H. Reek, *ChemCatChem*, 2013, **5**, 2785–2793.

31 N. Tsukada, T. Mitsuboshi, H. Setoguchi and Y. Inoue, *J. Am. Chem. Soc.*, 2003, **125**, 12102–12103.

32 N. Wheatley and P. Kalck, *Chem. Rev.*, 1999, **99**, 3379–3419.

33 R. C. Matthews, D. K. Howell, W. Peng, Spencer G. Train, W. D. Treleaven and G. G. Stanley, *Angew. Chem. Int. Engl.*, 1996, **35**, 2253–2256.

34 D. A. Aubry, N. N. Bridges, K. Ezell and G. G. Stanley, *J. Am. Chem. Soc.*, 2003, **125**, 11180–11181.

35 W. Peng, S. G. Train, D. K. Howell, F. R. Fronczek and G. G. Stanley, *Chem. Commun.*, 1996, **882**, 2607-2612.

36 R. Tudor and M. Ashley, *Platinum. Met. Rev.*, 2007, **51**, 164–171.

37 M. Diéguez, C. Claver, A. M. Masdeu-Bultó, A. Ruiz, P. W. N. M. van Leeuwen and G. C. Schoemaker, *Organometallics*, 1999, **18**, 2107–2115.

38 R. Davis, J. W. Epton and T. G. Southern, *J. Mol. Cat.*, 1992, **77**, 159–163.

39 G. M. Whitesides, M. Hackett, R. L. Brainard, J. P. M. Lavalleye, A. F. Sowinski, A. N. Izumi, S. S. Moore, D. W. Brown and E. M. Staudt, *Organometallics*, 1985, **4**, 1819–1830.

Chapter 4

Synthesis and characterization of water-soluble mono- and binuclear thiosemicarbazone Pd(II) complexes

This chapter forms part of the following publication:

Water-soluble Palladium(II) sulfonated thiosemicarbazone complexes: Facile synthesis and preliminary catalytic studies in the Suzuki-Miyaura cross-coupling reaction in water. **Leah C. Matsinha,** Jincheng Mao, Selwyn F. Mapolie, and Gregory S. Smith, *European Journal of Inorganic Chemistry*, 2015, 4088-4094.

4.1 Introduction

Thiosemicarbazone ligands are versatile ligands which can coordinate as neutral ligands or in their deprotonated form. This class of ligands has two tautomeric forms (**a**) and (**b**) as shown in Scheme 4.1.[1] These Schiff base type compounds have interesting coordination modes to a wide range of metals.[2] When additional donor groups such as $–PR_2$, NH_2, -OH or –SH are present, the resulting thiosemicarbazone ligands can coordinate in a tridentate fashion resulting in highly stable metal complexes.[1] It is believed that the metal chelating ability of thiosemicarbazone ligands accounts for the wide application of thiosemicarbazone complexes.[3]

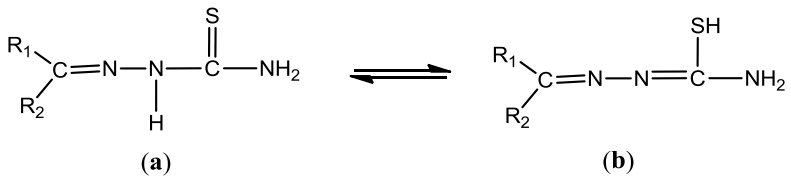

Scheme 4.1. Two tautomers of thiosemicarbazone ligands.

Transition metal complexes of thiosemicarbazones are of importance because of their interesting biological properties (anti-tumoral, anti-bacterial, anti-fungal).[3–14] The study of complexes of thiosemicarbazones for biological applications has been prolific and it was only

in 1998 that Pelagatti and co-workers first reported the application of thiosemicarbazone complexes for catalysis.[15] In this work, Pelagatti and co-workers report the homogeneous hydrogenation of phenylacetylene using a thiosemicarbazone Pd(II) catalyst which displays high chemoselectivity.

Several reports are available in the literature on the application of thiosemicarbazone complexes as catalysts for various cross-coupling reactions such as the Mizoroki-Heck, Suzuki-Miyaura and Sonogashira reactions.[16–21] However, in most of these reports the reactions were performed in an organic medium and catalysts could not be recovered for recycling. Using water as a reaction medium allows easy separation of catalysts from the organic products and consequently catalyst recycling becomes possible.

The synthesis of water-soluble Pd catalysts for the application in the Suzuki-Miyaura cross-coupling reaction in aqueous medium was first reported by Casalnuovo and co-workers.[22] In this work, the authors describe Pd-catalysed Suzuki-Miyaura cross-coupling reactions in a single basic aqueous phase. Water also has many advantages over conventional organic solvents because it is a green solvent (non-toxic, non-flammable, odourless and environmentally friendly).[23] This has motivated the synthesis of a series of new water-soluble Pd(II) sulfonated thiosemicarbazone complexes. These Pd(II) complexes have been evaluated as catalyst precursors in the Suzuki-Miyaura cross-coupling reactions in neat water. In this chapter, the synthesis of a series of water-soluble salicylaldimine thiosemicarbazone ligands and their corresponding water-soluble Pd(II) thiosemicarbazone salicylaldimine complexes is discussed.

4.2 Synthesis and characterization of water-soluble sulfonated salicylaldimine thiosemicarbazone ligands

4.2.1 Synthesis and characterization of sulfonated monothiosemicarbazone salicylaldimine ligand 4.1

The salicylaldimine monothiosemicarbazone **4.1** was prepared *via* a Schiff base condensation reaction between the sulfonated salicylaldehyde **2.1** (preparation discussed in Chapter 2) and thiosemicarbazide in ethanol under reflux conditions (Scheme 4.2). The ligand was isolated in 93% yield as an off-white solid, with good water-solubility at room temperature (8 mg/mL). The ligand decomposes without melting at 225 ˚C.

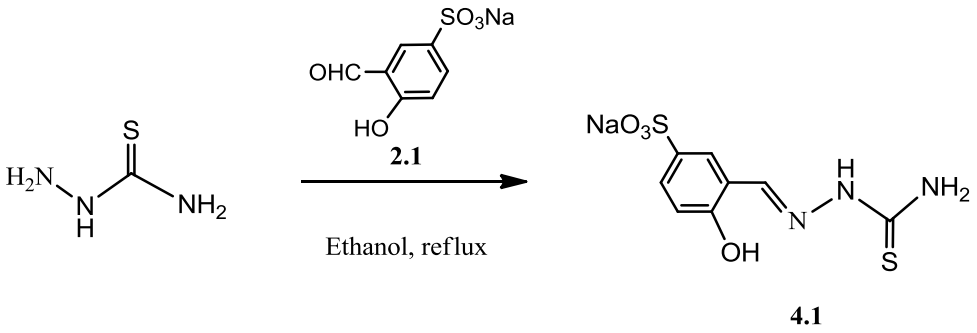

Scheme 4.2. Synthesis of water-soluble salicylaldimine monothiosemicarbazone **4.1**

The ligand **4.1** was characterized using various techniques such as nuclear magnetic resonance spectroscopy, mass spectrometry, infrared spectroscopy and elemental analysis. The ^{1}H NMR assignments were compared to literature assignments for similar compounds and are consistent with previous reports.[9] The most important signal to note is that for the imine proton at 8.36 ppm which confirms a successful Schiff base condensation reaction between the sulfonated salicylaldehyde and thiosemicarbazide. At 11.32 ppm a signal for the hydrazinic proton is observed due to the electron withdrawing effects of the hydrazinic nitrogen and the imine nitrogen adjacent to it. A broad singlet is observed at 9.96 ppm for the phenolic proton. The terminal amino protons are observed as two separate singlets at 8.06 ppm and 7.69 ppm. This is due to restricted rotation of the amino group about the C-N bond which results from delocalization of the NH_2 lone pair of electrons (Scheme 4.3). This phenomenon has also been observed in the literature.[9]

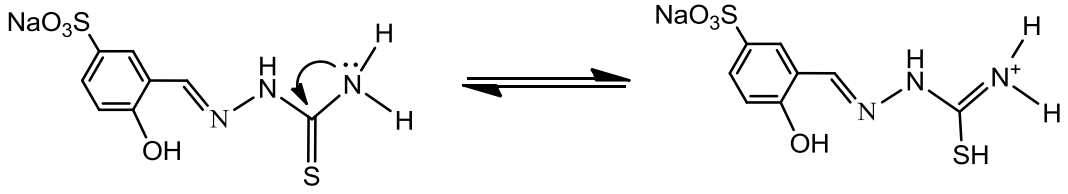

Scheme 4.3 Tautomers of ligand **4.1**.

The aromatic protons are observed at 6.78 ppm, 7.45 ppm and 7.92 respectively. The ^{13}C{H} NMR spectrum of ligand **4.1** shows the expected number of carbon signals which further supports the proposed structure.

In the infrared spectrum of the ligand, an intense absorption band is observed at 1630 cm^{-1} for the C=N functionality. This further confirms the success of the Schiff base condensation

reaction between the thiosemicarbazide and the sulfonated salicylaldehyde **2.1**. The C=S absorption band is observed at 831 cm^{-1}. The electrospray ionisation mass spectrum of the ligand was recorded in the negative ion-mode and shows the molecular ion peak for $[M]^-$ at m/z = 273.9901, where M represents the anionic ligand. The elemental analytical data of the ligand is consistent with its composition and includes two molecules of water.

4.2.2 Synthesis and characterization of sulfonated dithiosemicarbazone salicylaldimine ligand 4.3.

The preparation of the dithiosemicarbazone, entailed a nucleophilic addition reaction of hydrazine to benzene-1,4-diisothiocyanate to afford the dithiosemicarbazide **4.2**.[24] This was followed by a Schiff base condensation reaction with two equivalents of the sulfonated salicylaldehyde **2.1** and dithiosemicarbazide **4.2** under reflux conditions to afford **4.3** as an off-white solid in 78% yield (Scheme 4.4).

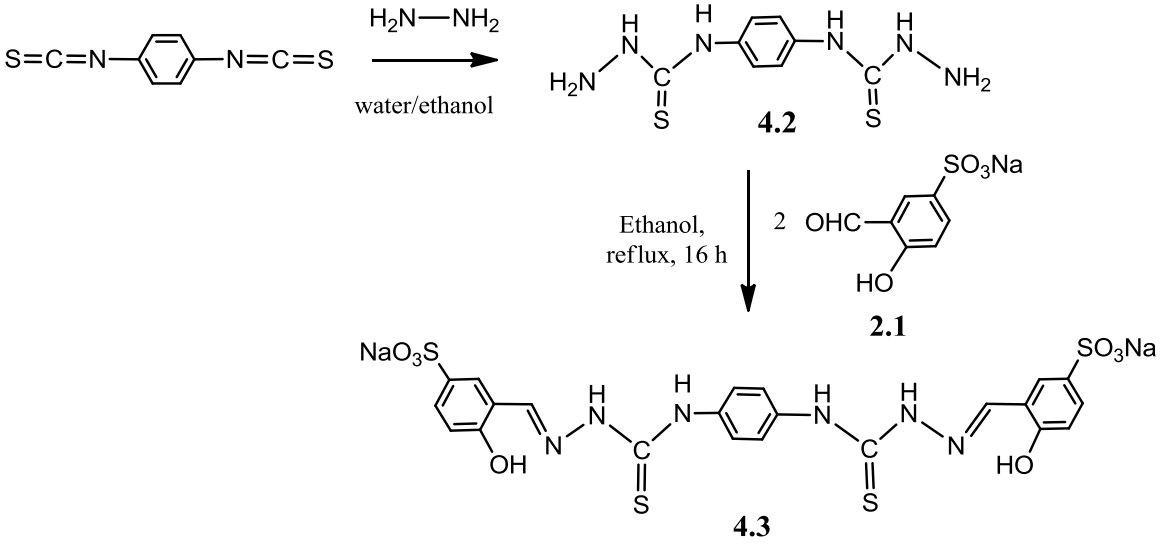

Scheme 4.4. Synthesis of water-soluble dithiosemicarbazone ligand **4.3**.

The ^1H NMR spectrum of ligand **4.2** shows a characteristic singlet at 8.48 ppm for the two imine protons (Figure 4.1). This confirms the success of the Schiff base condensation reaction between the sulfonated salicylaldehyde **2.1** and the dithiosemicarbazide **4.2**.

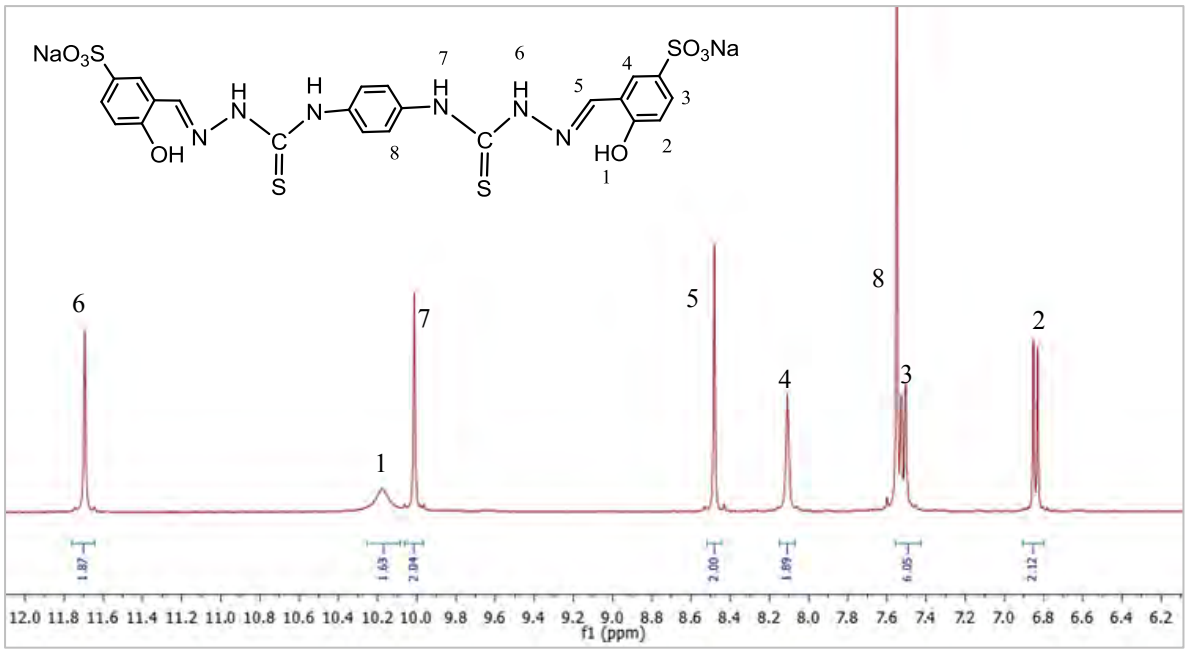

Figure 4.1. ^{1}H NMR spectrum of **4.3** in DMSO-d_6 at 30 ˚C.

The two hydrazinic protons (H-6) are the most deshielded protons and are observed as a singlet at 11.70 ppm. Further upfield, a broad singlet is observed at 10.13 ppm for the phenolic protons (H-1) whilst the protons (H-7) are observed as a singlet at 10.01 ppm. The aromatic protons H-4, H-3 and H-2 are observed in the expected region at 8.11 ppm, 7.52 ppm and 6.84 ppm respectively. H-2 appears as a doublet with coupling constant of 8.5 Hz. Of interest are the aromatic protons (H-8) which are observed as a singlet integrating for 4 protons. This confirms the symmetrical nature of the molecule since these protons exist in the same chemical environment. The ^{13}C{H} NMR spectrum of the ligand shows the expected number of carbon signals. The thione carbon and the imine carbon are observed at 176.3 ppm and 157.3 ppm respectively which further confirms the structure of the ligand. This is in close agreement with the chemical shifts for the same carbon signals in the monothiosemicarbazone **4.1** which are observed at 176.1 ppm and 156.98 ppm respectively.

In the infrared spectrum of the **4.3**, an intense absorption band for the C=N functionality is observed at 1616 cm^{-1} and at 830 cm^{-1} for the C=S functionality. The electrospray mass spectrum of the ligand was recorded in the negative ion-mode. The molecular ion peak was observed at m/z = 622.9965 for $[M]^{2-}$ where M is the anionic ligand. The elemental analysis of **4.3** was also found to be consistent with the calculated values with inclusion of water-

molecules which could be due to the presence of the hydrophilic sulfonate moiety in the ligand.

4.3 Synthesis and characterization of water-soluble Pd(II) sulfonated salicylaldimine thiosemicarbazone complexes

4.3.1 Synthesis and characterization of water-soluble mononuclear Pd(II) sulfonated salicylaldimine thiosemicarbazone complexes 4.4 and 4.5.

The mononuclear palladium(II) complexes **4.4** and **4.5** were prepared by deprotonating the hydroxyl functionality of the phenol moiety of the monothiosemicarbazone ligand **4.1** using sodium hydride in ethanol, followed by the addition of either *cis*-$[PdCl_2(PPh_3)_2]$ or *cis*-$[PdCl_2(PTA)_2]$, where PTA is 1,3,5-triaza-7-phosphaadamantane (Scheme 4.5). The metal precursors *cis*-$[PdCl_2(PPh_3)_2]$[25] or *cis*-$[PdCl_2(PTA)_2]$[26] were prepared following previously reported literature methods. Complexes **4.4** and **4.5** where isolated as bright yellow solids with water-solubility of 7 mg/mL and 2.3 mg/mL respectively.

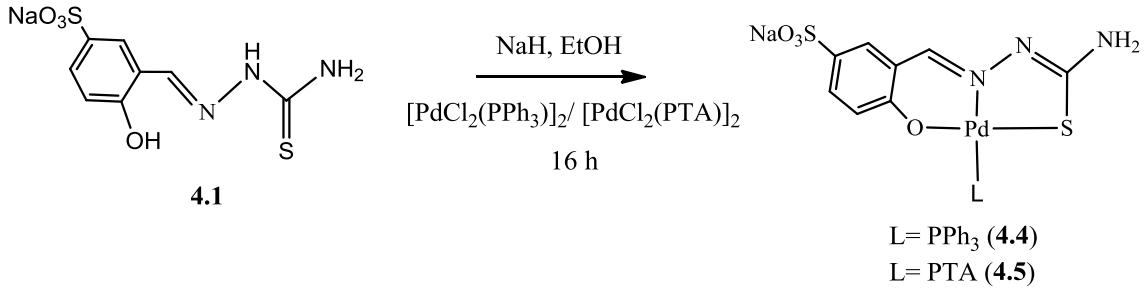

Scheme 4.5 Synthesis of water-soluble mononuclear Pd(II) thiosemicarbazone complexes **4.4** and **4.5**.

Analysis of the ^{1}H NMR spectroscopic data reveals that complexation of free ligand **4.1** to the Pd metal occurs in a tridentate fashion, through the thiolato sulfur, the imine nitrogen and phenolic oxygen. The ^{1}H NMR spectra of the complexes show a characteristic imine doublet for each complex at either 8.23 ppm (J_{H-P} = 13.9 Hz) or 8.19 ppm (J_{H-P} = 13.1 Hz) for **4.4** and **4.5** respectively. Figure 4.2 is a representative ^{1}H NMR spectra for complexes such as **4.4** and **4.5** which display similar trends.

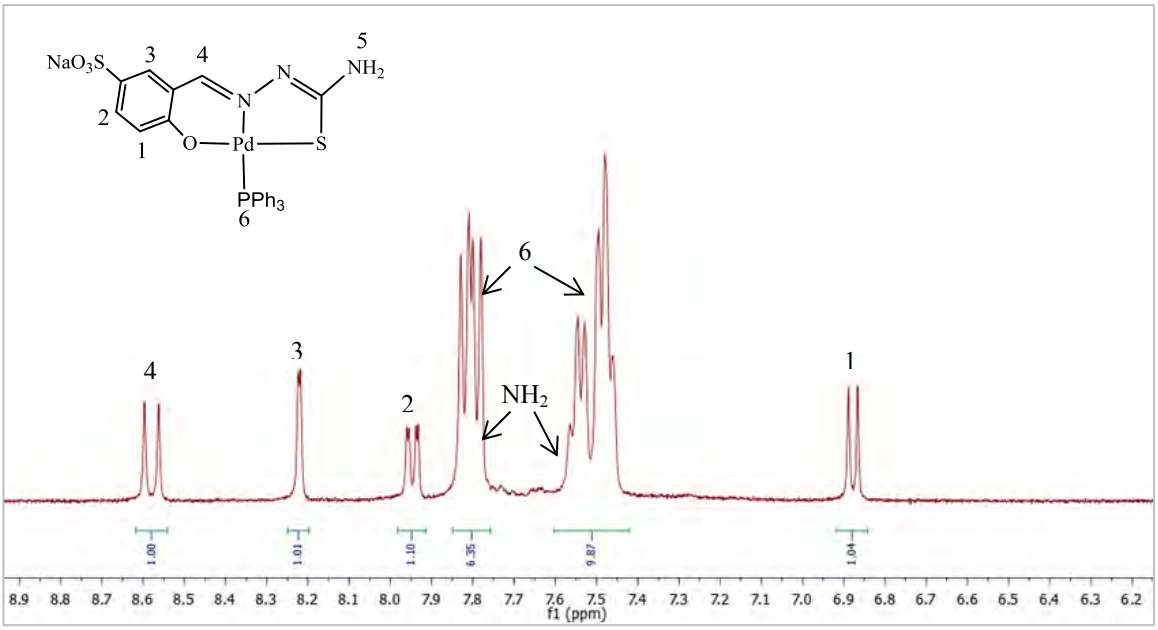

Figure 4.2. ^{1}H NMR spectrum of **4.4** in DMSO-d_6 at 30 ˚C.

The coupling of the imine proton to the phosphorus atom has been observed for similar compounds in the literature.[9] This is evidence of coordination of the ligand to the Pd metal *via* the imine nitrogen. The aromatic protons appear at 7.70 ppm, 7.38 ppm, 7.45 ppm and 6.78 ppm for H-3, H-2, H-6 and H-1 respectively. H-1 appears as a doublet with a coupling constant of ^{3}J =8.4 Hz and this as a result of H-1 coupling with H-2 which is three bonds away. The terminal amino proton signals overlap with the triphenylphosphine proton signals and this is reflected by the integration of the signals for H-6. The ^{1}H NMR spectrum for complex **4.5** shows similar trends except the protons for the 1,3,5-triaza-7-phosphaadamantane appear upfield between 4.30 ppm and 4.60 ppm.

The ^{31}P{H} NMR spectra of the complexes were also analysed and for both complexes, one singlet was observed in both cases. The signal was observed at 24.3 ppm for complex **4.4** and at -41.5 ppm for complex **4.5**. The number of carbon signals observed in the ^{13}C{H} NMR spectra of the complexes corresponds to the number of carbons in the complexes. The thiol carbons are observed in the expected regions at either 171.4 ppm or 171.8 ppm for complexes **4.4** and **4.5** respectively, whilst the imine carbons appear at 162.1 ppm and 162.3 ppm respectively.

The infrared spectra of the complexes confirm the coordination mode of the thiosemicarbazone ligands to the Pd metal. The ligand coordinates in the thiolate form

resulting in two imine functionalities in the metal complexes. For complex **4.4** the absorption bands for the two imines are observed at 1600 cm^{-1} and 1598 cm^{-1}, whilst for complex **4.5** an intense absorption band is observed at 1597 cm^{-1} with a shoulder at 1602 cm^{-1} for the second imine functionality (Figure 4.3).

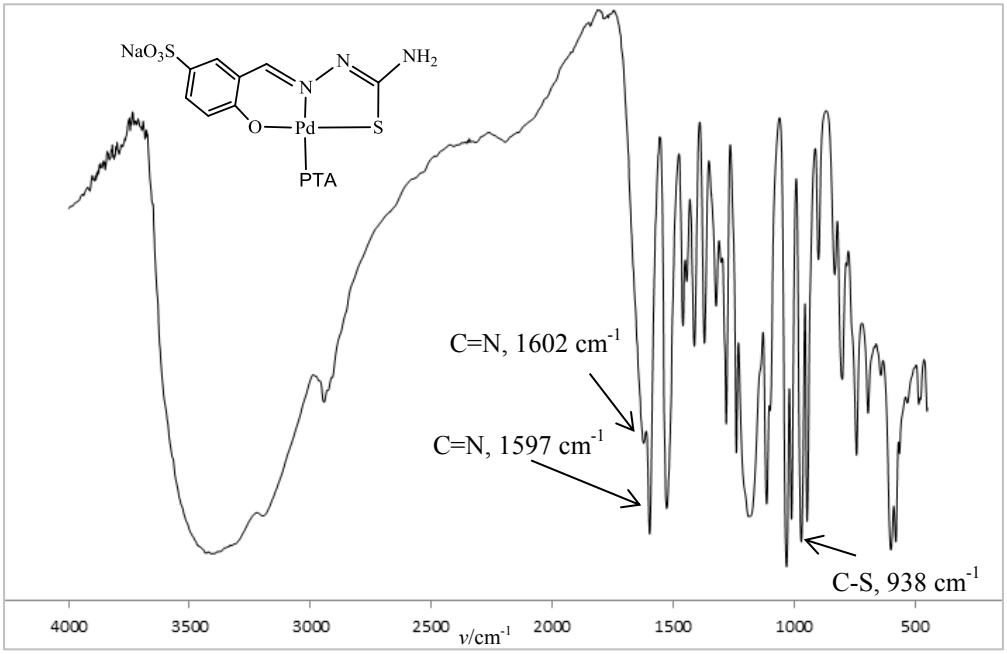

Figure 4.3 Infrared spectrum of complex **4.5**.

Another absorption band for the C-S functionality is observed at 933 cm^{-1} and 938 cm^{-1} for **4.4** and **4.5** respectively. Of interest is the shift of the imine absorption from 1616 cm^{-1} in the free ligand to lower wave numbers. This is further confirmation that the imine nitrogen immediately adjacent to the aromatic ring has coordinated the metal. A broad OH band is observed in the spectrum and this could be due to the alcoholic solvent used in the reaction.

The complexes **4.4** and **4.5** were also characterized using high resolution electrospray mass spectrometry in the negative ion-mode. The molecular ion peaks for **4.4** and **4.5** were observed at m/z = 639.9780 and m/z = 534.9614 for $[M]^-$, respectively, where M is the anionic complex.

4.3.2 Synthesis and characterization of water-soluble binuclear Pd(II) sulfonated salicylaldimine thiosemicarbazone complexes 4.6 and 4.7.

The water-soluble palladium(II) dithiosemicarbazone complexes **4.6** and **4.7** were prepared by deprotonating the phenolic protons of the dithiosemicarbazone ligand **4.3** using sodium hydride in ethanol, followed by the addition of two equivalents of either *cis*-$[PdCl_2(PPh_3)_2]$ or *cis*-$[PdCl_2(PTA)_2]$ (Scheme 4.6). After stirring for 16 hours, the products were isolated as yellow solids with water-solubility values of 7 mg/mL (**4.6**) and 4.5 mg/mL (**4.7**). The complexes are stable at room temperature and both complexes (**4.6** and **4.7**) decompose without melting.

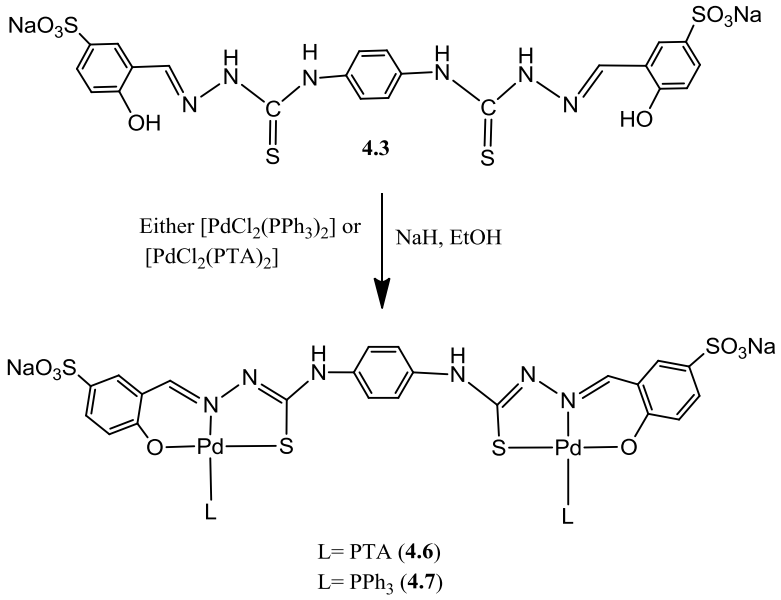

Scheme 4.6. Synthesis of water-soluble binuclear Pd(II) dithiosemicarbazone complexes **4.6** and **4.7**.

The ^{1}H NMR spectra of the binuclear complexes **4.6** and **4.7** are similar to those of the mononuclear analogues **4.4** and **4.5**. Absence of the phenolic and hydrazinic protons indicates that ligand **4.3** has coordinated to the Pd metal centres. Further evidence is the appearance of the imine protons as a doublet with coupling constants of 13.0 Hz and 13.8 Hz for **4.6** and **4.7** respectively. This is due to coupling of the imine proton with the phosphorus which is four bonds away. Each doublet integrates for two protons as expected. The aromatic protons appear in the expected regions between 6.40 ppm and 7.80 ppm for both complexes. A representative ^{1}H NMR spectrum of **4.7** is shown in Figure 4.4.

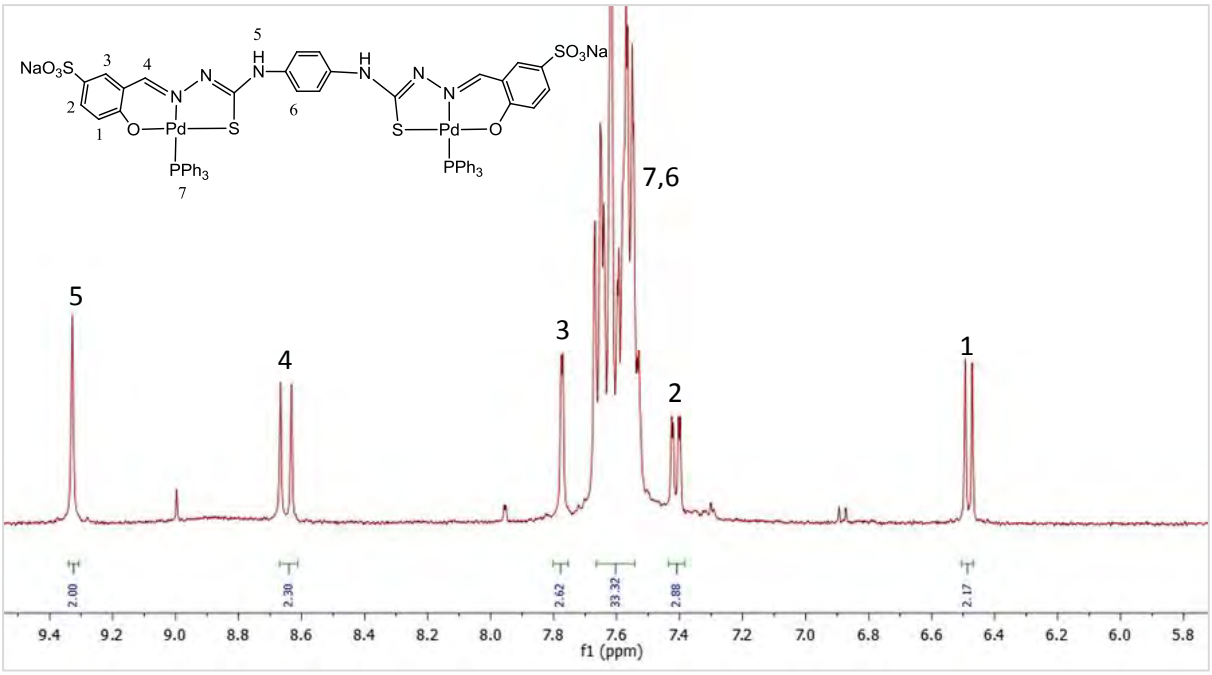

Figure 4.4. ^{1}H NMR spectrum of **4.7** in DMSO-d_6 at 30 ˚C.

The amino protons H-5 are observed furthest downfield at 9.33 ppm. The imine protons are observed at 8.65 ppm as a doublet. The aromatic protons are observed between 6.48 ppm and 7.77 ppm. Similar to the mononuclear complexes, H-5 appears as a doublet with a coupling constant of ^{3}J = 8.7 Hz. Integration of the multiplet between 7.50 ppm and 7.70 ppm indicates the presence of 34 protons due to overlapping of the signals of the aromatic spacer protons and the signals of triphenylphosphine protons. However, the integration of the protons H-1, H-2, H-3, H-4 and H-5 support the dimeric nature of the complex **4.7**. For complex **4.6 (**with PTA ligand), a singlet is observed at 7.66 ppm which integrates for the 4 aromatic protons (H-6) of the aromatic spacer. This confirms the symmetric structure of the complex. The ^{13}C{H} NMR spectra of the binuclear complexes **4.6** and **4.7** show the expected number of carbon signals. The thiol carbon and the two imine carbon signals are observed in the expected regions for both complexes.

The ^{31}P{H} NMR spectra of the binuclear complexes **4.6** and **4.7** show the presence of a single phosphorus species. The singlet is observed at -37.4 ppm and 24.4 ppm for **4.6** and **4.7** respectively. This data is similar to what was observed for the mononuclear analogues **4.4** and **4.5**.

The complexes (**4.6** and **4.7**) were also characterized using infrared spectroscopy. Similar to the mononuclear derivatives **4.4** and **4.5**, two imine absorption bands were observed

confirming coordination of the ligand **4.3** in the thiol form. The imine absorption bands are observed at 1603 cm^{-1} and 1599 cm^{-1} for **4.6** and at 1601 cm^{-1}, 1596 cm^{-1} for **4.7**. The C-S vibration was observed for both complexes at 943 cm^{-1} (**4.6**) and 937 cm^{-1} (**4.7**).

Further characterization was performed using high resolution electrospray ionisation mass spectrometry. The high resolution mass spectra were recorded in the negative ion-mode due to the anionic nature of the complexes. Molecular ion peaks are observed at m/z = 572.9680 (**4.6**) and m/z = 677.9856 (**4.7**) for $[M]^{2-}$ where M is the anionic complex. The elemental analysis results of the complexes are consistent with the calculated values with inclusion of water molecules which could be due to the presence of the sulfonate moiety which makes the complexes slightly hygroscopic.

4.4 Stability experiments for the water-soluble Pd(II) complex 4.4 in water at 70 ˚C.

The stability of metal-based compounds in solution is of great importance in catalysis. NMR experiments were conducted using complex **4.4** as a representative example. Monitoring the $^{31}P\{H\}$ NMR and ^{1}H NMR spectrum of the complex over a 24 hour period in D_2O gave an indication of the stability of the compound in solution. The $^{31}P\{H\}$ NMR spectra obtained over a 24 hour period are shown in Figure 4.5.

Throughout the course of the experiment, a single peak at 24.3 ppm was observed in the $^{31}P\{H\}$ NMR spectrum. Triphenylphosphine usually undergoes slow oxidation in air to give triphenylphosphine oxide, however in the $^{31}P\{H\}$ NMR experiments of **4.4** this oxide is not observed. Similarly, in the ^{1}H NMR spectra of the complex, the imine functionality is not hydrolysed and this was confirmed by the imine proton doublet that remained unaltered (Figure 4.6). Hydrolysis of imines results in formation of aldehydes and absence of an aldehyde proton in all ^{1}H NMR spectra indicates that there was no imine hydrolysis.

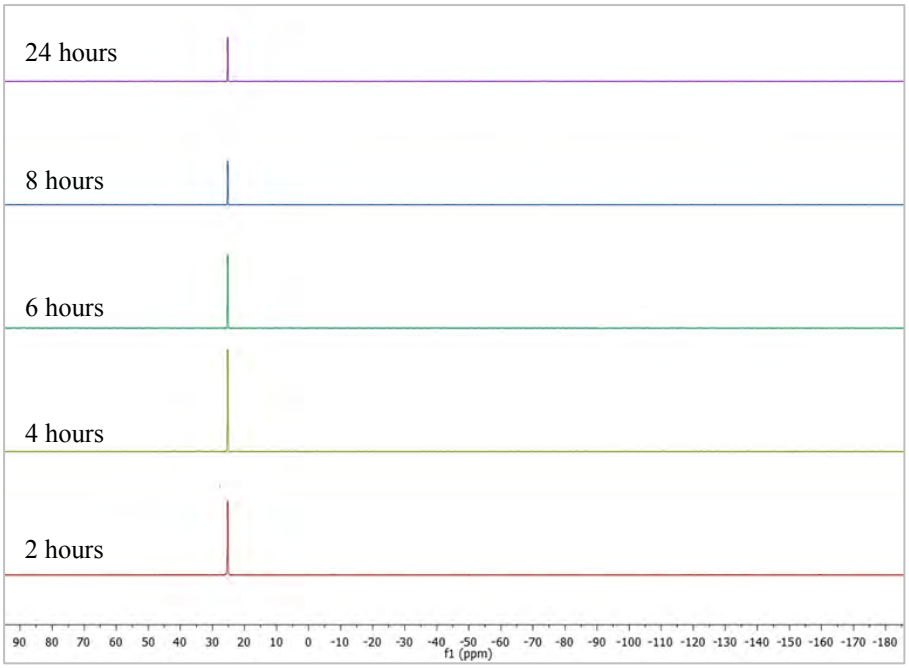

Figure 4.5 Stacked $^{31}P\{H\}$ NMR spectra of complex **4.4** in D_2O at 70 ˚C over a 24 hour period.

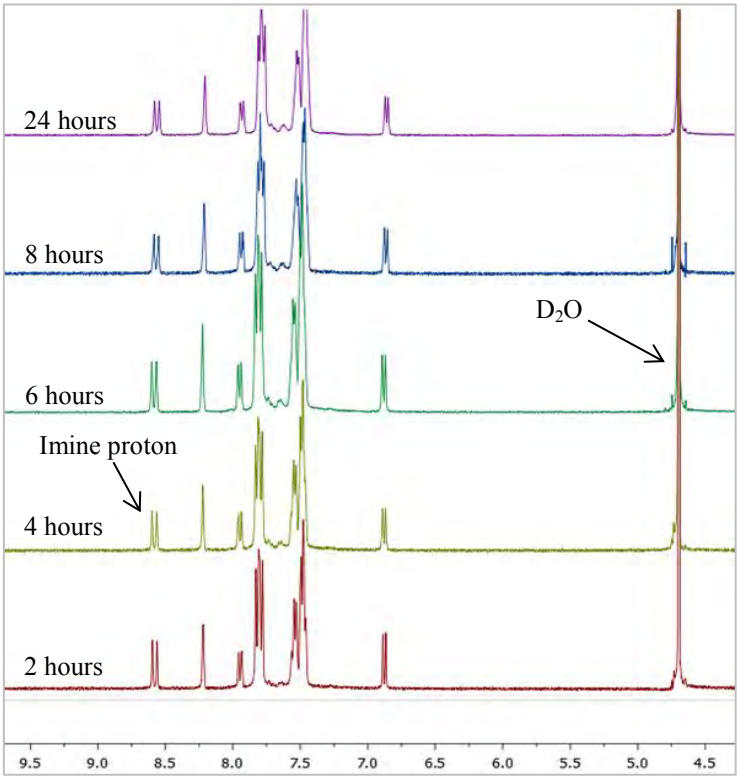

Figure 4.6 Stacked ^{1}H NMR spectra of complex **4.4** in D_2O at 70 ˚C over a 24 hour period.

The absence of aquation or imine hydrolysis indicates that complex **4.4** is stable in water at this temperature. This stability of thiosemicarbazone complexes in water and various organic

solvents has also been reported by Abram and co-workers.[28]

4.5 Overall Summary

New water-soluble mono- and dithiosemicarbazone ligands (**4.1** and **4.3**) have been synthesized and characterized. Both ligands display excellent water-solubility at room temperature. These were reacted with either $[PdCl_2(PPh_3)_2]$ or $[PdCl_2(PTA)_2]$ to afford a series of water-soluble mono- and binuclear Pd(II) thiosemicarbazone complexes (**4.4**-**4.7**). All the complexes have been characterized using ^1H NMR, $^{13}C\{^1H\}$ NMR, $^{31}P\{^1H\}$ NMR and infrared spectroscopy, high resolution mass spectrometry, elemental analysis and melting points. The characterization proves that the ligands coordinate to the Pd metal *via* the imine nitrogen, thiolato sulfur and phenolic oxygen in a tridentate fashion. The complexes also display excellent water-solubility at room temperature and in addition, ^1H and $^{31}P\{^1H\}$ NMR spectroscopic experiments reveal that mononuclear complex **4.4** is very stable in water at 70 ˚C.

4.6 Experimental

General Details

All reagents and solvents were purchased from Sigma-Aldrich and were used as received. Palladium chloride was received as a kind donation from Anglo-Platinum Corporation / Johnson Matthey Limited. The sodium sulfonate aldehyde,[29] dithiosemicarbazide **4.2**,[24] **[**$PdCl_2(PPh_3)_2$**]**[25] and $[PdCl_2(PTA)_2]$[26] were prepared following previously reported literature methods. Nuclear magnetic resonance (NMR) spectra were recorded on either a Varian XR300 MHz (^1H at 300.08 MHz, $^{13}C\{H\}$ at 75.46 MHz) or a Bruker Biospin GmbH (^1H NMR at 400.22 MHz, $^{13}C\{H\}$ NMR at 100.65 MHz, $^{31}P\{H\}$ NMR at 162.01 MHz) spectrometer at ambient temperature. Elemental analysis for C, H, N and S were carried out using a Thermo Flash 1112 Series CHNS-O Analyser. Infrared absorptions were measured using a Perkin-Elmer Spectrum 100 FT-IR spectrometer as KBr pellets. Mass spectrometry was carried out on a Waters API Quattro Micro Triple Quadrupole electrospray ionisation mass spectrometer. Data were recorded in the negative ion-mode.

4.7 Synthesis and characterization of water-soluble sulfonated thiosemicarbazone ligands

4.7.1 Synthesis and characterization of sulfonated monothiosemicarbazone salicylaldimine ligand 4.1

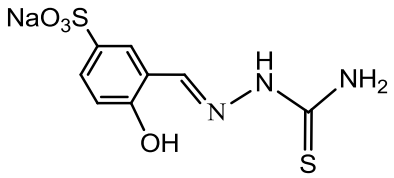

The sulfonated salicylaldehyde **2.1** (0.213 g, 0.950 mmol) was dissolved in distilled water (10 mL) in a round bottomed flask. The thiosemicarbazide (0.0860 g, 0.945 mmol) was suspended in ethanol (50 mL) and this was added drop-wise to the stirring aldehyde. The resulting solution was refluxed at 80 ^{o}C for 4 hours after which the mixture was filtered by gravity and the solvent removed under reduced pressure. The white solid recovered was dried under vacuum to afford the desired product as a white solid. **Yield** 0.261 g, 93%. **Mp**: Decomposes without melting, onset at 225 ^{o}C. **FT-IR** (ν_{max}/cm^{-1}, KBr): 1630 (C=N), 831 (C=S). **^{1}H NMR** (DMSO-d_6, δ, ppm): 11.32 (br s, 1 H, NN**H**CS), 9.96 (br s, 1 H, O**H**), 8.36 (s, 1 H, **H**$_{imine}$), 8.06 (s, 1 H, N**H**$_2$), 7.92 (s, 1 H, **H**$_{Ar}$), 7.69 (s, 1 H, N**H**$_2$), 7.45 (d, ^{3}J = 8.1 Hz, 1 H, **H**$_{Ar}$), 6.78 (d, ^{3}J = 8.4 Hz, 1 H, **H**$_{Ar}$). **^{13}C{^{1}H} NMR** (DMSO-d_6, δ, ppm): 176.1, 156.9, 138.9, 130.5, 127.0, 124.6, 121.9, 119.3. **Elemental Analysis**: Calculated for $C_8H_8N_3NaO_4S_2.2H_2O$: C, 28.83; H, 3.63; N, 12.61; S, 19.24; Found: C, 28.63; H, 3.72; N, 13.29; S, 19.75. **ESI-MS** (negative): m/z 273.9901 [M]$^{-}$ where M is the anion. **S$_{20^{o}C}$** = 8 mg/mL in water.

4.7.2 Synthesis and characterization of sulfonated dithiosemicarbazone salicylaldimine ligand 4.3

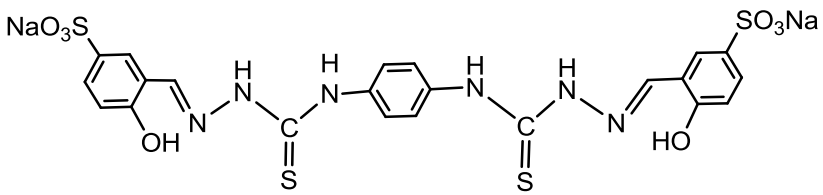

The dithiosemicarbazide **4.2**[24] (0.257 g, 1.00 mmol) was suspended in 20 mL ethanol. To this was added the sulfonated salicylaldehyde **2.1** (0.449 g, 2.00 mmol) dissolved in a 1:1 water/ethanol mixture (10 mL). An off-white precipitate was formed immediately and this

was left to reflux at 80 ^{o}C for 16 hours. The mixture formed was filtered using a Hirsch funnel and washed with cold ethanol and dried under vacuum. **Yield** 0.522 g, 78%. **Mp**: Decomposes without melting, onset at 258 ^{o}C. **FT-IR** (ν_{max}/cm^{-1}, KBr): 1616 (C=N), 830 (C=S). **^{1}H NMR** (DMSO-d_6, δ, ppm): 11.70 (s, 2 H, C**H**=NNH), 10.13 (s, 2 H, O**H**), 10.01 (s, 2 H, S=CN**H**Ph), 8.48 (s, 2 H, $\mathbf{H}_{imine}$), 8.11 (s, 2 H, $\mathbf{H}_{Ar}$), 7.55 (s, 4 H, $\mathbf{H}_{Ar}$), 7.52 (m, 2 H, $\mathbf{H}_{Ar}$), 6.84 (d, ^{3}J = 8.5 Hz, 2 H, $\mathbf{H}_{Ar}$). **^{13}C{^{1}H} NMR** (DMSO-d_6, δ, ppm): 176.3, 157.3, 141.7, 139.9, 136.6, 129.4, 129.4, 125.4, 119.3, 115.7. **Elemental Analysis**: Calculated for $C_{22}H_{18}N_6Na_2O_8S_4.14H_2O$: C, 28.69; H, 5.03; N, 9.13; S, 13.93, Found: C, 28.77; H, 4.09; N, 9.28; S, 13.89. **ESI-MS** (negative): m/z 622.9965 [M]$^{-}$ where M is the anion. $\mathbf{S_{20°C}}$ = 1.5 mg/mL in water.

4.8 Synthesis and characterization of water-soluble sulfonated thiosemicarbazone Pd(II) complexes

4.8.1 Synthesis and characterization of sulfonated mononuclear Pd(II) thiosemicarbazone complex 4.4.

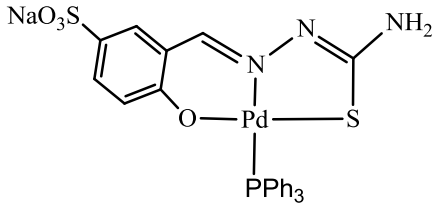

The monothiosemicarbazone ligand **4.1** (0.0810 g, 0.271 mmol) was suspended in ethanol (20 mL) and to it was added an equimolar amount of sodium hydride and this was stirred at room temperature for 2 hours. [$PdCl_2(PPh_3)_2$] (0.190 g, 0.271 mmol) was added to the ligand and the resulting solution was stirred at room temperature for 16 hours. The mixture was filtered using a Hirsch funnel, the solid collected was washed with ethanol and dried under vacuum to afford the desired product as a bright yellow solid. **Yield** 0.163 g, 91%. **Mp**: Decomposes without melting, onset at 276 ^{o}C. **FT-IR** (ν_{max}/cm^{-1}, KBr): 1600, 1598 (C=N), 933 (C-S). **^{1}H NMR** (DMSO-d_6, δ, ppm): 8.23 (d, ^{4}J = 13.9 Hz, 1 H, $\mathbf{H}_{imine}$), 7.70 – 7.50 (m, 15 H, $\mathbf{H}_{Ar}$), 7.38 (d, ^{3}J = 8.6 Hz, 1 H, $\mathbf{H}_{Ar}$), 7.69 (s, 1 H, N$\mathbf{H}_2$), 7.45 (d, ^{3}J = 8.1 Hz, 1 H, $\mathbf{H}_{Ar}$), 6.78 (d, ^{3}J = 8.4 Hz, 1 H, $\mathbf{H}_{Ar}$). **^{13}C{^{1}H} NMR** (DMSO-d_6, δ, ppm): 171.4, 162.1, 148.5, 135.7, 134.6, 131.8, 131.6, 129.6, 129.2, 129.1, 119.5, 116.7. **^{31}P{H} NMR** (DMSO-d_6, δ, ppm): 24.3. **Elemental Analysis**: Calculated for $C_{14}H_{18}N_6NaO_4PPdS_2.4H_2O$: C, 26.65; H, 4.15; N, 13.32; S, 10.16, Found: C, 26.29; H, 4.29; N, 13.35; S, 6.32. **ESI-MS** (negative): m/z 639.9780 [M]$^{-}$ where M is the anion. $\mathbf{S_{20°C}}$ = 7 mg/mL in water.

4.8.2 Synthesis and characterization of sulfonated mononuclear Pd(II) thiosemicarbazone complex 4.5.

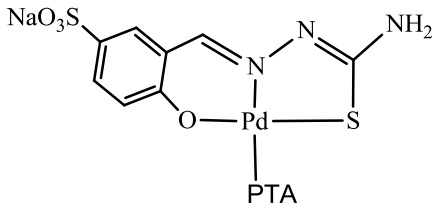

The monothiosemicarbazone ligand **4.1** (0.0801 g, 0.268 mmol) was suspended in ethanol 20 mL. To it was added an equimolar amount of sodium hydride, the colourless solution immediately turned yellow and this was left to stir at room temperature for 2 hours. The metal precursor $PdCl_2(PTA)_2$ (0.130 g, 0.286 mmol) was suspended in ethanol (10 mL) and this was added drop-wise to the deprotonated ligand. The bright yellow suspension formed was left to stir at room temperature overnight. The mixture was filtered using a Buchner funnel and the yellow solid was washed with ethanol and dried under vacuum. **Yield** 0.120 g, 82%. **Mp**: Decomposes without melting, onset at 281 ^{o}C. **FT-IR** (ν_{max}/cm^{-1}, KBr): 1602, 1597 (C=N), 938 (C-S). **^{1}H NMR** (DMSO-d_6, δ, ppm): 8.19 (d, ^{4}J = 13.1 Hz, 1 H, $\mathbf{H}_{imine}$), 7.62 (d, ^{3}J = 2.2 Hz, 1 H, $\mathbf{H}_{Ar}$), 7.45 (dd, ^{3}J = 8.7 Hz, ^{4}J = 2.3 Hz, 1 H, $\mathbf{H}_{Ar}$), 6.80 (d, ^{3}J = 8.7 Hz,1 H, $\mathbf{H}_{Ar}$), 6.71 (s, 2 H, N$\mathbf{H}_2$), 4.58 (m, 6 H, PTA), 4.32 (s, 6 H, PTA). **^{13}C{^{1}H} NMR** (DMSO-d_6, δ, ppm): 171.8, 162.3, 148.1, 135.6, 131.9, 130.9, 120.2, 116.7, 72.44, 50.6. **^{31}P{H} NMR** (DMSO-d_6, δ, ppm): -41.5. **Elemental Analysis**: Calculated for $C_{26}H_{21}N_3NaO_4PPdS_2.15H_2O$: C, 33.43; H, 5.50; N, 4.50; S, 6.86; Found: C, 33.29; H, 3.33; N, 4.22; S, 6.79. **ESI-MS** (negative): m/z 534.9614 [M]$^{-}$, where M is the anion. $\mathbf{S_{20^{o}C}}$ = 2.3 mg/mL in water.

4.8.3 Synthesis and characterization of sulfonated mononuclear Pd(II) thiosemicarbazone complex 4.6.

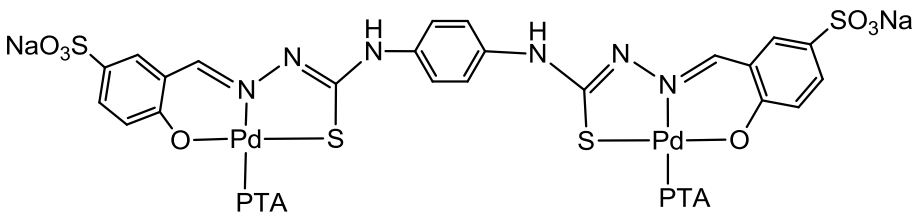

The dithiosemicarbazone ligand **4.3** (0.0400 g, 0.0590 mmol) was suspended in 20 mL

water/ethanol mixture. To this was added an equimolar amount of sodium hydride and two equivalents of $[PdCl_2(PTA)_2]$ (0.0570 g, 0.118 mmol) in 10 mL ethanol. The solution was left to reflux at 80 ^oC overnight. The orange brown mixture formed was filtered using a Hirsch funnel and washed with cold ethanol and dried under vacuum to afford the desired product asa bright yellow powder. **Yield** 0.0620 g, 64%. **Mp**: Decomposes without melting onset at 268 ^oC. **FT-IR** (ν_{max}/cm^{-1}, KBr): 1603, 1599 (C=N), 943 (C-S). **^{1}H NMR** (DMSO-d_6, δ, ppm): 9.49 (s, 2 H, CN**H**C), 8.65 (d, ^4J = 13.0 Hz, 2 H, $\mathbf{H}_{imine}$), 7.80 (d, ^3J = 2.2 Hz, 2 H, $\mathbf{H}_{Ar}$), 7.66 (s, 4 H, H_{Ar}), 7.54 (dd, ^3J = 8.7 Hz, ^4J = 2.2 Hz, 2 H, $\mathbf{H}_{Ar}$), 6.84 (d, 8.4 Hz, 2 H, H_{Ar}), 4.68 (m, 12 H, PTA). 4.39 (s, 12 H, PTA). **^{13}C{^{1}H} NMR** (DMSO-d_6, δ, ppm): 162.6, 155.5, 146.5, 136.4, 132.7, 124.7, 115.9, 1.9.8, 71.5, 52.2. **^{31}P{H} NMR** (DMSO-d_6, δ, ppm): -37.4. **Elemental Analysis**: Calculated for $C_{34}H_{38}N_{12}Na_2O_8P_2Pd_2S_4.12H_2O$: C, 29.00; H, 4.44; N, 11.94; S, 9.11; Found: C, 28.73; H, 4.72; N, 11.29; S, 9.75. **ESI-MS** (negative): m/z 572.9680 $[M]^{2-}$, where M is the anion. $\mathbf{S_{20^oC}}$ = 7 mg/mL in water.

4.8.4 Synthesis and characterization of sulfonated mononuclear Pd(II) thiosemicarbazone complex 4.7.

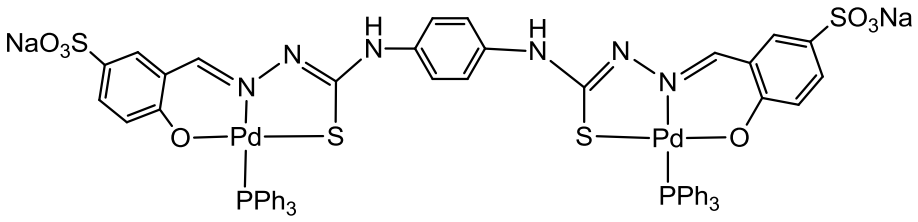

The dithiosemicarbazone ligand **4.3** (0.113 g, 0.168 mmol) was suspended in 20 mL ethanol. To this, an equimolar amount of sodium hydride was added and the mixture was left to stir at room temperature for 2 hours. $[PdCl_2(PPh_3)_2]$ (0.236 g, 0.336 mmol) was suspended in ethanol (10 mL) and this was added to the ligand. This was left to stir at room temperature for 16 hours. The yellow precipitate formed was filtered using a Hirsch funnel and washed with ethanol and dried under vacuum. **Yield** 0.219 g, 93%. **Mp**: Decomposes without melting onset at 332 ^oC. **FT-IR** (ν_{max}/cm^{-1}, KBr): 1601, 1596 (C=N), 937 (C-S). **^{1}H NMR** (DMSO-d_6, δ, ppm): 9.33 (s, 2 H, NNC**H**), 8.65 (d, ^4J = 13.8 Hz, 2 H, $\mathbf{H}_{imine}$), 7.77 (d, ^3J = 2.2 Hz, 2 H, $\mathbf{H}_{Ar}$), 7.70 – 7.50 (m, 34 H, $\mathbf{H}_{Ar}$), 7.41 (dd, ^3J = 8.7 Hz, ^4J =2.2 Hz, 2 H, $\mathbf{H}_{Ar}$), 6.48 (m, 2 H, $\mathbf{H}_{Ar}$). **^{13}C{^{1}H} NMR** (DMSO-d_6, δ, ppm): 162.4, 152.4, 151.3, 136.3, 134.6, 133.9-130.1, 129.6, 124.7, 119.2, 116.5, 46.3. **^{31}P{H} NMR** (DMSO-d_6, δ, ppm): 24.4. **Elemental Analysis**: Calculated for $C_{58}H_{44}N_6Na_2O_8P_2Pd_2S_4.5H_2O$: C, 46.69; H, 3.65; N, 5.63; S, 8.60;

Found: C, 46.21; H, 3.73; N, 5.21; S, 8.96. **ESI-MS** (negative): m/z 677.9856 $[M]^{2-}$, where M is the anion. $\mathbf{S_{20°C}}$ = 4.5 mg/mL in water.

4.9 References

1 I. G. Santos, U. Abram, R. Alberto, E. V. Lopez and A. Sanchez, *Inorg. Chem.*, 2004, **43**, 1834–1836.

2 F. Basuli, S. M. Peng and S. Bhattacharya, *Inorg. Chem.*, 2000, **39**, 1120–1127.

3 P. Chellan, S. Nasser, L. Vivas, K. Chibale and G. S. Smith, *J. Organomet. Chem.*, 2010, **695**, 2225–2232.

4 J. Pisk, B. Prugovečki, D. Matković-Čalogović, R. Poli, D. Agustin and V. Vrdoljak, *Polyhedron*, 2012, **33**, 441–449.

5 M. Belicchi-Ferrari, F. Bisceglie, C. Casoli, S. Durot, I. Morgenstern-Badarau, G. Pelosi, E. Pilotti, S. Pinelli and P. Tarasconi, *J. Med. Chem.*, 2005, **48**, 1671–1675.

6 G. Pelosi, F. Bisceglie, F. Bignami, P. Ronzi, P. Schiavone, M. C. Re, C. Casoli and E. Pilotti, *J. Med. Chem.*, 2010, **53**, 8765–8769.

7 D. R. Richardson, D. S. Kalinowski, V. Richardson, P. C. Sharpe, D. B. Lovejoy, M. Islam and P. V. Bernhardt, *J. Med. Chem.*, 2009, **52**, 1459–1470.

8 V. Vrdoljak, I. Dilović, M. Rubčić, S. Kraljević Pavelić, M. Kralj, D. Matković-Čalogović, I. Piantanida, P. Novak, A. Rožman and M. Cindrić, *Eur. J. Med. Chem.*, 2010, **45**, 38–48.

9 P. Chellan, N. Shunmoogam-Gounden, D. T. Hendricks, J. Gut, P. J. Rosenthal, C. Lategan, P. J. Smith, K. Chibale and G. S. Smith, *Eur. J. Inorg. Chem.*, 2010, 3520–3528.

10 W. Hernández, J. Paz, F. Carrasco, A. Vaisberg, E. Spodine, J. Manzur, L. Hennig, J. Sieler, S. Blaurock and L. Beyer, *Bioinorg. Chem. Appl.*, 2013, **2013**, 20–22.

11 P. Chellan, T. Stringer, A. Shokar, P. J. Dornbush, G. Vazquez-Anaya, K. M. Land, K. Chibale and G. S. Smith, *J. Inorg. Biochem.*, 2011, **105**, 1562–1568.

12 M. Adams, C. De Kock, P. J. Smith, K. Chibale and G. S. Smith, *J. Organomet. Chem.*, 2013, **736**, 19–26.

13 M. Adams, Y. Li, H. Khot, C. De Kock, P. J. Smith, K. Land, K. Chibale and G. S. Smith, *Dalton Trans.*, 2013, **42**, 4677–85.

14 S. D. Khanye, G. S. Smith, C. Lategan, P. J. Smith, J. Gut, P. J. Rosenthal and K. Chibale, *J. Inorg. Biochem.*, 2010, **104**, 1079–1083.

15 P. Pelagatti, A. Venturini, A. Leporati, M. Carcelli, M. Costa, A. Bacchi and C. Pelizzi, *J. Am. Chem. Soc. Dalton Trans.*, 1998, 2715–2721.

16 G. Xie, P. Chellan, J. Mao, K. Chibale and G. S. Smith, *Adv. Synth. Catal.*, 2010, **352**, 1641–1647.

17 S. Datta, D. K. Seth, R. J. Butcher and S. Bhattacharya, *Inorganica Chim. Acta*, 2011, **377**, 120–128.

18 P. Paul, S. Datta, S. Halder, R. Acharyya, F. Basuli, R. J. Butcher, S. M. Peng, G. H. Lee, A. Castineiras, M. G. B. Drew and S. Bhattacharya, *J. Mol. Catal. A Chem.*, 2011, **344**, 62–73.

19 I. D. Kostas, F. J. Andreadaki, D. Kovala-Demertzi, C. Prentjas and M. A. Demertzis, *Tetrahedron Lett.*, 2005, **46**, 1967–1970.

20 D. Kovala-Demertzi, P. N. Yadav, M. A. Demertzis, J. P. Jasiski, F. J. Andreadaki and I. D. Kostas, *Tetrahedron Lett.*, 2004, **45**, 2923–2926.

21 I. D. Kostas, G. A. Heropoulos, D. Kovala-Demertzi, P. N. Yadav, J. P. Jasinski, M. A. Demertzis, F. J. Andreadaki, G. Vo-Thanh, A. Petit and A. Loupy, *Tetrahedron Lett.*, 2006, **47**, 4403–4407.

22 A. L. Casalnuovo and J. C. Calabrese, *J. Am. Chem. Soc.*, 1990, **112**, 4324–4330.

23 R. A. Sheldon, *Green Chem.*, 2005, **7**, 267–278.

24 M. Christlieb, H. S. R. Struthers, P. D. Bonnitcha, A. R. Cowley and J. R. Dilworth, *Dalton Trans.*, 2007, 5043–54.

25 W. A. Herrmann, G. Brauer and A. Salzer, *Synth. Meth. Organomet. Inorg. Chem.*, 1996, **1**, 160–161.

26 A. M. M. Meij, S. Otto and A. Roodt, *Inorg. Chim. Acta*, 2005, **358**, 1005–1006.

27 I. G. Santos, A. Hagenbach and U. Abram, *Dalton Trans.*, 2004, 677–682.

28 E. B. Hager, B. C. E. Makhubela and G. S. Smith, *Dalton Trans.*, 2012, **41**, 13927–13935.

Chapter 5

Aqueous phase Suzuki-Miyaura cross-coupling reactions using water-soluble Pd(II) complexes as catalyst precursors

This chapter forms part of the following publication:

Water-Soluble Palladium(II) Sulfonated Thiosemicarbazone Complexes: Facile Synthesis and Preliminary Catalytic Studies in the Suzuki-Miyaura cross-coupling reaction in Water. **Leah C. Matsinha,** Jincheng Mao, Selwyn F. Mapolie, and Gregory S. Smith, *European Journal of Inorganic Chemistry*, 2015, 4088-4094.

5.1 Introduction

Carbon-carbon bond formation reactions are some of the most important reactions that provide key steps in the synthesis of more complex molecules from simple precursors. The simplest of these reactions are metal-catalysed reactions that were developed in the 1970s, for the formation of carbon-carbon bonds between groups such as vinyl, aryl or alkynyl moieties.[1] The Suzuki-Miyaura reaction is a cross-coupling reaction between aryl boronic acids and aryl halides (and other derivatives such as triflates) (Scheme 5.1).[2]

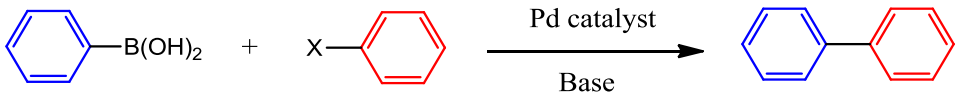

Scheme 5.1. The Suzuki-Miyaura cross-coupling reaction.

This reaction is one of the most efficient cross-coupling reactions due to the many advantages of organoboron reagents which include; their high stability in water and other solvents, tolerance towards an extensive range of functional groups and that they are readily available.[3] A base is usually required for the reaction to be efficient because the negatively charged base can coordinate to the boron atom, which increases nucleophilicity of the boron atom and

consequently results in easy transfer of the organic group on the boron to the adjacent electrophilic centre.[1]

One of the important motivations for using water as a reaction medium is that it simplifies the separation of homogeneous transition metal catalysts from the reaction products.[4] The application of water-soluble catalysts for the Suzuki-Miyaura cross-coupling reaction in water was first reported by Casalnuovo in the 1990s.[5] Thereafter, a lot of research has been carried out using high water-soluble catalysts in aqueous medium for this reaction.[4,6–12] In this Chapter, the application of water-soluble mononuclear and binuclear thiosemicarbazone Pd(II) complexes as catalysts for the Suzuki-Miyaura cross-coupling reaction is discussed. Various substrates are investigated and the potential recyclability of one mononuclear catalyst is also explored.

5.2 Aqueous phase Suzuki-Miyaura cross-coupling reactions using water-soluble thiosemicarbazone complexes 4.4-4.7.

The four water-soluble Pd(II) thiosemicarbazone complexes (**4.4**-**4.7**), whose synthesis and characterization has been discussed in Chapter 4, were evaluated as catalyst precursors in the Suzuki-Miyaura cross-coupling reaction in a monophasic aqueous solution (Figure 5.1). The complexes were placed in a Schlenk tube, together with the base, aryl halide, arylboronic acid, phase transfer agent, tetrabutylammonium bromide (TBAB), and water (2 mL). The reaction was allowed to proceed at the set temperature for 24 hours. In this study TBAB was used as an additive and its importance as a phase transfer agent is well documented in the literature.[10–15]

At the end of the reaction, the reaction mixture was cooled, the products were either extracted with toluene and analysed using gas chromatography or extracted with ethyl acetate, separated on a short column and product analysed using ^{1}H NMR and ^{13}C{H} NMR spectroscopy.

The first step in the mechanism of the Suzuki-Miyaura cross-coupling reaction is the oxidative addition of the aryl halide to Pd(0). The process results in the formation of an organopalladium complex. It has generally been accepted that this complex is initially in the *cis*-conformation but isomerises to the *trans*-conformation.[16–18] The most commonly known oxidative addition mechanism for the Suzuki-Miyaura cross-coupling reaction follows a

Pd(0) to Pd(IV) mechanism,[17,19–23] but a Pd(II) to Pd(IV) mechanism is also possible.[24–27] This feasibility this Pd(II)/Pd(IV) redox during oxidative addition will be investigated and discussed in more detail in Chapter 6 as a possible mechanism using thiosemicarbazone Pd(II) complexes.

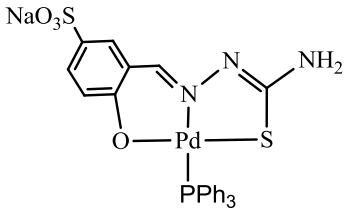

4.4

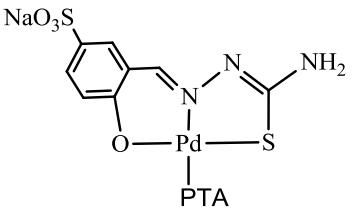

4.5

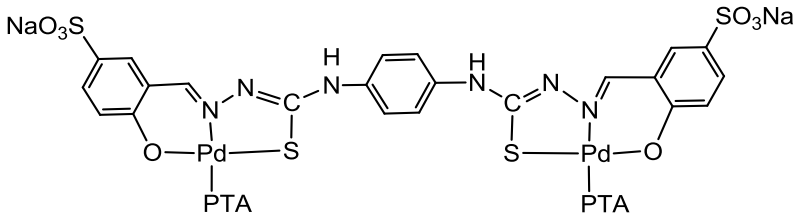

4.6

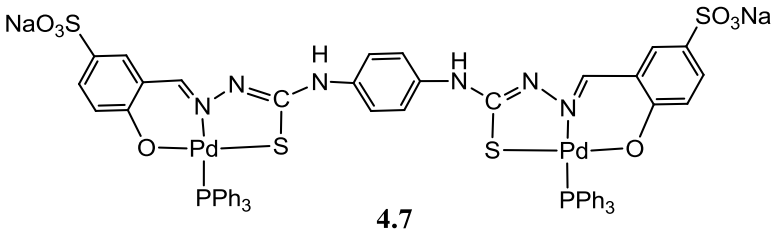

4.7

Figure 5.1. Water-soluble Suzuki-Miyaura Pd(II) thiosemicarbazone catalyst precursors **4.4-4.7.**

After oxidative addition, the transmetallation step follows. In this step, the base activates the boron containing reagent and also facilitates the formation of the alkoxy species R-Pd-OR from R-Pd-X (where X is the halide). Different bases influence this step differently and therefore it is of high importance to investigate the performance of a variety of bases for Suzuki-Miyaura cross-coupling reaction. The final step gives the desired product and this step is called the reductive elimination step (Figure 5.2). In this step the Pd catalyst is regenerated and the catalyst has to revert back to the *cis*-conformation before reductive elimination can occur.[16]

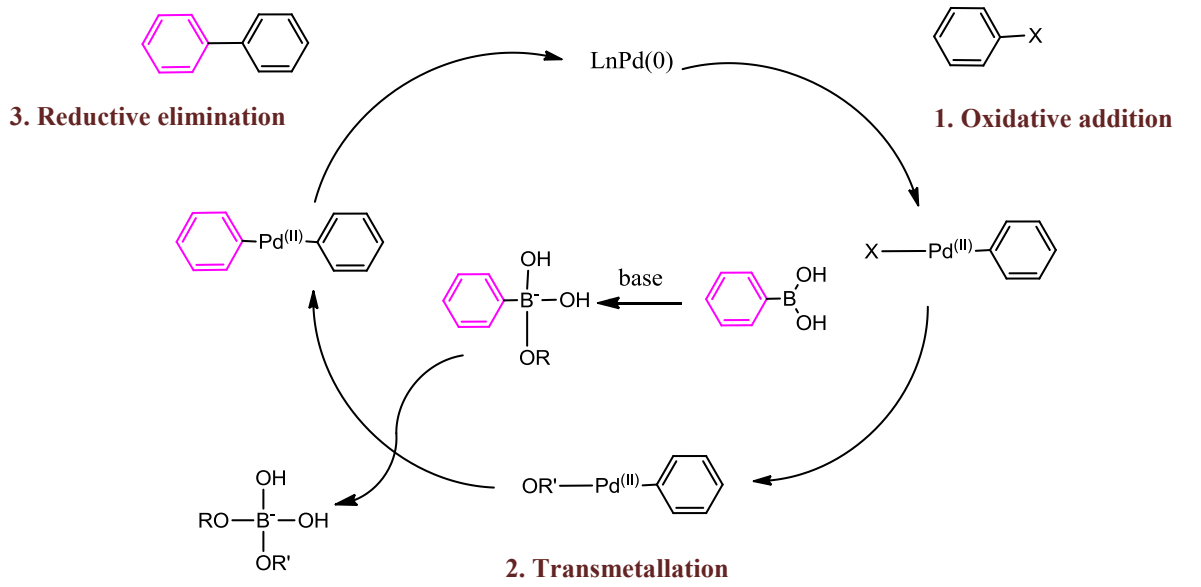

Figure 5.2 The Suzuki-Miyaura cross-coupling reaction mechanism.[16]

Various reaction parameters have to be considered to find the optimum reaction conditions. In the screening experiments, the effects of the base, temperature and nuclearity of catalysts were investigated in neat water.

5.3 Effects of the base

The performance of the catalysts was evaluated using four inorganic bases. The cross-coupling reaction was performed using *p*-methoxyphenylboronic acid and iodobenzene. The reactions were performed at 90 ˚C for 24 hours. A slight excess of phenylboronic acid was used and this is similar to what was reported previously for similar complexes in the Suzuki-Miyaura cross-coupling reaction.[28] The results obtained using the water-soluble catalyst precursors are summarised in Figure 5.3.

All bases give excellent conversions, except K_2CO_3 which gives moderate conversions of iodobenzene (76% and 66%) with catalysts **4.4** and **4.5** respectively. The results show that each of the four different bases works better with a particular catalyst. K_2CO_3 is the best base for catalyst **4.7**, whilst Na_2CO_3 gives impressive results with catalyst **4.5**. However, Na_2CO_3 and Cs_2CO_3 generally give excellent results with all four catalysts (**4.4**-**4.7**) and hence these two bases were selected for further experiments. It has been previously reported that there is a beneficial role of using water as a solvent for Suzuki-Miyaura cross-coupling reaction in the presence of carbonates as bases and hence this could be reason why these two carbonates give excellent results in these reactions.[29]

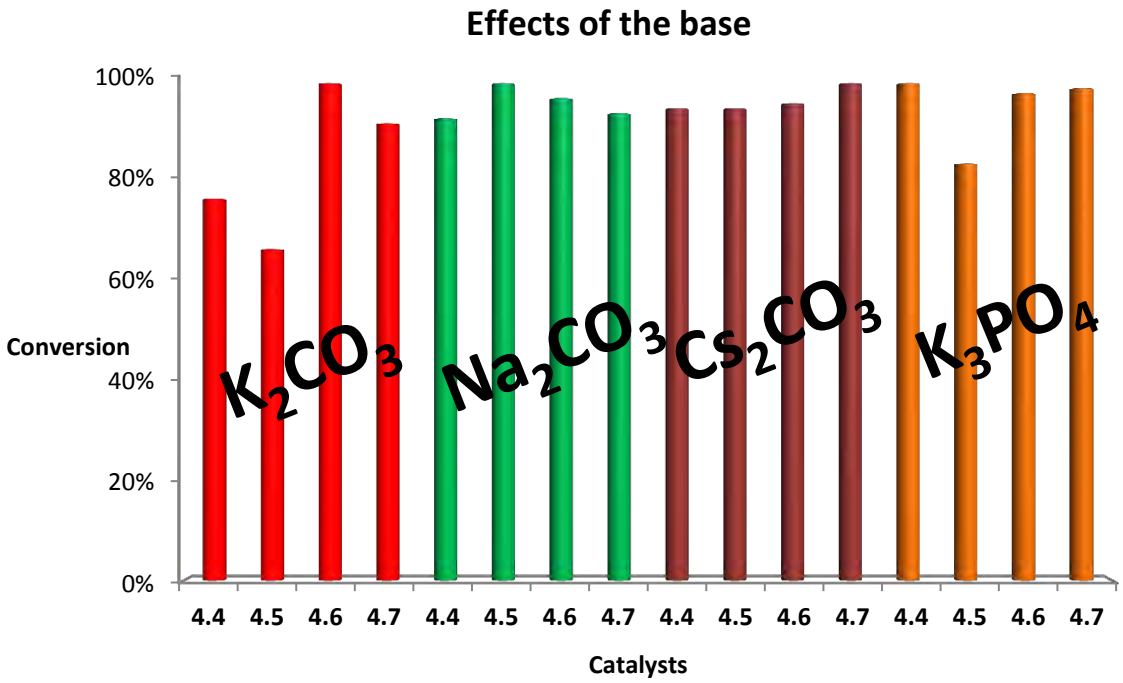

Reactions carried out in 2 mL water, 24 h, at 90 ˚C, 1 mol% Pd loading, 0.8 mmol phenylboronic acid, 0.5 mmol iodobenzene, TBAB 0.25 mmol, base 1 mmol. All reactions were monitored by GC and conversion of aryl halide is average of two identical catalytic experiments.

Figure 5.3. Effect of base on the conversion of iodobenzene.

A time dependant base optimisation was then carried out between Na_2CO_3 and Cs_2CO_3. This experiment was carried out at 90 ˚C for 24 hours and each reaction mixture was analysed every 4 hours in order to determine which base gives the best conversion in the shortest time. The results obtained in this experiment are summarised in Figure 5.4.

The conversion of iodobenzene was plotted as a function of time. The two bases show comparable iodobenzene conversion over the 24 hour period. After 24 h, over 90% conversion of aryl halide was observed in both cases with all catalysts. As a result of this comparable performance, Na_2CO_3 was selected as the suitable base for these reactions using catalysts **4.4**-**4.7**, only because Na_2CO_3 is the cost-effective alternative. The effect of temperature on the reactions using **4.4**-**4.7** was the next parameter to be investigated.

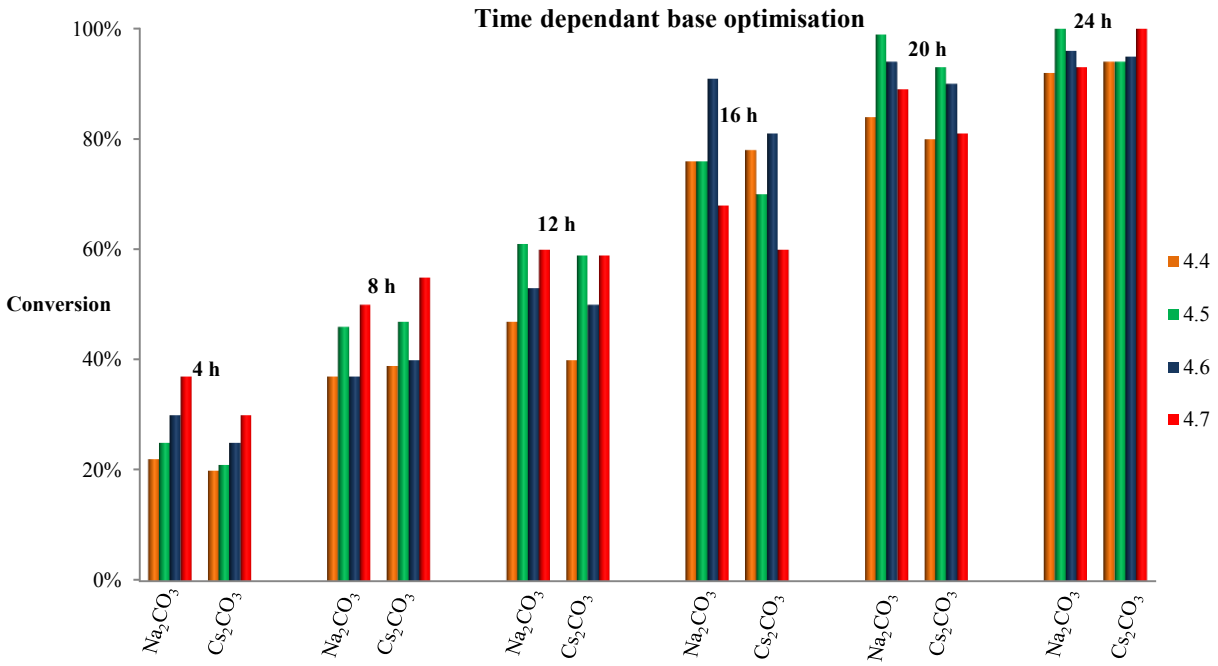

Reactions carried out in 2 mL water, 24 h, 90 ºC, 1 mol % Pd loading, 0.8 mmol Phenylboronic acid, 0.5 mmol iodobenzene, TBAB 0.25 mmol, base 1 mmol, n-decane internal standard. All reactions were monitored by GC and conversion iodobenzene is average of two identical catalytic experiments.

Figure 5.4. Time dependant base optimisation for the Suzuki-Miyaura cross-coupling reaction using Na_2CO_3 and Cs_2CO_3.

5.4 Effects of temperature

Base screening was performed at 90 ˚C, therefore the effects of lowering the temperature of the reaction were evaluated. Temperatures below 90 ˚C were selected in an effort to search for milder reaction conditions. Similar to the base screening experiments, iodobenzene and *p*-methoxyphenylboronic acid were used as the substrates. At 70 ºC, the mononuclear and binuclear complexes maintain iodobenzene conversion above 90% (Figure 5.5).

At 50 **°**C, the catalysts containing triphenylphosphine ligand (**4.4** and **4.7**) perform poorly as compared to their PTA counterparts (**4.5** and **4.6**). At this temperature the type of phosphine coordinated to the Pd centre seems to have a significant role on the performance of the catalysts. This could also be due to the slightly better water-solubility of the PTA derivatives than the triphenylphosphine derivatives at room temperature.

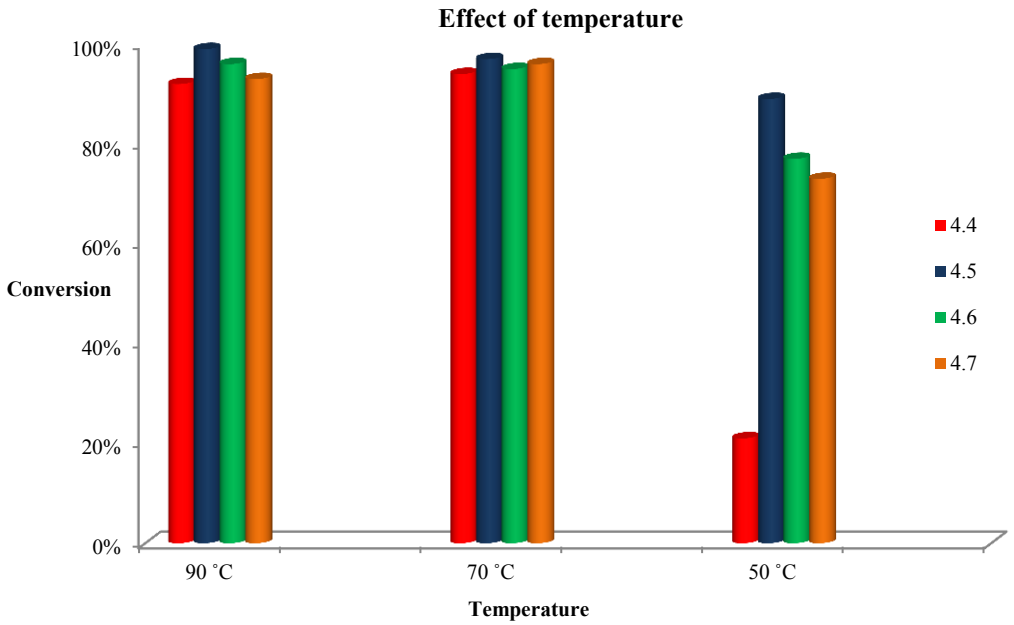

Reactions carried out in 2 mL water, 24 h, 1 mol % Pd, 0.8 mmol phenyl boronic acid, 0.5 mmol iodobenzene, TBAB 0.25 mmol, Base 1 mmol, n-decane internal standard. All reactions were monitored by GC and conversion of aryl halide is the average of catalytic experiments.

Figure 5.5. Effect of temperature on the Suzuki-Miyaura cross-coupling reaction.

Another important observation from these results is that the binuclear catalysts **4.6** and **4.7** do not show improved activity as expected for multinuclear catalysts; however this phenomenon is further investigated in the next section. Since the results at 90 ˚C and 70 ˚C are similar, 70 ˚C was selected as the optimum temperature for this reaction using the water-soluble thiosemicarbazone catalyst precursors (**4.4-4.7**).

5.3.3 Effects of nuclearity

This experiment was carried out at 70 ˚C for 24 hours using sodium carbonate as the base. Iodobenzene and *p*-methoxyphenylboronic acid were also used as the substrates. The effect of the presence two of metal centres in catalysts **4.6** and **4.7** was investigated by performing experiments using the same loading of Pd for each of the catalysts. The Pd loading was doubled by using 1 mol% catalyst loading for **4.6** and **4.7**. This was due to their binuclear nature which resulted in double Pd loading. Figure 5.6 shows the results obtained.

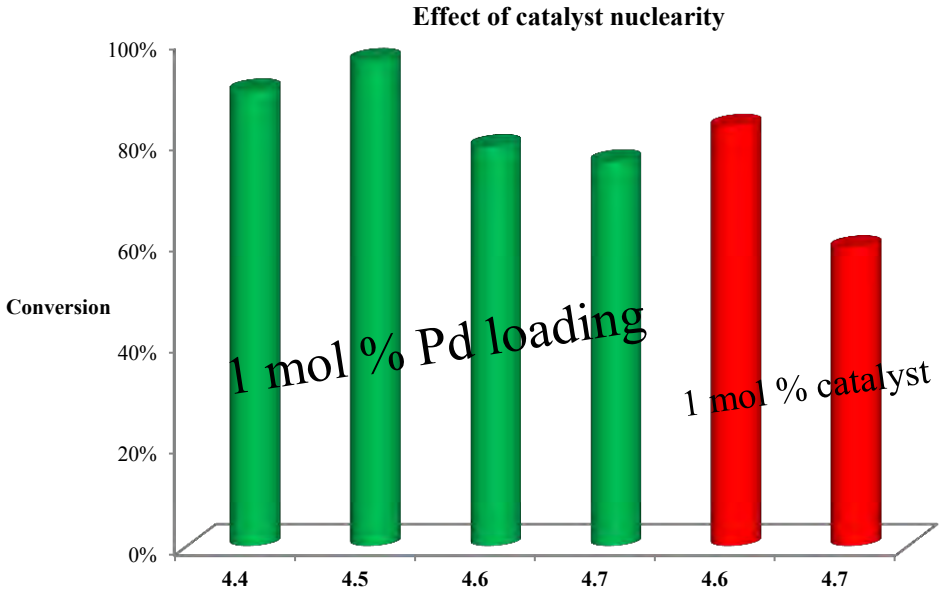

Reactions carried out in 2 mL water, 70 °C, 24 h, 1 mol % Pd, 0.8 mmol phenyl boronic acid, 0.5 mmol iodobenzene, TBAB 0.25 mmol, base 1 mmol, n-decane internal standard. All reactions were monitored by GC and conversion of aryl halide is average of two identical catalytic experiments.

Figure 5.6 Effect of catalyst nuclearity on the Suzuki-Miyaura cross-coupling reaction.

At the same loading of Pd (1 mol% Pd), the mononuclear catalysts **4.4** and **4.5** show higher iodobenzene conversion (90% and 96% respectively). The presence of two metal centres in **4.6** and **4.7** does not result in improved performance (results in green), which iodobenzene conversions of 79% and 76% respectively. Upon doubling the amount of Pd (1 mol% catalyst) for the binuclear catalysts (results in red) iodobenzene conversion do not show any improvement (83% and 59%). It is possible that there is no cooperativity between the two metal centres which usually results in better catalyst activity. This is similar to Hanhan's observations for Suzuki-Miyaura cross-coupling reactions in water using water-soluble diamine Pd(II) catalyst precursors.[30] In this work, the authors observed that the two metal centres in each catalyst work independently of each other and they operate as mononuclear catalysts. As a result of these observations, we conclude that the mononuclear catalyst precursors (**4.4** and **4.5**) have superior activity than the binuclear counterparts and therefore the catalytic activity of the mononuclear catalysts **4.4** and **4.5** using various substrates was evaluated.

5.4 Suzuki-Miyaura cross-coupling reactions between various substrates using 4.4 and 4.5.

The Suzuki-Miyaura cross-coupling reactions (Scheme 5.2) were carried out under the afore-mentioned optimised reaction conditions. Both hydrophobic and hydrophilic substrates were tested and the percentage yields of the products were moderate to excellent. The results for the Suzuki-Miyaura cross-coupling reactions show that the catalysts are compatible with a range of functional groups on the substrates. Both catalysts (**4.4** and **4.5**) showed notable activity when using 1 mol% Pd loading under the test conditions (Table 5.1).

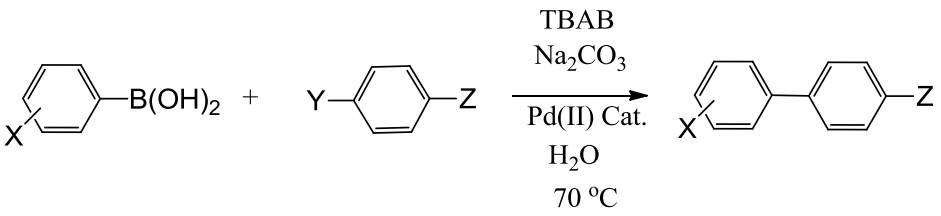

Scheme 5.2. Suzuki-Miyaura cross-coupling reactions between various substrates.

The results indicate that catalysts **4.4** and **4.5** are highly efficient. When employing catalyst **4.4**, the presence of an electron-withdrawing substituent on the phenylboronic acid such as –COOH (Entry 6) results in very low yield of biphenyl product (33%). However, when the iodobenzene is used in place of the bromobenzene, (Entry 6 and 11), a 38% yield is obtained. It shows that iodobenzene couples more readily with the phenylboronic acid than bromobenzene. This halogen effect is also observed in Entries 5 and 9. The yield of biphenyl product almost triples when iodobenzene is utilised. However, with catalyst **4.5**, this is not observed when the halogen is changed (Entries 16 and 23).

When unsubstituted starting materials are used (Entry 1), a yield of 76% is obtained using catalyst **4.4**. However, when catalyst **4.5** is used, a pronounced decrease in the performance of the catalyst is observed, with 49% yield of product (Entry 18). Introduction of a nitro-substituent (Entry 12) on the phenylboronic acid results in a 67% yield of product. The absence of the nitro- group (Entry 10) results in a conversion of 80%. Moderate yields are obtained with the carboxyl substituents and this is probably due to their good water-solubility (Entries 11, 18, 20). However, a significant drop in catalyst performance is observed when bromobenzene was used. Both mononuclear catalysts gave moderate results (Entries 11, 18, 20).

Table 5.1. Suzuki-Miyaura cross-coupling reactions between various substrates using catalyst **4.4** and **4.5**.

Entry	Catalyst	X	Y	Z	Isolated Yield (%)
1	**4.4**	H	Br	H	76
2	**4.4**	H	Br	CH_3	72
3	**4.4**	H	Br	OMe	93
4	**4.4**	4-CH_3,2-NO_2	Br	H	94
5	**4.4**	4-^{t}Bu	Br	H	32
6	**4.4**	4-COOH	Br	H	33
7	**4.4**	H	I	CH_3	81
8	**4.4**	4-CHO	I	H	45
9	**4.4**	4-^{t}Bu	I	H	84
10	**4.4**	4-CH_3	I	H	80
11	**4.4**	4-COOH	I	H	38
12	**4.4**	4-CH_3,3-NO_2	I	H	67
13	**4.4**	4-COOH	I	CH_3	69
14	**4.5**	H	Br	OMe	25
15	**4.5**	H	Br	CH_3	54
16	**4.5**	4-^{t}Bu	Br	H	98
17	**4.5**	4-COOH	Br	H	61
18	**4.5**	H	I	H	49
19	**4.5**	4-COOH	I	H	85
20	**4.5**	4-COOH	I	CH_3	42
21	**4.5**	H	I	CH_3	70
22	**4.5**	4-CH_3	I	H	74
23	**4.5**	4-^{t}Bu	I	H	63

Reactions carried out in 2 mL water, 70 °C, 24 h, 1 mol % Pd, 0.8 mmol phenyl boronic acid, 0.5 mmol aryl halide, TBAB 0.25 mmol, Na_2CO_3 1 mmol.

The complexes display good stability in solution, therefore it is possible that a vacant coordination site can be difficult to form for oxidative addition to take place. Therefore a Pd(II) to Pd(IV) oxidative addition could be the possible mechanism for oxidative addition to occur. However, catalyst **4.4** generally showed superior activity in the reactions. Therefore, complex **4.4** was further tested in recyclability experiments.

5.5 Catalyst recycling in the aqueous phase Suzuki-Miyaura cross-coupling reactions using catalyst 4.4.

The potential for recyclability of catalyst **4.4** was tested using iodobenzene and *p*-methoxy phenylboronic acid as substrates. After cooling the reaction vessel, the product was extracted

from the aqueous solution using toluene and analysed using gas chromatography. The aqueous layer was then reused. The conversions obtained are an average of two identical reactions and were based on the conversion of aryl halide. The results are shown in Figure 5.7.

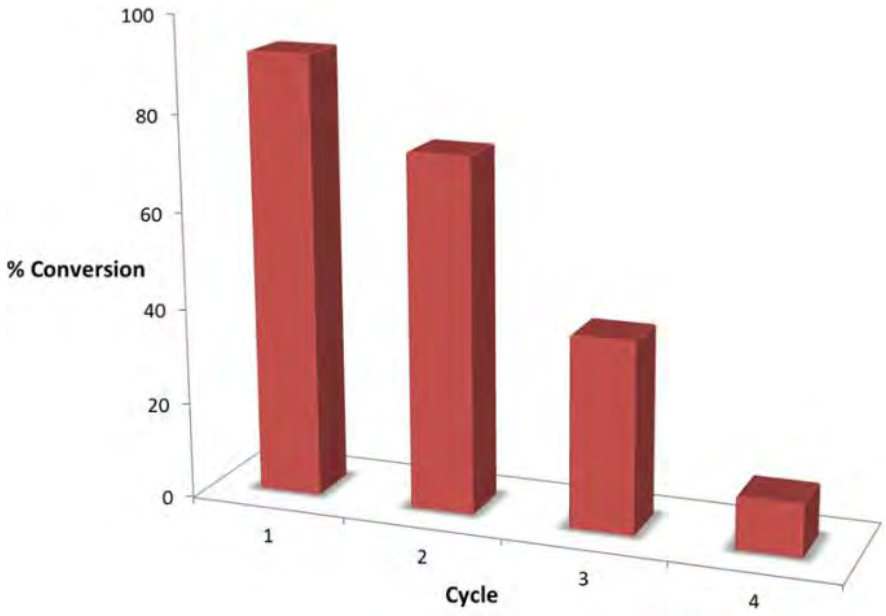

Figure 5.7 Recycling of catalyst **4.4.**

There is a gradual decrease in iodobenzene conversion with each recycle (Figure 5.7). The catalyst could be recycled efficiently twice. 92% of the iodobenzene was converted to biphenyl product in the first cycle and this dropped to 74% in the second recycle. In the third and fourth cycles 40% and 11% conversion was observed, respectively. This could be due to partial decomposition of the active species at the elevated temperatures during each catalytic cycle.[31] This decomposition could have occurred after 24 hours since the catalyst proved to be stable over a 24 hour period.

No palladium black was observed during the experiments ruling out the presence of palladium nanoparticles. This was confirmed in a mercury poisoning experiment. This experiment was performed in a recycling experiment in the presence of mercury. In the first run, the conversion of iodobenzene is 86% which is comparable to 92% conversion in the absence of mercury. Upon further catalyst reuse, the iodobenzene conversion in the second, third and fourth recycle was 72%, 46% and 17% respectively, which is comparable to the results obtained in the absence of mercury.

This indicates the absence of nanoparticle mediated catalysis and confirms that the water-soluble catalyst **4.4** acts a homogeneous catalyst in this reaction.

5.6 Overall Summary

The water-soluble Pd(II) thiosemicarbazone complexes (**4.4**-**4.7**) were evaluated as catalyst precursors in the Suzuki-Miyaura cross-coupling reaction in aqueous medium. Sodium carbonate was used as the base. The presence of 2 metal centres in the binuclear catalyst precursors **4.6** and **4.7** did not improve the activity of the catalysts, with **4.6** and **4.7** having comparable activity as the mononuclear analogues **4.4** and **4.5**. The monothiosemicarbazone complexes **4.4** and **4.5** were therefore further tested in the Suzuki-Miyaura cross-coupling reactions of various substrates. Catalysts **4.4** and **4.5** were versatile and could couple various substrates, with iodobenzene giving better results than bromobenzene as expected. Catalyst **4.4** could be recycled efficiently twice with a significant drop in conversion of aryl halide in the third and fourth recycles. Mercury poisoning tests confirm that the reaction follows a homogeneous pathway.

5.7 Experimental

General Details

Nuclear magnetic resonance (NMR) spectra were recorded on either a Varian XR300 MHz (^{1}H at 300.08 MHz, ^{13}C{H} at 75.46 MHz) or a Bruker Biospin GmbH (^{1}H NMR at 400.22 MHz, ^{13}C{H} NMR at 100.65 MHz) spectrometer at ambient temperature. The Suzuki-Miyaura cross-coupling products were analysed on a Perkin Elmer Clarus 580 GC.

General Suzuki-Miyaura cross-coupling procedure

The palladium loading was (1.00 mol%), phenylboronic acid (0.80 mmol), aryl halide (0.50 mmol), tetrabutylammonium bromide (0.25 mmol), base (1.00 mmol) and water (2 mL) were charged into a 50 mL Schlenk tube. The mixture was heated to appropriate temperature and the reaction allowed to proceed at this temperature for 24 h in air. For the gas chromatography analyses, the products were extracted with toluene and analysed. Conversions reported are an average of two identical reactions and were based on the aryl halide. For NMR spectroscopy determination, the reaction mixture was cooled and ethyl acetate (2 mL) was added. The organic layer was dried over magnesium sulphate and the

product formed was recovered after separation on a short column using petroleum ether: ethyl acetate solvent mixture. The recovered product was dried under vacuum.

Catalyst recycling procedure

The Schlenk tube was charged with catalyst **4.4** (1.00 mol%), phenylboronic acid (0.80 mmol), aryl halide (0.50 mmol), tetrabutylammonium bromide (0.25 mmol), sodium carbonate (1.00 mmol) and water (2 mL). The mixture was heated to 70 ˚C and the reaction was allowed to proceed at this temperature for 24 h in air. The reaction mixture was cooled to room temperature and 2 mL of toluene added and this was stirred for 5 minutes. The organic layer was separated and analysed using gas chromatography. The aqueous layer was transferred to a clean Schlenk tube for the next reaction cycle.

5.8 Characterization of the Suzuki-Miyaura cross-coupling reaction products.

The products have been characterized using ^{1}H NMR and ^{31}C NMR spectroscopy and the spectroscopic data compares favourably with the literature and confirms the authenticity of the coupled products.

5.8.1 Characterization of 1,1-biphenyl[32]

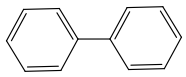

Yield (76%). **^{1}H NMR**: $CDCl_3$, δ (ppm): 7.69 (d, ^{3}J = 7.5 Hz, 4 H, $\mathbf{H}_{Ar}$), 7.51 (t, ^{3}J = 7.2 Hz, 4 H, $\mathbf{H}_{Ar}$), 7.42 (t, ^{3}J = 7.2 Hz, 2 H, $\mathbf{H}_{Ar}$). **^{13}C{H} NMR**: $CDCl_3$, δ (ppm): 141.3, 129.8, 127.3, 127.2.

5.8.2 Characterization of 4-methyl-1,1-biphenyl[32]

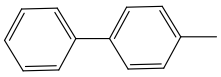

Yield (72%). **^{1}H NMR**: DMSO-d_6, δ (ppm): 8.00-7.99 (m, 1 H, $\mathbf{H}_{Ar}$), 7.80-7.76 (m, 2 H, $\mathbf{H}_{Ar}$), 7.61-7.59 (m, 2 H, $\mathbf{H}_{Ar}$), 7.43-7.35 (m, 2 H, $\mathbf{H}_{Ar}$), 7.03-7.01 (m, 2 H, $\mathbf{H}_{Ar}$), 2.26 (m, 3 H, $C\mathbf{H}_3$). **^{13}C{H} NMR**: DMSO-d_6, δ (ppm): 141.3, 139.7, 138.8, 137.4, 134.5, 131.9, 130.4, 127.8, 20.9.

5.8.3 Characterization of 4-methoxyl-1,1-biphenyl[33]

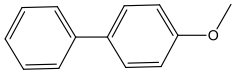

Yield (93%). **^{1}H NMR**: DMSO-d_6, δ (ppm): 7.59 (t, ^3J = 7.2 Hz, 4 H, $\mathbf{H}_{Ar}$), 7.35 (t, ^3J = 6.1 Hz, 2 H, $\mathbf{H}_{Ar}$), 7.32 (m, 1H, $\mathbf{H}_{Ar}$), 7.04 (d, ^3J = 8.4 Hz, 2 H, $\mathbf{H}_{Ar}$), 3.89 (s, 3 H, C$\mathbf{H}_3$). **^{13}C{H} NMR**: DMSO-d_6, δ (ppm): 159.2, 140.8, 133.9, 128.7, 128.1, 126.7, 126.5, 114.3, 55.4.

5.8.4 Characterization of 4-methyl-2-nitro-1,1-biphenyl[34]

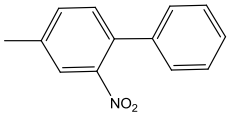

Yield (94%). **^{1}H NMR**: $CDCl_3$, δ (ppm): 7.90 (s, 1 H, $\mathbf{H}_{Ar}$) 7.58-7.52 (m, 1 H, $\mathbf{H}_{Ar}$) 7.45-7.42 (m, 1 H, $\mathbf{H}_{Ar}$), 7.37-7.27 (m, 4 H, $\mathbf{H}_{Ar}$) 7.24-7.20 (m, 1 H, $\mathbf{H}_{Ar}$) 2.20 (s, 3 H, C$\mathbf{H}_3$). **^{13}C{H} NMR**: $CDCl_3$, δ (ppm): 149.3, 139.3, 137.9, 137.6, 137.2, 134.8, 135.5, 131.0, 130.1, 128.1, 20.5.

5.8.5 Characterization of 4-(tert-butyl)-1,1-biphenyl[35]

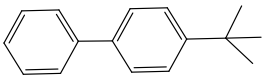

Yield (39%). **^{1}H NMR**: $CDCl_3$, δ (ppm): 7.59 (t, ^3J = 7.2 Hz, 4 H, $\mathbf{H}_{Ar}$), 7.35 (t, ^3J = 6.1 Hz, 2 H, $\mathbf{H}_{Ar}$), 7.32 (m, 1 H, $\mathbf{H}_{Ar}$), 7.04 (d, ^3J = 8.4 Hz, 2 H, $\mathbf{H}_{Ar}$), 3.89 (s, 9 H, C$\mathbf{H}_3$). **^{13}C{H} NMR**: $CDCl_3$, δ (ppm): 159.2, 140.8, 133.9, 128.7, 128.1, 126.7, 126.5, 114.3, 55.36, 31.2.

5.8.6 Characterization of [1,1-biphenyl]-4-carboxylic acid[36]

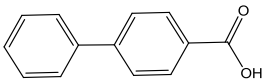

Yield (33%). **^{1}H NMR**: DMSO-d_6, δ (ppm): 7.72 (m, 2 H, $\mathbf{H}_{Ar}$), 7.37 (m, 2 H, $\mathbf{H}_{Ar}$), 7.15 (m, 5 H, $\mathbf{H}_{Ar}$). **^{13}C{H} NMR**: DMSO-d_6, δ (ppm): 168.0, 137.6, 134.3, 132.5, 132.0, 131.1, 130.8, 128.6, 128.1.

5.8. Characterization of 4-methyl-1,1-biphenyl[32]

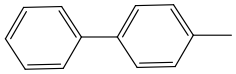

Yield (81%). **^{1}H NMR**: DMSO-d_6, δ (ppm): 8.00-7.98 (m, 1 H, H_{Ar}), 7.82-7.77 (m, 2 H, H_{Ar}), 7.62-7.58 (m, 2 H, H_{Ar}), 7.40-7.36 (m, 2 H, H_{Ar}), 7.00-6.99 (m, 2 H, H_{Ar}), 2.26 (m, 3 H, CH_3). **^{13}C{H} NMR**: DMSO-d_6, δ (ppm): 141.1, 139.6, 137.3, 134.5, 131.9, 130.4, 127.8, 21.0.

5.8.8 Characterization of [1,1'-biphenyl]-4-carbaldehyde[37]

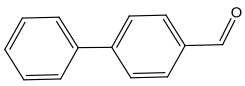

Yield (45%). **^{1}H NMR**: DMSO-d_6, δ (ppm): 10.11 (s, 1 H, C**H**O), 7.79-7.73 (m, 2 H, $\mathbf{H}_{Ar}$) 7.41-7.34 (m, 2 H, $\mathbf{H}_{Ar}$), 7.18-7.12 (m, 5 H, $\mathbf{H}_{Ar}$). **^{13}C{H} NMR**: DMSO-d_6, δ (ppm): 190.0, 146.1, 140.2, 135.9, 130.4, 129.2, 128.4, 127.9, 127.6.

5.8.9 Characterization of 4-(tert-butyl)-1,1-biphenyl[35]

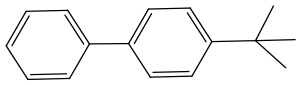

Yield (32%). **^{1}H NMR**: DMSO-d_6, δ (ppm): 7.82 (m, 5 H, $\mathbf{H}_{Ar}$), 7.43 (m, 2 H, $\mathbf{H}_{Ar}$), 7.03 (m, 2 H, $\mathbf{H}_{Ar}$), 1.98 (s, 9 H, C$\mathbf{H}_3$). **^{13}C{H} NMR**: DMSO-d_6, δ (ppm): 155.9, 138.6, 136.3, 134.6, 131.9, 130.0, 126.6, 124.7, 35.6, 30.9.

5.8.10 Characterization of 4-methyl-1,1-biphenyl[32]

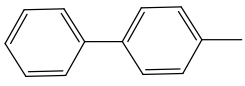

Yield (80%). **^{1}H NMR**: DMSO-d_6, δ (ppm): 7.99-7.96 (m, 1 H, $\mathbf{H}_{Ar}$), 7.82-7.78 (m, 2 H, $\mathbf{H}_{Ar}$), 7.60-7.58 (m, 2 H, $\mathbf{H}_{Ar}$), 7.40-7.34 (m, 2 H, $\mathbf{H}_{Ar}$), 7.03-7.01 (m, 2 H, $\mathbf{H}_{Ar}$), 2.30 (m, 3 H, C$\mathbf{H}_3$). **^{13}C{H} NMR**: DMSO-d_6, δ (ppm): 140.1, 139.1, 138.8, 137.6, 132.5, 131.6, 130.9, 127.2, 20.9.

5.8.11 Characterization of [1,1-biphenyl]-4-carboxylic acid[36]

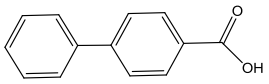

Yield (38%). **^{1}H NMR**: DMSO-d_6, δ (ppm): 7.72 (m, 2 H, $\mathbf{H}_{Ar}$), 7.37 (m, 2 H, $\mathbf{H}_{Ar}$), 7.15 (m, 5 H, $\mathbf{H}_{Ar}$). **^{13}C{H} NMR**: DMSO-d_6, δ (ppm): 168.0, 139.9, 137.8, 134.64, 132.5, 131.1, 128.6, 128.1, 127.8.

5.8.12 Characterization of 4-methyl-2-nitro-1,1-biphenyl[34]

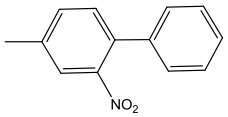

Yield (67%). **^{1}H NMR**: DMSO-d_6, δ (ppm): 8.44 (s, 1 H, $\mathbf{H}_{Ar}$), 8.05 (d, ^{3}J = 7.6 Hz, 1 H, $\mathbf{H}_{Ar}$), 7.74-7.70 (m, 2 H, $\mathbf{H}_{Ar}$), 7.41-7.34 (m, 4 H, $\mathbf{H}_{Ar}$), 7.20-7.17 (m, 3 H, $\mathbf{H}_{Ar}$), 2.51 (s, 3 H, CH_3). **^{13}C{H} NMR**: DMSO-d_6, δ (ppm): 149.3, 139.3, 137.8, 137.6, 17.3, 134.8, 132.5, 131.0, 130.1, 128.1.

5.8.13 Characterization of [1,1-biphenyl]-4-carboxylic acid[36]

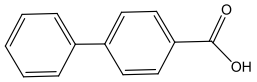

Yield (69%). **^{1}H NMR**: DMSO-d_6, δ (ppm): 7.98 (m, 2 H, $\mathbf{H}_{Ar}$), 7.02 (m, 2 H, $\mathbf{H}_{Ar}$), 6.98 (m, 5 H, $\mathbf{H}_{Ar}$). **^{13}C{H} NMR**: DMSO-d_6, δ (ppm): 167.4, 140.2, 138.6, 137.3, 135.1, 131.9, 128.9, 128.0, 126.3.

5.8.14 Characterization of 4-methoxyl-1,1-biphenyl[33]

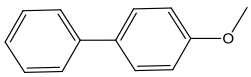

Yield (25%). **^{1}H NMR**: $CDCl_3$, δ (ppm): 7.61 (m, 5 H, $\mathbf{H}_{Ar}$), 7.30 (m, 2 H, $\mathbf{H}_{Ar}$), 7.00 (m, 2 H, $\mathbf{H}_{Ar}$), 3.85 (s, 3 H, $C\mathbf{H}_3$). **^{13}C{H} NMR**: $CDCl_3$, δ (ppm): 160.1, 141.9, 136.9, 128.6, 127.9, 126.3, 126.0, 115.9, 54.2.

5.8.15 Characterization of 4-methyl-1,1-biphenyl[32]

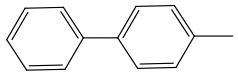

Yield (54%). **^{1}H NMR**: DMSO-d_6, δ (ppm): 8.00-7.98 (m, 1 H, $\mathbf{H}_{Ar}$), 7.77-7.80 (m, 2 H, $\mathbf{H}_{Ar}$), 7.59-7.61 (m, 2 H, $\mathbf{H}_{Ar}$), 7.40-7.30 (m, 2 H, $\mathbf{H}_{Ar}$), 7.03-7.00 (m, 2 H, $\mathbf{H}_{Ar}$), 2.25 (m, 3 H, C$\mathbf{H}_3$). **^{13}C{H} NMR**: DMSO-d_6, δ (ppm): 141.1, 139.6, 138.0, 137.3, 134.5, 131.9, 130.5, 127.8, 20.8.

5.8.16 Characterization of 4-(tert-butyl)-1,1-biphenyl[35]

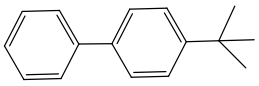

Yield (58%). **^{1}H NMR**: DMSO-d_6, δ (ppm): 7.72 (m, 5 H, $\mathbf{H}_{Ar}$), 7.37 (m, 2 H, $\mathbf{H}_{Ar}$), 7.15 (m, 2 H, $\mathbf{H}_{Ar}$), 1.27 (s, 9 H, C$\mathbf{H}_3$). **^{13}C{H} NMR**: DMSO-d_6, δ (ppm): 152.9, 137.6, 135.2, 134.6, 131.0, 130.4, 128.1, 124.5, 34.8, 31.6.

5.8.17 Characterization of [1,1-biphenyl]-4-carboxylic acid[36]

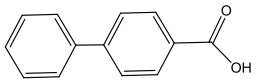

Yield (61%). **^{1}H NMR**: DMSO-d_6, δ (ppm): 7.75-7.70 (m, 2 H, $\mathbf{H}_{Ar}$), 7.40-734 (m, 2 H, $\mathbf{H}_{Ar}$), 7.20-7.12 (m, 5 H, $\mathbf{H}_{Ar}$). **^{13}C{H} NMR**: DMSO-d_6, δ (ppm): 161.1, 143.9, 140.9, 134.2, 128.6, 128.0, 127.3, 126.1, 118.9.

5.8.18 Characterization of 1,1-biphenyl[32]

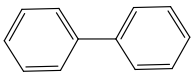

Yield (49%). **^{1}H NMR**: DMSO-d_6, δ (ppm): 7.71-7.69 (m, 4 H, $\mathbf{H}_{Ar}$), 7.52-7.51 (m, 4 H, $\mathbf{H}_{Ar}$), 7.45-7.40 (m, 2 H, $\mathbf{H}_{Ar}$). **^{13}C{H} NMR**: DMSO-d_6, δ (ppm): 141.3, 128.8, 127.3, 127.2.

5.8.19 Characterization of [1,1-biphenyl]-4-carboxylic acid[36]

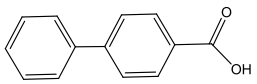

Yield (85%). **^{1}H NMR**: DMSO-d_6, δ (ppm): 7.92-7.81 (m, 2 H, $\mathbf{H}_{Ar}$), 7.62-7.59 (m, 2 H, $\mathbf{H}_{Ar}$), 7.29-7.23 (m, 5 H, $\mathbf{H}_{Ar}$). **^{13}C{H} NMR**: DMSO-d_6, δ (ppm): 169.9, 145.3, 141.3, 133.6, 129.1, 128.0, 127.8, 127.0, 119.9.

5.8.20 Characterization of [1,1-biphenyl]-4-carboxylic acid[36]

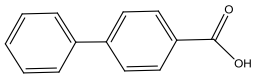

Yield (42%). **^{1}H NMR**: DMSO-d_6, δ (ppm): 7.91-7.95 (m, 2 H, $\mathbf{H}_{Ar}$), 7.39-7.36 (m, 2 H, $\mathbf{H}_{Ar}$), 7.22-7.19 (m, 5 H, $\mathbf{H}_{Ar}$). **^{13}C{H} NMR**: DMSO-d_6, δ (ppm): 169.6, 145.1, 140.4, 135.2, 128.7, 128.5, 127.9, 126.8, 120.9.

5.8.21 Characterization of 4-methyl-1,1-biphenyl[32]

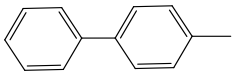

Yield (30%). **^{1}H NMR**: DMSO-d_6, δ (ppm): 8.00-7.99 (m, 1 H, $\mathbf{H}_{Ar}$), 7.80-7.79 (m, 2 H, $\mathbf{H}_{Ar}$), 7.61-7.59 (m, 2 H, $\mathbf{H}_{Ar}$), 7.42-7.30 (m, 2 H, $\mathbf{H}_{Ar}$), 7.03-7.00 (m, 2 H, $\mathbf{H}_{Ar}$), 2.26 (m, 3 H, C$\mathbf{H}_3$). **^{13}C{H} NMR**: DMSO-d_6, δ (ppm): 140.7, 139.6, 138.6, 137.3, 134.5, 131.9, 130.4, 127.8, 20.9.

5.8.22 Characterization of 4-methyl-1,1-biphenyl[32]

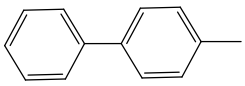

Yield (74%). **^{1}H NMR**: DMSO-d_6, δ (ppm): 7.99-7.98 (m, 1 H, $\mathbf{H}_{Ar}$), 7.80-7.77 (m, 2 H, $\mathbf{H}_{Ar}$), 7.61-7.59 (m, 2 H, $\mathbf{H}_{Ar}$), 7.40-7.31 (m, 2 H, $\mathbf{H}_{Ar}$), 7.03-7.00 (m, 2 H, $\mathbf{H}_{Ar}$), 2.26 (m, 3 H, C$\mathbf{H}_3$). **^{13}C{H} NMR**: DMSO-d_6, δ (ppm): 141.1, 139.7, 138.9, 137.4, 134.5, 131.9, 130.4, 127.8, 20.9.

5.8.23 Characterization of 4-(tert-butyl)-1,1-biphenyl[35]

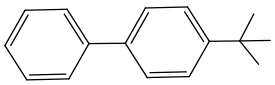

Yield (63%). **^{1}H NMR**: DMSO-d_6, δ (ppm): 7.64-7.54 (m, 4H $\mathbf{H}_{Ar}$), 7.51-7.28 (5H, m, $\mathbf{H}_{Ar}$), 1.40 (s, 9H, C$\mathbf{H}_3$). **^{13}C{H} NMR**: DMSO-d_6, δ (ppm): 154.1, 138.6, 135.5, 134.8, 132.0, 130.9, 129.3, 125.8, 36.8, 30.3.

5.9 References

1 A. Suzuki, *J. Organomet. Chem.*, 2002, **653**, 83–90.

2 C. S. Callam and T. L. Lowary, *J. Chem. Educ.*,**78**, 2001, 948-949.

3 N. Miyaura and A. Suzuki, *Chem. Rev.*, 1995, **95**, 2457–2483.

4 K. H. Shaughnessy, *Metal-Catalysed Reactions in Water*, Wiley-VCH Verlag GmbH & Co. KGaA, Weinheim, 2013, pp 1-46.

5 A. L. Casalnuovo and J. C. Calabrese, *J. Am. Chem. Soc.*, 1990, **112**, 4324–4330.

6 R. Huang and K. H. Shaughnessy, *Organometallics*, 2006, **25**, 4105–4112.

7 R. Zhong, A. Pöthig, Y. Feng, K. Riener, W. A. Herrmann and F. E. Kühn, *Green Chem.*, 2014, **16**, 4955–4962.

8 J. Zhou, X. Guo, C. Tu, X. Li and H. Sun, *J. Organomet. Chem.*, 2009, **694**, 697–702.

9 J. Zhou, X. Li and H. Sun, *J. Organomet. Chem.*, 2010, **695**, 297–303.

10 L. Bai, J. Wang and Y. Zhang, *Green Chem.*, 2003, **5**, 615–617.

11 C. Baleizao, A. Corma, H. Garcia and A. Leyva, *ChemInform*, 2003, **34**, 606–607.

12 S. N. Chen, W. Y. Wu and F. Y. Tsai, *Tetrahedron*, 2008, **64**, 8164–8168.

13 M. Makosza, *Pure Appl. Chem.*, 2000, **72**, 1399–1403.

14 L. Botella and C. Na, *J. Organomet. Chem.*, 2002, **663**, 46–57.

15 A. Roucoux and H. Patin, *Adv. Synth. Catal.*, 2002, **344**, 266–267.

16 J. So, K. Olech, Ś. Agnieszka, D. Zaj and J. Cabaj, *J. Chem. Educ.*, 2013, **3**, 19–32.

17 A. A. C. Braga, G. Ujaque and F. Maseras, *Organometallics*, 2006, **25**, 3647–3658.

18 L. J. Goossen, D. Koley, H. L. Hermann and W. Thiel, *Organometallics*, 2005, **24**, 2398–2410.

19 N. Miyaura and A. Suzuki, *Chem. Rev.*, 1995, **95**, 2457–2483.

20 M. Joshaghani, E. Faramarzi, E. Rafiee, M. Daryanavard, J. Xiao and C. Baillie, *J. Mol. Catal. A Chem.*, 2006, **259**, 35–40.

21 S. Kotha, K. Lahiri and D. Kashinath, *Tetrahedron*, 2002, **58**, 9633–9695.

22 H. M. Senn and T. Ziegler, *Organometallics*, 2004, **23**, 2980–2988.

23 A. J. J. Lennox and G. C. Lloyd-Jones, *Chem. Soc. Rev.*, 2014, **43**, 412–443.

24 K. M. Engle, D. Wang and P. J. Yu, *Angew. Chem. Int. Engl.*, 2009, **48**, 5094–5115.

25 W. De Graaf, J. Bowsma and G. Van Koten, *Organometallics*, 1990, **9**, 1479–1484.

26 D. Kalyani, N. Deprez, L. V Desai and M. S. Sanford, *J. Am. Chem. Soc.*, 2005, **127**, 7330–7331.

27 P. K. Byers, A. J. Canty, B. W. Skelton and A. H. White, *J. Chem. Soc. Chem. Commun.*, 1986, **3**, 1722-1723.

28 H. Yan, P. Chellan, T. Li, J. Mao, K. Chibale and G. S. Smith, *Tetrahedron Lett.*, 2013, **54**, 154–157.

29 C. Amatore, A. Jutand and G. Le Duc, *Chem. Eur. J.*, 2012, **18**, 6616–6625.

30 M. E. Hanhan, C. Cetinkaya and M. P. Shaver, *Appl. Organomet. Chem.*, 2013, **27**, 570–577.

31 W. A. Herrmann, V. P. Böhm and C. P. Reisinger, *J. Organomet. Chem.*, 1999, **576**, 23–41.

32 R. Bandari, T. Höche, A. Prager, K. Dirnberger and M. R. Buchmeiser, *Chem. A Eur. J.*, 2010, **16**, 4650-4658.

33 A. Emilio and N. Carmen, *Org. lett.*, 2008, **10**, 5011-5014.

34 H. Wenkun, Q. Yatao, Y. Zhiyi, W. Zhaoyang and J. Sheng, *Tetrahedron Lett.*, 2011, **52**, 4916-4919.

35 L. Hu, S. Chang-Liang, Y. Miao, Y. Da-Gang, L. Bi-Jie and S. Zhang-Jie, *Chem. A. Eur. J.*, 2011, **17**, 3593-3597.

36 D. Zhengyin, Z. Wanwei, W. Fen and W. Jin-Xian, *Tetrahedron*, 2011, **67**, 4914-4918.

37 Z. Guolin, *Synthesis*, 2005, **4**, 537-542.

Chapter 6

Theoretical study on the oxidative addition of iodobenzene to Pd(II) thiosemicarbazone complex

6.1 Introduction

Theoretical experiments on the oxidative addition of aryl halides to Pd(0) in the Suzuki-Miyaura cross-coupling reaction have been studied extensively.[1–7] The generally accepted mechanism for this reaction is shown in Figure 6.1.[2] The catalytic cycle involves three steps; (a) oxidative addition, (b) transmetallation and (c) reductive elimination. The oxidative addition step and the reductive elimination steps have been studied extensively in the literature, both experimentally[8–10] and theoretically.[11,12]

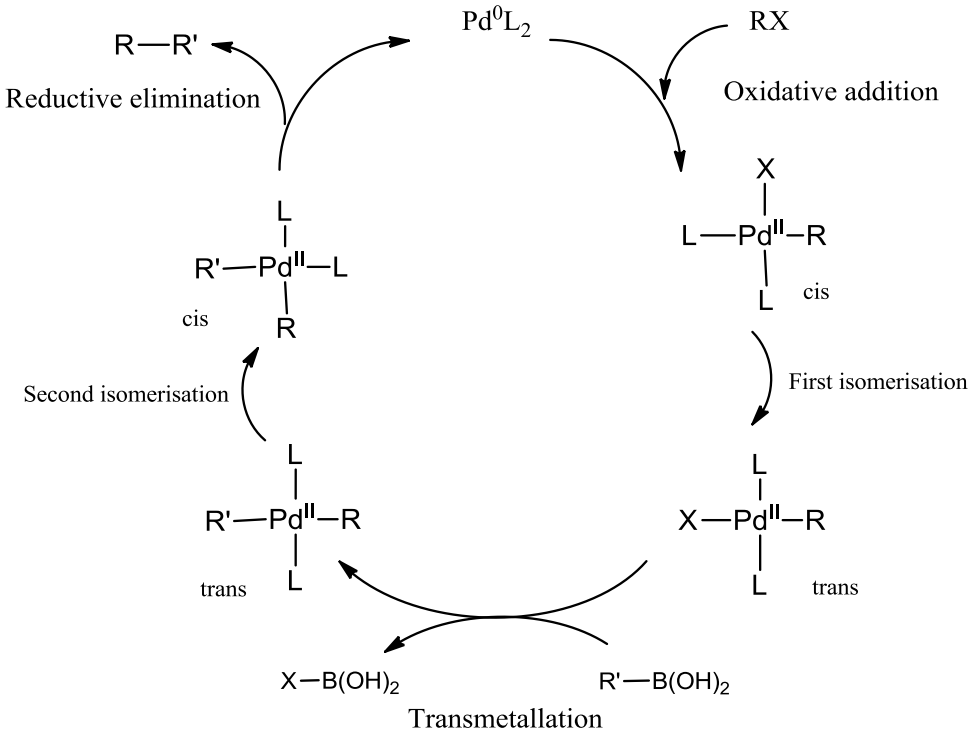

Figure 6.1. Generally accepted Suzuki-Miyaura cross-coupling reaction mechanism.

The oxidative addition step results in the formation of an organopalladium complex. It has generally been accepted that this complex is initially in the *cis*-conformation but isomerises to the *trans*-conformation as shown in Figure 6.1.[2,4,13] The most commonly known oxidative

addition mechanism for the Suzuki-Miyaura cross-coupling reaction follows a Pd(0) to Pd(II) mechanism.[1,2,14–17] After oxidative addition, the transmetallation step follows. In this step, the base activates the boron containing reagent and also facilitates the formation of the alkoxy species R-Pd-OR from R-Pd-X (where X is the halide). The final step (reductive elimination) gives the desired product and results in the regeneration of Pd catalyst and in this step it reverts back to the *cis*-conformation before reductive elimination can occur.[13]

Although the Pd(0) to Pd(II) redox is popular for oxidative addition, a Pd(II) to Pd(IV) mechanism is also possible.[18–21] Pd(IV) complexes are formed by oxidative addition of aryl halides to Pd(II). The catalytic roles of Pd(IV) complexes have also been investigated by Canty.[22]

Pincer-type palladium catalysts have been reported to undergo oxidative addition *via* a Pd(II)/Pd(IV) redox couple.[23,24] Unlike other Pd(II) complexes such as $Pd(PPh_3)_4$ and $Pd(PPh_3)_2(OAc)_2$, which serve as sources of Pd nanoparticles, pincer-type complexes are reported to have high thermal stability, which has led to the proposal of Pd(II)/Pd(IV) catalytic mechanisms. Computational studies on this class of compounds have also proved that a Pd(II)/Pd(IV) mechanism exists.[24]

Bautista and co-workers have demonstrated the possibility of synthesis of aryl Pd(IV) complexes by oxidative addition of aryl halides to Pd(II) complexes and their application as catalysts for C-C coupling reactions.[25] The Pd(IV) complexes synthesised were very stable and this was attributed to the pincer ligand present. A Pd(II) intermediate was formed during the oxidative addition and this was detected using spectroscopic techniques. The catalysts were used for the C-C coupling reactions in the presence of an excess amount of mercury and over 80% product was formed, indicating that Pd nanoparticles were not involved in the reaction. The results from this study point to the fact that Pd(IV) complexes can be formed by oxidative addition of an aryl halide to Pd(II). The catalytic results also suggest that Pd(II) to Pd(IV) is the favoured redox for these stable complexes.

In another study, involving a ligand promoted $C(sp^3)$-H activation and arylation reaction, the authors proved that the Pd(II) complexes could undergo oxidative addition with iodobenzene to form Pd(IV) complexes.[26] The authors demonstrated the possibility of a Pd(II)/Pd(IV) redox couple during oxidative addition of iodobenzene to Pd(II).

The water-soluble thiosemicarbazone complex **4.4** (preparation and characterization discussed in Chapter 4) was found to be very stable in water at elevated temperatures. Moreover, in the Suzuki-Miyaura cross-coupling reactions discussed in Chapter 5, nanoparticle formation was not observed in the catalytic reactions. The mercury poisoning experiment also supported the fact that the Suzuki-Miyaura cross-coupling reactions were entirely homogeneous. As a result of these findings, the possibility of reduction of Pd(II) to Pd(0) for oxidative addition of the aryl halide to occur was ruled out. In this Chapter we seek to investigate a possible Pd(II)/Pd(IV) redox couple during the oxidative addition of iodobenzene to the thiosemicarbazone complex (**4.4**) using DFT computational studies. The computational details for this investigation are given in section 6.4.

6.2 Mechanism of Oxidative addition of iodobenzene to Pd(II) thiosemicarbazone complex 4.4

The optimised structures of the two starting materials **6.1** (metal complex) and **6.2** (iodobenzene) are shown in Figure 6.2. The sodium counter-ion was included during the calculations to achieve an overall neutral charge on the metal complex.

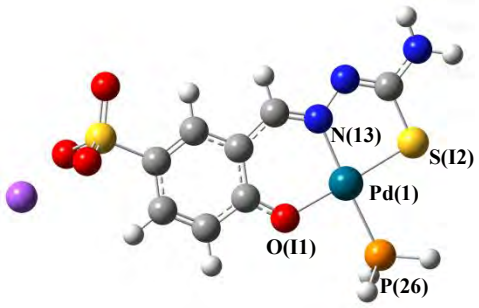

6.1

Pd(1)-P(26) = 2.292
O(11)-Pd(1)-P(26) = 88.4
S(12)-Pd(1)-P(26) = 93.3
N(13)-Pd(1)-S(12) = 84.2
N(13)-Pd(1)-O(11) = 94.1

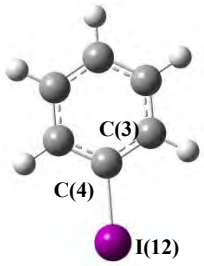

6.2

C(4)-I(12) = 2.108
C(4)-C(3) = 1.396

Figure 6.2. Optimised structures of the starting materials PBE0/def2-SVP/SDD(Pd) with selected bond lengths (Å) and angles (˚).

The structure of the metal complex shows a square-planar geometry at the Pd metal centre with bond angles between 84.2˚ and 94.1˚ which is similar to previously reported experimental data for Pd thiosemicarbazone complexes.[27,28] The distance between Pd(1) and P(26) is 2.292 Å. The bond length between C(4) and I(12) in iodobenzene is 2.108 Å and this

is also similar to previously reported data for this molecule.[4] The charge assigned to the Pd metal using natural bond orbitals analysis (NBO) is 0.204*e*. As shown by other computational studies involving aryl halides and Pd, the oxidative addition of iodobenzene (**6.2)** to Pd(II) complex (**6.1)** can occur *via* several intermediates. The proposed mechanism (Figure 6.3) follows a pathway similar to previously reported pathways in the literature.[4,23,26]

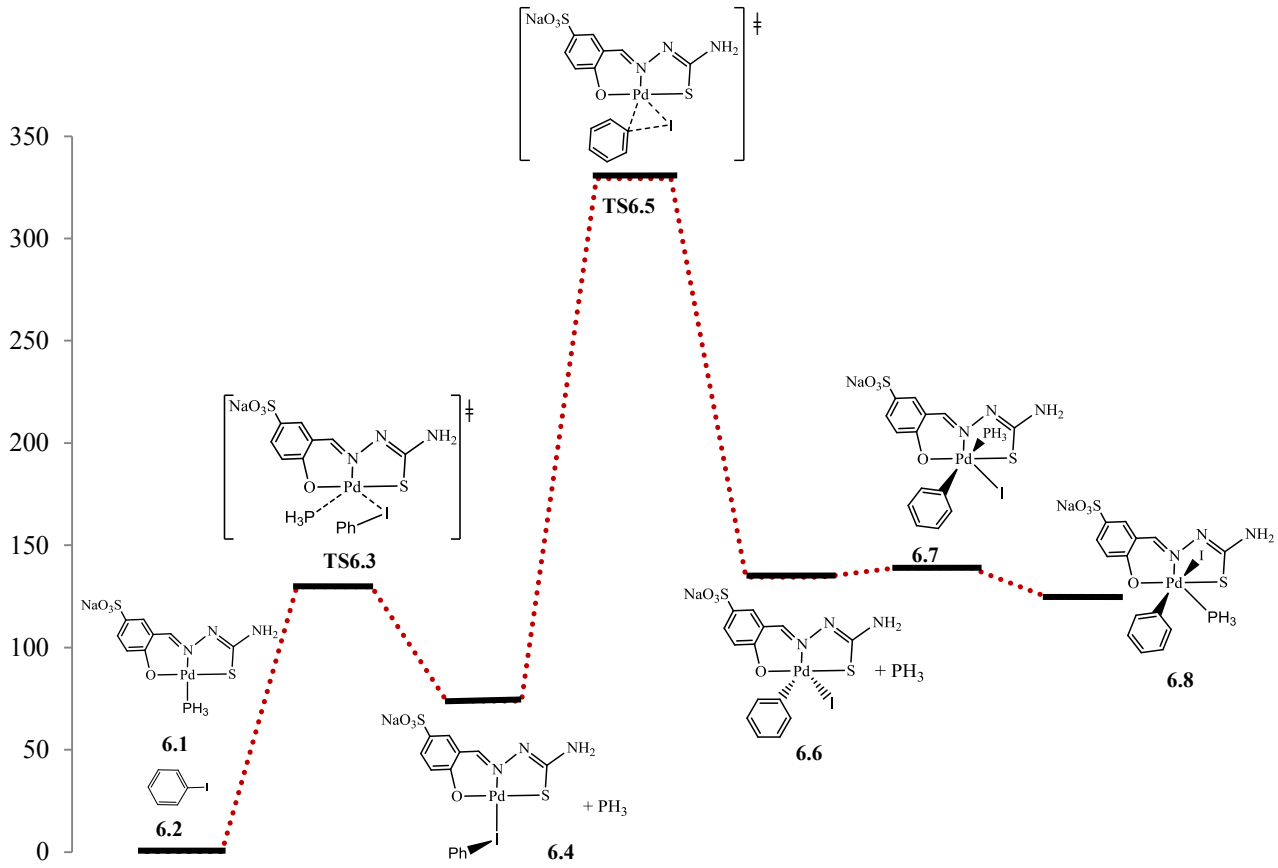

Figure 6.3. Free energy profile for the oxidative addition of **6.2** to **6.1** leading to product **6.8**.

The first step involves substitution of the phosphine with iodobenzene *via* transition state **TS6.3** (Figure 6.3). The product of this substitution (**6.4**) is a square-planar intermediate with the aryl halide bound to Pd *via* the iodine atom. The second step involves cleavage of the Ph-I bond and subsequent formation of a 5-coordinate Pd complex **6.6** *via* transition state **TS6.5**. Intermediate **6.6** then coordinates with a PH_3 to form an octahedral Pd(IV) complex (**6.7**) with a *cis* conformation which then isomerises to a more stable *trans* isomer **6.8**.

The located transition state structure (**TS6.3**) suggests dissociation of the PH_3 as the iodobenzene approaches the Pd metal with the Pd(1)-P(26) bond increasing from 2.835 Å to

2.907 Å. Upon coordination of the iodobenzene to Pd, intermediate **6.4** is formed, which shows a clear change in the bond distances. The distance between the Pd(1) and P(26) in **6.4** has increased to 3.716 Å, which suggests complete dissociation of the PH_3 ligand from the metal. The bond distance Pd(1)-I(12) is 2.680 Å, which is shorter than 2.907 Å observed in the transition state structure **TS6.3** (Figure 6.4). The charge on the Pd metal has increased slightly to 0.292*e* from 0.204*e* in the starting complex. The overall free energy change of this step is +73 kJ/mol with a free energy barrier of 129.6 kJ/mol.

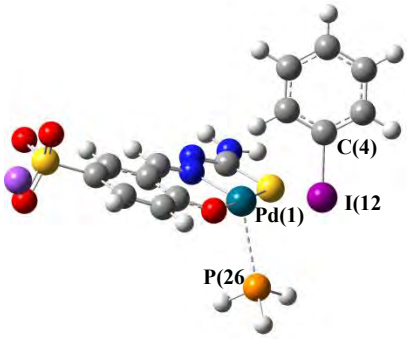

TS6.3

Pd(1)-P(26) = 2.835
Pd(1)-I(12) = 2.907

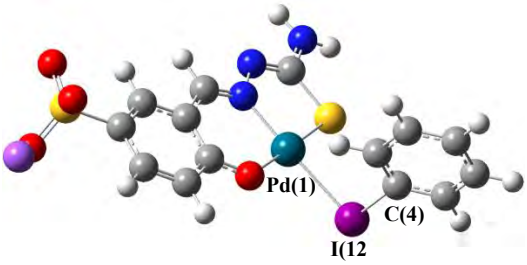

6.4

S(12)-Pd(1)-I(12) = 91.8
N(13)-Pd(1)-S(12) = 84.4
Pd(1)-P(26) = 3.716

N(13)-Pd(1)-O(11) = 94.3
O(11)-Pd(1)-I(12) = 89.5
Pd(1)-I(12) = 2.680

Figure 6.4. Optimised structures of **TS6.3** and **6.4** with selected bond lengths (Å) and angles (˚).

Intermediate **6.4** has a square-planar geometry around the metal centre. The substitution of PH_3 brings the C-I bond (of iodobenzene) into close proximity with the Pd metal centre which consequently facilitates the oxidative addition. Intermediates of this type have previously been observed in a Pd(II)/Pd(IV) redox during oxidative addition of iodobenzene to a Pd(II) catalyst.[26] Coordination of the iodine atom to the Pd centre has also been reported by Thiel and co-workers during oxidative addition of aryl halides.[29] A linear structure was considered for **6.4** where the Pd(1)-I(12)-C(4) angle is 180˚. This is because linearly bound aryl halides have been previously reported in the literature.[4,29] However, after several attempts to locate a linearly bound iodobenzene, this was abandoned and further calculations were performed with **6.4** with a Pd(1)-I(12)-C(4) angle of 99.8˚.

Coordination of Pd to the phenyl ring of iodobenzene and subsequent dissociation of the C(4)-I(12) bond then follows *via* transition state **TS6.5** to form **6.6** with a trigonal bipyramidal geometry at the Pd centre. This step has an overall free energy change of 60.6

kJ/mol and a free energy barrier of 255.6 kJ/mol. The transition state structure of **TS6.5** is shown in Figure 6.5.

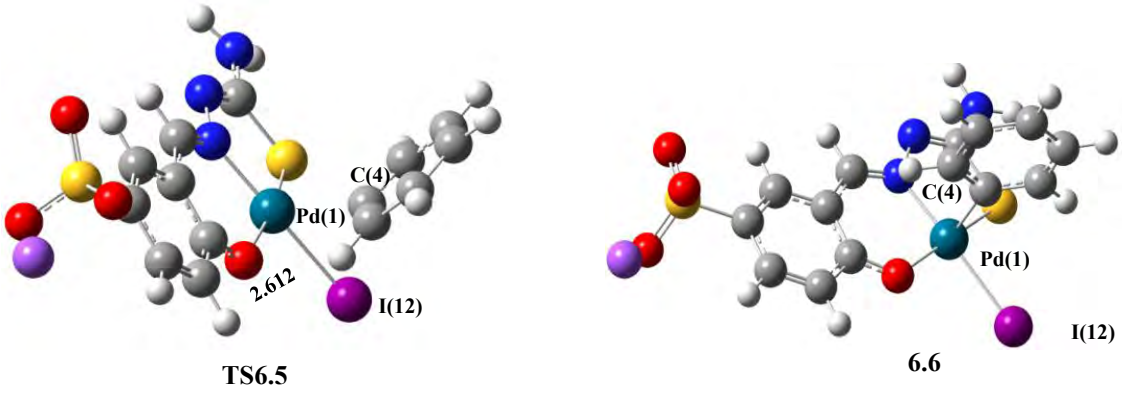

Figure 6.5 Transition state structure **TS6.2** and structure for **6.6**

Analysis of the occupied molecular orbital for the transition state structure **TS6.5** shows the metal-to-ligand interactions. The involvement of the Ph-I π* orbital (see insert) in the HOMO of transition state structure **TS6.5** is quite evident (Figure 6.6).

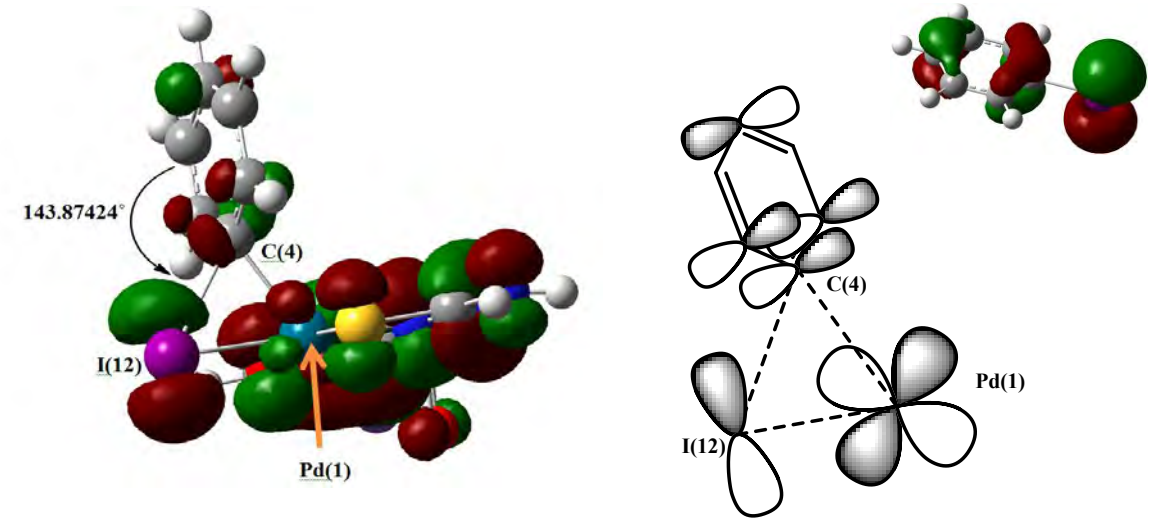

Figure 6.6. Highest occupied molecular orbital showing the metal-to-ligand interactions in the transition state **TS6.5**.

The transition state structure also shows bending of the C(4)-I(12) bond away from the plane of the phenyl ring. The bending results in a 143.9˚ angle being formed as illustrated in Figure 6.5. This bending has also been documented by Lin and co-worker in the oxidative addition of bromobenzene to a Pd(0) complex.[30] The authors reported that this bending can allow mixing of the Ph-halogen π* and the σ orbitals resulting in a new hybrid orbital that can

overlap with the occupied Pd d-orbitals and thus increasing the donor-acceptor orbital interactions.

An IRC (intrinsic reaction coordinate) path was computed for the transition state (**TS6.5**) to confirm that this structure connects to **6.4** and **6.6**. A number of structures along the reaction coordinate were obtained. The reaction was followed backwards and forwards starting from the located transition state **TS6.5**. The path is shown in Figure 6.7.

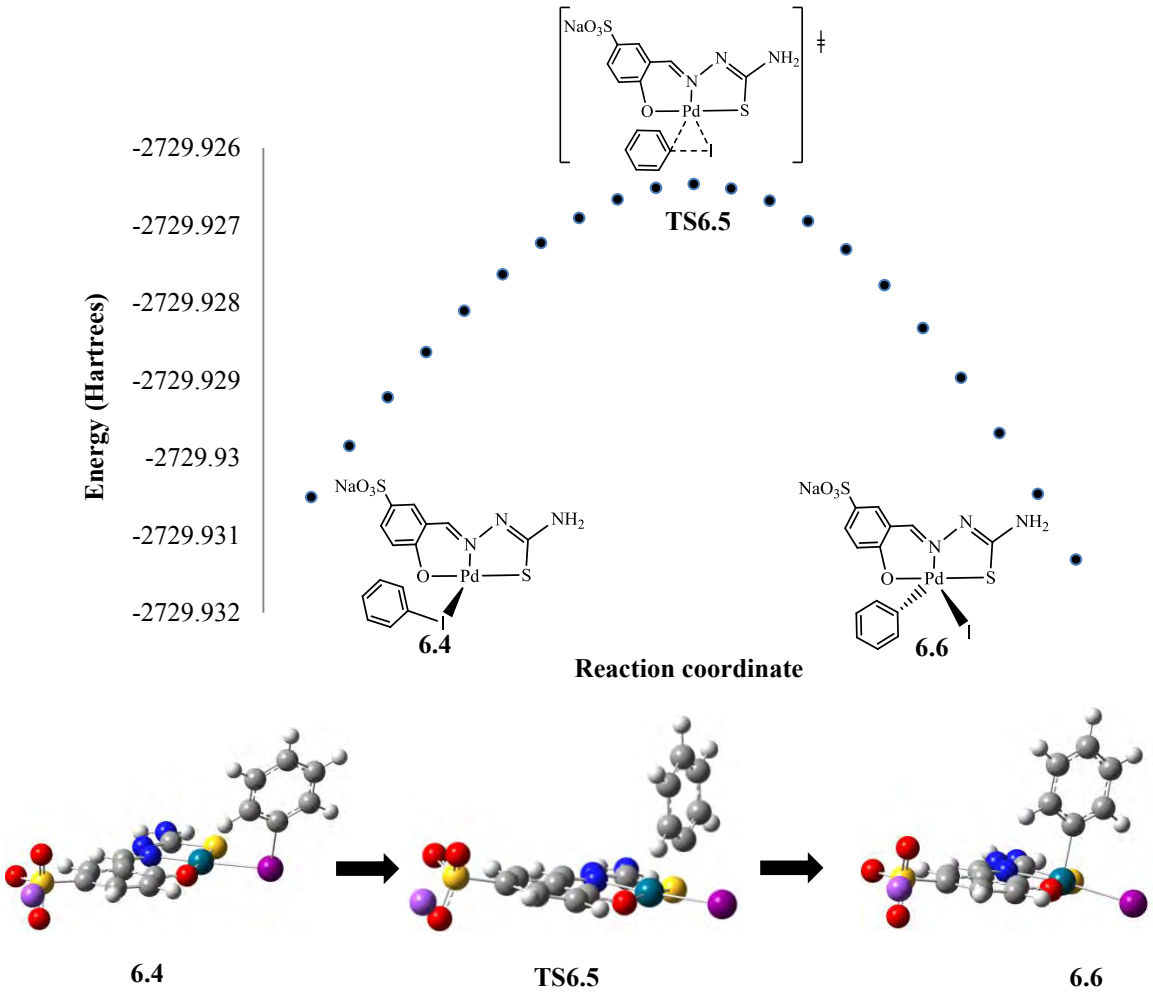

Figure 6.7. Illustrations of the reaction centre structures for **6.4**, **TS6.5** and **6.6** along the IRC.

The IRC path shows that there is a definite change in the geometry at the Pd centre. A 4-coordinate square-planar complex is observed for **6.4**, but changes to a 5-coordinate square pyramidal intermediate **6.6** with the iodine and the phenyl ring in the *cis* conformation. A significant increase in the charge on the Pd metal centre is observed for **6.6**. The charge is 0.443*e* and this is indicative of the fact that oxidative addition has occurred on the Pd metal.

After the addition of iodobenzene, **6.6** coordinates with PH_3 to form an octahedral Pd(IV) **6.7** (Figure 6.8). The oxidative addition product **6.7** then isomerises to form the *trans* product **6.8**.

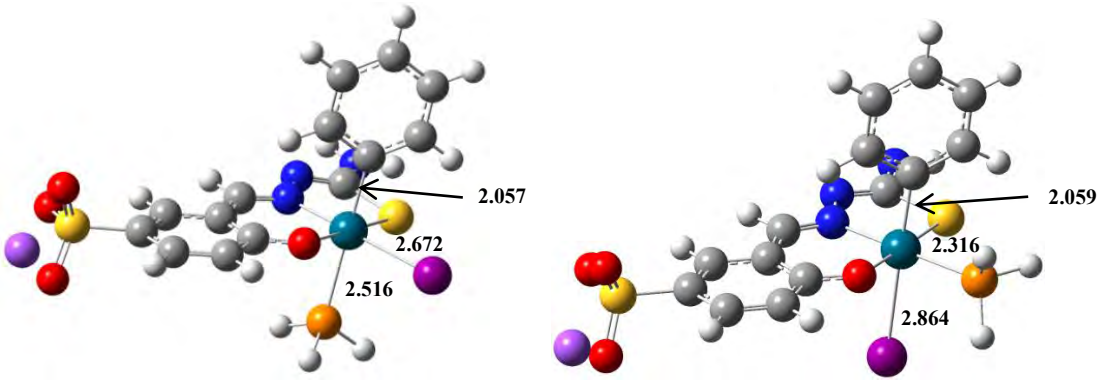

6.7 (*cis*) **6.8** (*trans*)

Figure 6.8. Optimised structures for **6.7 and 6.8** PBE0/def2-SVP/SDD(Pd) with selected bond lengths (Å).

The energy barrier for the coordination of PH_3 to **6.6** is 4.5 kJ/mol to form complex **6.7** (*cis* conformation) which further isomerises to **6.8** with the iodine and the phenyl ring *trans* to each other. The *trans* isomer (**6.8**) is 9.5 kJ/mol more stable than the *cis* isomer (**6.7**). Slight changes in the bond lengths are observed after isomerisation; however the geometry around the metal is maintained. The overall oxidative addition reaction is endergonic with a positive free energy of 138.8 kJ/mol.

6.3 Overall Summary

DFT calculations have been utilised to elucidate the oxidative addition of iodobenzene to a new water-soluble thiosemicarbazone Pd(II) complex (**6.1**). The proposed mechanism begins with substitution of PH_3 with iodobenzene with the iodine coordinated to the Pd(II) centre to form a square planar complex **6.3**. This step has a free energy barrier of 129.6 kJ/mol and overall reaction energy of +73.8 kJ/mol. This substitution brings the Ph-I close to the Pd centre to facilitate the ensuing oxidative addition. The oxidative addition then occurs resulting in a 5-coodinate intermediate (**6.6**) and the free energy of the step is + 60.6 kJ/mol with a free energy barrier of 255.6 kJ/mol. This 5-coodinate intermediate (**6.6**) coordinates with PH_3 resulting in the formation of an octahedral Pd(IV) oxidative addition product (**6.7**) which isomerises to the *trans* isomer (**6.8**). The *trans* isomer is 9.5 kJ/mol more stable than

the *cis* isomer (**6.7**). The overall oxidative addition reaction is endergonic with a positive free energy of 138.8 kJ/mol and is not consistent with literature examples that follow a similar pathway.[4, 26, 29] This suggests that the oxidative addition of iodobenzene to thiosemicarbazone complex **4.4**, may occur *via* alternative pathways, since the experimental results discussed in Chapter 5 show that the reaction is feasible.

6.4 Computational details

PH_3 was used in place of triphenylphosphine to reduce the computational effort. Geometry optimizations and frequency calculations were performed at the PBE0/def2-SVP/SDD(Pd, I)[31–33] level of theory in aqueous solution using the SMD[34] implicit solvent model. The notation above denotes a mixed basis set of def-2SVP[31] on the organic atoms (C, H, N, P, S) and the SDD[33] pseudopotential on I and Pd. Harmonic force constraints were computed at the optimized geometries to characterise the stationary points as minima or saddle points. Zero-point vibrational corrections were determined from the harmonic vibrational frequencies to convert the total energies E_e to ground state energies E_0. The rigid-rotor harmonic-oscillator approximation was applied for evaluating the thermal and entropic contributions. The transition states were computed using the QST2 method. The TS structures (**TS6.3** and **TS6.5**) are characterized by a single imaginary frequency while the rest of the optimised structures possess only real frequencies. All calculations were carried out by employing the Gaussian09 package.[35]

6.5 References

1 H. M. Senn and T. Ziegler, *Organometallics*, 2004, **23**, 2980–2988.

2 A. A. C. Braga, G. Ujaque and F. Maseras, *Organometallics*, 2006, **25**, 3647–3658.

3 A. A. C. Braga, N. H. Morgon, G. Ujaque and F. Maseras, *J. Am. Chem. Soc.*, 2005, 9298–9307.

4 L. J. Goossen, D. Koley, H. L. Hermann and W. Thiel, *Organometallics*, 2005, **24**, 2398–2410.

5 L. J. Goossen, D. Koley, H. L. Hermann and W. Thiel, *Organometallics*, 2006, 54–67.

6 S. Kozuch, S. Shaik, A. Jutand and C. Amatore, *Chem. Eur. J.*, 2004, **10**, 3072–3080.

7 M. Sumimoto, N. Iwane, T. Takahama and S. Sakaki, *J. Am. Chem. Soc.*, 2004, **126**, 10457–10471.

8 F. Barrios-Landeros and J. F. Hartwig, *J. Am. Chem. Soc.*, 2005, **127**, 6944–6945.

9 A. L. Casado and P. Espinet, *Organometallics*, 1998, **17**, 954–959.

10 A. Gillie and A. Gillie, *J. Am. Chem. Soc.*, 1980, **102**, 4933–4941.

11 V. P. Ananikov, D. G. Musaev and K. Morokuma, *J. Am. Chem. Soc.*, 2002, **124**, 2839–2852.

12 E. Zuidema, P. W. N. M. van Leeuwen and C. Bo, *Organometallics*, 2005, **24**, 3703–3710.

13 J. So, K. Olech, Ś. Agnieszka, D. Zaj and J. Cabaj, *J. Chem. Educ.*, 2013, **3**, 19–32.

14 N. Miyaura and A. Suzuki, *Chem. Rev.*, 1995, **95**, 2457–2483.

15 M. Joshaghani, E. Faramarzi, E. Rafiee, M. Daryanavard, J. Xiao and C. Baillie, *J. Mol. Catal. A Chem.*, 2006, **259**, 35–40.

16 S. Kotha, K. Lahiri and D. Kashinath, *Tetrahedron*, 2002, **58**, 9633–9695.

17 A. J. J. Lennox and G. C. Lloyd-Jones, *Chem. Soc. Rev.*, 2014, **43**, 412–43.

18 K. M. Engle, D. Wang and P. J. Yu, *Angew. Chem. Int. Engl.*, 2009, **48**, 5094–5115.

19 W. De Graaf, J. Bowsma and G. Van Koten, *Organometallics*, 1990, **9**, 1479–1484.

20 D. Kalyani, N. Deprez, L. V Desai and M. S. Sanford, *J. Am. Chem. Soc.*, 2005, **127**, 7330–7331.

21 P. K. Byers, A. J. Canty, B. W. Skelton and A. H. White, *J. Chem. Soc. Chem. Commun.*, 1986, **3**, 1722.

22 B. A. J. Canty, *Platin. Met. Rev.*, 1993, **37**, 2–7.

23 K. J. Szabó, *J. Mol. Catal. A Chem.*, 2010, **324**, 56–63.

24 O. Blacque and C. M. Frech, *Chem. Eur. J.*, 2010, **16**, 1521–1531.

25 J. Vicente, A. Arcas, F. Juliá-Hernández and D. Bautista, *Angew.Chem. Int. Ed.*, 2011, **50**, 6896–6899.

26 Y. Dang, S. Qu, J. W. Nelson, H. D. Pham, Z.-X. Wang and X. Wang, *J. Am. Chem. Soc.*, 2015, **137**, 2006–2014.

27 P. Chellan, N. Shunmoogam-Gounden, D. T. Hendricks, J. Gut, P. J. Rosenthal, C. Lategan, P. J. Smith, K. Chibale and G. S. Smith, *Eur. J. Inorg. Chem.*, 2010, 3520–3528.

28 J. Dutta and S. Bhattacharya, *RSC Adv.*, 2013, **3**, 10707.

29 L. J. Goossen, D. Koley, H. Hermann and W. Thiel, *Chem. Commun.*, 2004, 2141–2143.

30 A. Ariafard and Z. Lin, *Organometallics*, 2006, **25**, 4030–4033.

31 F. Weigend and R. Ahlrichs, *Phys. Chem. Chem. Phys.*, 2005, **7**, 3297–3305.

32 J. P. Perdew, M. Ernzerhof and K. Burke, *J. Chem. Phys.*, 1996, **105**, 9982–9985.

33 M. Dolg, U. Wedig, H. Stoll and H. Preuss, *J. Chem. Phys.*, 1987, **86**, 866–872.

34 A. V. Marenich, C. J. Cramer and D. G. Truhlar, *J. Phys. Chem. B*, 2009, **113**, 6378–6396.

35 Gaussian 09, Revision D.01, M. J. Frisch, G. W. Trucks, H. B. Schlegel, G. E. Scuseria, M. A. Robb, J. R. Cheeseman, G. Scalmani, V. Barone, B. Mennucci, G. A. Petersson, H. Nakatsuji, M. Caricato, X. Li, H. P. Hratchian, A. F. Izmaylov, J. Bloino, G. Zheng, J. L. Sonnenberg, M. Hada, M. Ehara, K. Toyota, R. Fukuda, J. Hasegawa, M. Ishida, T. Nakajima, Y. Honda, O. Kitao, H. Nakai, T. Vreven, J. A. Montgomery, Jr., J. E. Peralta, F. Ogliaro, M. Bearpark, J. J. Heyd, E. Brothers, K. N. Kudin, V. N. Staroverov, T. Keith, R. Kobayashi, J. Normand, K. Raghavachari, A. Rendell, J. C. Burant, S. S. Iyengar, J. Tomasi, M. Cossi, N. Rega, J. M. Millam, M. Klene, J. E. Knox, J. B. Cross, V. Bakken, C. Adamo, J. Jaramillo, R. Gomperts, R. E. Stratmann, O. Yazyev, A. J. Austin, R. Cammi, C. Pomelli, J. W. Ochterski, R. L. Martin, K. Morokuma, V. G. Zakrzewski, G. A. Voth, P. Salvador, J. J. Dannenberg, S. Dapprich, A. D. Daniels, O. Farkas, J. B. Foresman, J. V. Ortiz, J. Cioslowski, and D. J. Fox, Gaussian, Inc., Wallingford CT, 2013.

Chapter 7

Overall summary, conclusions and future outlook

7.1 Synthesis and characterization of water-soluble Rh(I) complexes and application as catalysts precursors in the aqueous biphasic hydroformylation of 1-octene

The main objectives of this study were to prepare a series of new water-soluble mononuclear and binuclear transition metal complexes and evaluate their potential as recyclable catalysts for various organic transformations. This would contribute to the area of green chemistry and application of water as a reaction medium as opposed to the use of conventional organic solvents for catalysis.

A series of new water-soluble sulfonated salicylaldimine ligands was prepared *via* Schiff base condensation reactions between various amines and a water-soluble aldehyde. The ligands were characterized using various spectroscopic and analytical techniques. Both the monomeric (**2.3**-**2.6**) and dimeric ligands (**2.7**-**2.10**) displayed excellent water-solubility in water at room temperature. These ligands (**2.3**-**2.10**) were reacted with the $[RhCl(COD)]_2$ *via* a bridge-splitting reactions to afford a series of new Rh(I) complexes (**2.11**-**2.18**). All the complexes were characterized using ^{1}H NMR, ^{31}C NMR and infrared spectroscopy, electrospray ionisation mass spectrometry (negative ion-mode), elemental analysis, single crystal X-ray diffraction (**2.14**) and melting point determinations.

These water-soluble Rh(I) complexes were used as aqueous biphasic hydroformylation of 1-octene catalyst precursors. The mononuclear catalysts (**2.11**-**2.14**) displayed excellent chemoselectivity for aldehydes (>99%), whilst the binuclear Rh(I) analogues (**2.15**-**2.18**) showed slightly lower aldehyde chemoselectivity (>89%). Hydrogenation of 1-octene was not observed. The hydrogenation of 1-octene was prevented in the present catalysts most importantly by using Rh-based catalysts as opposed to Ru-based catalysts which are well-known to be active hydrogenation catalysts. Through recycling experiments, the mononuclear catalysts (**2.11**-**2.14**) could be recycled up to five times while the binuclear analogues (**2.15**-**2.18**) could be recycled three times. Inductively coupled plasma optical

spectrometry experiments confirm that no leaching of the mononuclear and binuclear catalysts (**2.11**-**2.18**) into the organic layer occurs. Analyses of the aqueous layers after the recycling experiments show that <1% metal is present in solution. The mercury drop experiments show suppressed catalyst activity and therefore the activity is due to a combination of homogeneous catalysis and catalysis mediated by Rh nanoparticles suspended in the aqueous layer.

The advantages of the present Rh catalysts include:

(i) Moderate to good activity in the hydroformylation of a higher olefin (with poor water-solubility) in an aqueous biphasic system.

(ii) Good recyclability of the catalysts without significant changes in activity and chemoselectivity.

(iii) Easy catalyst recovery due to the biphasic nature of the system.

7.2 Synthesis and characterization of water-soluble Pd(II) thiosemicarbazone complexes and their application in aqueous phase Suzuki-Miyaura cross-coupling reactions

The synthesis and characterization of new water-soluble thiosemicarbazone ligands (**4.1** and **4.3**) *via* Schiff base condensation reactions has been done. Both ligands displayed excellent water-solubility at room temperature and were characterized using various analytical and spectroscopic techniques. The ligands were used in the synthesis of new mononuclear and binuclear water-soluble thiosemicarbazone Pd(II) complexes. The complexes (**4.4**-**4.7**) were characterized using ^{1}H NMR, ^{31}C{H} NMR, ^{31}P{H} and infrared spectroscopy, electrospray ionisation mass spectrometry (negative ion-mode), elemental analysis, single crystal X-ray diffraction (**2.14**) and melting point determinations. The stability of the complexes display excellent stability in water at 70 ˚C over a period of 24 hours and this was confirmed using ^{1}H NMR and ^{31}P{H} NMR spectroscopy.

The Pd(II) thiosemicarbazone complexes were tested as catalyst precursor in the Suzuki-Miyaura cross-coupling reaction in water. The binuclear catalysts (**4.6**-**4.7**) displayed comparable activity to the mononuclear analogues (**4.4**-**4.5**). Both catalysts (**4.4**-**4.5**) proved to be versatile and were able to couple substrates containing various substituents. The recyclability of catalyst **4.4** was evaluated and the catalyst-containing aqueous layer

could only be recycled efficiently twice. Mercury poisoning tests rule out the formation of any catalytic active nanoparticles, suggesting that the catalytic reaction follows a homogeneous pathway.

The advantages of the Pd catalysts include:

(i) Easy catalyst recovery for recycling.
(ii) Ability of the catalysts to couple various substrates with varying electronic effects.
(iii) Easy catalyst preparation.
(iv) The Pd catalysts are very stable in solution.

7.3 Theoretical investigation of the oxidative addition of iodobenzene to water-soluble thiosemicarbazone complex in aqueous medium

The feasibility of a Pd(II)/Pd(IV) mechanism during the oxidative addition of iodobenzene to thiosemicarbazone complex was investigated. Geometric optimizations and frequency calculations were performed at the PBE0/def2-SVP/SDD(Pd, I)[1–3] level of theory in aqueous solution using the SMD[4] implicit solvent model. The notation above denotes a mixed basis set at def-2SVP[1] on the organic atoms (C, H, N, P, S) and the SDD[3] pseudopotential on I and Pd. All calculations were carried out by employing the Gaussian09 package.[5] A Pd(II)/Pd(IV) redox during oxidative addition of iodobenzene was established using complex **4.4**. The overall oxidative addition reaction is endergonic with a ΔG^o = +138.8 KJ/mol.

7.4 Future outlook

7.4.1 Aqueous biphasic hydroformylation reactions

The mononuclear complexes displayed excellent aldehyde chemoselectivity and recyclability. However, the regioselectivity was not impressive. The experiments displayed that the presence of bulky substituents results in better regioselectivity for the linear products. It is therefore important that in future, catalysts with similar structure can be designed and synthesized but the presence of bulky substituents is essential for high *n*:*iso* ratios to be obtained.

It could be useful to explore another route for generating Rh(I) species to produce efficient and recyclable catalysts by adding an oxidising agent for Rh(0) salts. However, it is

important to note the influence of ligands in fine-tuning catalyst regioselectivity and chemoselectivity. This makes proper catalyst design and synthesis very important as opposed to simply oxidising Rh(0) salts.

For the binuclear series, the design and synthesis of stable complexes is important to reduce nanoparticle formation which ultimately alters catalysts' chemoselectivity. The distance between the metal centres is also important for cooperativity to be ensured which results in higher catalyst activity.[6–10]

7.4.2 Aqueous phase Suzuki-Miyaura cross-coupling reactions

In the Suzuki-Miyaura cross-coupling experiments, the performance of the catalysts with aryl chlorides was not tested. This is important that these reactions are investigated with more difficult substrates in the future. Similar to the Rh(I) catalysts, the presence of two Pd centres did not result in improved catalytic activity. The binuclear complexes seemed to operate as two mononuclear catalysts and hence there was comparable activity between the binuclear catalysts and their mononuclear analogues. In future, the distance between the metals must be considered during catalyst design in order for cooperativity effects between metal centres to be possible.

7.4.3 Theoretical studies on the oxidative addition of iodobenzene to thiosemicarbazone Pd(II) complex

Since Canty and co-workers reported the oxidative addition of MeI to Pd(II) complexes to form Pd(IV) species, there has been growing interests in investigating oxidative addition reactions following Pd(II)/Pd(IV).[11,12] The possibility of a Pd(II)/Pd(IV) redox during the oxidative addition of iodobenzene has been established in this work. Future work entails investigation of the transmetallation and reductive elimination steps in Suzuki-Miyaura cross-coupling mechanism using the Pd(II) thiosemicarbazone complexes. Apart from this, there could be other possible pathways followed during the oxidative addition step and hence further studies using DFT experiments can be carried out to find these pathways.

7.5 References

1 F. Weigend and R. Ahlrichs, *Phys. Chem. Chem. Phys.*, 2005, **7**, 3297–3305.

2 J. P. Perdew, M. Ernzerhof and K. Burke, *J. Chem. Phys.*, 1996, **105**, 9982–9985.

3 M. Dolg, U. Wedig, H. Stoll and H. Preuss, *J. Chem. Phys.*, 1987, **86**, 866–872.

4 A. V. Marenich, C. J. Cramer and D. G. Truhlar, *J. Phys. Chem. B*, 2009, **113**, 6378–6396.

5 Gaussian 09, Revision D.01, M. J. Frisch, G. W. Trucks, H. B. Schlegel, G. E. Scuseria, M. A. Robb, J. R. Cheeseman, G. Scalmani, V. Barone, B. Mennucci, G. A. Petersson, H. Nakatsuji, M. Caricato, X. Li, H. P. Hratchian, A. F. Izmaylov, J. Bloino, G. Zheng, J. L. Sonnenberg, M. Hada, M. Ehara, K. Toyota, R. Fukuda, J. Hasegawa, M. Ishida, T. Nakajima, Y. Honda, O. Kitao, H. Nakai, T. Vreven, J. A. Montgomery, Jr., J. E. Peralta, F. Ogliaro, M. Bearpark, J. J. Heyd, E. Brothers, K. N. Kudin, V. N. Staroverov, T. Keith, R. Kobayashi, J. Normand, K. Raghavachari, A. Rendell, J. C. Burant, S. S. Iyengar, J. Tomasi, M. Cossi, N. Rega, J. M. Millam, M. Klene, J. E. Knox, J. B. Cross, V. Bakken, C. Adamo, J. Jaramillo, R. Gomperts, R. E. Stratmann, O. Yazyev, A. J. Austin, R. Cammi, C. Pomelli, J. W. Ochterski, R. L. Martin, K. Morokuma, V. G. Zakrzewski, G. A. Voth, P. Salvador, J. J. Dannenberg, S. Dapprich, A. D. Daniels, O. Farkas, J. B. Foresman, J. V. Ortiz, J. Cioslowski, and D. J. Fox, Gaussian, Inc., Wallingford CT, 2013.

6 D. G. H. Hetterscheid, S. H. Chikkali, B. de Bruin and J. N. H. Reek, *ChemCatChem*, 2013, **5**, 2785–2793.

7 S. W. S. Choy, M. J. Page, M. Bhadbhade and B. A. Messerle, *Organometallics*, 2013, 1–4.

8 R. K. Das, B. Saha, S. M. W. Rahaman and J. K. Bera, *Chem. A Eur. J.*, 2010, **16**, 14459–14468.

9 S. W. S. Choy, M. J. Page, M. Bhadbhade and B. A. Messerle, *Organometallics*, 2013, **32**, 4726–4729.

10 D. A. Aubry, N. N. Bridges, K. Ezell and G. G. Stanley, *J. Am. Chem. Soc.*, 2003, **125**, 11180–11181.

11 P. K. Byers, A. J. Canty, B. W. Skelton and A. H. White, *J. Chem. Soc. Chem. Commun.*, 1986, **3**, 1722.

12 B. A. J. Canty, *Platin. Met. Rev.*, 1993, **37**, 2–7.